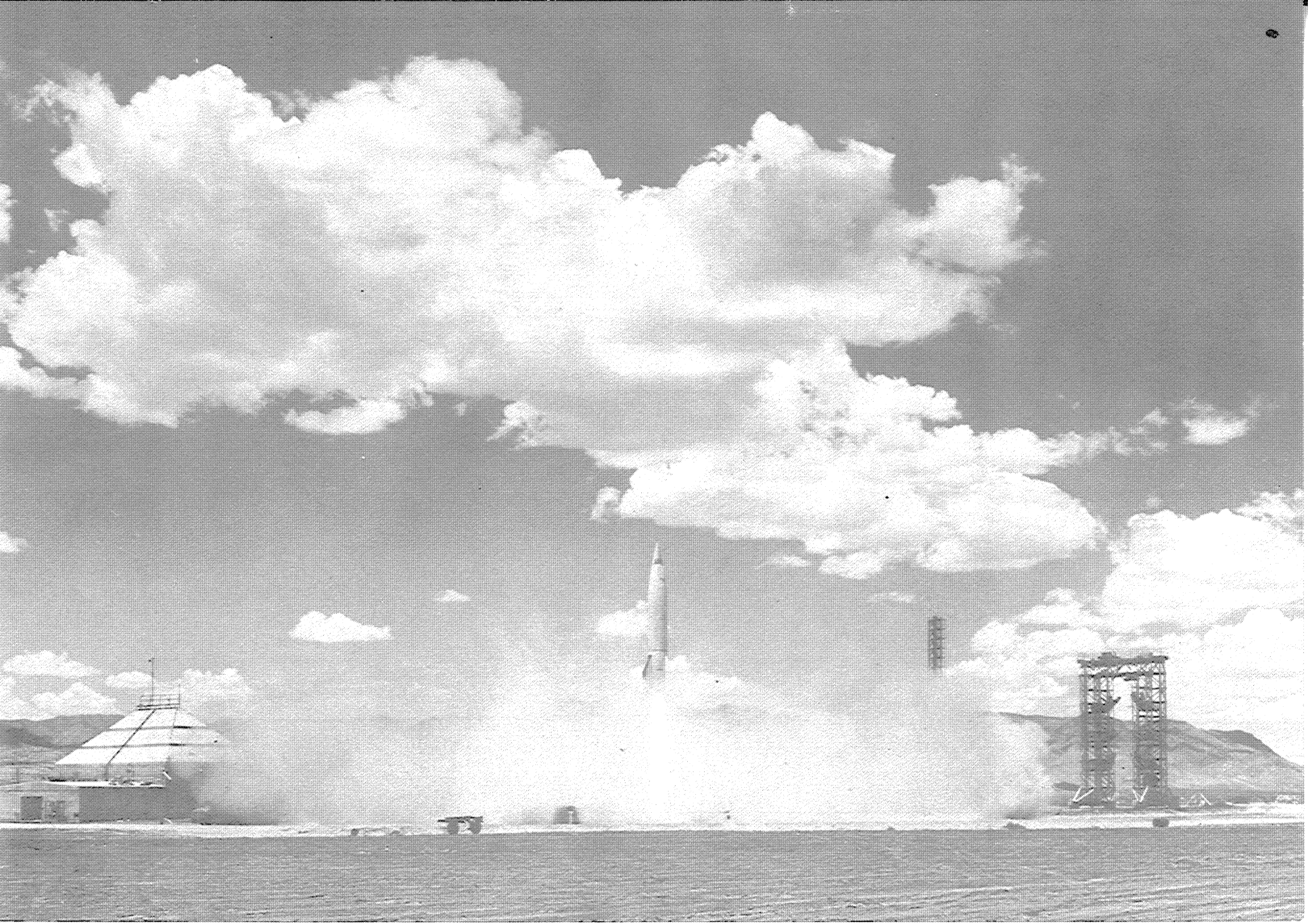

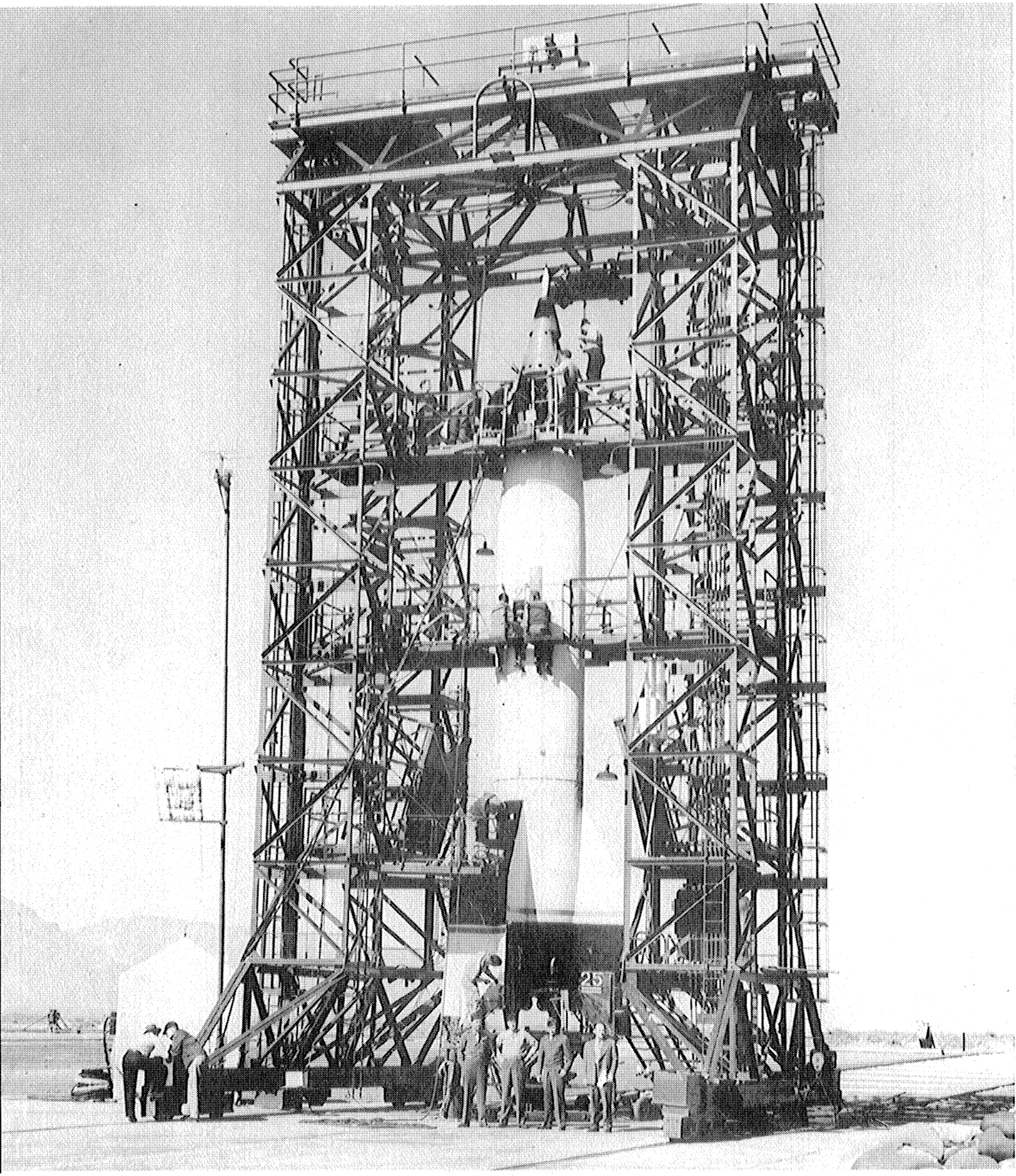

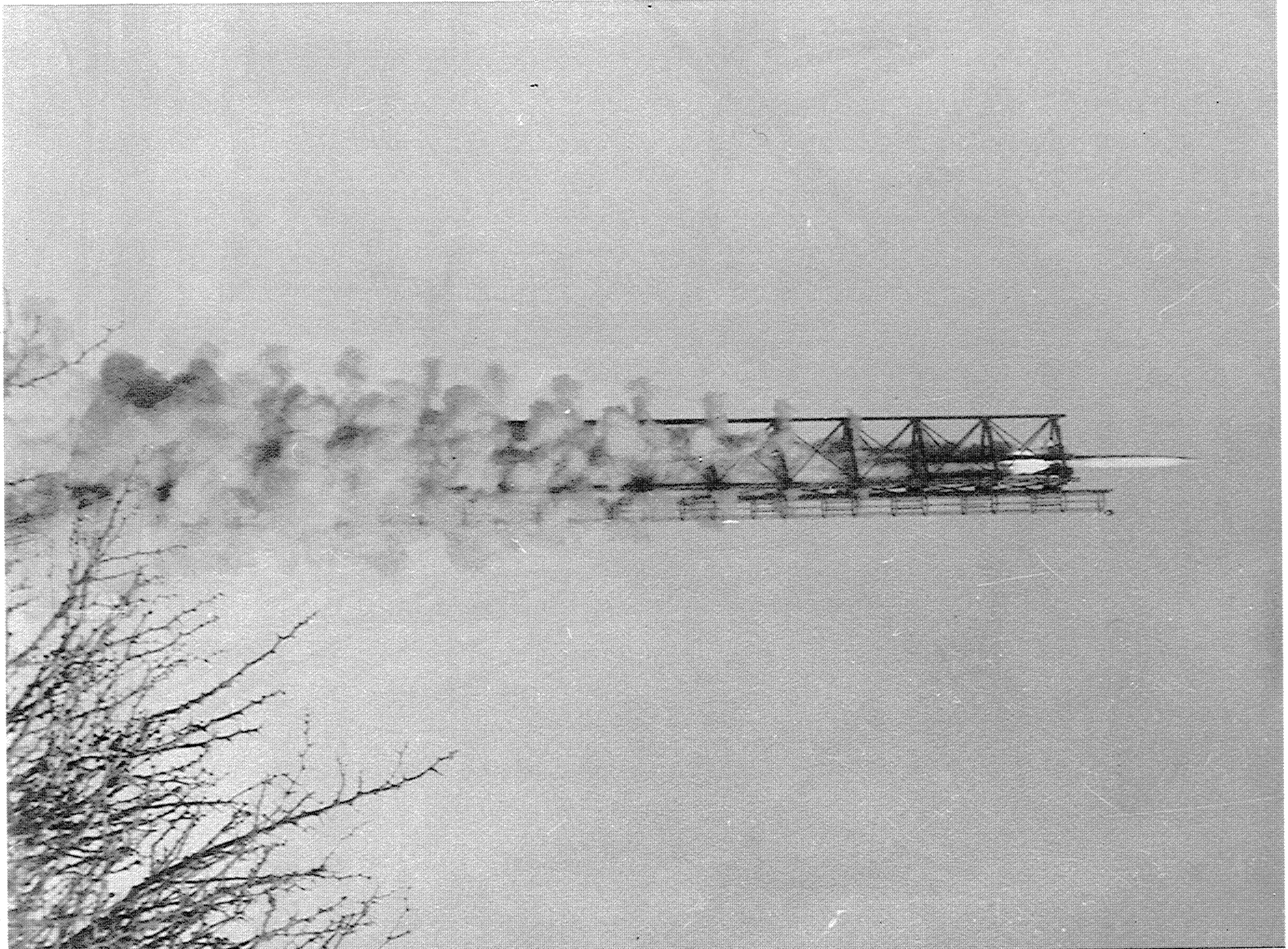

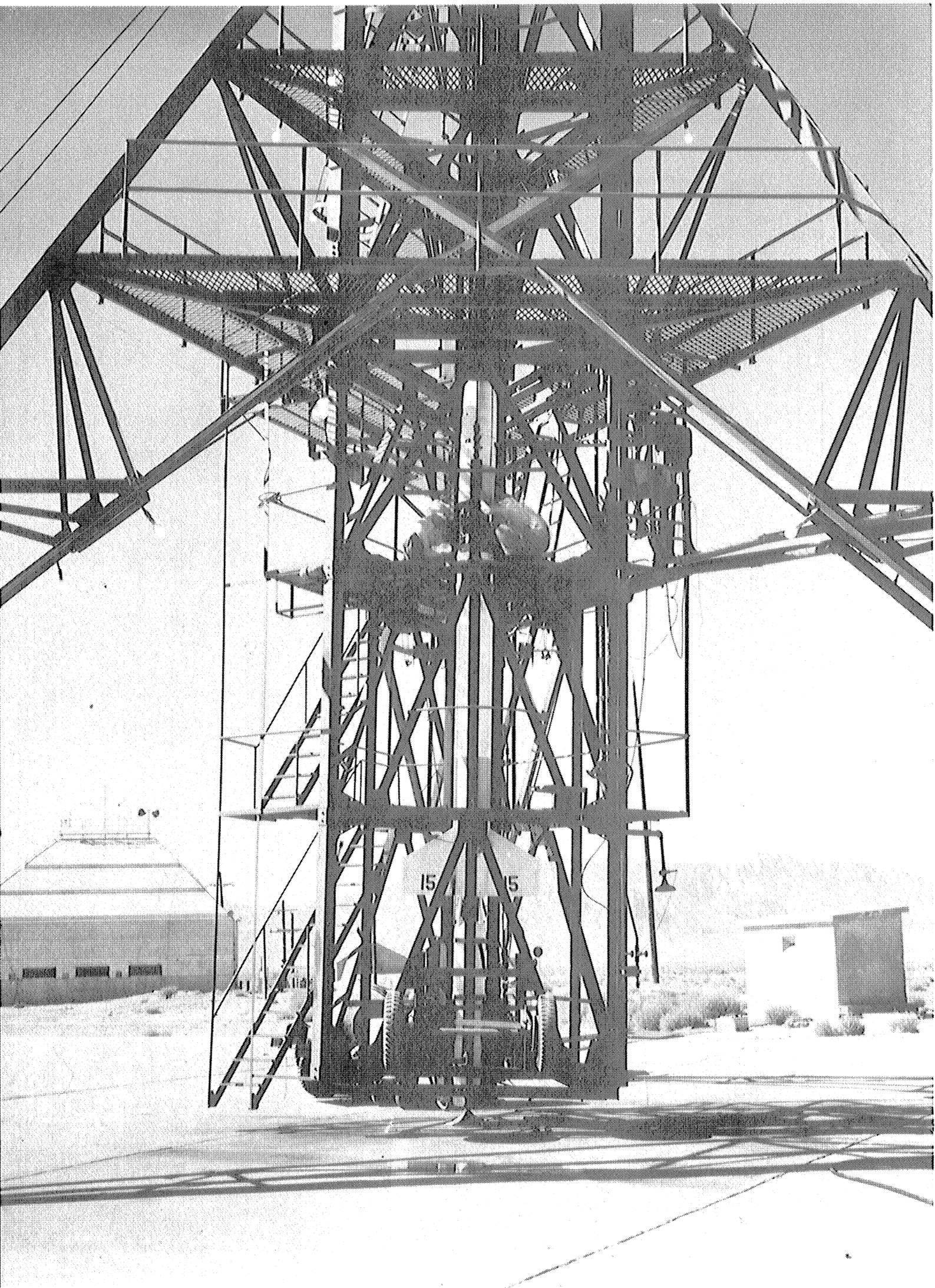
15
5

ENGINEERING RESEARCH INSTITUTE
UNIVERSITY OF MICHIGAN

Ann Arbor

ATMOSPHERIC PHENOMENA AT HIGH ALTITUDES

U. S. War Department
Contract No. W-36-039 sc-32307
(Meteorological Branch, Signal Corps)

Final Progress Report

for the period

July 15, 1946 to August 31, 1950

Department of the Army Project: No. 3-99-07-022
Signal Corps Project: No. 172B

Submitted for the project by:

L. M. Jones
H. W. Neill

UNIVERSITY OF MICHIGAN PROJECT PERSONNEL

Both Part Time and Full Time

* Bartman, Fred L., M.S., Research Engineer
Boothroyd, Alma C., Secretary
* Bozeman, Herbert C., Laboratory Assistant
Cohan, Alice F., Secretary
Collins, T. Kirkwood, B.S., Research Associate
Cooper, James B., Research Technician
Courtney, Howard W., B.S., Research Engineer
Goetz, Warren, B.S. Research Technician
Grabowski, Walter, Lab Technician
Hagelbarger, David T., PhD, Instructor, Dept. of Aeronautical Engineering
Henry, George, Laboratory Assistant
* Jones, Leslie M., B.S., Project Supervisor
* King, Jay B., B.A., Research Assistant
Lally, Frank I., Laboratory Assistant
* Leite, Richard J., M.S., Research Associate
* Liu, Vi-Cheng, PhD, Research Engineer
* Loh, Leslie T., M.S., Chemist
Mills, Robert G., M.S., Research Associate
* Munroe, Hugh F., B.S., Designer
Neill, Elizabeth, B.A., Research Technician
* Neill, Howard W., M.S., Research Engineer
* Nichols, Myron H., PhD, Consultant
Rutledge, Wyman T., M.S., Research Associate
* Schaefer, Edward J., M.S., Research Engineer
Schellinger, Richard T., Metalsmith
Sturgeon, Stocker S., Research Technician
* Swets, Maxine, Secretary
* Titus, Paul A., Research Technician
Turner, Eugene B., M.S. Research Associate
* Wenk, Norman J., B.S., Research Engineer
* Wenzel, Elton A., Research Technician
Whittington, Robert G., Laboratory Assistant
Williams, Ralph O., Research Technician

Degrees and titles shown were those held at time of leaving the project.

From July 1946 until August 1949 the research was under the direction of Dr. M. H. Nichols who is now Associate Professor of Electrical Engineering at the California Institute of Technology. We are fortunate in having Dr. Nichols' continued association and invaluable aid as consultant.

* Currently with the project.

TABLE OF CONTENTS

Section	Topic	Page
1.	INTRODUCTION	1
2.	PURPOSE	1
3.	PROGRAM	2
4.	REPORTS	3
5.	COMPOSITION	6
	5.1 Sampling	6
	5.11 Preparation of Sampling Bottles	6
	5.12 Sampling Bottle Openers	8
	5.13 Sampling Bottle Sealers	11
	5.14 Sampling Bottle Installations and Air Scoop Arrangements	16
	5.15 Recovery of Sampling Bottle After Rocket Flight	25
	5.16 Extraction of Upper Air Samples from Sampling Bottles	27
	5.17 Possible Contamination of the Upper Air Samples by Sampling Technique	29
	5.18 Establishment of Sampling Heights	32
	5.19 Sampling Efficiency	33
	5.2 Analyses of Upper Air Samples	38
	5.21 Charcoal Adsorption Analyses - University of Durham	38
	5.22 Charcoal Adsorption Analyses - University of Michigan	40
	5.23 Mass Spectrometric Analyses - Westinghouse Laboratory	46
	5.24 Mass Spectrometric Analyses - National Bureau of Standards	47
	5.25 Analyses for Oxides of Nitrogen - University of Michigan and Columbia University	50
	5.26 Attempted Analyses for Oxygen - University of Michigan	54
	5.27 Nitrogen Isotope Ratio Analyses - University of Virginia	55
	5.28 Discussion of Apparent Discrepancy Between the Nitrogen Isotope Ratio Analyses and the Paneth-Glückauf Type Analyses	57

TABLE OF CONTENTS (continued)

Section	Topic	Page
6.	MEASUREMENTS OF PRESSURE AND TEMPERATURE	69
	6.1 Ambient Pressure at a Neutral Point	69
	6.2 Measurement of Ambient Temperature by Measurement of the Aerodynamic Properties of a Supersonic Cone	71
	6.21 Theory	71
	6.22 Experimental Attempt on V-2 25	73
	6.23 Experimental Attempt on V-2's 33 and 50	78
	6.3 Measurement of Ambient Temperature by Measurement of the Angle of the Shock Wave Formed by a Supersonic Cone	85
	6.31 Theory	85
	6.32 Experimental Attempts on V-2's 33 and 50	88
	6.33 Experimental Attempt on V-2 56	89
	6.34 Adaptation to Aerobees	94
	6.4 Pressure Gages and Circuits	98
	6.41 Alphatrons	99
	6.42 Pirani Gages	106
	6.43 Pirani Gage Time Constants	111
	6.44 Pirani Gage Circuits	113
	6.45 Circuits for Probe Aerobee - Magnetic Recorder	123
	6.46 Constant Resistance Circuits for Probe Piranis	126
	6.5 Shadowgraph	134
	6.6 Subsidiary Experiments Related to the Measurement of Pressure and Temperature	138
	6.61 Probe Temperatures and Signals in Flight	138
	6.62 Model Test of Probes	140
	6.63 Shock Wave Curvature Investigation	141
	6.64 Evaluation of Shadowgraph and Schlieren Techniques for Measuring Temperatures in the Upper Atmosphere	148
7.	WINDS	153
8.	AUXILIARY ROCKET COMPONENTS	153
	8.1 Timers	153
	8.2 Cook Magnetic Recorder	154
9.	RECOMMENDATIONS	157
	9.1 Composition	157
	9.2 Pressure, Density, Temperature	157

TABLE OF CONTENTS (continued)

Section	Topic	Page
10.	ACKNOWLEDGMENT	157
11.	REFERENCES	160

ATMOSPHERIC PHENOMENA AT HIGH ALTITUDES

Department of Aeronautical Engineering

1. INTRODUCTION

This report summarizes the program of upper atmosphere research carried out by the Aeronautical Engineering Department of the University of Michigan in fulfillment of Signal Corps Contract No. W-36-039 sc-32307 with the Engineering Research Institute of the University. The work was started on July 15, 1946, and through extensions to the contract continued until August 31, 1950. The program is continuing on Signal Corps Contract DA 36-039 sc-125. The report consists of new material and edited excerpts from the project reports listed below. The excerpts are not shown as quotations or noted in the list of references.

2. PURPOSE

The purpose of the research as originally set forth in the contract was as follows:

a) "Develop the necessary techniques, and confirm them by field experiments, leading to measurement of pressure, temperature, and constituency of the atmosphere in the region of 30 to 80 kilometers altitude, the upper limit to be extended beyond 80 kilometers if phenomena are found which are considered by the government to warrant additional investigation.

b) "Develop methods for measuring wind direction and velocity throughout the altitude interval given in paragraph (a) above.

c) "Follow closely the progress of other investigations in research on other associated atmospheric phenomena such as ozone tracing, cosmic ray phenomena, etc., and participate in and extend investigations into these phenomena if deemed by the Government to be meteorologically significant.

d) "Pursue studies on the basis of information gained as a result of the investigations under paragraphs (a)

and (b) above, leading to evaluation of the role of observable upper atmosphere quantities in a better understanding of meteorological phenomena and weather forecasting.

e) "Assist with the evaluation, design and operation of special meteorological rockets, and design, test in operation, and evaluate the necessary instruments and techniques for obtaining required data."

3. PROGRAM

The first rockets to become available for high altitude experimentation were captured German V-2's (A-4's). A program of test firings at White Sands Proving Ground by Army Ordnance was inaugurated. Various agencies interested in the upper atmosphere were invited by Ordnance to use space on the V-2's for research instrumentation. Accordingly, a series of experiments was planned by the Meteorological Branch, ESL, and the University of Michigan to measure the fundamental variables of the upper atmosphere that have meteorological significance.

The first experiments planned by ESL were:

a) Measurement of the velocity of sound as a function of altitude by observations of explosions of grenades ejected from the V-2.

b) Optical tracking of smoke puffs from grenades ejected from the V-2. Designed to give information on upper atmosphere winds.

c) Optical observation of smoke trails generated on the V-2 after burnout. (In cooperation with Edgewood Arsenal)

The first experiments planned by the University of Michigan were:

a) Sampling of the upper atmosphere by means of bottles carried in the V-2. Designed to give information on the constituency of the upper atmosphere of importance in the evaluation of mixing vs. diffusion in the atmosphere.

b) Measurement of the ambient temperature of the upper atmosphere by aerodynamic measurements on the V-2.

The early major effort at the University went into preparing sampling bottles for V-2's, instrumenting V-2's for aerodynamic measurement of temperature and providing the circuits for the grenade and smoke experiments. Through the courtesy of other agencies, space for sampling bottles and a shadowgraph was made available on several V-2's other than those for which Michigan was the cognizant agency. When the Aerobee became available

the sampling experiment was designed for use with this rocket and several flights were made. Also, work was started on the application of the probe aerodynamic measurement of temperature to the Aerobee and the first flight will be made in December 1950. During the same period ESL adapted the grenade experiment to the Aerobee and made several successful flights.

Four V-2's and eight Aerobees were instrumented by the University of Michigan and fired. A total of 46 sampling bottles were flown on these rockets and on seven V-2's on which space was made available by other agencies. The V-2's were also equipped with apparatus for the aerodynamic measurement of ambient pressure and temperature. A shadowgraph was flown on Signal Corps V-2 42 for which Edgewood Arsenal was the chief instrumenting agency. Table 1 summarizes the firings for which Michigan was the chief instrumenting agency.

The major laboratory effort throughout the program has been applied to the preparation of flight instrumentation and experimentation subsidiary to the flight experiments. Three of the more important related developments have been the construction and operation of a selective adsorption gas analyzer, the investigation of shock wave curvature and the development of a flight magnetic recorder.

During the period February 1948 to February 1949 a related program of research on the generation of smoke at high altitudes was carried on under the supervision of Dr. C. M. Sliepcevich. The progress of the work was reported in the Progress Reports for the period (see Section 4) and in a Final Report dated February 1949.

4. REPORTS

The following Technical Reports were issued:

a) Mills, R. G., Calculations of Pressures on Cones Moving at Supersonic Velocities in the Upper Atmosphere, October 1946.

b) Neill, H. W., Physical Status of the Atmosphere, March 1947.

c) Leite, R. J. and Liu, V. C., Technical Report on Analysis of Pressure Measurements Recorded During the Flight of V-2 No. 25, April 1949.

d) Turner, E. B. and Liu, V. C., An Evaluation of Shadowgraph and Schlieren Optical Methods for Determining Temperatures in the Upper Atmosphere, July 1949.

e) Bartman, F. L., Liu, V. C. and Schaefer, E. J., An Aerodynamic Method of Measuring the Ambient Temperature of Air at High Altitudes, July 1950.

TABLE 1

Summary of Rocket Firings by the University of Michigan

Rocket No.	Date	Time MST	Peak Altitude MSL Feet		Kilometers	Major Objectives or Apparatus
V-2 25	4-2-48	0640	475,600		145.0	Ambient temperature and pressure by measuring pressure at "neutral point" and by measuring pressures on a cone. Air sampling. Ambient temperature and winds by grenades (SCEL). Solar spectrograph (NRL). Cosmic ray telescope (NRL). Classified experiment (AMC).
V-2 33	9-2-48	1800	543,100		165.5	Ambient temperature and pressure by measuring pressures on a cone. Ambient temperature by probing shock wave. Air sampling. Ambient temperature and winds by grenades (SCEL).
Aerobee SC-1	12-9-48	1538	304,200		92.7	Air sampling.
V-2 50	4-11-49	1505	286,200		87.2	Ambient temperature and pressure by measuring pressures on a cone. Ambient temperature by probing shock wave. Air sampling.
Aerobee SC-2	6-2-49	0610	271,300	*	82.7	Air sampling.
Aerobee SC-4	7-21-49	0901	250,000	*	76.2	Air sampling.
Aerobee SC-5	9-20-49	1002	196,000	*	59.7	Air sampling.

TABLE 1 (continued)

Rocket No.	Date	Time MST	Peak Altitude MSL Feet	Kilometers	Major Objectives or Apparatus
V-2 56	11-18-49	0903	405,700	123.7	Ambient temperature by probing shock wave. Air sampling. Ambient temperature and winds by grenades (SCEL). Classified experiment (AEC).
Aerobee SC-3	12-6-49	1132	212,600	64.8	Air sampling.
Aerobee SC-7	12-6-49	1716	198,100	60.4	Air sampling.
Aerobee SC-9	2-21-50	1754	165,000	50.3	Air sampling.
Aerobee SC_11	4-25-50	1812	328,000	* 100.0	Air sampling.

Occasional small experiments and devices such as exposing seeds to radiation (Harvard), x-ray densitometer plates (NRL) and thermal luminescence detectors (NRL) have been carried. These are not noted in the table. Devices for measuring missile performance such as heliographs, beacons and dopplers or for gathering data such as telemeters and recorders are not listed but are mentioned when necessary in the discussions of experiments in the report.

* Not tracked to peak. Peak altitude based on assumed vacuum trajectory.

The following Quarterly Progress Reports were issued:

Progress Report No.	Quarterly Report No.	Period
3	2	10-1-46 to 1-15-47
4	3	1-15-47 to 4-15-47
5	4	4-15-47 to 7-15-47
6	5	7-15-47 to 10-15-47
4		10-15-47 to 1-15-48
5		1-15-48 to 4-15-48
6		4-15-48 to 7-15-48
10	7	7-15-48 to 10-15-48
11	8	10-15-48 to 1-15-49
12	9	1-15-49 to 4-15-49
13		4-15-49 to 5-14-49
14		5-15-49 to 6-14-49
15	10	6-15-49 to 9-14-49
16	Interim	9-15-49 to 11-14-49
17	11	11-14-49 to 2-13-50
18	12	2-14-50 to 5-13-50
19	13	5-14-50 to 8-31-50

A series of one page letter-type progress reports was also issued monthly during the course of the work.

5. COMPOSITION

The primary objective of the air sampling experiment has been to ascertain the amount of diffusive separation of gases in the atmosphere at altitudes between 30 and 80 km. In addition some work was done in attempting to detect oxides of nitrogen in upper air samples.

5.1 Sampling

It was determined that air samples of sufficient amount for known methods of analysis could be obtained at ambient pressures up to 80 km altitude in bottles of suitable size for rocket use. Therefore, no technique for increasing the air capture by cooling was developed. The bottles used were 500 cu. in. steel oxygen breathing bottles.

5.11 Preparation of Sampling Bottles

The bottles were found to be quite suited for the purpose of air sampling. The original welds were found to be vacuum tight and did not open upon impact after the rocket flight. For the V-2 flights the bottles had additional protection from opening upon impact by a specially designed steel jacket. See Fig. 1. The sampling bottles were prepared for evacuation by soldering the sealer and opener components directly to the bottle wall. The bottles were washed in water and alcohol or acetone and dried. The bottles were then evacuated on the preflight pumping system shown in Fig. 2. They were pumped for 24-48 hours while being held at a temperature of about 150°C.

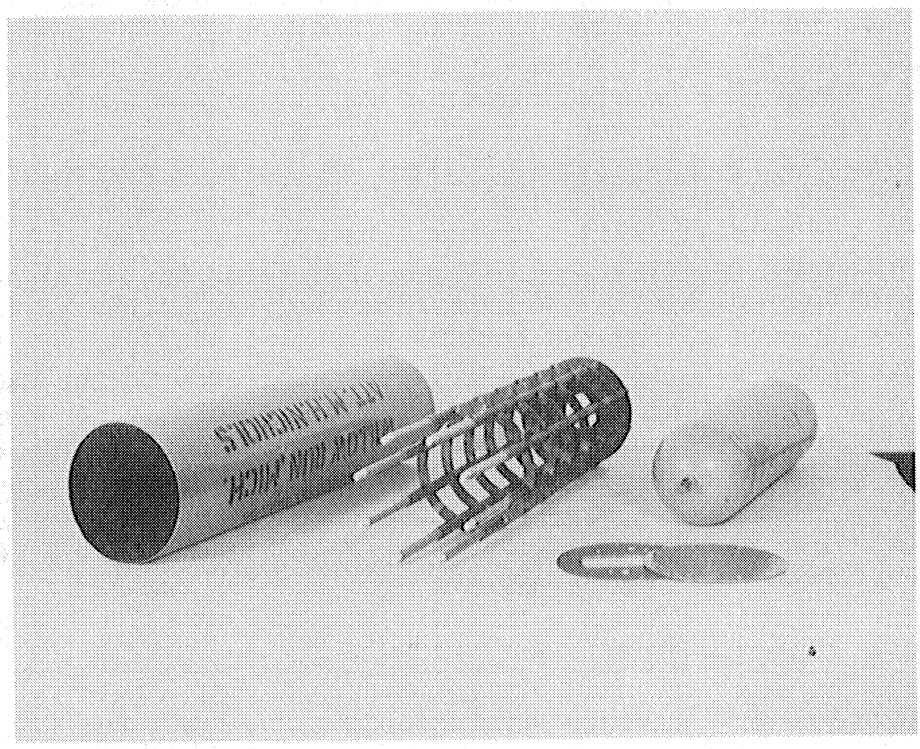

Fig. 1. Sampling Bottle and Shield Assembly (V-2 only)

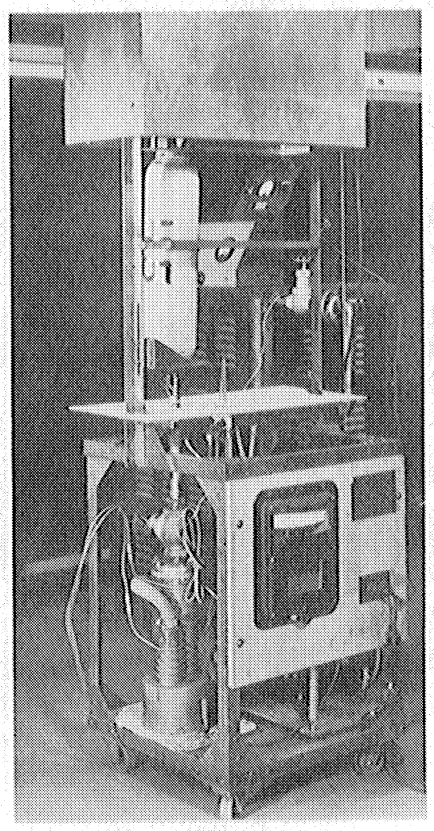

Fig. 2. Vacuum System for Evacuating Sampling Bottle

This was the highest temperature that could be maintained for any protracted period of time due to the presence of soft solders in the construction of the sampling bottle. While on the pumping system the bottles were tested for leaks by means of a General Electric helium leak detector. The bottles that showed leaks were removed and the faults corrected. The bottles were finally sealed off from the pumping system by means of a modified C-clamp which was used to pinch the 1/4 inch copper tube through which the air was removed from the bottle. This 1/4 inch tube had been previously tinned with a thin coat of soft solder so the bottle was sealed vacuum-tight by application of pressure and heat to the modified C-clamp. After seal-off from the preflight pumping system the bottles were monitored for possible leaks by means of a small hot-wire Pirani gage soft-soldered in the neck of the sampling bottle. Sampling bottles were checked carefully for possible leaks in this way before installation on the rockets themselves. The characteristic of the hot-wire gage is shown by Fig. 3. Although the gages are not suitable for measurement of pressures less than one or two microns mercury, they are sufficiently sensitive to detect small leaks within a few days after seal-off from the pumping system.

5.12 Sampling Bottle Openers

Five types of openers were developed. These were:

a) Frangible glass seal-off tube. Never used on account of fragility. (Fig. 4).

b) Spring-operated knife and copper "roof-top". Discontinued because of uncertainty in trigger action. (Fig. 5).

c) Pyrotechnic-operated knife and copper "roof-top". Used successfully on many bottles. (Fig. 6).

d) Pyrotechnic-soldered disc. Discontinued because of complexity. Used on Aerobee SC-11. (Fig. 8, 9, 10).

e) Motor-operated knife. Most promising because it leaves an unrestricted opening. To be used on Aerobees SC-13 and SC-17. (Fig. 7).

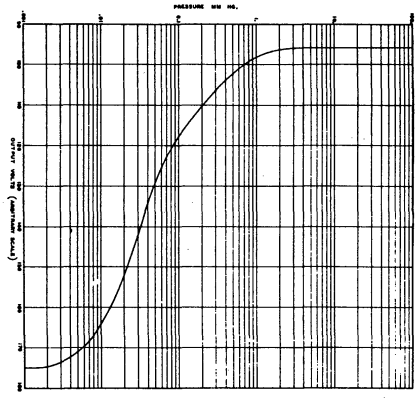

Fig. 3. Characteristic of Hot Wire Gages Installed in the Sampling Bottles

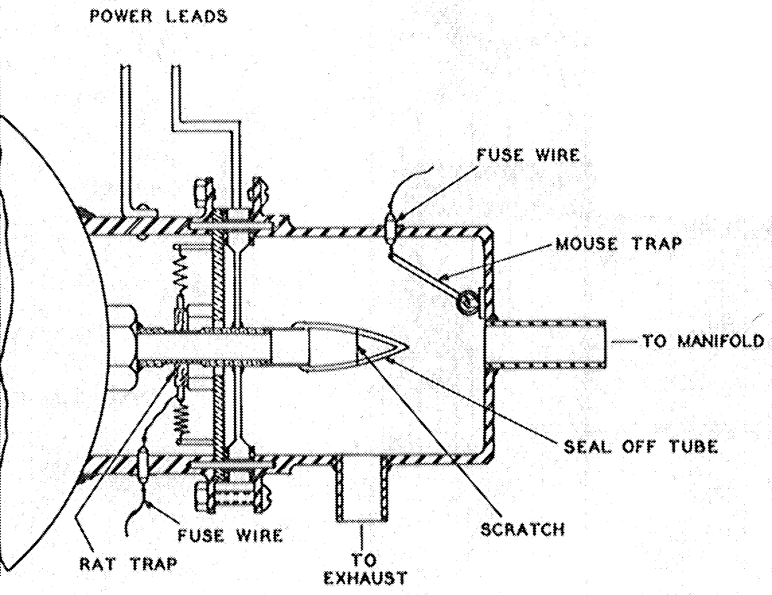

Fig. 4. Glass Seal-Off Tube

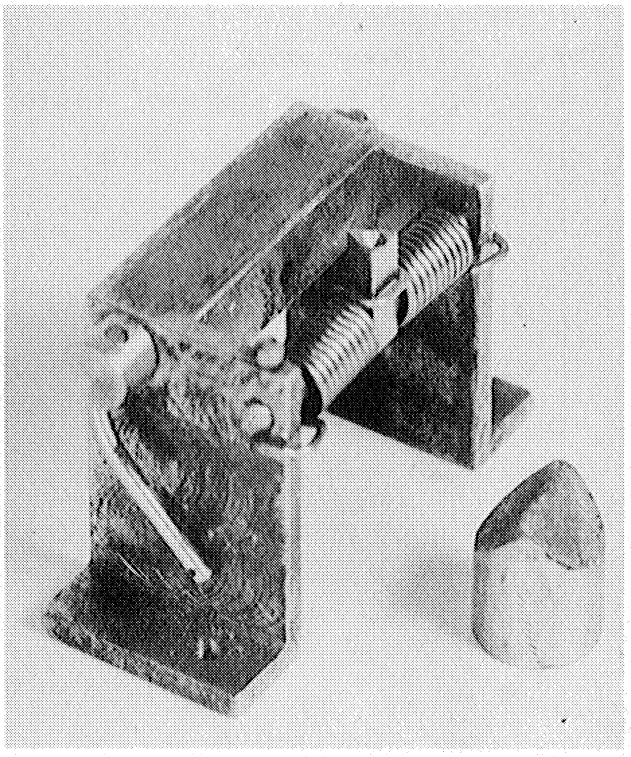

Fig. 5. Spring-Operated Knife

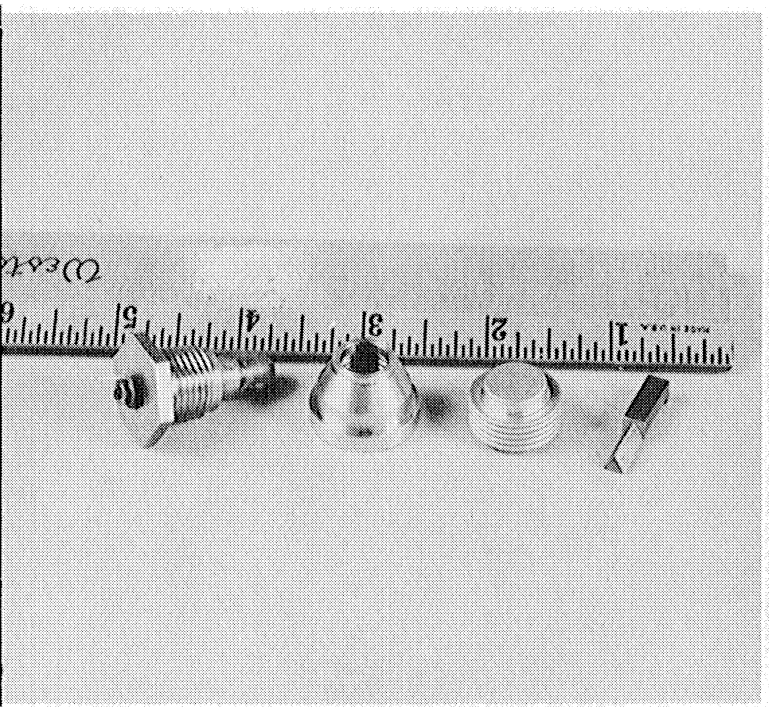

Fig. 6. Pyrotechnic-Operated Knife

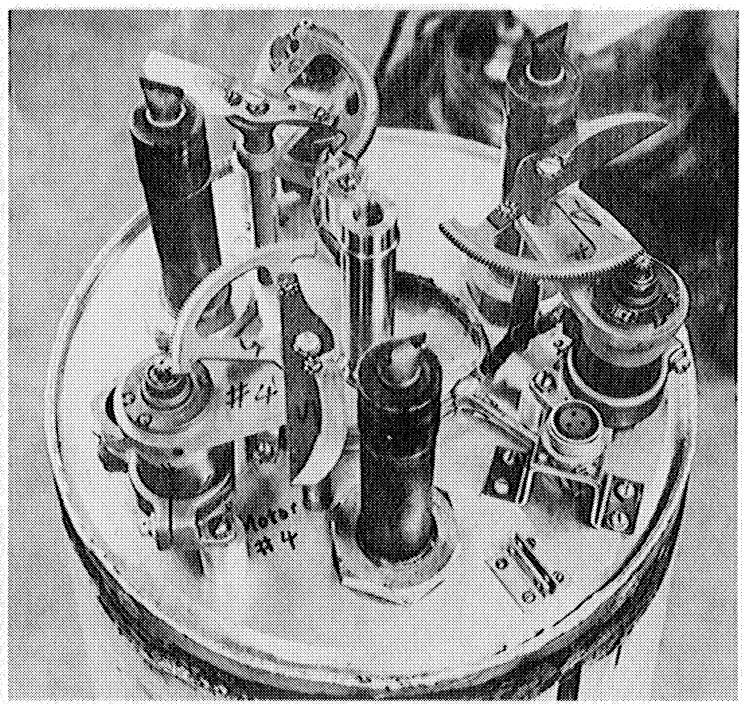

Fig. 7. Motor-Operated Knife

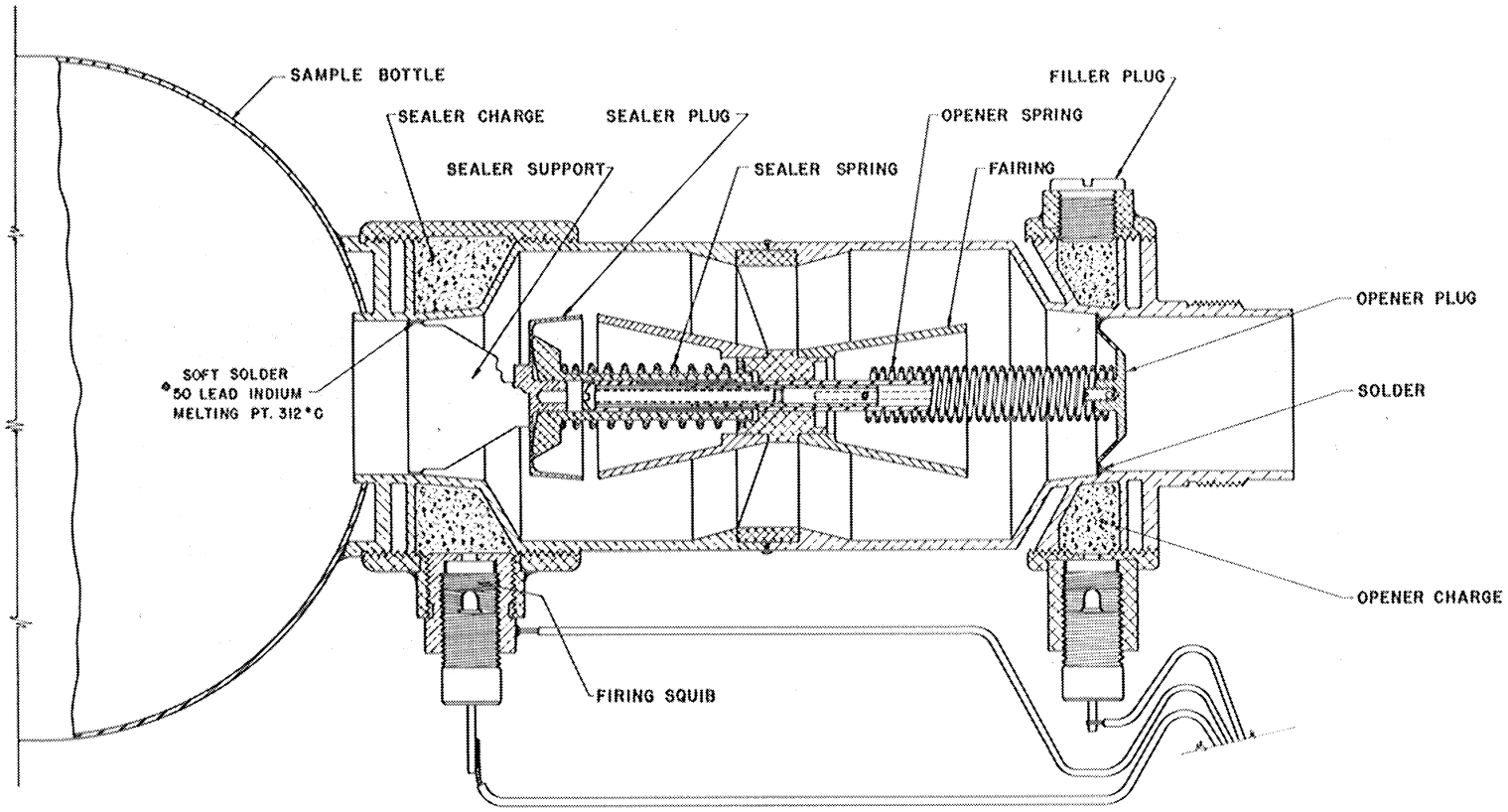

Fig. 8. Schematic of Pyrotechnic-Soldered Disc Sealer-Opener

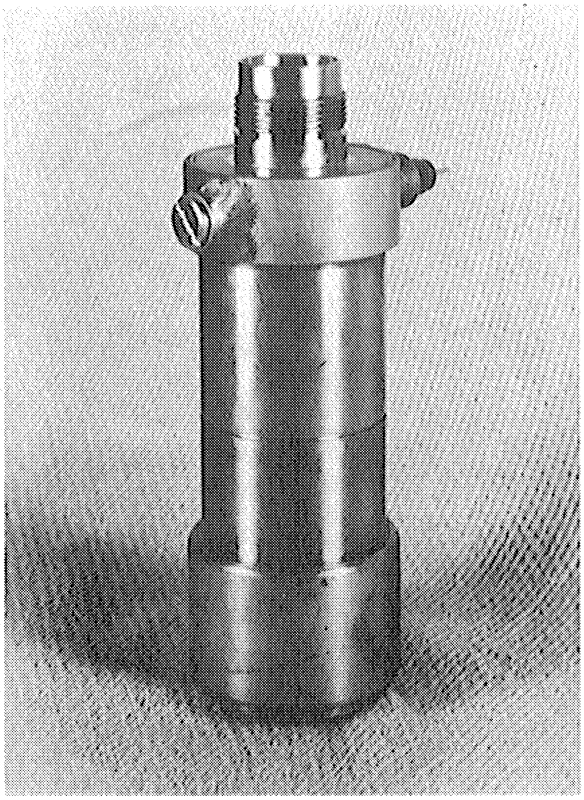

Fig. 9.
Pyrotechnic-Soldered Disc Sealer-Opener

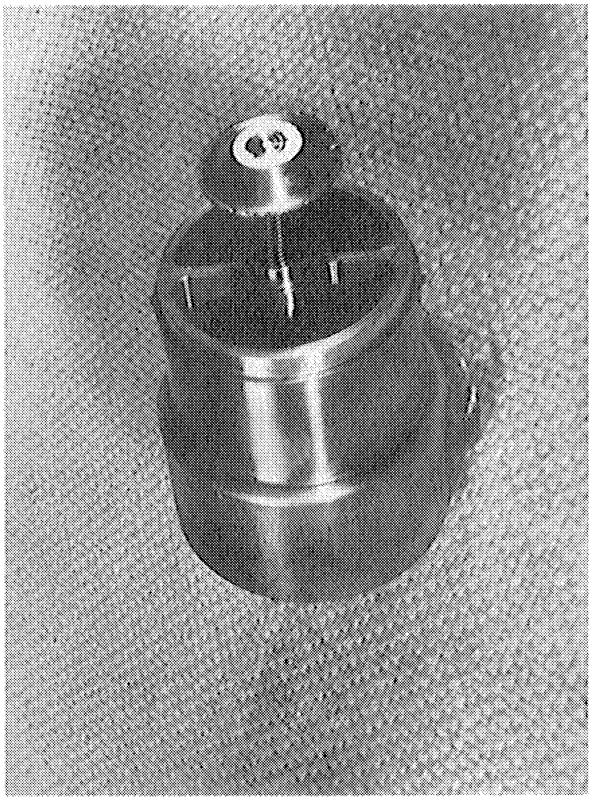

Fig. 10.
Detail of Opener Plug and Spring

5.13 Sampling Bottle Sealers

Five types of sealers were developed, of which two were flown and one is to be flown. These were:

a) Cone-soldered type. Discontinued because of power requirement and complexity. Never flown. (Fig. 11, 12).

b) Spring-operated jaws with electric soldering. Discontinued because of large amount of power required. Mounted on V-2 25 but never flown due to rocket failure. (Fig. 13).

c) Pyrotechnic hammer and anvil and pyrotechnic soldering. Used on all successful samplings to this date. (Fig. 14 and 15). Designed by Picatinny Arsenal.

d) Pyrotechnic-soldered disc. Discontinued because of complexity and generated gas. Used on Aerobee SC-11. (Fig. 8, 9, and 10).

e) Pyrotechnic-operated jaws for cold-weld of copper tube. Most promising from a standpoint of gas sorption by bottle seal-off. To be used on Aerobees SC-13 and SC-17. (Fig. 17 and 18).

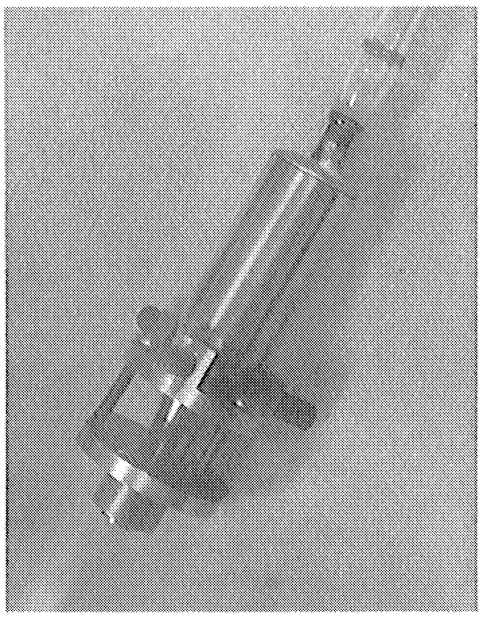

Fig. 11.
Cone-Soldered Sealer

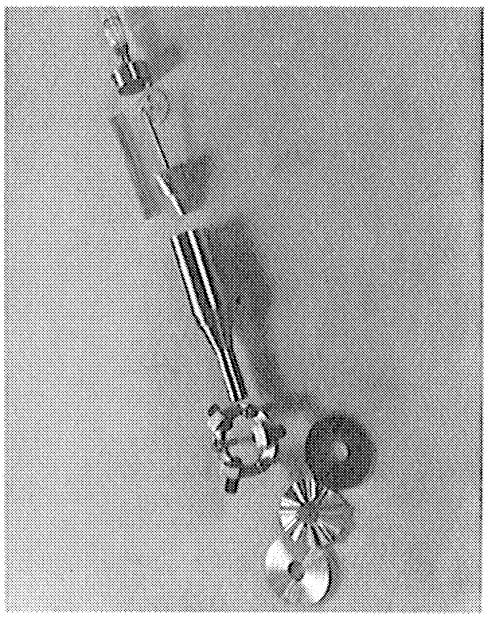

Fig. 12.
Cone-Soldered Sealer, Exploded View

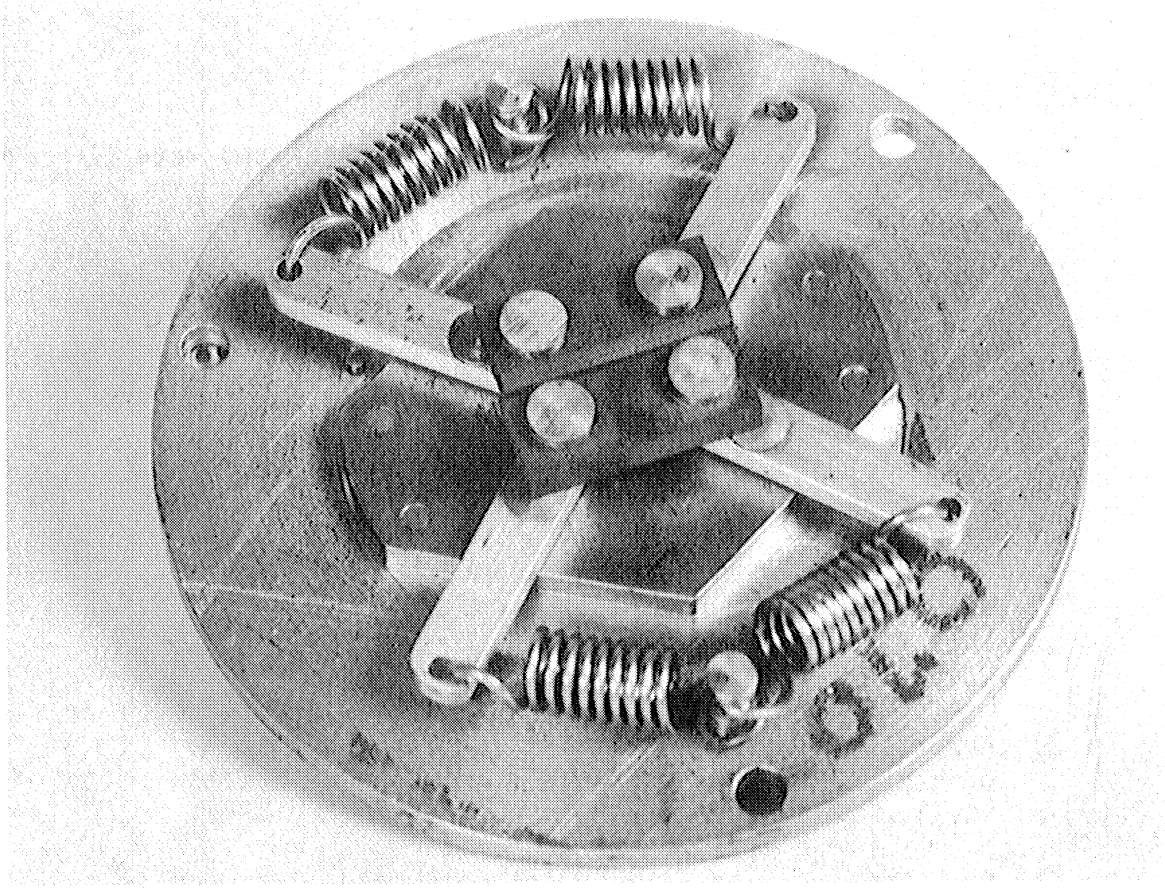

Fig. 13. Spring-Operated Sealer

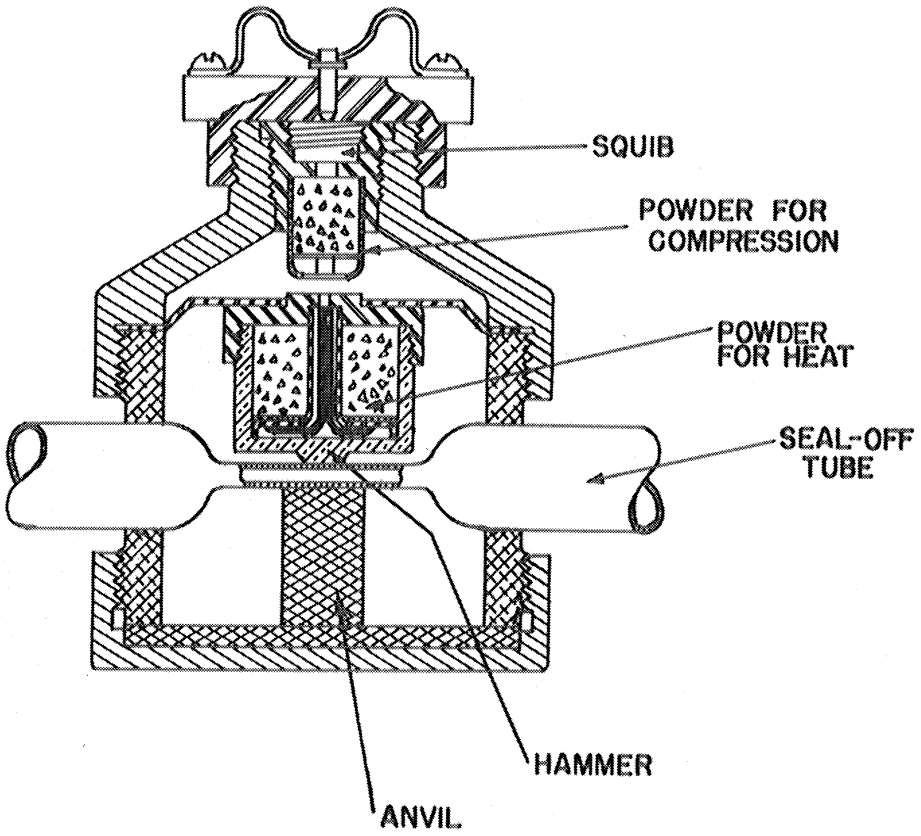

Fig. 14. Schematic of Pyrotechnic-Operated Hammer-Anvil Sealer

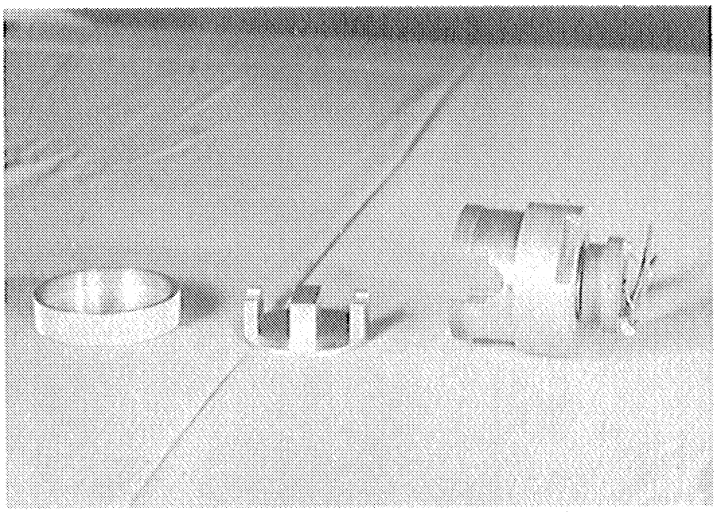

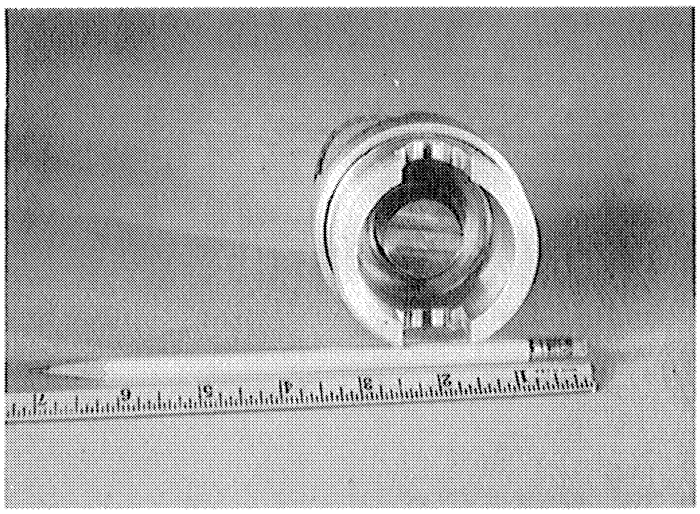

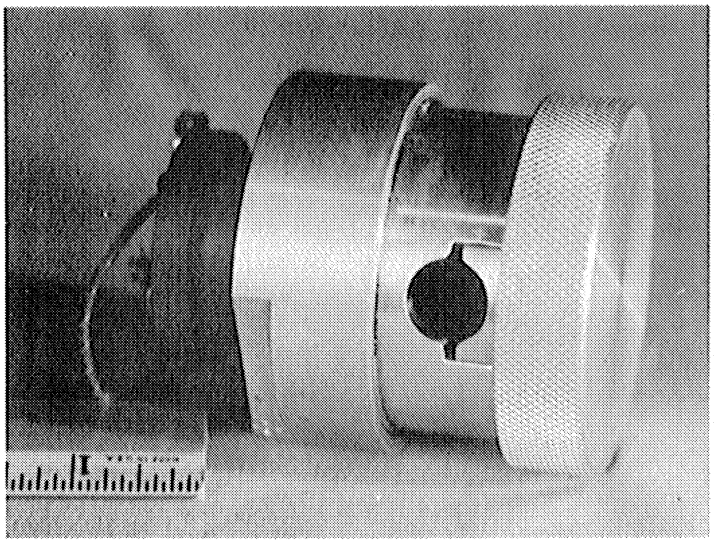

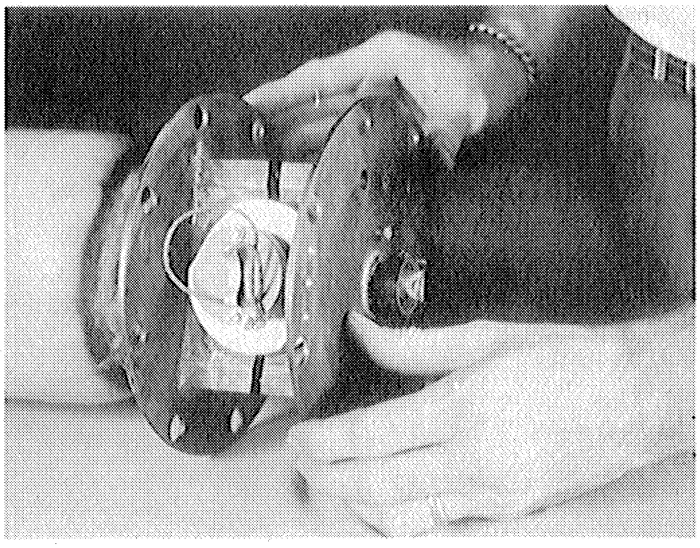

Fig. 15. Construction and Installation Details of Pyrotechnic-Operated Hammer-Anvil Sealer

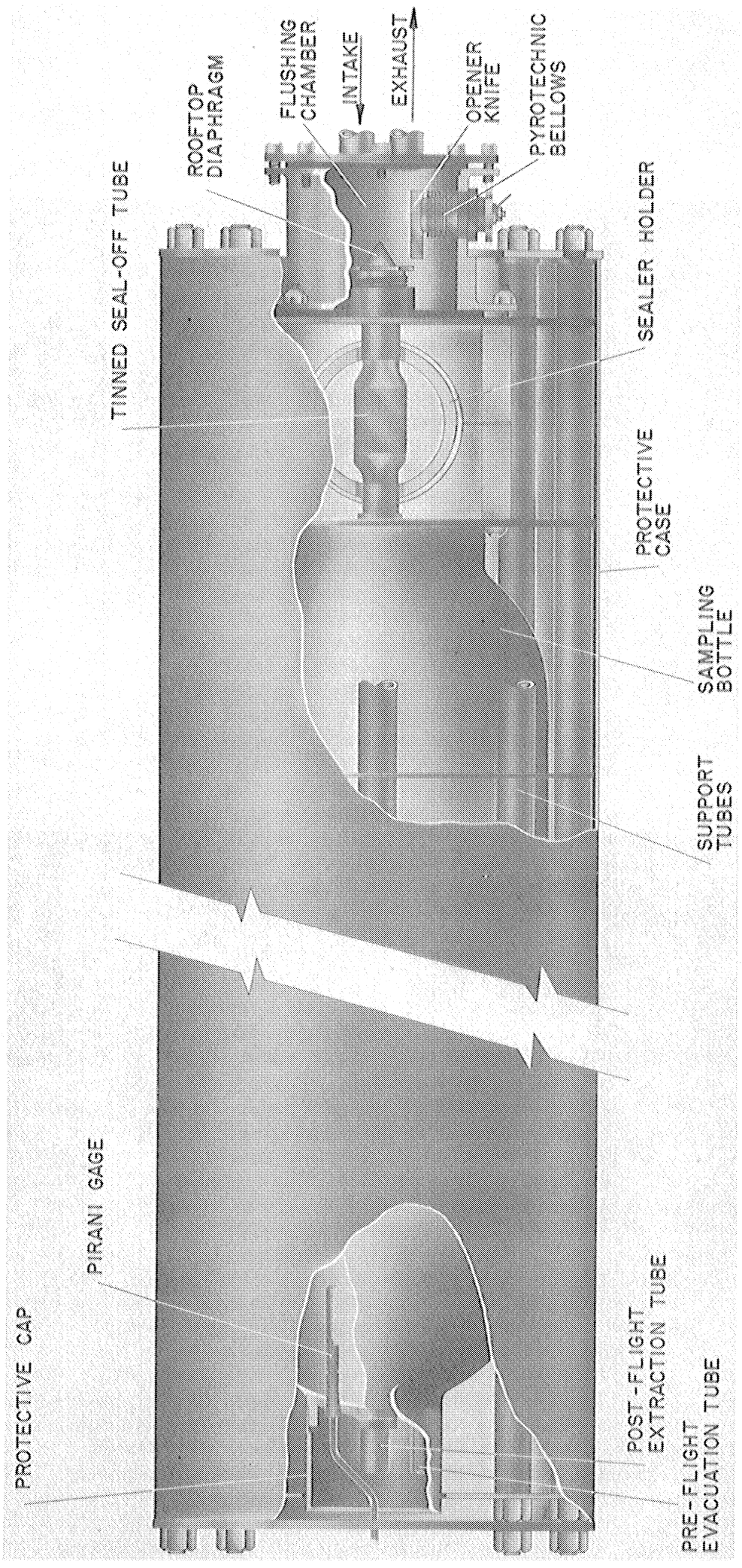

Fig. 16. Opener-Sealer Manifold Typical of V-2's and Aerobees

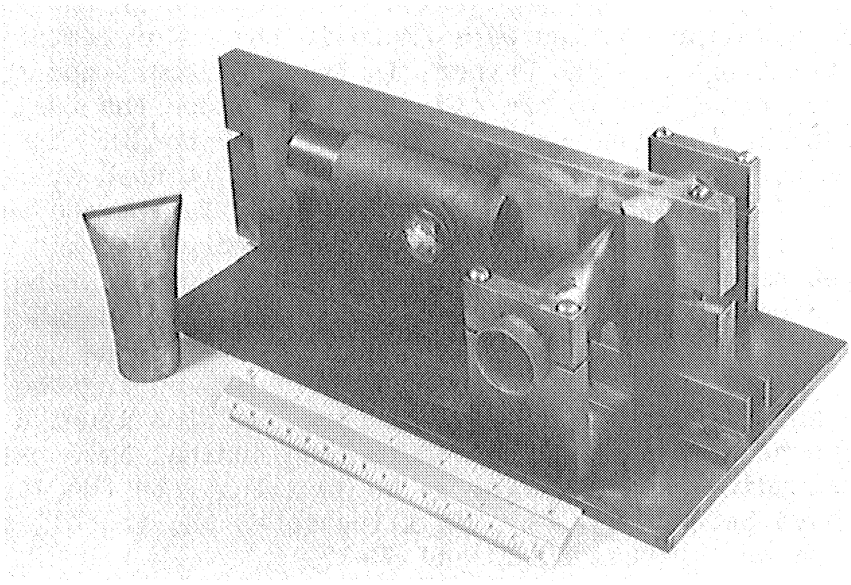

Fig. 17. Laboratory Model of
Pyrotechnic-Operated Cold-Weld Sealer

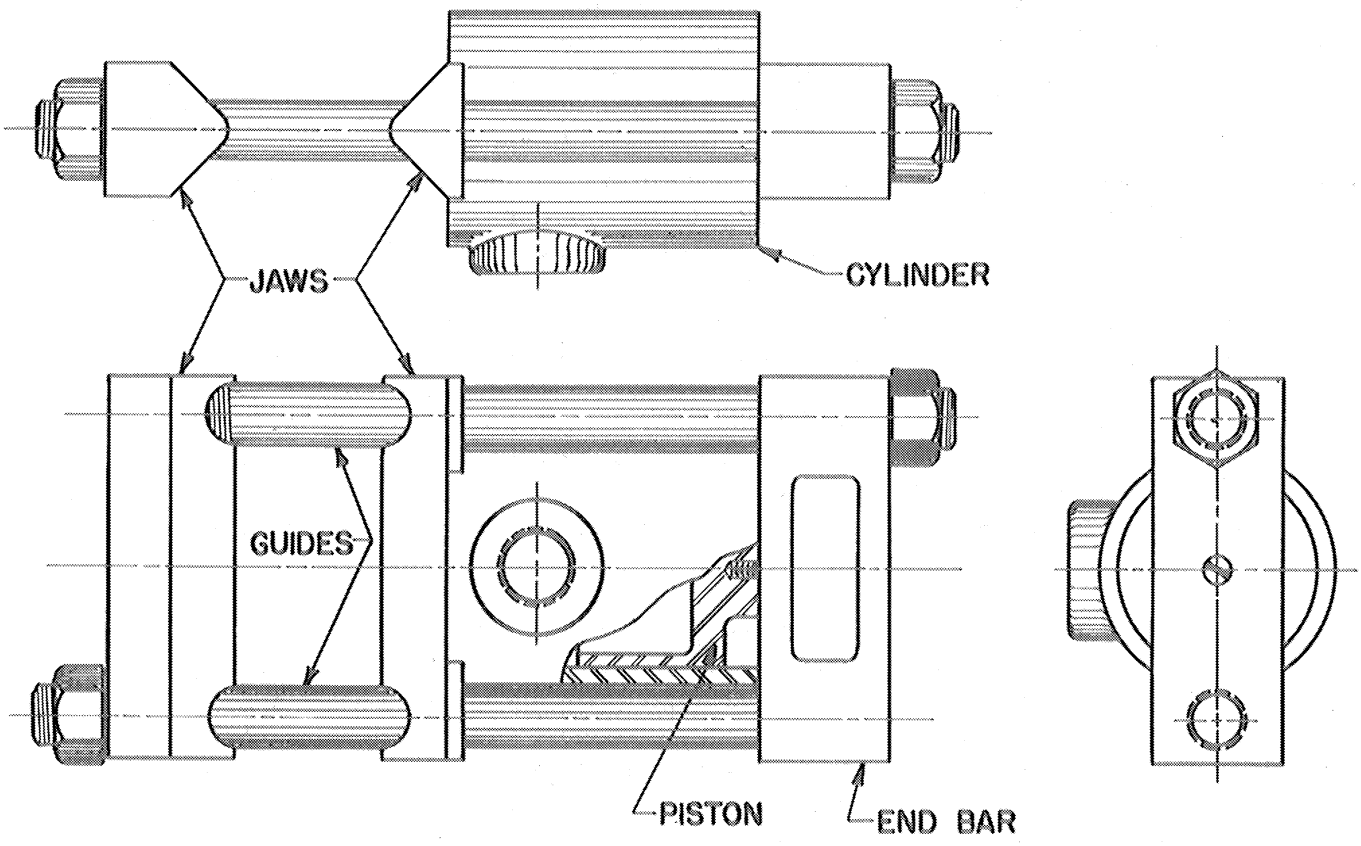

Fig. 18. Schematic of Cold-Weld Sealer

5.14 Sampling Bottle Installations and Air Scoop Arrangements

Several mounting configurations were used in the various flights. On V-2's the sampling bottles were flown in the motor compartment between the lower fuel tanks and the burner, in the instrument compartment just below the nose cone, and in the mid-section between the fuel tanks. The types of installation used are shown in Figs. 19 to 22. The mid-section installation was the one most widely used since it used space not adaptable to other experiments, was the easiest for installation and resulted in the least damage to the sampling bottles. Its big disadvantage was the requirement that the sampling bottles be available for installation a few months before the actual rocket flight since this installation had to be completed before the fuel tank assembly. This meant that sampling bottles could not be replaced in case of leak development or damage during the rocket assembly. All Aerobee installations consisted of three bottles mounted in about the center of the nose cone with the bottle longitudinal axes parallel to the missile longitudinal axis. Figs. 23 to 30 illustrate the Aerobee installations that have been used. Fig. 31 illustrates the installations contemplated for use on Aerobees SC-13 and SC-17.

In the first V-2 firings the air intake and exhaust scoops lay close to the skin so that relatively little increase in pressure over ambient pressure was realized. Fig. 20 shows these scoops. In addition it was soon realized that there was a definite possibility of the samples containing a certain amount of contamination from air carried along with the rocket. This point will be discussed shortly. On later flights, intake scoops projecting beyond the boundary layer into the free stream were used. Fig. 19 shows the newer type intake scoop. Still later, an attempt was made to increase capture efficiency of the sampling procedure by design and use of supersonic nozzles and diffusers. Fig. 22 shows how V-2 50 was fitted with one of these special designs and one of the earlier extended scoops for comparison purposes. Unfortunately, both bottles were badly crushed and burned on impact so that the samples were lost and no check on the increased efficiency of the supersonic scoops was made. V-2 56 was fitted with two sets of the supersonic scoops, but no samples were obtained. The supersonic scoops were also used on Aerobees SC-3 and SC-7. Close-in scoops were used on the remaining Aerobees with the exception of SC-11 where the air was admitted through 1" diameter straight tubing that ran to the tip of the rocket, except for the final spring-ejected tip. On Aerobees SC-13 and SC-17, yet to be fired, the intake system consists of 1" diameter tube, 11" long, with no curves or restrictions of any kind. The forward end of the tubes is the most forward part of the rocket at the time of sampling so that the ram pressure beyond a normal shock wave may be expected in the tubes.

As a result of an invitation by the Army Air Forces, three completely non-magnetic sampling bottles were prepared for inclusion in the Blossom II-A canister of V-2 39. The bottles were fabricated from brass and each had a capacity of 250 cubic inches. The Picatinny Arsenal furnished pyrotechnic hammer-anvil sealers of non-magnetic material. A photograph of the bottles installed in the canister is shown in Fig. 33. It was planned to take the samples before the canister was ejected from the rocket and

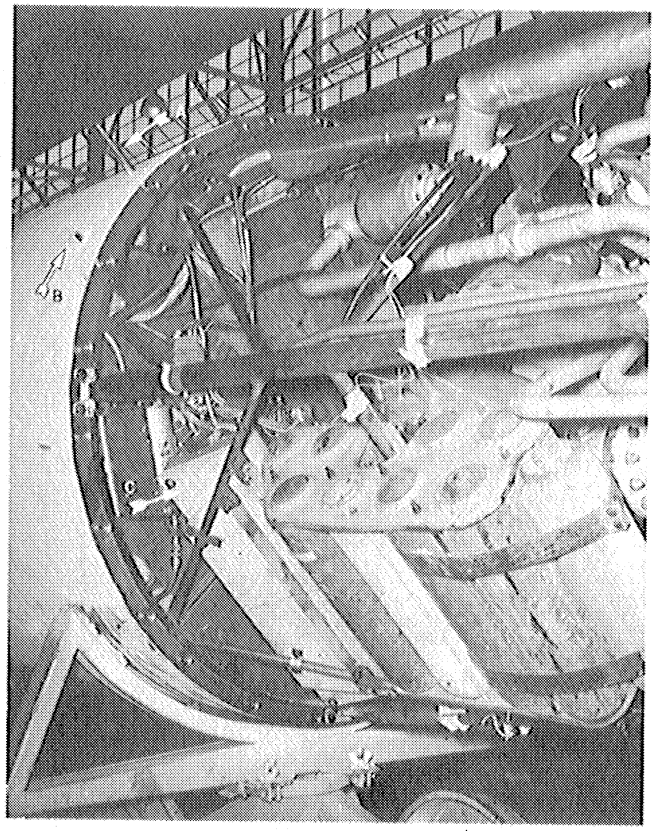

Fig. 19. Sampling Bottle Installation in Motor Section of V-2
A - Modified Intake Scoop
B - Close-in Exit Scoop
C - Sampling Bottle

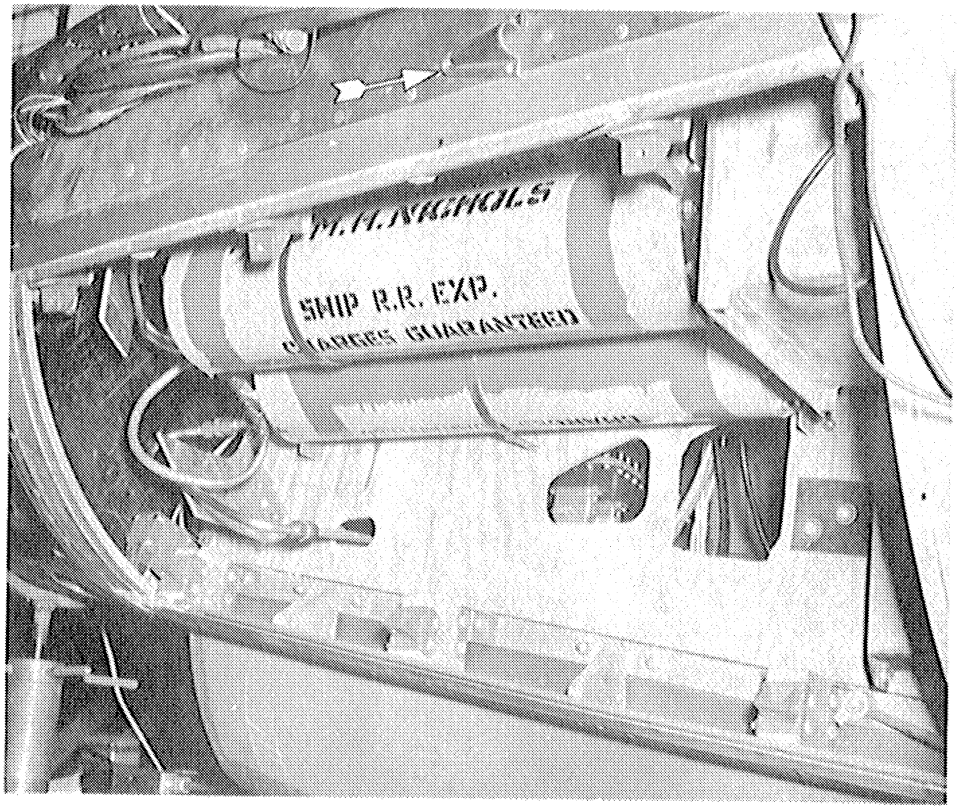

Fig. 20. Sampling Bottle Installation in Instrument Compartment of V-2
Only the close-in exit scoop is shown.

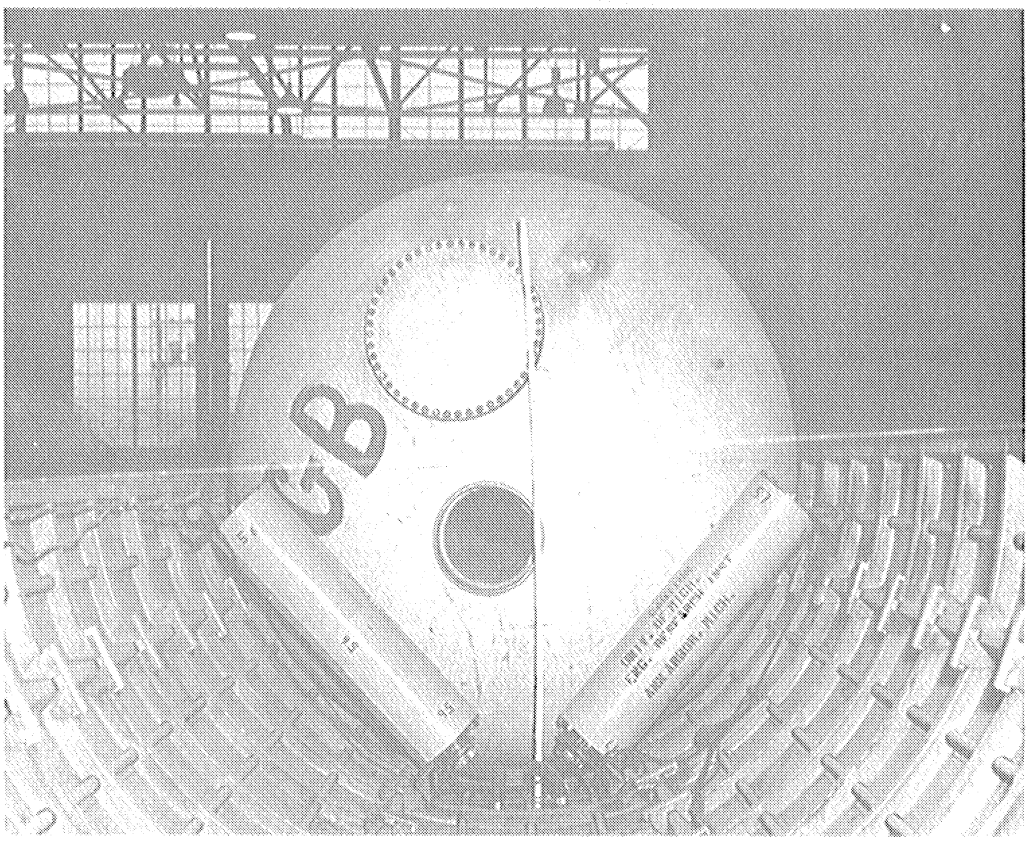

Fig. 21. View of Mid-Section Installation of Sampling Bottles Between V-2 Fuel Tanks During Course of Assembly.

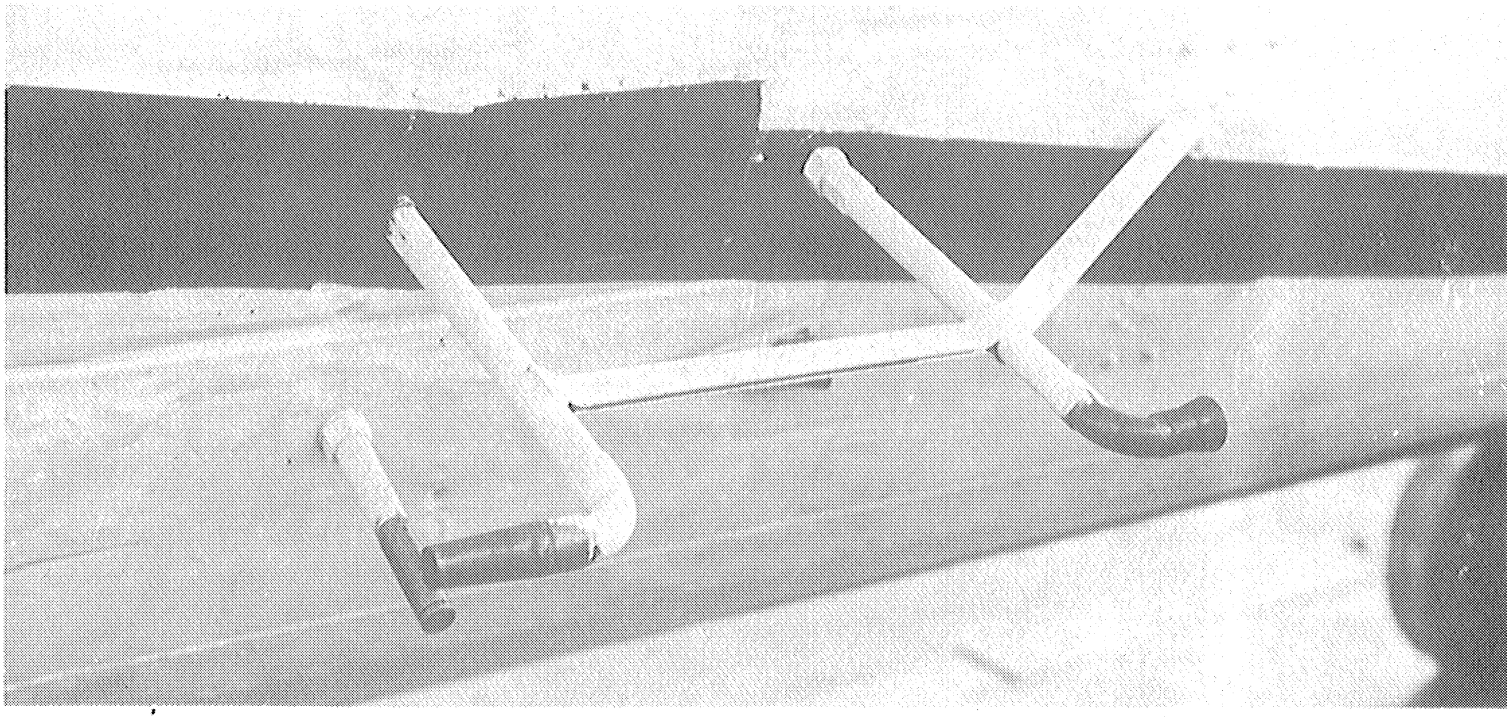

Fig. 22. Exterior View of Mid-Section Installation on V-2 This shows both old-type extended scoop and newer supersonic nozzle and diffuser.

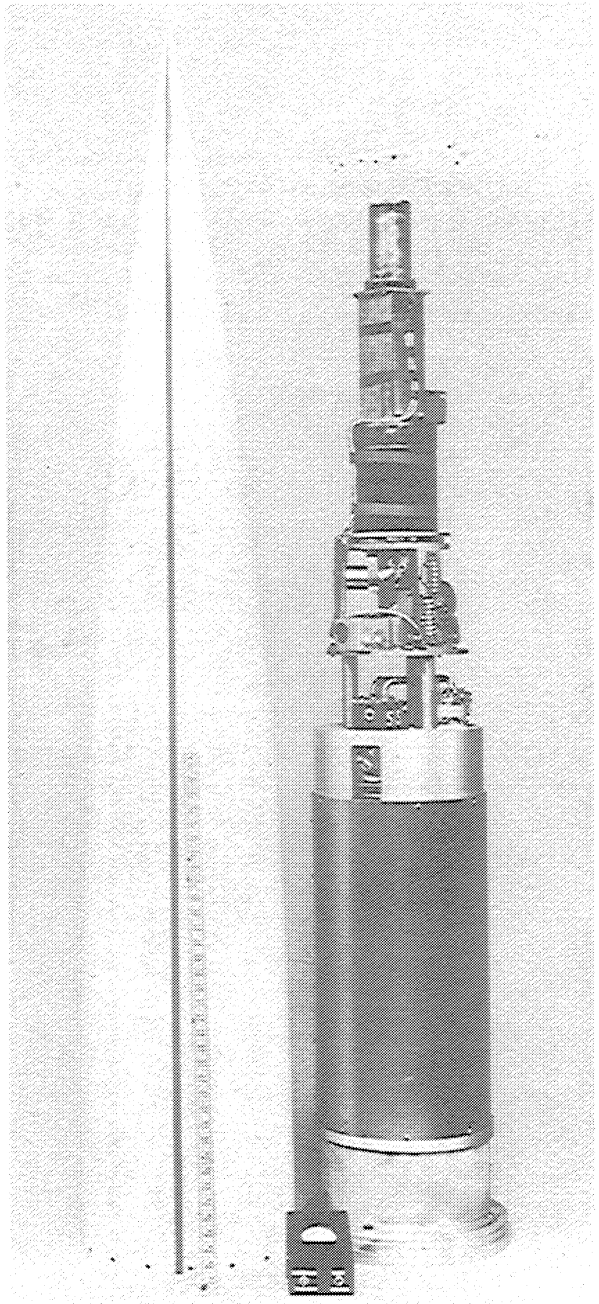

Fig. 23. Aerobee SC-1
This shows the arrangement of instrumentation and the nose cone. The scoops are not shown.

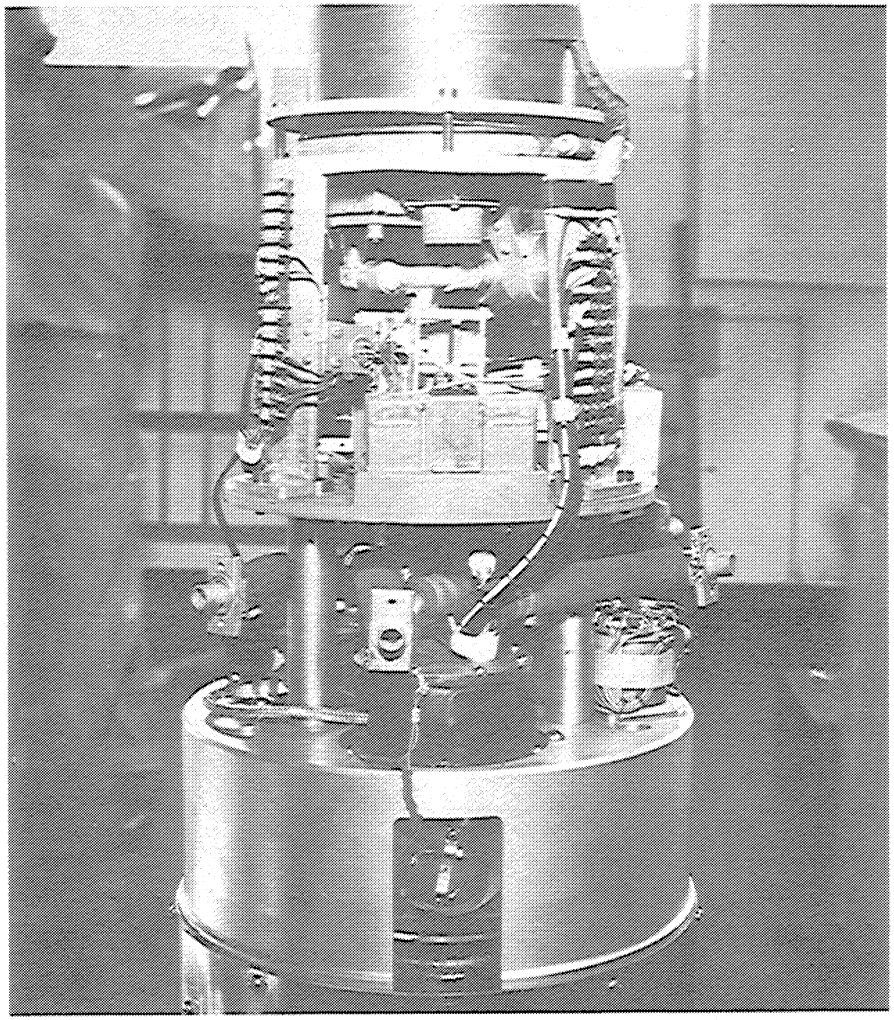

Fig. 24.
Close-Up View of SC-1 Showing Beacon, Timer, and Upper Part of Sampling Bottles.

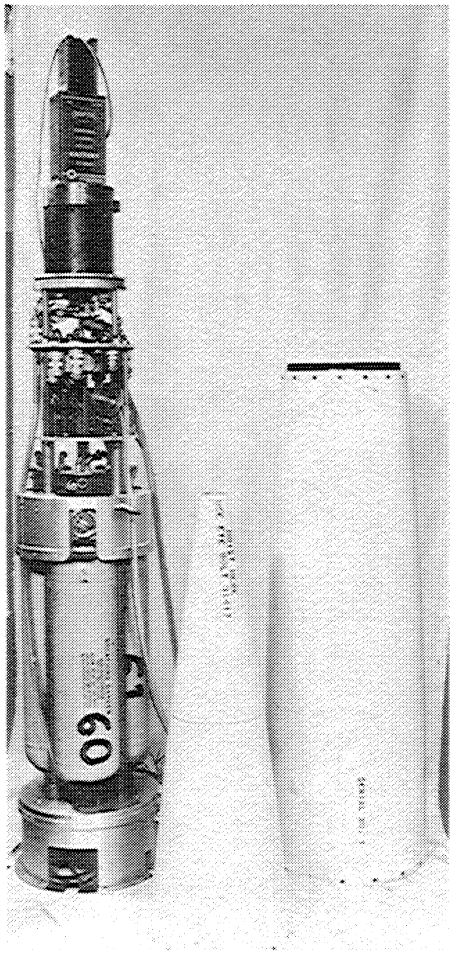

Fig. 25.
Sampling Bottle Arrangement with Split Nose Cone
Scoops are not shown.

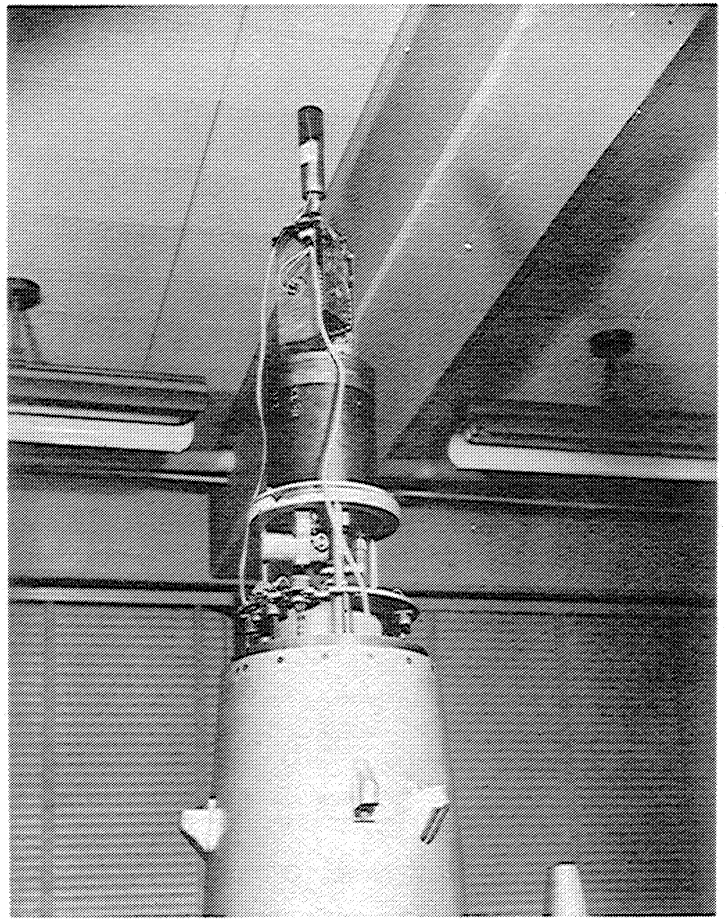

Fig. 26.
Lower Part of Split Nose Cone with Upper Assembly
The small scoops were used on this installation.
The CO_2 cylinder is at the top of the assembly.

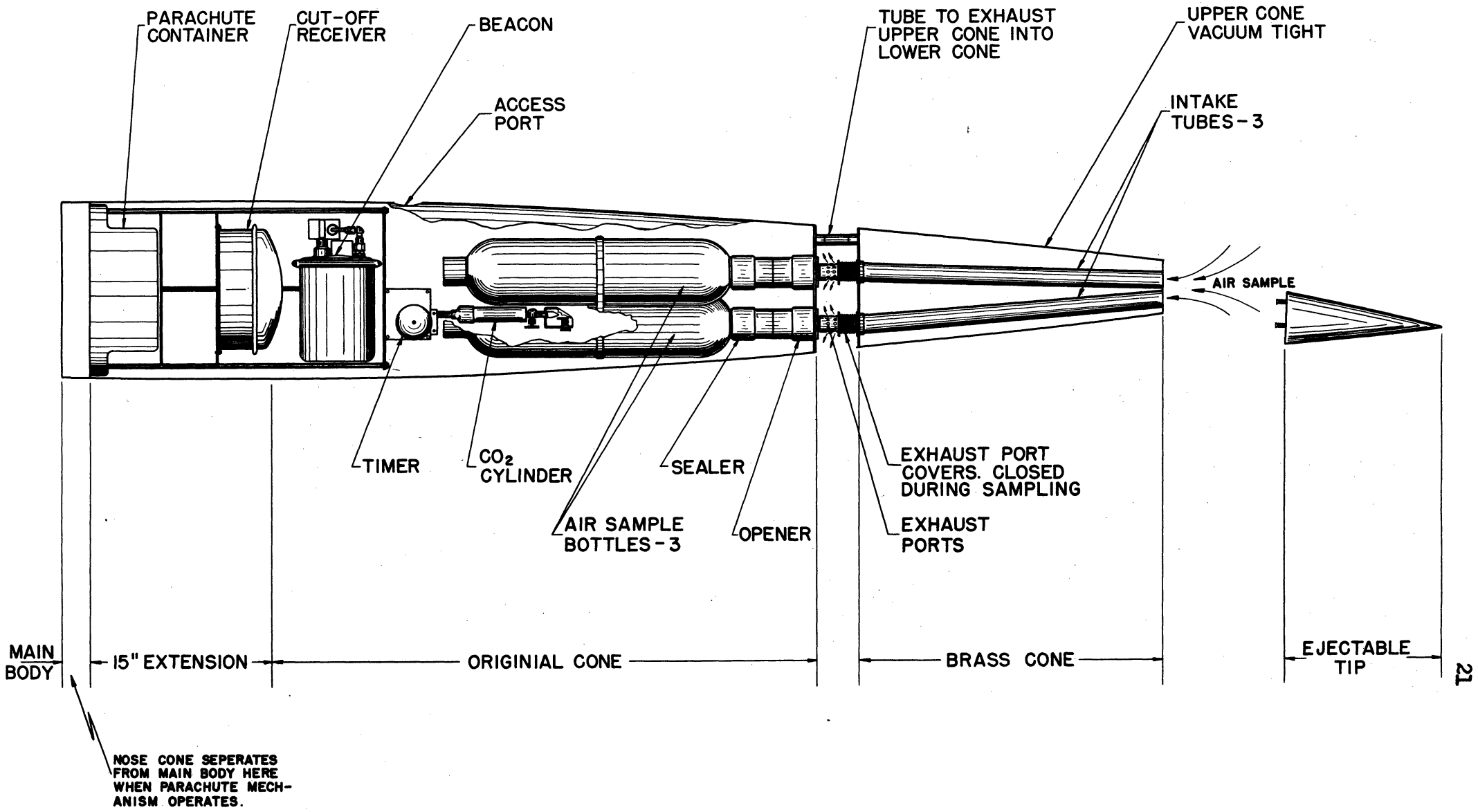

Fig. 27. Schematic of Sampling Bottle Installation Used on SC-11

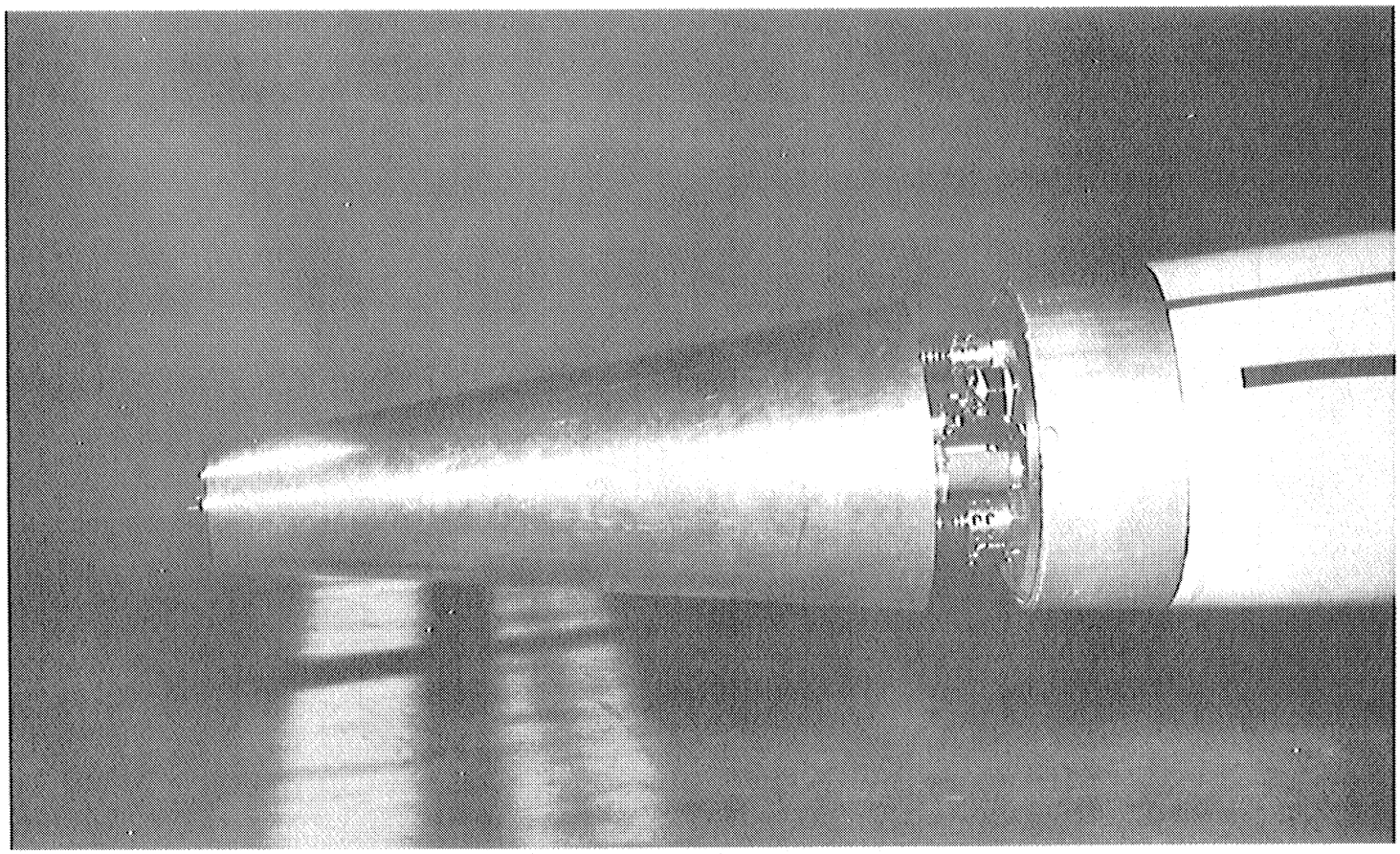

Fig. 28. Nose Cone of SC-11.
Spring-ejected tip is not shown.

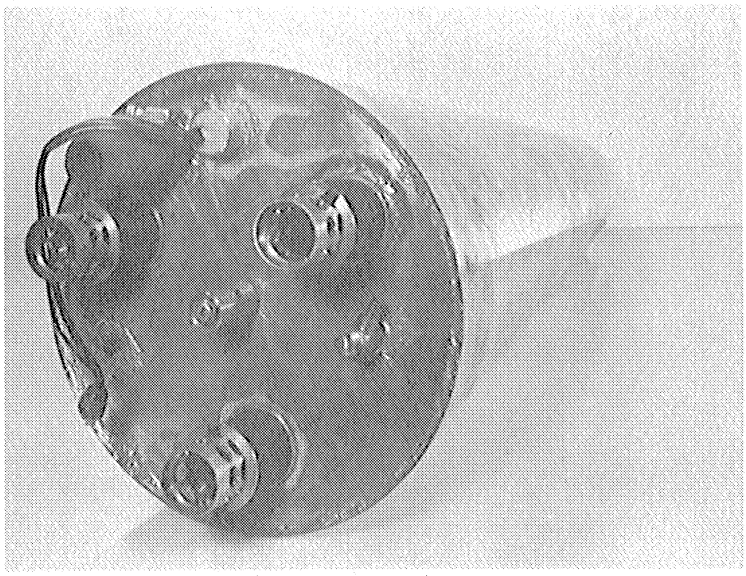

Fig. 29.
Brass Nose Cone of SC-11

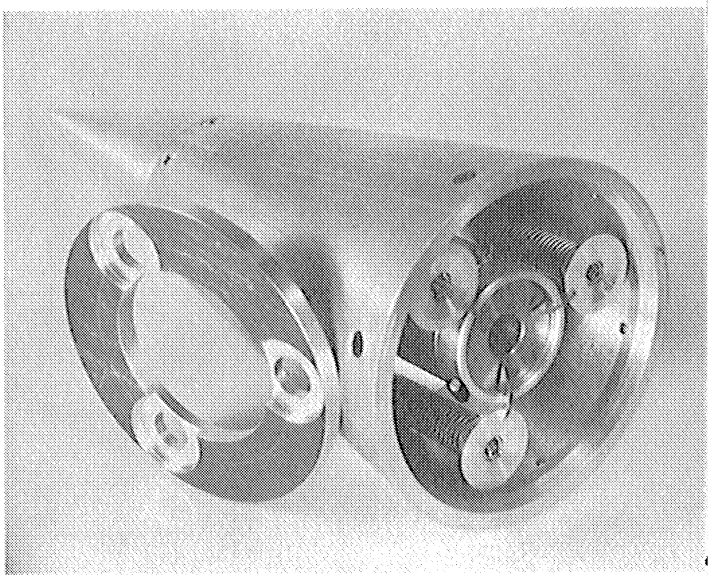

Fig. 30.
Spring-Ejected Nose Cone Tip

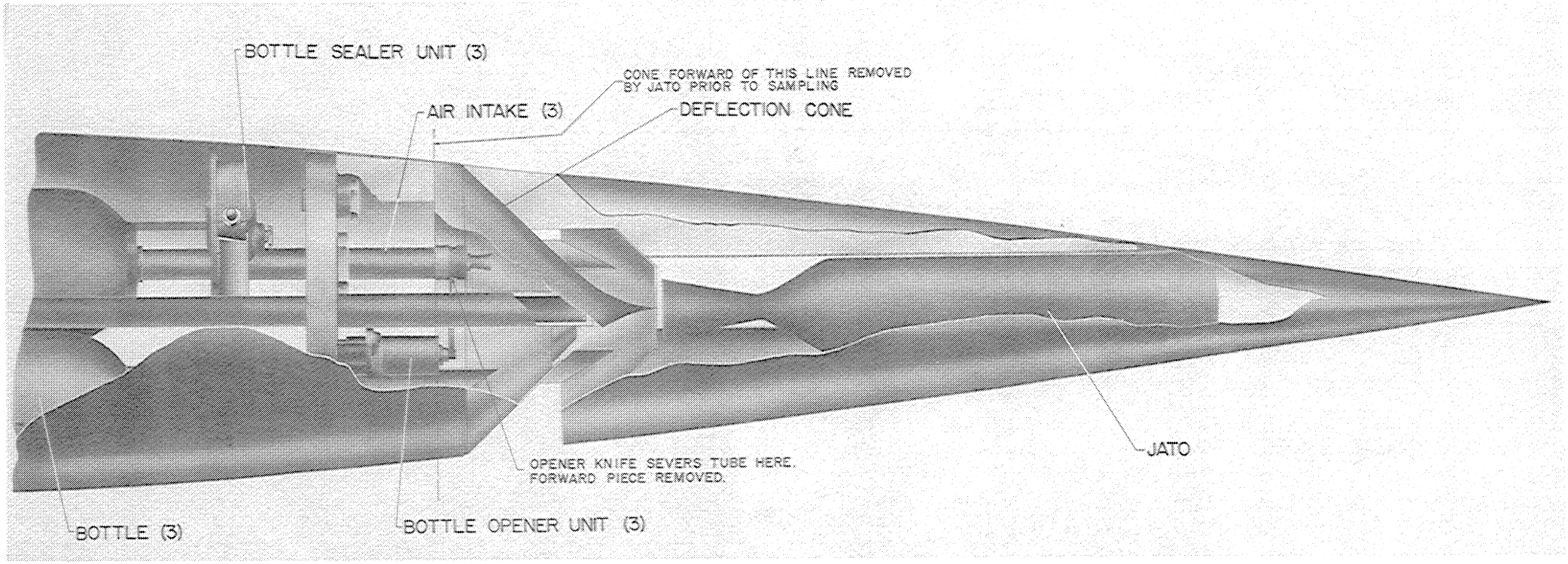

Fig. 31. Sampling Bottle Installation to be used on SC-13 and SC-17

Fig. 32. Recovery of SC-3
This shows the minimum damage obtained with parachute recovery. The supersonic scoop and diffuser shown were also used for SC-7.

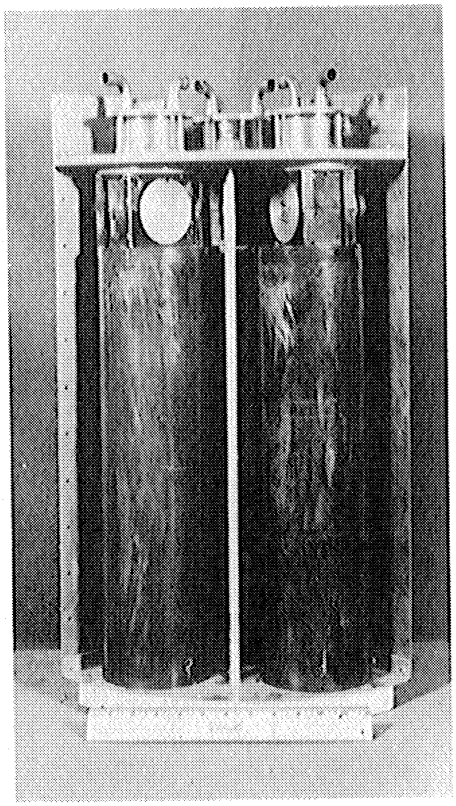

Fig. 33. Non-Magnetic Sampling Bottle
Installation in Canister of Blossom II-A

lowered by means of a parachute. Unfortunately, no samples were obtained due to an extremely poor rocket flight. However, the parachute on the Blossom II-A functioned so that the bottles suffered only minor damage and could probably be used over again.

On all flights the samples were taken during the upward flight of the rocket, the timing sequence of the openers and sealers being controlled by a timing circuit. The final timer developed and its circuit are described in Section 8.1.

5.15 Recovery of Sampling Bottles After Rocket Flight

Unlike the rocket experiments in which the data may be telemetered to the ground during the rocket flight, recovery of the sampling bottles is necessary to the obtaining of the sample itself. All of the sampling bottles were recovered except the two bottles in the instrument compartment of V-2 27. These two bottles were never found. In general, recovery was accomplished within a few days after the rocket flight, although some sampling installations were not recovered for several months. In the V-2 it was found that the mid-section installation was best from the standpoint of recovery since the fuel tanks usually separated upon the controlled detonation at the end of the rocket flight. This usually released the bottles from their detachable mountings between the fuel tanks. Even here the mortality has been quite high as can be seen from Table 2. In the first two Aerobee firings (SC-1 and SC-2) recovery of the bottles in good

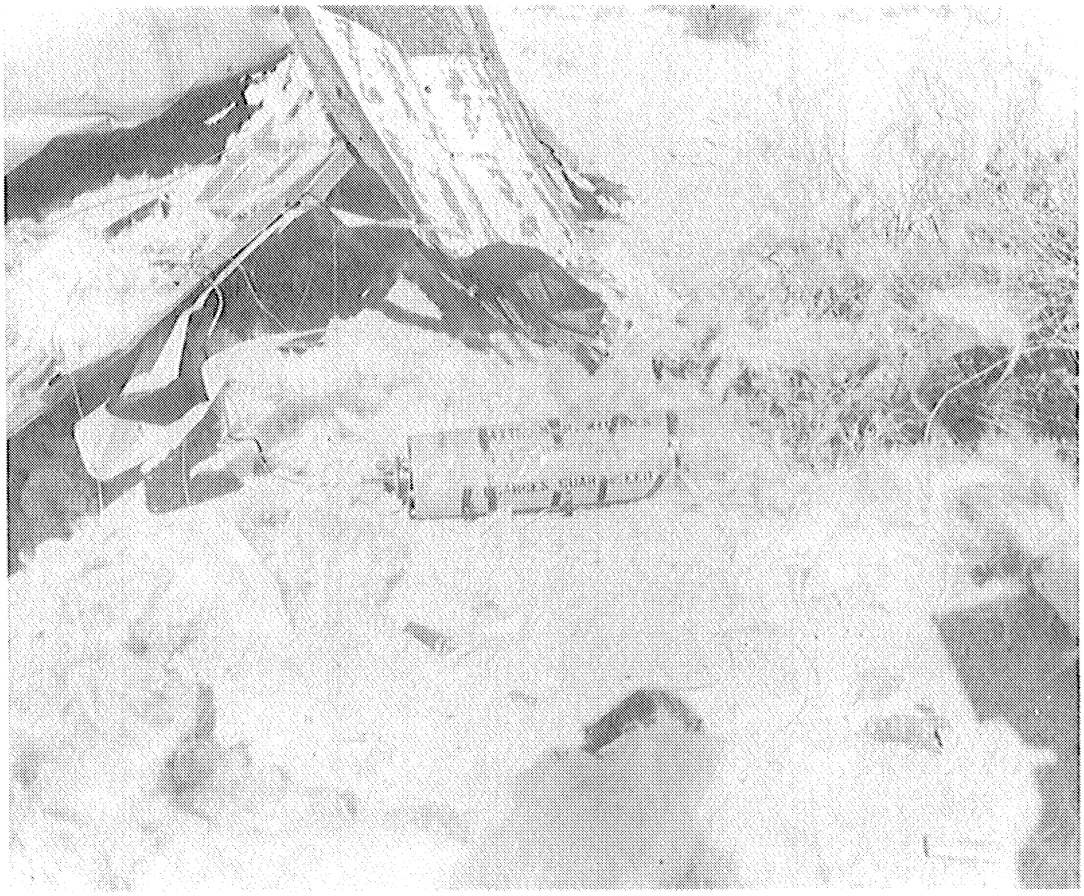

Fig. 34. View of V-2 and Sampling Bottles After Rocket Flight

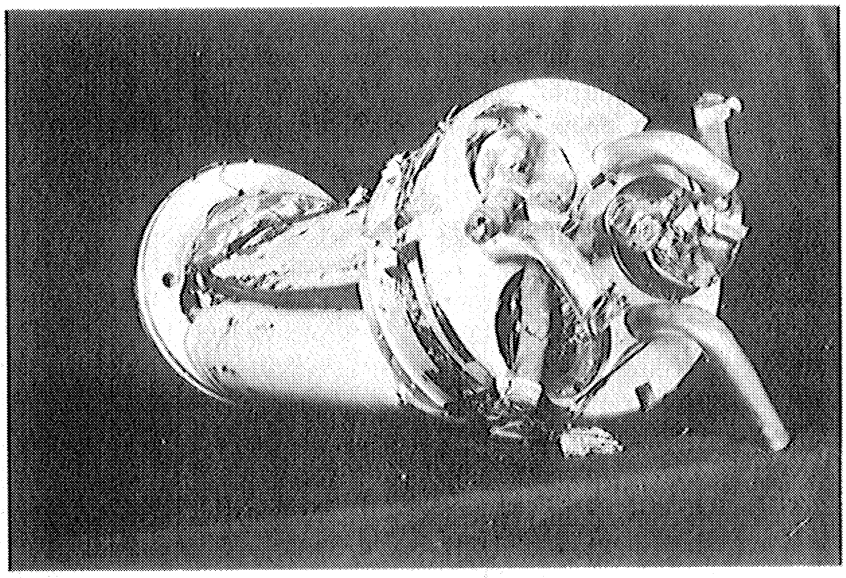

Fig. 35. Typical Aerobee Recovery (no parachute)
This view shows the general crushed condition of the sampling bottles after Aerobee flight where there was no parachute recovery.

condition was hoped for by means of pyrotechnic separation of the tail fins from the main missile body. Although two good bottles were recovered from SC-2, the general crushed condition of the bottles on account of the high velocity impact necessitated an attempt at parachute recovery. A parachute mechanism was developed by ESL and has been used for the other six sampling Aerobee firings. Of these, parachute recovery was not obtained for SC-4 and SC-11, but for the others it has been highly successful and has resulted in only slight damage to the sampling bottles.

5.16 Extraction of Upper Air Samples from Sampling Bottles

After completion of the rocket flight and recovery of the sampling bottles from the wreckage, the bottle installations were carefully inspected for any information that might be useful to future flights. The bottles that failed to collect upper air samples are listed in Table 2* with some information on them and their respective rockets. More complete information is given in Table 3* for the bottles from which upper air samples were extracted. The samples were extracted from the steel bottles by a mercury-glass pumping system which made use of the so-called Toepler pump. The extraction was originally attempted through use of a continuous "Archimedes pump" which operated by means of a glass-covered iron armature mounted perpendicular to the axis of the pumping system and a rotating external magnetic field. A schematic of this system is shown in Fig. 36. This proved to be unsatisfactory and was replaced by an air-operated Toepler pump. The modification has been quite satisfactory and has enabled the transfer of the major part of the upper air "capture" from each successful sampling bottle to four lime glass vials without contamination by the outside air.

The transfer is made possible by means of a small copper diaphragm of 0.003" shim stock soldered in the sampling bottle at the time of bottle preparation. After the extraction system has been pumped and outgassed by heating the vial system is closed off from the mercury diffusion pump by means of a mercury shut-off valve. The sample is then allowed to enter the extraction system on puncturing the copper diaphragm in the sampling bottle by means of the steel plunger. See Fig. 37. The pressure of the sample is then increased in the vial end of the extraction system by action of the air-operated Toepler pump and the magnetic mercury float valve which retains the higher pressure in the vial portion of the extraction system. After operation of the automatic air-operated Toepler pump for about two hours, at the end of which nearly all of the air sample is in the vial end of the extraction system, the glass vials are pulled off from the system by means of a hot glass seal-off. Each of the upper air samples were transferred to four glass vials in this way. The vials were labeled A, B, C, D following the appropriate arabic numeral representing the extraction number (and not the original bottle number). Vials A and D are all of 50 cc. capacity, while vials B and C are 25 cc. capacity. The products of these volumes with the vial pressures of Table 3 give the amount of air sample in each vial available for analysis. From these figures it is seen that the amounts vary from 9.1 cc NTP (vials 28A and 28D) to 0.29 cc NTP (vials 18B and 18C).

---

* For convenience Tables 2 and 3 are given at the end of Section 5.28.

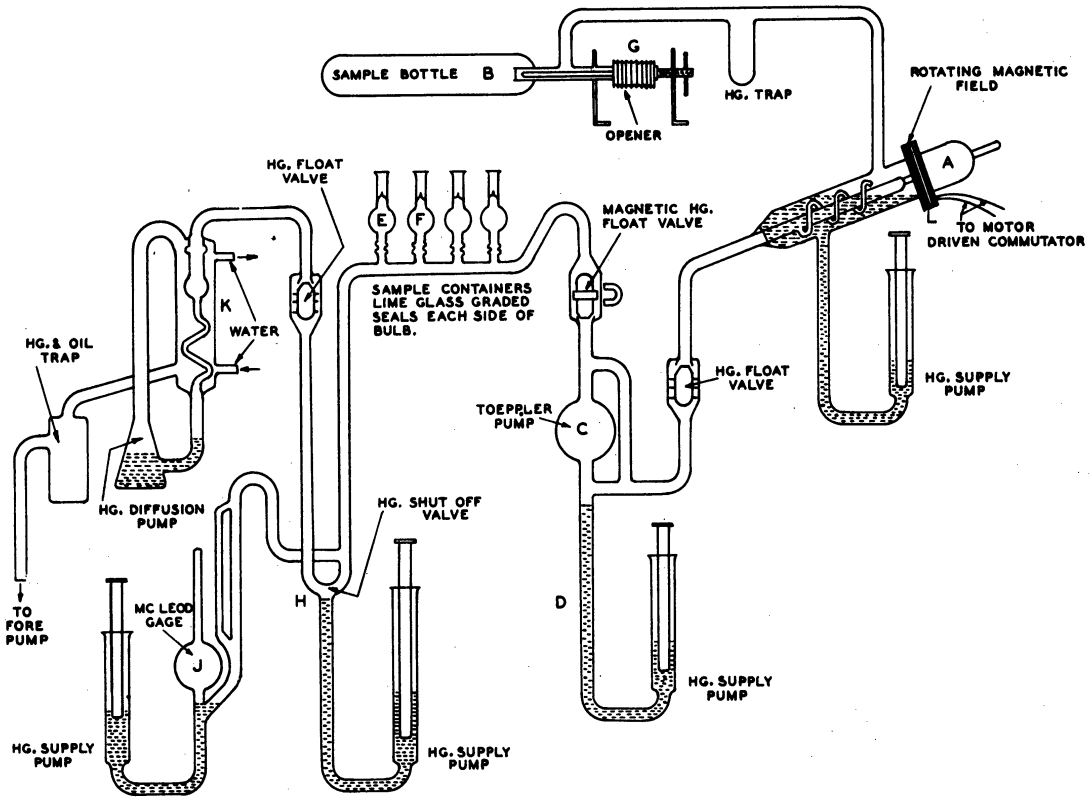

Fig. 36. Schematic of Sample Extraction System
The rotary pump shown was later replaced
by an air-operated Toepler pump.

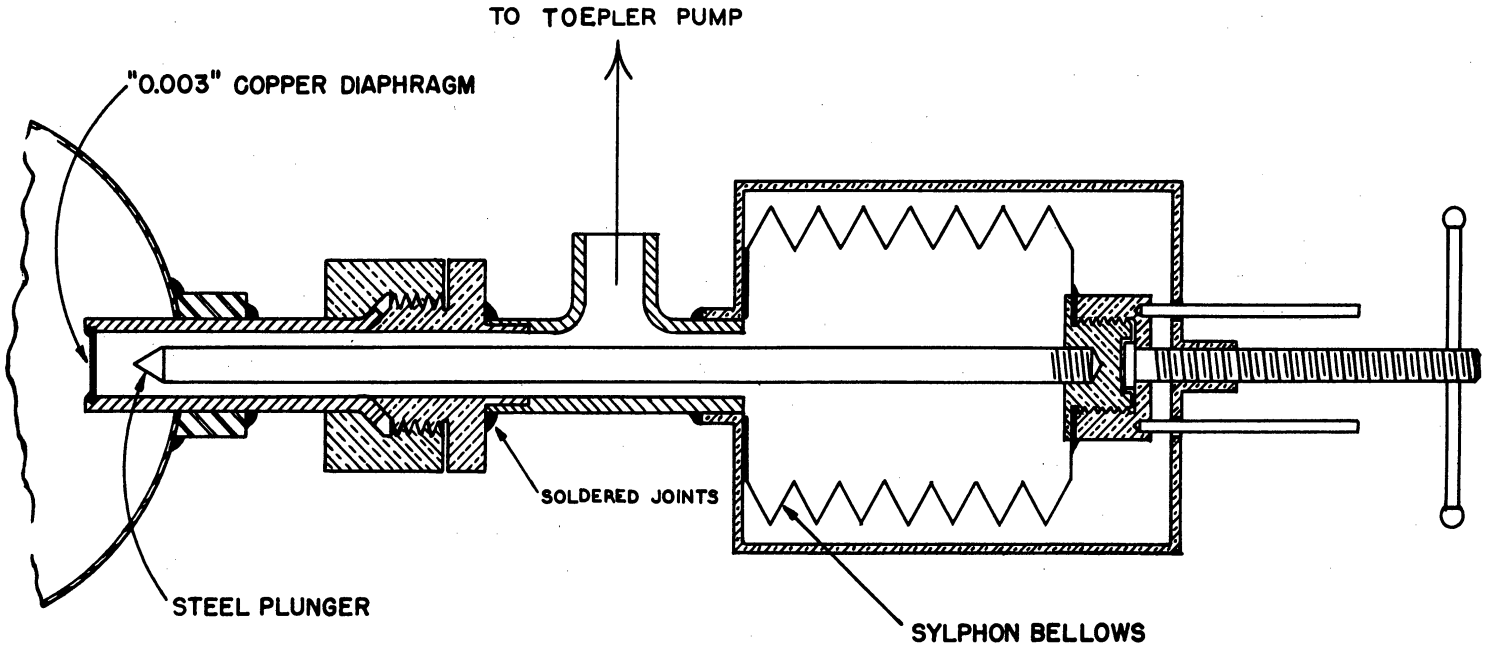

Fig. 37. Detail of Extraction System Showing Plunger Mechanism

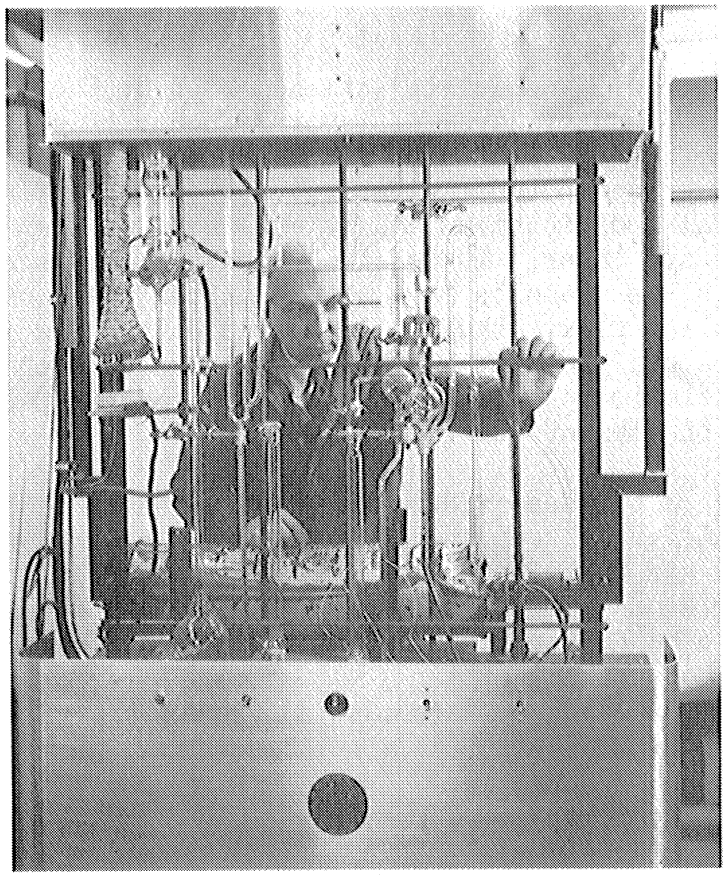

Fig. 38. Operation of the Present Sample Extraction System

After extraction of a sample from its steel sampling bottle a leak check of the bottle was made by raising the mercury cut-off valves and repumping the entire extraction system to a high vacuum. The mercury diffusion pump was then cut off from the extraction system and the rate of pressure increase, if any, in the extraction system was measured by means of the attached McLeod gage. The leak rates are given in Table 3. Several sampling bottles were found to have rather high leak rates so that their samples were not considered valid and the sealed-off vials were rejected for analysis. These particular bottles were not included in Table 3 but rather in Table 2.

5.17 Possible Contamination of the Upper Air Samples by Sampling Technique

Since the upper air samples from V-2 flights were obtained from installations in which the scoops were located well back of the tip of the rocket, these experiments were subjected to the possibility that the upper air samples have been contaminated by ground air carried along by the interior of the missile. Rough estimates indicate that the air will be discharging from an effective volume of about 100 cu. ft. during the upward flight of the V-2. The time constant for this discharge (time for the pressure to decrease to 1/e of its original volume) was estimated to be of the order of 20 seconds. Against this, the V-2 at a height of 225,000 feet (68 km) and a velocity of 4000 feet/sec., is sweeping out an air volume of 10 cu. ft. (NTP) per second. Thus the volume of air swept out appears to be somewhat greater (possibly a factor of 10 or more) than the rate of leakage from the missile body above the sampling intake scoops. The conclusion to be drawn so far is that this possible source of sample contamination can not result in more than 10% impurity by ground air carried along by the rocket.

However, aerodynamicists estimate that at the location of the intake scoops the boundary layer is several inches thick at zero angle of attack. Outside this distance the velocity is essentially that of the main stream. The intake scoop tubes were made as long as appeared feasible without structural modifications and it was intended that they should extend outside the boundary layer. It is likely that air leakage from the compartments above the scoops results in a thickening of the boundary layer and may even cause turbulent flow. Thus it is possible that the intake scoop does not actually extend beyond the boundary layer and that the air taken into the sampling bottle is contaminated by the trapped air perhaps by as much as 1 to 1 ratio of ambient to trapped air.

In regard to these views the attitude has been taken that if there is appreciable diffusive separation in the upper atmosphere at the height of the samples, the air taken in at the intake scoops should show a difference from surface air since samples should contain some stratospheric air. This, in itself, would be an important result. If no difference were found in several flights, one would certainly expect little diffusive separation. If there is a difference from surface air, the quantitative difference might be questionable because of the possible contamination.

It appeared that sampling by means of the Aerobee rocket might eliminate these objections since this would be a single-experiment rocket and the design could be manipulated so that the intake scoops were well ahead of the out-gassing ports of the missile body. For SC-1 the nose cone was fitted down over the sampling installation and the scoops attached. For the later Aerobees provisions were made to cut the nose cone about two-thirds the way towards the tip so as to greatly increase the ease of assembly and trouble shooting. By use of ring seals it has been possible to eliminate any air leakage at this joint. Thus, if the Aerobee nose cones are sealed and leak-tested forward of the intake scoops, upper air samples will be uncontaminated provided the angle of attack is not more than about 90°. Unfortunately, in view of the sparse attitude data of the Aerobees, and indications from the attitude data that do exist, it appeared that it would be desirable to design an experiment to estimate the contamination from trapped air inside the nose cone in case a large angle of attack occurs after fuel burnout.

An experiment was designed making use of the radioactive carbon isotope C^{14} in the form of $C^{14}O_2$. The CO_2 is contained in a 100 cc steel cylinder at one atmosphere pressure and is opened by means of a pyrotechnic opener similar to the sampling bottle pyrotechnic openers at an altitude of 35 km where the pressure is 1/150 of one atmosphere. Fig. 39 shows the cylinder and opener mechanism. The cylinders were in the nose cone of the Aerobee near the tip. See Fig. 26. The CO_2 should be sufficient to displace the 15,000 cc of the unoccupied volume of the cone when the CO_2 cylinder is opened at this altitude. It was calculated that .000025 cc NTP of the CO_2 could be detected by present Geiger counter techniques. Since the test vials usually contain about .3 cc NTP, this means it would be possible to detect 0.008% contamination by this gas. In this way it was hoped, in the design, that such measurements would give evidence one way or the other regarding contamination of the sample by air leaking from the nose cone either through seals or through the intake tubing. This would also cover the case where

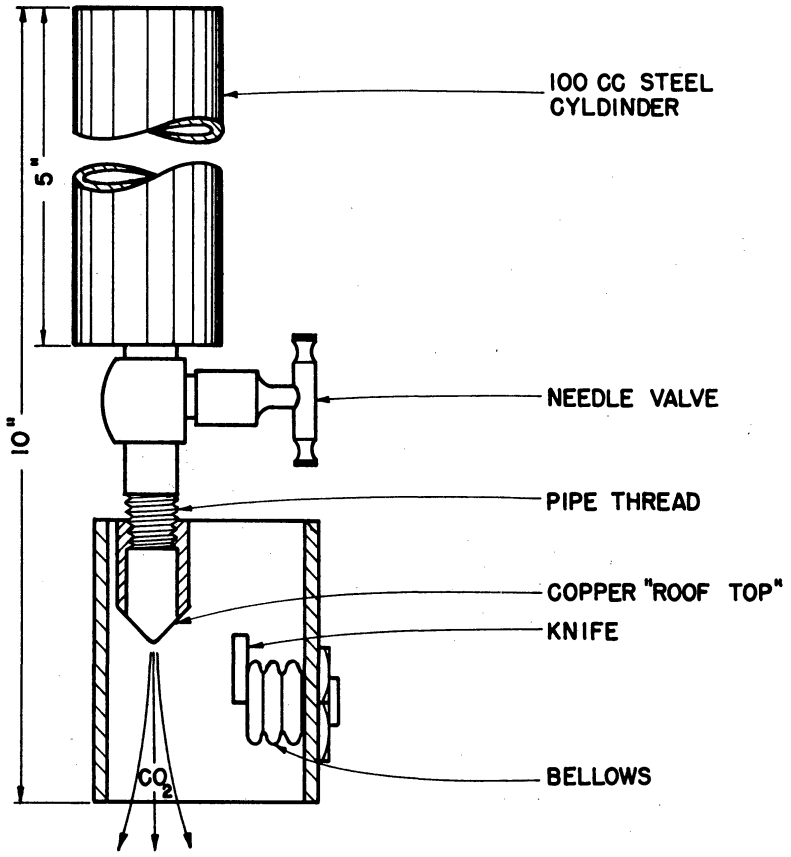

Fig. 39. Cylinder and Opener

there is a large angle of attack and the outgassing of the nose cone occurs in the trajectory ahead of the intake scoops. The contaminator was installed on SC-3, SC-7, SC-9 and SC-11 but, because of failure of the device to open, contamination checks have been restricted to bottle 77 on SC-3. The results were quite encouraging since the beta-ray count gave a contamination of 0.002% with background at the same value. The beta-ray count was accomplished by isolating a part of the sample from bottle 77 at the time of extraction. This was sent to Tracerlab, Inc., Boston, Massachusetts, for measurement by standard Geiger counter technique.

There are still a number of possible sources of sample contamination. The first arises from small leaks in the sampling bottle before sampling. Since the Pirani gages soldered inside of the sampling bottles were insensitive to pressures less than one or two microns of mercury, it is conceivable that the bottles may have leaked this amount. However, since the collecting pressures were at least two orders of magnitude higher than this value the amount of air contamination would not be objectionable provided (for the Glückauf analyses) the helium content of air in the pumping room was not too much above normal.* Some attempt was made to store the sampling bottles after evacuation in a room separate from the pumping room containing the preflight pumping system, so that this possibility was reduced considerably. In addition, it is important to note that such a contamination would increase the helium to nitrogen ratio above and beyond the increase

* The leak detector required the release of a small amount of helium in the pumping room a few minutes a week.

that might be obtained from diffusive separation of the sample itself - none was detected (Section 5.21 and 5.22).

A more serious possibility of air contamination exists in the bottle seal-off techniques. All of the successful samples obtained used the seal-off involving the pyrotechnique hammer sealer. The sealer appears to evolve about two microns of gas in the sampling bottle when operated. It seems reasonable that some of this gas will consist of gaseous hydrocarbons from the rosin flux that was found to be necessary for successful seals. The rest is probably water vapor and carbon dioxide. None of these gases would affect any of the analyses used to determine diffusive separation in the upper atmosphere. The outgassing of the pyrotechnic soldered-disc sealer was more serious than for the pyrotechnic hammer sealer since the amount of hot metal available for outgassing was considerably larger than for the hammer sealer. Since this type of sealer was not successful on SC-11 and since this model has been discontinued, these objections will not be discussed in detail.

One objection to the sealers is the partial or complete loss of oxygen apparently due to the hot metal at the time of seal-off. If this loss were eliminated, as in a cold-weld seal, a measurement of the ratio of the oxygen isotopes would allow a check on the internal consistency of the analysis technique discussed in Section 5.27.

The slight contamination of the samples by oxides of nitrogen formed at the time of the hot glass seal-off of the vials from the extraction system is discussed in detail in Section 5.25. Suffice to say that it does not appear able to nullify any of the interpretations of the analyses used to determine diffusive separation.

The possibility that some of the sample is atmospheric air that has leaked in due to poor seals at sampling time has been discussed in Section 5.16. The leak rate data of Table 3 show that this source of sample contamination by ground air is considerably less than 1% except for bottle 63 (vials 19A to 19D) and bottle 65 (vials 18A to 18D). For the former the contamination appears to have been about 8%, while for the latter 5%. These values are not enough to change the deviations given on pages 64 and 65 of Table 3.

Another effect that should be mentioned, as far as the Glückauf analysis is concerned, is the slight solubility of helium and neon in the soda glass vials mentioned by Chackett, Paneth, and Wilson.[1] Examination of the laboratory notebooks reveals little possibility that any of the samples extractions have been treated in a different manner than the others, so that this question remains unsettled. Because of this there remains a number of controlled sorption experiments which will have to be done eventually.

Another possibility of sample contamination is discussed in Section 5.19.

5.18 Establishment of Sampling Heights

The sampling bottle openers and sealers were actuated by timers

described briefly in Section 8.1. The timing sequences were arranged so that the bottles were opened at the height to be sampled and were then closed after a period of five seconds. This value was calculated from the "time constant" of the bottle and found to be adequate. Previous to the flight the times for actuation of the opener and sealer were determined from the rocket trajectory to be expected and the height of the atmosphere to be sampled. The timing mechanisms were started at rocket takeoff. On V-2 flights the timing circuits were monitored by means of one channel of the telemeter system so that it was usually possible to check the actuating times quite accurately. On the Aerobee flights the timing sequence was monitored by means of pulse widening of the beacon transponder in the rocket. This was done since there were no telemetering systems in the Aerobees. Unlike the V-2 flights, the timing mechanism for the Aerobees begin operating at booster separation rather than at the official starting time so that the pulse widening times, in terms of official time, have to be adjusted by about 2 1/2 seconds.

When all flight and ground equipment operated as intended, the sampling heights were determined quite easily from the monitored timing sequence and the official rocket trajectories issued by the Ballistic Research Laboratories, Aberdeen Proving Ground, Maryland. On many of the Aerobee flights optical tracking of the rockets was limited to heights below the fuel burnout of the missile. In these cases the radar tracking data were used. If neither were available the sampling heights were calculated on the assumption of a vacuum trajectory after fuel burnout. As can be noted by reference to the previous progress reports the sampling heights originally given do not always agree with the data in Table 3. This is explained, of course, by the procurement of more accurate rocket trajectory data from the Ballistic Research Laboratories as a result of more detailed calculations.

5.19 Sampling Efficiency

As was to be expected, the mortality of the sampling bottles was quite high since the sampling apparatus required basic development, had to be completely automatic, had to withstand large accelerations and had to survive high velocity impacts with the ground after the rocket flight. The efficiency of sampling is given in the following table:

	V-2	Aerobee
Bottle never found	2	
Poor rocket performance	4	
Bottle damaged as a result of impact	5	5
Failure of instrumentation to operate properly	6	10
Total bottles without samples	17	15
Total bottles with samples	5	9
Total bottles flown	22	24

Some of the details of the sampling failures are given in Table 2. During the development of sampling procedure it was found that the mortality of the sampling bottles on V-2's was decreased by mid-section installations and, in particular, by not lashing the bottles to the missile structure. This meant that the sampling bottles were freed from their mountings when the main body broke as it entered the dense part of the atmosphere. By virtue of this, the bottles often fell a few to a few hundred feet from the main wreckage and not strictly with it. See Fig. 34. For the Aerobee the loss of sampling bottles as a result of impact has been almost completely nullified through the use of parachute recovery. The mortality as a result of instrumentation to operate properly has apparently been due to a variety of reasons. It has not always been possible to ascertain the reason for failure. Of the sixteen failures which have been attributed to instrumentation, four of the instrumentations operated properly but failed to seal vacuum tight as was evidenced by their leakage after extraction of the sample. For the rest, the sealers and/or the openers failed to operate. It was not always possible to ascertain the basic trouble. It may be pointed out that the design had been changed a number of times even after becoming stabilized and flight-tested in an attempt to increase the "capture efficiency" and to avoid alteration of sample constitution. This has been no small matter in sampling bottle mortality.

It was deemed extremely important to evaluate all available information on the performance of the rockets on the premise that their performance might, in some way, affect the fourteen sampling bottles whose contents were to be considered representative of the chemical constitution of the upper atmosphere. Unfortunately, it has not been possible to determine all desired rocket performance and attitude, but the following information has been obtained:

a) V-2 27 (bottle 32). There was an explosion of this rocket at about 82 seconds. This appears to have been a premature warhead blow-off since Doppler radar, beacon and telemeter ceased functioning. It was thought, at the time of recovery, that this may have likewise disrupted the bottle operations since the installation was programmed for bottle opening at 80 seconds and bottle closing at 88 seconds. This does not appear to have been the case, since the sampling wiring circuit was completely independent of the other circuit. The possible effects of this explosion as far as sampling is concerned will be discussed shortly.

b) V-2 35 (bottles 35 and 37). Rocket with excellent performance. Bottle performance as planned.

c) V-2 40 (bottle 42). Rocket motor burned irregularly at 43 seconds but it apparently corrected itself in a second or so. Bottle performance as planned.

d) V-2 44 (bottle 45). Rocket with excellent performance. Bottle performance as planned.

e) Aerobee SC-2 (bottles 60 and 61). In the PRELIMINARY RADAR DATA sheet issued by SCEL Beacon Radar Unit and White Sands Annex, BRL, it was stated that "Examination of ballistic camera films disclosed that the missile was detonated at 67.0 seconds." There has been no verification of this from the tracking telescopes since no tracking information was obtained at this particular time, except from a single tracking telescope, Telescope IV. Even from this tracking telescope the missile images were faint after 60 seconds. The apparent angle of the missile axis from the vertical as observed from telescope IV was 350° to 357° between 60 and 70 seconds, and 345° to 352° at 71 seconds. The missile was nose up at 71 seconds when the image faded. It was impossible to determine from the telescope IV record at 77 seconds whether the missile axis remained at 350° or turned nose down. Bottle No. 60 was set to open at 67 1/2 seconds and close at 72 1/2 seconds, while bottle 61 was to open at 72 1/2 seconds and close at 77 1/2 seconds. Thus it appears that the missile apparently detonated just previous to the opening of bottle 60 and it is conceivable that it was nose down by the time of closing of bottle 61.

f) Aerobee SC-4 (bottles 63 and 65). Nothing is known definitely about the attitude of this missile at sampling time since there was little tracking information after the burnout at 42 seconds. The angle between the missile trajectory vector and the missile axis was only a few degrees at the time of burnout.

g) Aerobee SC-5 (bottle 68 and 69). At the postflight conference it was revealed that this rocket was stable in the first 70 seconds of flight; thereafter, flight instability prevailed with the rocket being in a horizontal position at 100 seconds. The first report on this firing gave some of the angles of missile with respect to vertical at the tracking telescopes, but the attitude calculations of this missile have yet to be received. From an examination of the data it appears that during sampling times of bottles 68 (70.5 - 76 sec) and 69 (76 - 82 sec) the angle between the missile trajectory and missile axis was at least 50°.

h) SC-3 (bottle 77). Tracking telescopes TI, TIII, and TIV were able to follow the missile as high as the sampling altitude. There is evidence of considerable yaw of the missile after burnout, but it appears that the angle between the missile trajectory and the missile axis was not more than 20° at the time of sampling (83 - 89 sec).

i) SC-7 (bottles 74 and 79). The Aerobee was tracked very well for the entire flight. However, elevation angles of the missile axis before 91 seconds are not obtainable due to poor quality of missile image on the film. Extrapolating several seconds for bottle 79 (opened 81 sec., closed 87 sec.), it appears that the angle between the missile trajectory and missile axis was about 15°. Extrapolating farther, it seems that for bottle 74 (69 - 75 sec.) this angle is even smaller.

Summarizing these investigations, it was revealed that, for missiles V-2 27 and Aerobee SC-2, there were explosions of the rockets of some sort shortly before the times of sampling. The orientation of the air scoops with respect to the body of gas released at the time of explosion can not be determined, but it is possible that some of this gas was captured. Since the V-2 burns alcohol by means of liquid oxygen the combustion products, CO_2 and H_2O, may have also entered the sampling bottles since there are considerable gaseous products available even after burnout. This in itself would not affect the analyses described in Sections 5.21 and 5.22. A much more serious possibility lies in the rupture of the high pressure nitrogen lines used to actuate numerous mechanisms in the V-2. The effect of such a contamination in the sample will be discussed in Section 5.21.

For the Aerobee it is not certain what the combustion products are since it burns aniline by means of nitric acid with an excess of nitrogen dioxide, NO_2. These fuels are fed to the burner by means of high pressure air or nitrogen. Thus, for the case of SC-2, it is not known what effect of the rocket explosion on the sampling may be expected. One can only treat the analyses of their contents (vial 15A - 15D and 16A - 16D) with some discretion.

In Fig. 40 the pressures in the sampling bottles corrected for volume deformation upon impact are plotted against mean sampling height. The ambient pressure as a function of altitude (after Whipple[2]) is also plotted. This plot shows rather vividly the increased "ramming" effect of the higher velocity V-2 with respect to the Aerobee. It is rather interesting that the points for the V-2 flights are scattered along a straight line. Those for the Aerobee flights (except for bottles 60, 61, 65) lie along another straight line. It appears highly possible that the explosion of SC-2 shortly before the opening and closing of bottles 60 and 61 may have increased the "capture" of these bottles by virtue of the release of a large amount of gas in the vicinity of the rocket or by causing the missile to pitch badly so that the scoops were in the stream of the outgassing. The "capture" by bottle 32 on V-2 27 appears to be quite representative of the performance of the other V-2 sampling bottles. Thus, for bottle 32, this explosion may have had no effect on the sampling. It is possible that the small "capture" of bottle 65 was due to pitching and yawing of the missile; the scoop being in the streaming shadow of the nose cone at sampling time.

The fourteen sampling bottles whose contents have been considered, tentatively, to be representative of the constitution of the upper atmosphere were emptied and the samples put into 56 vials. Of these, 38 vials have been analyzed or committed for a specific analysis. The analyses completed to date are described in Section 5.2.

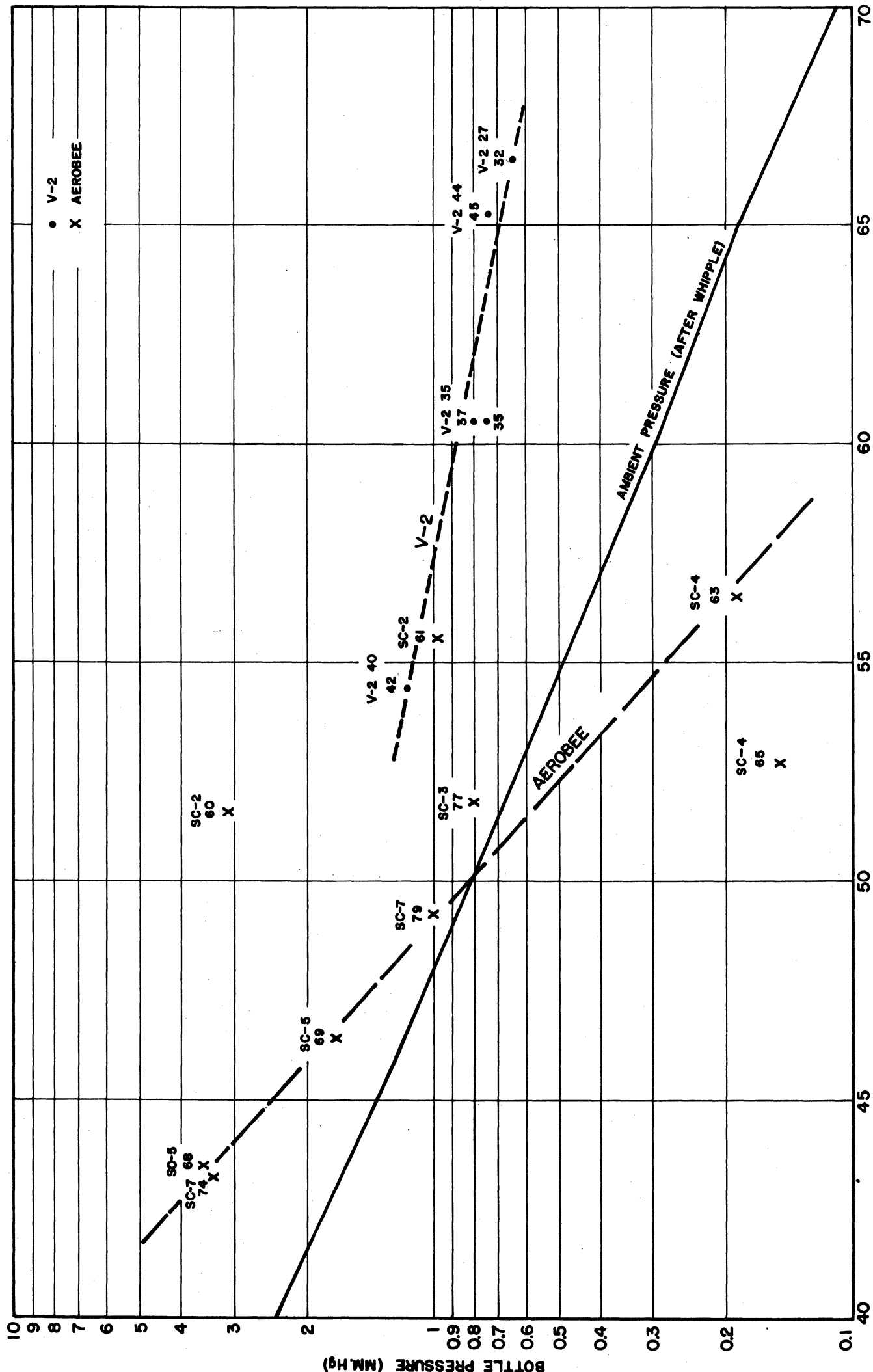

Fig. 40. Sampling Height vs Collecting Pressure for the 14 Successful Sampling Bottles

5.2 Analyses of Upper Air Samples

Shortly after the beginning of the work on the sampling program Professor F. A. Paneth of the University of Durham, England, heard of our program and offered to analyze some of the samples, when obtained, according to the methods developed by himself and his collaborators, in particular E. Glückauf, during the past twenty or so years[3]. It was decided that some of the samples would be sent to Professor Paneth and also that the Paneth-Glückauf analysis would be carried out at the University of Michigan. A large percentage of project effort went into the construction and calibration of this analyzer. The results of these two analytical programs concur in that there is little or no tendency for the lighter constituents of the upper atmosphere to separate out from the heavier constituents by molecular diffusion in the region of the atmosphere sampled from 40 to about 70 kilometers. This indicates that the main factor in controlling the general composition of the high atmosphere is a continual stirring which keeps the composition (other than for the constituents ozone, atomic oxygen, and water vapor) constant. It is hoped that these experiments can be extended to greater heights.

Analyses were also made of a few upper air samples by means of two analytical mass spectrometers, one at the Westinghouse Laboratory and the other at the National Bureau of Standards. The analytical mass spectrometers were found to have insufficient sensitivity and too large backgrounds to answer any of the outstanding questions. The mass spectrometric technique did, however, detect a new constituent which was interpreted as being due to nitric oxide (NO). By means of a modified colorimetric method of analysis this interpretation was found to be essentially correct and it appears that its formation resulted as a small interaction between the sample and hot glass during the sampling procedure. This effect is not large enough to influence the results of the Paneth-Glückauf technique.

Professor Beams and his collaborator, Dr. McQueen, of the University of Virginia made determinations of the nitrogen isotope ratio of some of the samples. Their tentative results indicate an inconsistency with the results of the two charcoal analyzers. Their analyses indicate considerable diffusive separation in some of the higher air samples obtained. This apparent discrepancy has yet to be cleared up.

It was found quite early in the analysis programs that a large percentage of the oxygen in the upper air samples was depleted by sampling technique so that one program had to be dropped. Also, an attempt was made to measure the oxygen content of the atmosphere during rocket flight, but this was not found feasible.

5.21 Charcoal Adsorption Analyses - University of Durham

The selective adsorption technique developed by Paneth, Glückauf and others for the separation and measurement of small concentrations of helium and neon in gas samples has been discussed in a series of papers over the last several decades[3]. In brief, it is the separation of two or more gaseous substances by fractional adsorption and desorption processes. That is, when the total gaseous mixture is brought into contact with an adsorption

unit the percentage of a gaseous constituent that goes into the adsorbed phase and the percentage that stays in the gaseous phase are governed by the particular adsorption coefficient for that constituent and that adsorptive material. If a series of adsorption units is used, the gaseous phase is transported from one adsorption unit to the next, each adsorption unit increasing the purity of the products as in fractional crystallization. This purification comes about since the absorbent of one stage is connected with an evacuated space into which the gases initially adsorbed can again expand according to their distribution equilibrium. This is repeated again and again as in fractional crystallization.

In this manner Glückauf[4] found that for adsorption units composed of 2.5 grams of hard nut charcoal it was necessary to have twelve adsorption units to be able to draw off 99% plus of the total helium (the helium here may be contaminated by a small amount of neon -- 0.5% or less) in a small air sample for measurement by a specially designed Pirani gage. The neon can then be drawn off and measured by continuing the adsorption stages. Glückauf devised an excellent method of operating the twelve adsorption units together and operating the twelve evacuated chambers together. These are connected so that mercury is raised and lowered at only two places but the net result is that of a 12-stage Toepler pump. The technique consists of first eliminating the oxygen together with a small amount of hydrogen, if present, and/or organic matter by a hot copper filament. Any H_2O and/or CO_2 formed are removed by solid NaOH and $CaCl_2$. In an air sample the remainder then consists of nitrogen, argon, neon, and helium. The amount of this mixture is determined by a manometric measurement of its pressure in a known volume and the amount of helium and neon is analyzed by the Paneth-Glückauf charcoal technique. The measurement of argon requires additional work and is described adequately in the recent paper by Chackett, Paneth, and Wilson[1]. In this manner the important ratios of argon, neon, and helium to that of nitrogen plus argon plus neon plus helium are obtained (hereafter to be called the argon to nitrogen ratio, the neon to nitrogen ratio, and the helium to nitrogen ratio, respectively) and may be compared with the ratios obtained for air samples gathered near the surface of the earth. Since it had been established by Paneth and Glückauf in a world wide survey[5] that these ratios can be considered to have the general nature of geophysical constants their comparison with the corresponding ratios from samples obtained at high altitudes give quantitative measurements of the net effect of molecular diffusion processes with respect to mixing processes in the atmosphere. Theory shows that the effect of molecular diffusion will be such as to increase the helium to nitrogen and neon to nitrogen ratios with respect to ground air but to lower the argon to nitrogen ratio.

Papers by Paneth[6] and Paneth and Glückauf[5] give the results of their analyses of the upper air samples obtained by balloons*, while the papers by Chackett, Paneth, and Wilson[1] give the analytical results for some of the upper air samples obtained by rocket. The latter results# are

---

* These samples were obtained by apparatus developed by L.H.G. Dines and reported in Quar. J. Roy. Met. Soc., 62, p. 379, 1936.

We have taken the liberty of publishing the separate analyses for vials 1B and 3B from figures furnished us by Professor Paneth.

reproduced on page 64 of Table 3. The suggestion was made that the deficit of helium in vials 1B and/or 3B and 16A may be due to the well-known slight solubility of helium -- and, to a much less extent, neon, in glass. The differences in these two vials being explained simply by a difference in the technique of evacuating and degassing the sample vials. However, this does not appear to be the cause of this discrepancy since these vials were handled no differently from any of the others. It is possible that the helium deficit detected by Chackett, Paneth, and Wilson in vials 1B (bottle 32 -- V-2 27) and 16A (bottle 60 -- Aerobee SC-2) might be due rather to an excess of nitrogen captured as a result of the rocket explosions discussed in Section 5.19. However, the neon to nitrogen and argon to nitrogen ratios do not appear to be consistent with this view since all of the ratios should be affected by the same amount.

The general conclusion of the work performed by Paneth and his collaborators at the University of Durham is that these ratios appear to have about the same values as those for ground air (within experimental error) even for upper air samples obtained as high as 67 kilometers. This seems to verify the theoretical work done by Maris[7], Epstein[8], and Mitra and Rakshit[9] that the diffusive processes are much too slow at these altitudes to compete with the much faster and more efficient stirring by means of large and small scale vertical convection.

5.22 Charcoal Adsorption Analyses - University of Michigan

In order to analyze the samples as soon as possible after they are taken and in order to carry out the numerous tests of possible effects such as selective adsorption on the walls of the sample bottles, storage flasks, etc., it seemed desirable to construct our own analysis system based on the techniques developed by Paneth and Glückauf. Because of the additional work required it was decided not to attempt the argon analysis. It appeared expedient to proceed by making the apparatus much like that of Glückauf[4] and to use ground air concentrations for calibrations. For additional calibration and absolute value determination it seemed desirable to construct a gas blending system of the type described by Langer[10] but with mercury cut offs and mercury-filled fritted glass plugs. This apparatus was constructed. See Fig. 41. The blending system developed a small leak in the interior glass construction and repair was delayed temporarily until the gas analyzer was completed. During the course of construction of the gas analyzer it was found necessary to devise methods of introducing small amounts of pure helium and neon for calibration purposes (this will be described shortly) and the change in technique removed the critical need for the gas blending system.

Although the analysis system was modeled much after the apparatus of Glückauf, unforeseen difficulties did arise. The period of construction, stabilization, and calibration continued for almost two years after the decision to check some of the University of Durham analyses at the University of Michigan#. The first difficulty that arose was the elimination of the effects of residual gases in the portion of the apparatus between the last fractionating steps and the Pirani gage used to measure the helium after

The details of this work is described in some detail in order to give better appreciation of the results given on page 65 of Table 3.

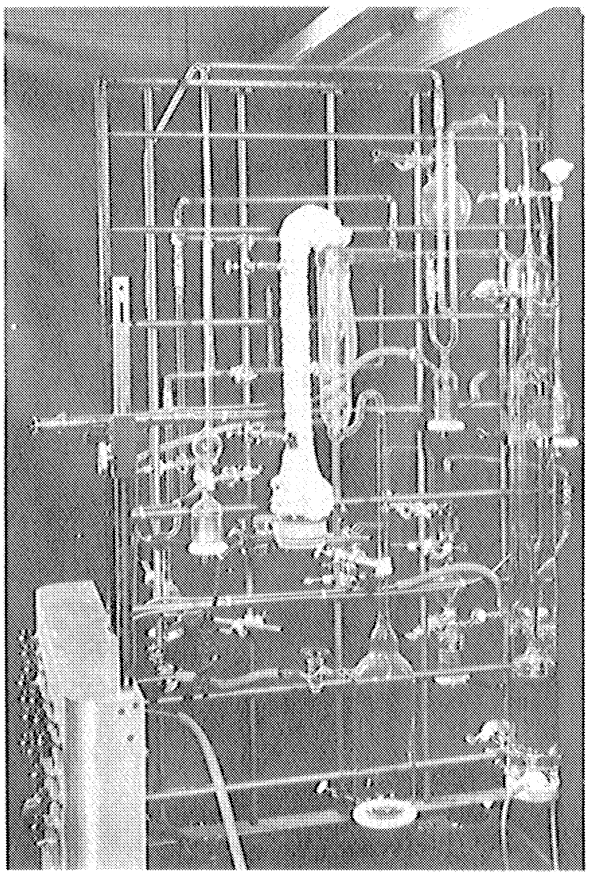

Fig. 41. Gas Blending System

separation. The earlier works on helium analysis described a method using the Pirani principle but which involved the measurement of helium pressures as low as 3.8×10^{-4} microns of mercury. In this method it is required to operate the Pirani gage at liquid nitrogen temperature and to have activated charcoal present in the bulb of the Pirani gage in order to adsorb residual gases for which the charcoal adsorption coefficients are much larger than those for helium and neon. This requires a volume calibration and other painstaking procedures. By reducing the volume of the Pirani gage to less than 0.1 cc., it was hoped to operate the Pirani gage at 0°C; and, by the elimination of stopcocks, torching the system, and using freshly distilled mercury in the Toepler pump used to compress the helium into the Pirani gage, it was hoped to eliminate the effects of residual gases. This, however, turned out to be impossible. The next step was to build a new Pirani gage with volume 0.5 cc which could be operated at liquid nitrogen temperature but without the charcoal. Preliminary tests indicated that the effects of residual gases could be reduced to less than 5%. Before completing these tests the final Pirani gage was broken and a new one had to be installed and calibrated. When Ann Arbor ground air was analyzed the results obtained for helium were 8.73 parts per million for the first run and 8.78 for the second run. The generally accepted value is 5.24 ppm.

The discrepancy mentioned above was thought to be due to an error in calibration of the Pirani gage caused by thermal transpiration resulting from the temperature differential between the Pirani gage and the McLeod gage used as a standard. The effect of thermal transpirations is well known from the kinetic theory of gases. This effect results when two chambers are

connected by an orifice whose cross sectional dimensions are small compared to the mean free path of the gas in the chambers. Since, at static equilibrium, the gas transport through the orifice must be equal and opposite between the two chambers it follows from kinetic theory considerations that the relation which follows is

$$\frac{P_a}{P_b} = \sqrt{\frac{T_a}{T_b}} \quad .$$

Since the McLeod gage was at room temperature, the Pirani gage at liquid nitrogen temperature, the two were connected by a 1 mm diameter capillary and the mean free path was about 4 cm, it appears that thermal transpiration could indeed account for the major portion of the discrepancy.

In order to check this result the analysis system was altered so that a known amount of helium or neon could be introduced into the Pirani gage. See Fig. 42. In this way the Pirani gage could be calibrated without making the necessary correction for thermal transpiration which at best was quite approximate. When this was done a series of five ground air analyses showed an average error of +5% for helium and -1.4% for neon when it was assumed that the adsorption units used have the same adsorption coefficients as those for the adsorption units in the apparatus described by Glückauf[4]. The policy decided on was to establish an instrumental correction in this way that could later be checked by analysis of accurate blends.

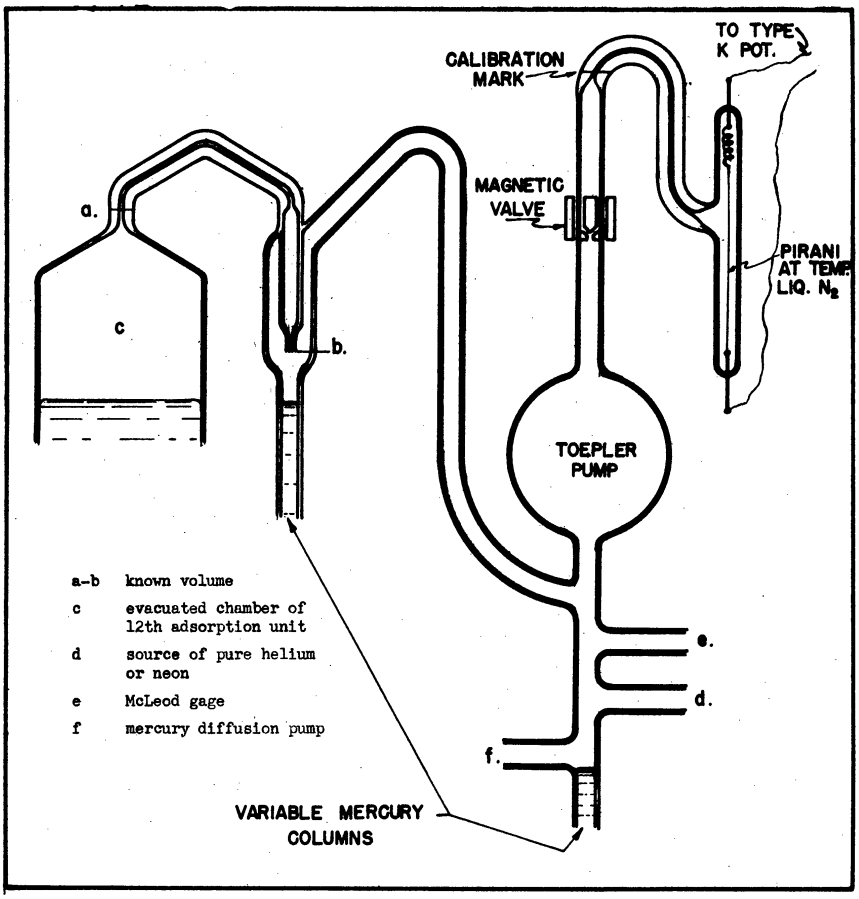

Fig. 42. Gas Analysis Calibrator

After check runs on ground air for helium were made, the Pirani (gage wire of tungsten) became very unstable. Investigation showed that one silver-solder to tungsten connection had failed. Because of the short tungsten terminal it was impossible to make another connection so a new Pirani gage wire was installed. The new gage was made of 0.0001" by 0.0025" nickel ribbon 6.3 cm long. Some of the resulting increased sensitivity was used up in increasing the volume of the gage from 0.68 cc to 1.0 cc. A small charcoal trap of 0.05 cc volume was included in the capillary to adsorb gas from the mercury column. See Fig. 43. An oven was wrapped around the charcoal volume to activate the charcoal and a thermocouple was inserted in the oven to measure its temperature. It was also found necessary to measure and correct for variations in the temperature of the liquid nitrogen in which the gage is immersed. This was thought desirable inasmuch as a change in temperature of 1°K could cause a change of 1.3% in the indicated pressure.

After calibration of the new Pirani gage a series of successful analyses of ground air was made. Following this, analyses of vials numbered 2A, 3A, and 15A were made. Shortly after this an instability of the Pirani gage was noted and thought to be due to moisture on the lead-in wires. The stability was improved by keeping the Pirani gage surrounded by a stoppered thermos flask except during the baking operation.

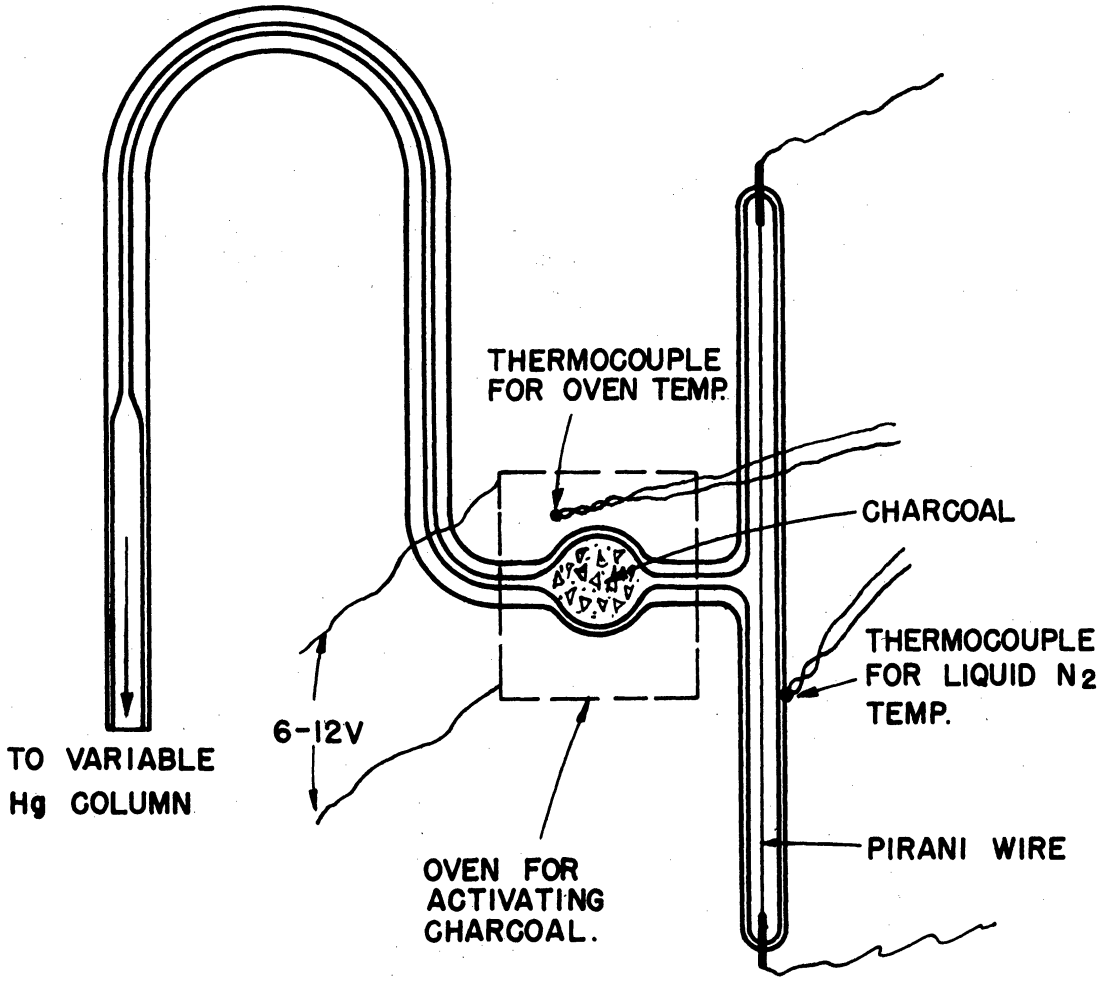

Fig. 43. Final Pirani Gage for Charcoal Analyzer

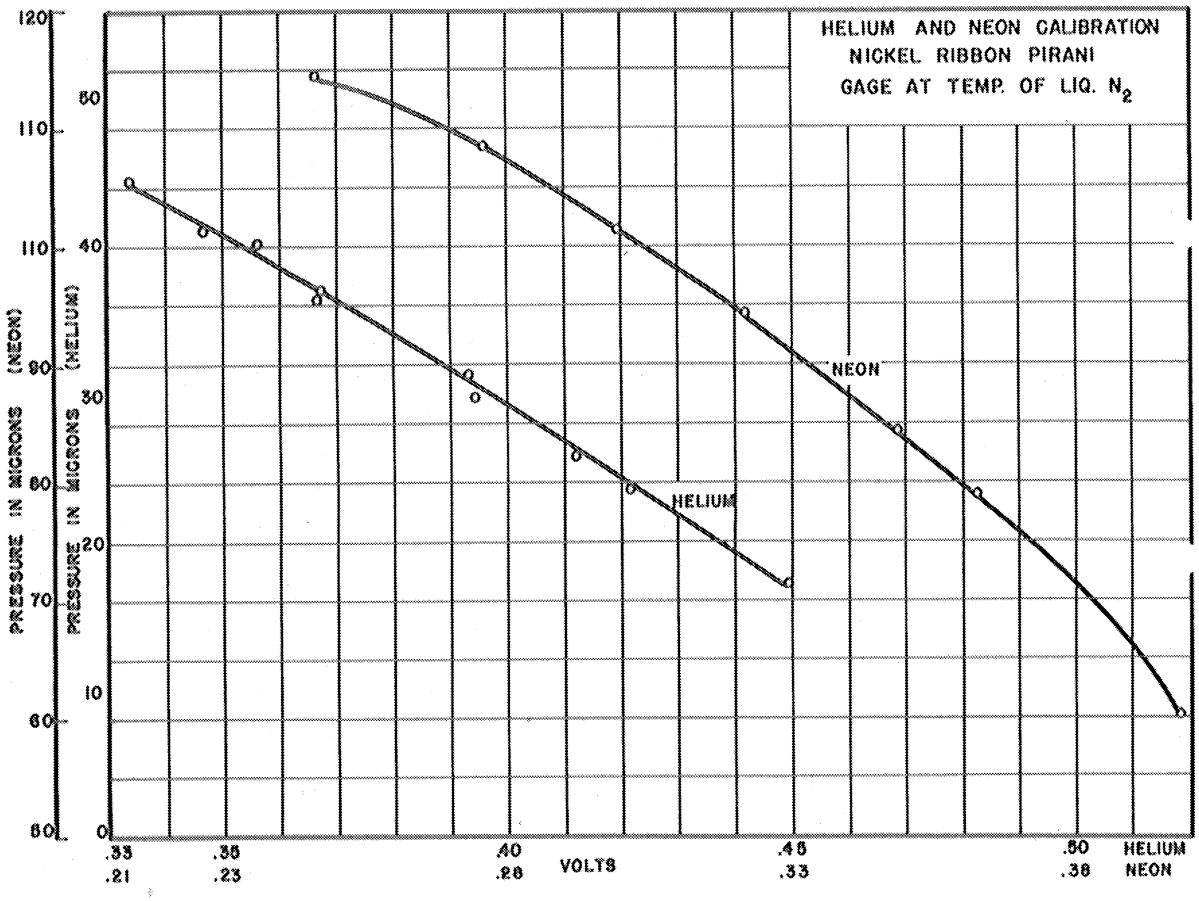

Fig. 44. Final Calibration of Charcoal Analyzer

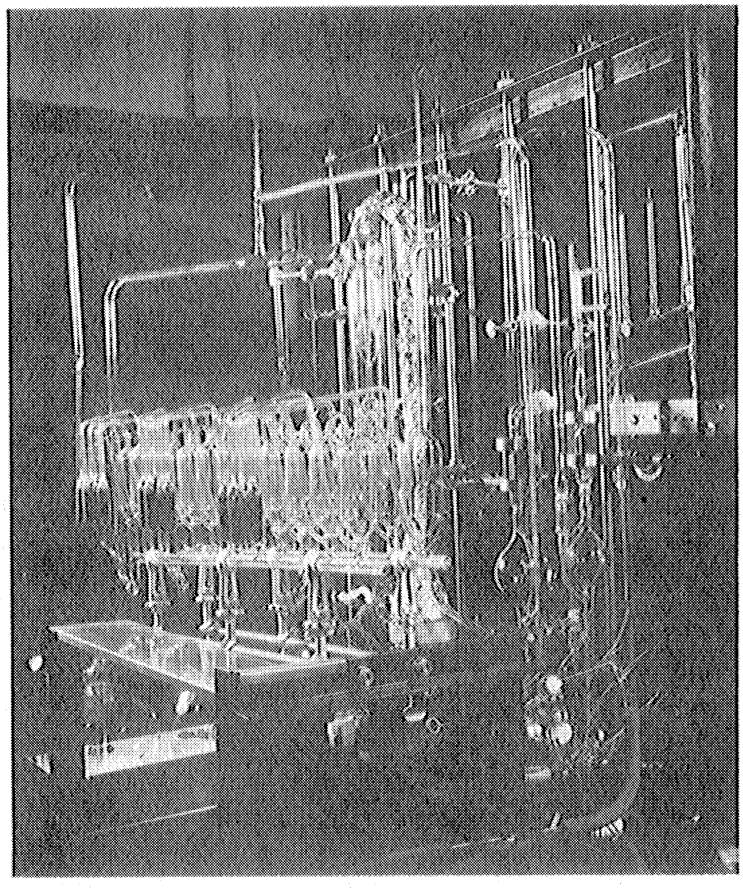

Fig. 45. Rear View of Charcoal Analyzer

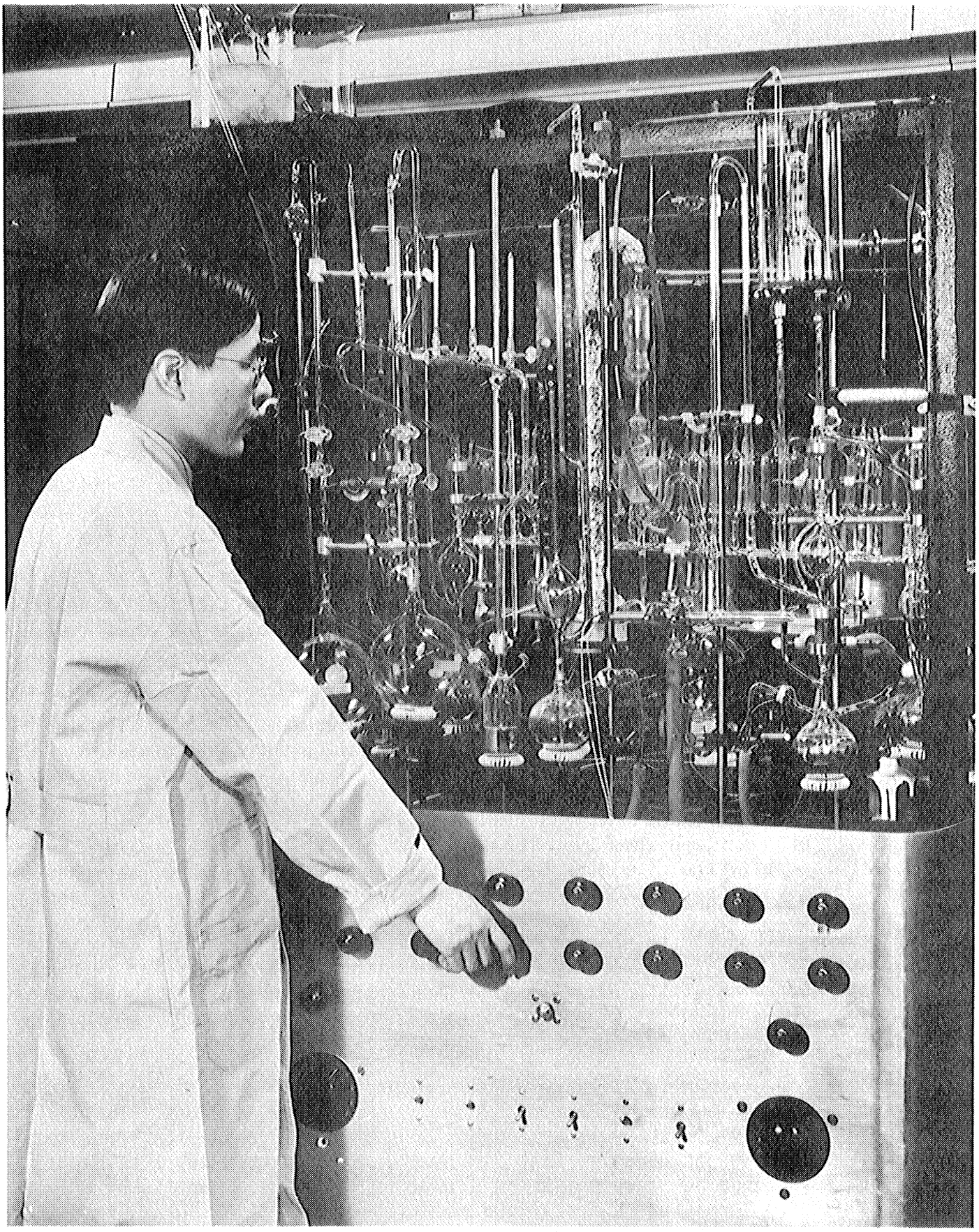

Fig. 46. Operation of Michigan Charcoal Analyzer
This view shows the operator transferring gas from one section of the analyzer to another by means of air-operated mercury Toepler pumps. All operations are controlled from the front console shown.

Following this modification two runs were made to determine the fractionations at which the separation of helium and neon is quantitative. It was known from Glückauf's publication[4] that nearly all of the helium would come over by the 24th fractionation, and that the neon would be recovered principally between the 24th and 50th fractionations. By fractionation of pure helium, it was found that the recovery of helium was 99.6% complete after the 22nd fractionation. By fractionation of pure neon, the amount of neon obtained in fractionations 23 and 24 was found to be 1.25%. Thus it was decided to take the fractionations 12 through 22 for helium. The recovery of helium is believed to be practically complete with very little contamination by neon. These tests enabled the total fractionation amounts to be corrected for residuals to a higher degree of accuracy. Following this, vials 1A, 19A and 5A were analyzed. Immediately after these analyses the system developed a leak and had to be repaired and outgassed. It was then necessary to run more calibrations and ground sample analyses. After that vial 12A was analyzed.

Shortly after this last analysis a number of changes in technique were made. The principal change was the flashing of the gage at fairly high temperatures and subsequent establishment of continuous operation of the gage wire at the correct operating temperature. The gage wire has been retained in a high vacuum at this temperature for the past several months. Following the establishment of the resulting increased stability of the gage, a series of ground samples and vials 21A and 28A were analyzed. These results are given in Table 3 and are self-explanatory.

Following the establishment of a stable and sensitive charcoal analyzer and initial check of the Glückauf technique it was decided that no more analyses would be run on the Michigan instrument until Professor Paneth and his collaborators had finished analyses of the sample vials that had already been sent him. This was deemed advisable due to the small backlog of upper air samples and the need for samples by other analytical schemes that will be described shortly. The work with the Michigan charcoal analyzer appears to verify the preliminary work of Paneth and his collaborators that the percentage of helium and neon in the upper air samples is about the same as for ground air. It is not now known whether the Michigan charcoal analyzer will be used to analyze more upper air samples. The most important piece of work that remains to be done on this instrument now appears to be the ultimate check of its reliability by analysis of accurately blended gas mixtures. It will not be discussed at this time how these accurate blends are to be obtained.

5.23 Mass Spectrometric Analyses - Westinghouse Laboratory

Shortly after the establishment of the upper air sampling program a visit to the Westinghouse at East Pittsburgh revealed that Dr. J.A. Hipple and his associates had just completed a leak detector which seemed to be much more sensitive to helium than previous models. At that time the helium in normal atmospheric air gave 20 divisions deflection on the ion collector meter with an accuracy of about 1 division (i.e. 5%). Dr. Hipple thought that with care the output could be increased by a factor of ten providing the analyzer was stable enough.

Following procurement of the first few rocket samples some months later, vials 1C, 1D, 2C*, and 2D were sent to the Westinghouse Laboratory for analysis by this technique. Unfortunately, due to the small amount of air in the rocket samples, it was not possible to follow the usual method in mass spectrometry applied to gas analysis of filling a fairly large volume to a standard pressure (usually about 50 microns mercury) and letting the sample leak through the slit to the analyzer tube. Instead, it was necessary to establish a relationship between output from the ion collector to pressure of helium in the volume back of the slit leading to the analyzer. The tentative results are given in column 3 on page 66. These results are taken directly from the report by Westinghouse Laboratory. Because of the difficulty of procurement of the upper air samples and the fact that the small amount of samples precludes the full exploitation of this method it was decided that this technique would not be followed up, at least for the time being.

Before the personnel of Westinghouse Laboratory (this work was now headed by Dr. R. E. Fox) made the previously described analyses for helium the vial contents were split so that the second portion of each sample available was analyzed by the Westinghouse Analytical Mass Spectrometer. The percentage composition correctly normalized to 100% that appeared to be the most reasonable are given on page 66 of Table 3*#. The presence of a fairly large but unexpected m/e peak of 18 was interpreted as being due to a small amount of water vapor left in the neck leading to the gas storage chamber after sealing of the glass vial to the analysis system≠. This appeared to be verified by the presence of a small amount of rust on the surface of the iron pellet used to break the thin glass septum of the glass vial. The m/e 30 peak which was present in the rocket sample spectra but not in the ground sample spectra was interpreted as being due to nitric oxide (NO). This peak evidently was not due to a hydrocarbon since there was no contribution to the m/e 29 peak. The suggestion by the Westinghouse analyses of the possible presence of nitric oxide in the rocket samples initiated a prolonged study which will be discussed in Sections 5.24 and 5.25 of this report.

5.24 Mass Spectrometric Analyses - National Bureau of Standards

Following our inability to find any analytical techniques (see Section 5.25) that could help settle the problem about possible oxides of nitrogen from the sampling bottles it was decided to use a few more of the scarce upper air samples and to exploit mass spectrometric techniques as

---

* Unfortunately the sample in vial 2C was lost completely in sealing the vial to the analysis system.

\# Sample 1C was lost due to a leaky valve which allowed atmospheric air to leak in and spoil the sample.

≠ It is possible that the water vapor detected in vial 1D was due to the explosion of V-2 27 discussed in Section 5.19, but the water vapor in vial 2D can hardly be explained in this way.

much as possible. Inquiry was directed to different investigators around the country and it was found that there appeared to be no essential differences as to sensitivity in the various commercial mass spectrometers in use in this country#. It was possible, of course, that there were certain special research installations which could detect smaller ion peaks but this did not appear to be the case. In the course of this inquiry Dr. Fred Mohler of the National Bureau of Standards became interested in this problem and kindly offered to place his entire staff and apparatus at our disposal for several days.* On this basis a number of blends of nitric oxide (NO) and nitrous oxide (N_2O) in air were prepared for calibration purposes. Previously, three upper air samples (5C, 16C, and 18B) had been split by a specially constructed mercury-glass gas handling system. As will be noted in the sections of Table 3 the four subdivisions of each of these three samples were given the additional numbers I, II, III, and IV respectively.

The procedure followed by Dr. Mohler and his collaborators in the interpretation of the m/e peaks into terms of percentage concentration was that of the standard use of the fragmentation ions and the choice between several possible interpretations (at times) by means of minimum residues. This technique can be applied quite efficiently even when there are several quite similar substances, e.g. mixtures of several hydrocarbons, but it is required that the fragmentation spectra for each possible constituent be available, and, for best results, the percentage compositions of each constituent should be at least a few percent. Fragmentation spectra for two oxides of nitrogen (NO and N_2O) were obtained and checked with blends where the nitrogen oxide concentrations were a few percent. When it came time to reduce the mass spectra of the upper air samples in terms of percentage compositions it was found that an unequivocal interpretation of the low percentage constituents could not be given. The best interpretation appeared to be the one given on page 67 of Table 3. There was another possible interpretation which appeared to be as good as far as the mass spectrometer was concerned, but did not agree with the results of the microwave spectrometer (see Section 5.25). In these spectra small but distinct m/e 30 peaks appeared in the upper air samples which did not appear in spectra of ground air. This was first detected in the mass spectra obtained on the Westinghouse instrument as noted in Section 5.23. The m/e peaks of 18, which were probably due to water vapor in the Westinghouse spectra, did not appear since the experience gained from the first analyses resulted in different techniques of gas handling. The reasons that an unequivocal interpretation, as far as possible oxides of nitrogen are concerned, could not be given follow from the following considerations:

Consolidated Engineering Corporation of Pasadena, California has just announced a new type mass spectrometer which appears to be better than previous commercial instruments, but this was not available at the time of this investigation.

* As was expected the experimental accuracy obtained at the Bureau of Standards was about the same as at the Westinghouse Laboratory. Because of the time lapse of one year between the Westinghouse analyses and the decision to repeat the mass spectrometric analyses it was felt that nothing would be lost and perhaps something might be gained by trying a different type of analytical mass spectrometer.

a) If nitric oxide (NO) is brought into contact with free oxygen the classical reversible reaction ensues:

$$O_2 + 2NO \underset{\text{dark}}{\overset{\text{light}}{\rightleftharpoons}} 2NO_2$$

Thus one should really talk about the possible presence of nitrogen dioxide (NO_2) rather than NO in an air sample in a dark container (this is not to be confused with the form from the inital source). However, the main m/e peak of NO_2 is 30 rather than 46[11]. Thus the presence of a small m/e peak of 30 and the absence of a 46 peak is not contradictory to the presence of one or both of these oxides of nitrogen.

b) Nitrous oxide (N_2O) is known to be present in the atmosphere in small amounts[12]. It has a m/e fragmentation peak of 30 but a much larger peak of 44[11]. One might then think that the m/e peak of 44 would give evidence as to possible interpretation of the m/e peak of 30. Unfortunately, carbon dioxide (CO_2) also has its main m/e peak at 44. The fragmentation peak of 28 for CO_2 can not be used to determine its amount since it is overlapped by the very much larger contribution to this peak by molecular nitrogen (N_2); the small fragmentation peak of 16 can not be used to any advantage due to the presence of some free oxygen; the peak of 12 can not be used efficiently due to its low value and large relative error. Thus, from the mass spectra, one can not distinguish between N_2O and CO_2 in small concentrations in air samples.*

c) An additional difficulty arises from the fact that most mass spectrometers do not give the correct value

---

* Slobod and Krogh (J. Amer. Chem. Soc., 72, p. 1175, 1950) have recently determined the amount of N_2O in ground air by means of mass spectrometry. Using a process of fractional distillation of a large amount of ground air they found that the percentage concentration of N_2O was 0.5 ± 0.1 ppm. If this concentration holds for all of the atmosphere, the resulting amount would be 4 mm atmospheres -- a value quite agreeable with the results from infra-red solar spectroscopy (see reference 12). At the 1950 conference on Molecular Spectroscopy, Columbus, Ohio, Mr. John Shaw of Ohio State University announced the result of another analytical method of measuring the N_2O content in ground air. By studying the absorption in the 3.9 micron region through a large amount of air (using a multiple reflection absorption cell) and specially prepared N_2O blends he concluded that the N_2O content in ground air appears to be less than 0.5 ppm. Thus it appears that the N_2O distribution in the atmosphere is still unresolved.

for the carbon dioxide content of atmospheric air (0.03%) but give a value about an order of magnitude too high. This seems to come about mainly from the fact that nearly all commercial instruments in use in this country are used, at time at least, for qualitative and quantitative analyses of hydrocarbon mixtures. This results in small ion backgrounds which can never be completely eliminated from any instrument once this type of analysis has been handled. Pumping of the spectrometer for several days (as was done at the Bureau of Standards) will lower this background but will never completely eliminate it. Some of the residual background apparently comes from the oils of the diffusion pump. It is now believed by this staff (University of Michigan) that the mass spectrometric technique could be exploited for air analyses for our purposes only by purchase of a new instrument (so designed that sensitivity is increased to the utmost, perhaps by loss of resolution) and its use only for air samples and blends of the approximate concentrations to be expected. This last point is important otherwise a new background might be introduced in the analyzer through the use of a pure constituent for the establishment of fragmentation spectra.

5.25 Analyses for Oxides of Nitrogen - University of Michigan and Columbia University

Following the interpretation of the m/e peak of 30 by Dr. Fox of Westinghouse Laboratory as possibly beind due to nitric oxide (NO) it was decided to look into the matter. It was quite clear, of course, that the sampling techniques developed were not fully adaptable to the capture and analysis for atmospheric constituents such as ozone, atomic oxygen, carbon dioxide, water vapor, and oxides of nitrogen. While these constituents are extremely important to a complete understanding of the photochemistry and of the radiation balance of the atmosphere, they are all of quite low concentration and their sorptive properties preclude correct analyses following their capture by such sampling techniques as could be developed for use in rockets. However, since the work of upper air sampling at such heights was unprecedented, it was deemed essential that this initial suggestion by Dr. Fox should be investigated quite thoroughly.

The present theoretical interest in the possible presence of oxides of nitrogen in the upper atmosphere arose from a suggestion by Chapman and Price[13]. These views have been expanded in a review article by Bamford[14] and in a number of publications by Nicolet[15]. It appears possible that certain oxides of nitrogen might be formed in the upper atmosphere much in the manner that has been offered as an explanation for the formation of the small amount of ozone present. A theoretical discussion of this will not be given in this report. Suffice to say that a number of possible mechanisms for their

formation and destruction have been suggested and indeed certain observations* in independent fields of scientific research point to the conclusion that oxides of nitrogen do exist in the atmosphere in measureable quantities.

In an attempt to find an analytical technique which could help throw light on the unsolved questions that arose from interpretation of the mass spectra a number of fields were investigated:

a) It soon became clear that Geissler emission techniques could not be used since one of the standard methods of producing NO electronic emissions bands is from Geissler emissions in an oxygen-nitrogen atmosphere.

b) Ultraviolet absorption spectroscopy can not be used since such high energy quanta would surely alter the equilibrium distribution of any of the oxides of nitrogen initially present or perhaps even form them[14].

c) Standard infra-red absorption spectroscopy gave little hope since the small amount of sample and the small concentration of the constituents to be identified and measured would give an absorption of less than 1% even in the strongest parts of the fundamental frequency absorption bands. There appeared to be some hope through the use of the so-called gas analyzer[16] which is a double-beam zero-dispersion instrument. These instruments have been used quite effectively for such purposes although the amount of gas sample necessary is usually of the order of 100 cc NTP or more. It was thought that this instrument could be modified for gas samples as small as 1 cc NTP. This

---

* The presence of N_2O in the atmosphere has been discussed in Section 5.24. There is some evidence which point to the presence of other oxides. Elvey, Swings, and Linke (Ap. J., 93, p. 337, 1941) have discussed the possible interpretation of certain emission lines of night sky spectra as arising from excited states of NO. On the basis of the first ultraviolet solar spectra (first reported in Phy. Rev., 70, p. 781, 1946) obtained by the Naval Research Laboratory above the ozone absorption, Götz (Experientia, 3, p.238, 1947 and Zeit. fur Met., 1, p. 298, 1947) discussed the possibility that the absorption below 2400 Å might be due to NO_2^+ or NO^+. In the later complete analysis of these spectra Durand, Oberly, and Tousey (Ap. J., 109, p. 1, 1949) mentioned that some unresolved absorption lies in the region where a strong band of NO centered at 2264 Å exists. Edgar and Paneth (J. Chem. Soc., p. 519, 1941) have detected NO_2 in ground air by means of fractional distillation. Hayhurst and Pring (Trans. Chem. Soc., 97, p. 868, 1910) apparently detected this gas at higher altitudes in the atmosphere. Sutherland and Callendar (Rep. Prog. Phy., IX, p. 18, 1942-43) have discussed the evidence for and against the presence of these oxides on the basis of infra-red spectra.

technique was not exploited since it would have required a great deal of experimentation and since the analytical precision that was calculated on the basis of present instruments did not leave a sufficiently large safety factor.

d) Initially, colorimetric techniques[17] were not thought to be applicable since they usually require gas samples orders of magnitude larger than would be available from upper air sampling. Later work revealed that these techniques could be modified. This work will be discussed shortly.

e) The recent development of the microwave spectrometer appeared to be applicable for the detection of N_2O but not for any of the other oxides of nitrogen. This technique follows from the development of microwave equipment in the radar program of World War II. Its use in spectroscopy lies in the fact that certain molecules have permanent electric dipole moments and thus exhibit active absorption bands from pure rotational transitions. Thus those molecules with permanent dipole moments can be detected in the microwave region provided their moments of inertia are such that some absorption bands lie in the relatively narrow workable microwave region. Such a case holds for N_2O[18] but not for NO. Professor Charles Townes of Columbia University has very kindly helped in this respect. The initial investigations indicate that there is less than 10 ppm N_2O in the upper air samples but this is still only tentative.* Dr. Townes is awaiting the construction of a new microwave spectrometer which promises to have more sensitivity than the previous instrument used. It is hoped that this work can be completed in the near future.

Following the repeat of mass spectrometric techniques at the National Bureau of Standards and the repeated but still slightly ambiguous results it was decided that all fields of analysis should be looked at again but in a more apprehensive manner. In addition a method was needed for study of certain sorptive processes. The result of this study was that the colorimetric techniques developed by Patty and Petty[19] could be used provided that the technique could be modified to handle a volume of gas about 50 times smaller than the amount required by them. It was found that this could be done but with a loss in sensitivity. Fortunately, this loss was not enough to nullify the use of the method.

---

* Any N_2O present in the samples can be concentrated by freezing it out with liquid nitrogen. This is feasible because of the very small amount of gas required by the microwave spectrometer.

The technique described by Patty and Petty was found to be an application of the long known Greiss-Ilosvay reagent which is a mixture of sulfanilic acid and alphanaphthylamine. It detects nitrites by the formation of a characteristic red dye which can be easily studied by standard quantitative colorimetric techniques the nitrites being formed from a water solution of the nitrogen oxides. Petty and Patty required 50 cc NTP of gas and found that the minimum detectable concentration of the nitrogen oxides was 5 ppm. By varying the technique slightly it was found that for 1 cc NTP of gas blend or sample the minimum detectable concentration was about 50 ppm. The reaction chamber developed is shown in Fig. 47.

Before proceeding with the check of possible adsorption or generation it was decided to check the mass spectrometric analyses by the Bureau of Standards since three vials had been split for this specific purpose. Sub-vials 16CIII and 5CIII (a sub-vial of 18B being unavailable at that time) were analyzed according to the techniques developed. These analyses gave 480 ppm (0.05%) by volume for 16CIII and 180 ppm (0.02%) by volume for 5CIII. These are to be compared with the analyses by the Bureau of Standards approximately 0.1% (sub-vial 16CIV) and a trace (less than 0.05%) (sub-vial 5CIV), respectively. In light of the rather crude colorimetric techniques used and the assumption in interpretation of the mass spectra data that the m/e 30 peak was due to nitric oxide (NO) alone, these results appeared to be consistent with the presence of a small concentration of oxides of nitrogen in the sample vials. It appeared advisable, at the time, to test one of the original vials (not split) for this constituent by the colorimetric technique. Unfortunately, the first vial 12C, was lost due to premature fracture

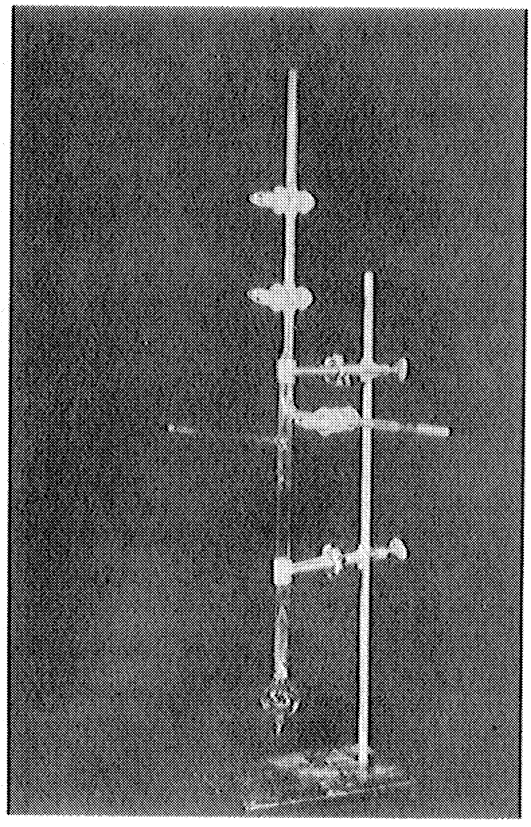

Fig. 47. Reaction Chamber for Colorimetric Analysis

of the septum, and it was necessary to choose another (vial 3C) from the stockpile. This analysis gave a percentage concentration of 83 ppm (0.01%) by volume. This appeared to be inconsistent with the other results and it seemed pertinent to make a careful check on the possible effects of sampling procedure.

When nitrogen oxide blends in air were prepared and introduced into the glass vials for analysis simulating the rocket sampling techniques as closely as possible, it was found that a number of inconsistencies were obtained. In short, the blends appeared to carry through the sampling technique somewhat but the percentage varied considerably. When unblended ground air was carried through a similar procedure it also gave an indication of the oxides but the concentrations did not appear to be a matter of the amount of air used. Rather, the amount (not concentration) appeared to be constant in each vial. This suggested that the oxides were formed as a result of the outgassing of the hot glass during the hot glass seal-off of the vial from the extraction system.

A literature check on the subject of the gases generated by hot glass revealed no mention of the oxides of nitrogen but experiments described in the literature mentioned release of water vapor and carbon dioxide. Upon inquiry, Dr. R. H. Dalton of the Corning Glass Works, Corning, New York suggested that these oxides are more likely resulting from the contact of air with the hot glass. This hypothesis was checked rather carefully by using evacuated vials with and without small amounts of air and this indeed appears to be the case.

It then became clear that the conflicting results could be resolved on the basis that these oxides of nitrogen detected by the various techniques are the result of a slight interaction of air with hot glass. The apparent "carrying-through" of the blends through the sampling technique was fallacious, and the concentration of these oxides in the split upper air samples was greater than for the one not split (vial 3C) as a result of greater dilution and a larger number of hot glass seal-offs. On the basis of average conditions encountered during these experiments (when air is present) it appears that one hot glass seal-off generates about 1×10^{-4} cc NTP of the gaseous oxides of nitrogen. Thus it is evident that this slight interaction of hot glass with the sample will be unable to discredit any of the results from the Glückauf charcoal analyzers.

The work of the analysis for the oxides of nitrogen has been concluded since the original question that arose from the interpretation of the mass spectra has been resolved. The relatively crude sampling techniques developed were not intended to study the concentrations of the sparse atmospheric constituents with strong sorptive qualities or of a temporary nature. The negative results of the analytical work described here is in full accord with this original view. There remains a slim chance, however, that rocket sampling techniques may help clear the unsettled problem regarding the height distribution of nitrous oxide (N_2O) in the atmosphere.

5.26 Attempted Analyses for Oxygen - University of Michigan

Since Regener[20] and Shepherd[21] had fair success in determining the ratio of oxygen pressure to total pressure in air samples obtained by means

of unmanned and manned balloons, respectively, it was decided that this technique was worth investigating. Since it appeared their analytical techniques require too much sample it was decided to attempt analyses by a technique suggested by Dr. Lipscomb of the Chemistry Department, University of Minnesota. This technique makes use of the unique paramagnetic property of oxygen through use of the Pauling oxygen analyzer[22] manufactured by the Arnold O. Beckman Company of Pasadena, California. Although an instrument was purchased, it was never used for analysis of upper air samples since the oxygen content of the samples is greatly depleted by the sampling technique. It is believed that this is due for the most part to the hot metal seal after the evacuated bottles have been opened and allowed to capture the sample. It is hoped that the new cold seal may dimish the depletion of the oxygen somewhat. It appears, even then, that this method will not be reliable. There is a possibility, however, that the analyses of the oxygen isotope ratios can be measured by a technique to be discussed in Section 5.27.

Another use of the paramagnetic property of oxygen was investigated by an instrument with which it was hoped to measure the oxygen content of the atmosphere during the rocket flight. Fig. 48 shows the instrument as designed while Fig. 49 shows the Wheatstone bridge circuit of the four hot wires used. Two of the hot wires are located in a strong inhomogeneous magnetic field. The gas in the vicinity of the wires is heated and has a lower magnetic susceptibility than the cooler gas, the paramagnetic susceptibility of a gas being directly proportional to the absolute temperature. It is therefore forced towards regions of lower flux density and is replaced with cooler gas. This gas flow produces a cooling effect on the wires in the magnetic field. The resistance of the wires is decreased as they are cooled. An unbalance current flows through the microammeter because of the resistance change of the wire in the magnetic field and no change in the other two wires outside of the field. It was found that the success of the instrument depended on balancing out the large pressure effects which tend to obscure the smaller oxygen effect. This could be attained only for the pressure range from 50 to 300 mm. of mercury, which is too high a pressure to be applicable to measuring oxygen content in the upper atmosphere. For this reason, investigation of the method for use on rockets was discontinued.

5.27 Nitrogen Isotope Ratio Analyses - University of Virginia

Upon reading of the success in obtaining samples from the upper atmosphere Professor J. W. Beams of the University of Virginia made a request for a few of these samples for the purpose of analysis by a high precision isotope-ratio mass spectrometer. This would give additional evidence as to relative importance of molecular diffusion processes and mixing processes in determining the general composition of the upper atmosphere. Since this research was compatible with our sampling program a number of samples were assigned for analysis by this technique. The results have been recently published by Dr. J. H. McQueen[23], a collaborator of Professor Beams, and, except for corrections in altitudes and dates, are reproduced on page 68 of Table 3. Regarding these analyses we quote directly from Dr. McQueen's paper:

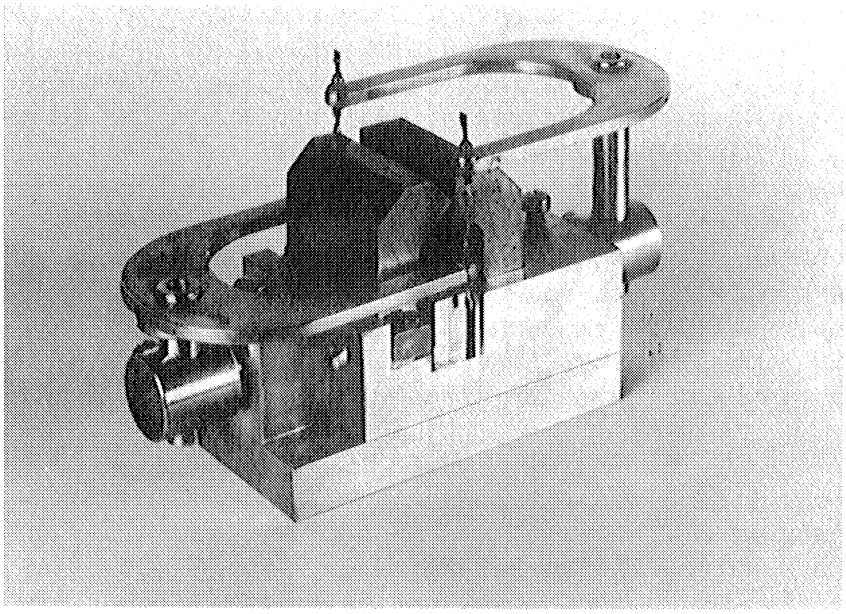

Fig. 48. Oxygen Analyzer - Laboratory Model

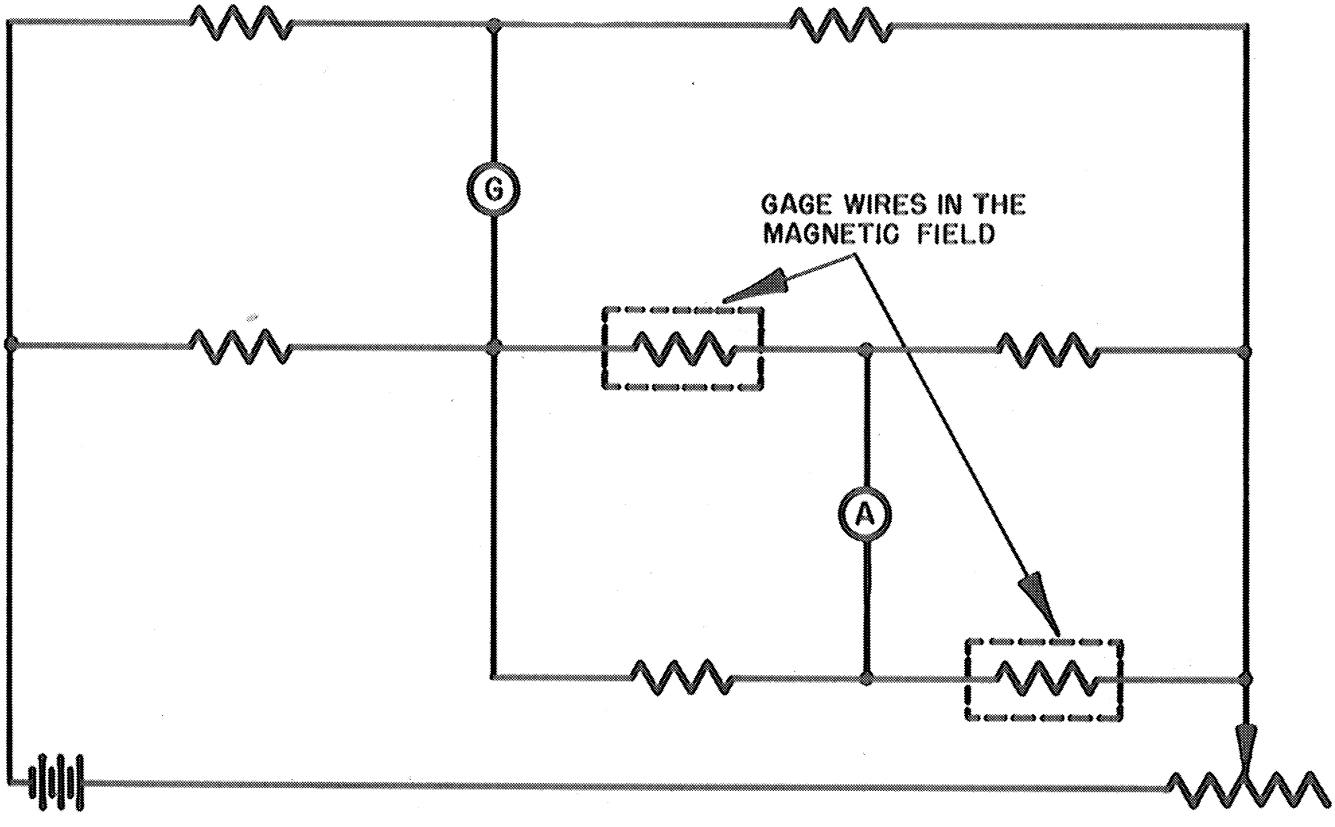

Fig. 49. Circuit of Oxygen Analyzer

"These samples were analyzed with a 60° Nier type mass spectrometer. Since the method of sampling was known to reduce the oxygen content of the samples, determinations were made only of the change in the abundance ratio of N^{14} and N^{15}. The method of analysis compared the ratio of the intensity of the $N^{14}N^{14}$ molecular ion beam (mass no. 28) to that of the $N^{14}N^{15}$ molecular ion beam (mass no. 29) in the sample to that in a standard sample collected at ground levels."

"The separation in percent were obtained from the abundance ratio of the mass numbers 28 to 29 in the sample minus that in the standard divided by that in the standard, the quantity multiplied by 100. The deviations indicated are the mean deviations of at least four sets of readings for each sample. The comparatively low precision of the analysis was due to a high background in the instrument at mass no. 29 (7 percent in some cases) which had to be subtracted from the readings."

5.28 Discussion of Apparent Discrepancy Between the Nitrogen Isotope Ratio Analyses and the Paneth-Glückauf Type Analyses

In light of the results published by Dr. McQueen it was decided to publish a short article noting the apparent discrepancy between his analyses and the analyses by the Paneth-Glückauf charcoal adsorption technique. Such an article is being written and should appear in the Physical Review in the near future. The apparent discrepancy arises in the following way:

In an atmosphere subject to a gravitational field and with no mixing the density of each constituent will fall off exponentially but each constituent will be governed by a different rate depending upon its molecular weight. If we consider the constituent i, of molecular weight M_i, in a layer of temperature T, then the density ρ_i^h of this constituent at a height h above some reference level o is

$$\rho_i^h = \rho_i^\circ e^{-\frac{M_i g}{RT} h} \qquad (1)$$

where ρ_i° is its density at the reference level. It is clear that, in an atmosphere with no convection or stirring, the ratio, $K_{i,j}^h$, of the density of two constituents i and j at the height h is

$$K_{i,j}^h = \frac{\rho_i^h}{\rho_j^h} = e^{\frac{-(M_i - M_j) g}{RT} h} \qquad (2)$$

From the dependence of the function $K_{i,j}$ upon the difference between the two molecular weights it is seen, under these assumptions, that the helium to nitrogen ratio will be at least 25 times more sensitive to the establishment of complete or partial diffusive separation than for the case of the isotopes of nitrogen ratio provided that "relaxation times" of the settling rates are about the same. A preliminary examination of the theoretical aspect of the problem indicates that this is approximately so. Comparisons of corresponding data of Table 3 from the two different analytical schemes show that this factor of 25 is not present. A more thorough examination of possible additional influences is underway.

TABLE 2

Sampling Bottles for Which Upper Air Samples Were Not Obtained

Bottle No.	Rocket No.	Firing Date	Instrumenting Agency	Installation	Reason for no Sample *
10	V-2 30	7-29-47	APL	Motor Comp.	a
30	V-2 27	10-9-47	GE	Inst. Comp.	b
34	V-2 27	10-9-47	GE	Inst. Comp.	b
I	V-2 39	3-19-48	GE	Blossom IIA	c
II	V-2 39	3-19-48	GE	Blossom IIA	c
IV	V-2 39	3-19-48	GE	Blossom IIA	c
36	V-2 25	4-2-48	U of M	Mid-Section	d
39	V-2 25	4-2-48	U of M	Mid-Section	d
43	V-2 40	7-26-48	APL	Mid-Section	d
40	V-2 33	9-2-48	U of M	Mid-Section	a
44	V-2 33	9-2-48	U of M	Mid-Section	d
52	V-2 44	11-18-48	GE	Mid-Section	a
51	SC-1	12-19-48	U of M	Nose Cone	a
53	SC-1	12-19-48	U of M	Nose Cone	a
54	SC-1	12-19-48	U of M	Nose Cone	d
57	V-2 48	2-17-49	APL	Mid-Section	e
58	V-2 50	4-11-49	U of M	Mid-Section	a
59	V-2 50	4-11-49	U of M	Mid-Section	a
62	SC-2	6-2-49	U of M	Nose Cone	a
66	SC-4	7-21-49	U of M	Nose Cone	a
70	SC-5	9-20-49	U of M	Nose Cone	f
72	V-2 56	11-18-49	U of M	Mid-Section	d
73	V-2 56	11-18-49	U of M	Mid-Section	d
71	SC-3	12-6-49	U of M	Nose Cone	f
76	SC-3	12-6-49	U of M	Nose Cone	f
78	SC-7	12-6-49	U of M	Nose Cone	a
75	SC-9	2-21-50	U of M	Nose Cone	f
80	SC-9	2-21-50	U of M	Nose Cone	d
67	SC-9	2-21-50	U of M	Nose Cone	d
101	SC-11	4-25-50	U of M	Nose Cone	d
102	SC-11	4-25-50	U of M	Nose Cone	d
103	SC-11	4-25-50	U of M	Nose Cone	d

* Reason for no Sample

(a) Bottle damaged as a result of ground impact after flight.
(b) Bottle never found.
(c) Poor rocket flight.
(d) Failure of some part of instrumentation to operate properly.
(e) Bottle punctured by high velocity fragment (probably from the steam turbine of the missile).
(f) Seal not perfect since leak rate after extraction was found to be quite large.

TABLE 3

Summary of Sample Bottle Information on Bottles

From Which Samples Were Obtained

(Bottles arranged by height of sampling)

Bottle No.	Rocket No.	Firing Date	Firing Time MST	Instrumenting Agency	Type of Installation (Fig No)
32	V-2 27	10-9-47		GE	19
45	V-2 44	11-18-48	1534	GE	21
35	V-2 35	5-27-48	0716	APL	21
37	V-2 35	5-27-48	0716	APL	21
63	SC-4	7-21-49	0901	U of M	25
61	SC-2	6-2-49	0610	U of M	25
42	V-2 40	7-26-48	1103	APL	21
65	SC-4	7-21-49	0901	U of M	25
77	SC-3	12-6-49	1132	U of M	25
60	SC-2	6-2-49	0610	U of M	25
79	SC-7	12-6-49	1716	U of M	25
69	SC-5	9-20-49	1002	U of M	25
68	SC-5	9-20-49	1002	U of M	25
74	SC-7	12-6-49	1716	U of M	25

TABLE 3 (continued)

Bottle No.	Sampling Height KM MSL	Mean Height MSL KM	1000's Feet	Intake Scoops (Fig No)	Exhaust Scoops (Fig No)	Opener (Fig No)	Sealer (Fig No)
32	61.1 - 72.0	66.5	218	19B	19B	5	14-15
45	60.8 - 69.5	65.2	214	19A	19B	6	14-15
35	55.4 - 65.5	60.5	198	19A	19B	6	14-15
37	55.4 - 65.5	60.5	198	19A	19B	6	14-15
63	54.7 - 58.3	56.5	185	26	26	6	14-15
61	53.6 - 57.7	55.6	182	26	26	6	14-15
42	49.0 - 59.8	54.4	178	19A	19B	6	14-15
65	50.7 - 54.7	52.7	173	26	26	6	14-15
77	50.4 - 53.3	51.8	170	32	32	6	14-15
60	49.6 - 53.6	51.6	169	26	26	6	14-15
79	48.0 - 50.6	49.3	162	32	32	6	14-15
69	45.0 - 47.8	46.4	152	26	26	6	14-15
68	42.0 - 45.0	43.5	143	26	26	6	14-15
74	41.4 - 44.9	43.2	142	32	32	6	14-15

TABLE 3 (continued)

Bottle No.	Crushed Volume (cc)	Pressure Corrected for Crushed Volume (mm Hg)	Ambient Pressure (mm Hg)	Mach No. of Rocket at Time of Sampling
32	-	0.65 est.	0.16	
45	7200	0.75	0.18	3.5
35	8050	0.75	0.29	3.2
37	8200	0.80	0.29	3.2
63	6350	0.19	0.43	1.6
61	8200	1.0	0.47	2.0
42	8050	1.18	0.52	2.4
65	6950	0.15	0.62	1.7
77	8200	0.8	0.68	1.3
60	7150	3.05	0.70	2.2
79	8200	1.0	0.88	1.3
69	8200	1.7	1.17	1.4
68	8200	3.6	1.40	1.6
74	8200	3.4	1.65	1.7

TABLE 3 (continued)

Bottle No.	Corrected Pressure* / Pitot Tube Pressure	Days Sample Was In Bottle	Vial Pressure After Extraction (Before sealing-off of first vial) (mm Hg)	Bottle Leak Check
32		180	36.5	no leak detected
45		20	29.1	.5μ/28 days
35		7	43.5	.25μ/3 days
37		8	48.5	.35μ/2 days
63		41	11.5	.25μ/12 hrs
61		7	46.2	.09μ/6 hrs
42		17	51.8	no check
65		34	8.9	2.0μ/5 days
77	0.46	16	28.5	.05μ/4 days
60		9	131.8	1.3μ/3 days
79	0.44	28	48.2	.05μ/1 day
69		15	64.0	0.1μ/1 day
68		22	125.3	.08μ/2 days
74	0.37	43	139.2	.04μ/2 days

* These ratios are given only for the sampling bottles with the supersonic scoops and diffusers.

TABLE 3 (continued)

University of Durham (Paneth) Charcoal Adsorption Analysis

Bottle No.	Vial No.	No. of Runs	% Deviation From Ground Values He/N_2	Ne/N_2	A/N_2	O_2(%)
32	1B	2	- 7.1	- 0.7	+ 0.6	1.0
45	12B					
35	2B	?	+ 0.9	- 0.4	0.0	< 0.5
37	3B	3	- 2.4	- 0.9	+ 0.2	< 0.1
63	19D					
61	15B	?	+ 0.3 ± 0.3	- 0.3 ± 0.4	+ 1.0 ± 0.6	
42						
65	18D					
77	25D					
60	16A	?	- 3.6 ± 0.3	- 2.0 ± 0.5	- 0.4 ± 0.2	
79	27D					
69	20D					
68	21D					
74	28D					

TABLE 3 (continued)

University of Michigan Charcoal Adsorption Analysis

Bottle No.	Vial No.	Run	% Deviation from Paneth's Ground Values He/N_2	% Deviation from Paneth's Ground Values Ne/N_2	% Deviation Corrected for Michigan Instrument * He/N_2	% Deviation Corrected for Michigan Instrument * Ne/N_2	% Conc. O_2
32	1A	1	+ 4.1	- 2.1			0.1
		2	+ 3.3	+ 2.3			0.0
		Avg	+ 3.7	+ 0.1	+ 0.4	+ 5.1	
45	12A	1	+ 6.8	+ 2.9			0.6
		2	+ 8.9	+ 1.7			0.3
		Avg	+ 7.8	+ 2.3	+ 4.5	+ 7.3	
35	2A	1	+ 3.3	-19.7			6.0
		2	- 1.5	- 5.2			6.1
		Avg	+ 0.7	-12.4	- 2.6	- 7.4	
37	3A	1	+ 3.2	-12.6			1.0
		2	+ 0.0	- 2.2			1.4
		Avg	+ 1.6	- 7.4	- 1.7	- 2.4	
63	19A	1	+ 4.0	+ 2.1	+ 0.7	+ 7.1	1.7
61	15A	1	+ 3.0	- 2.7	- 0.3	+ 2.3	
		2#	+46.4	+32.9			
		Avg					
42	5A	1	+ 9.8	+ 1.8			10.5
		2	+ 6.0	0.0			10.0
		Avg	+ 7.9	+ 0.9	+ 4.6	+ 5.9	
65	18A	1#	-66.0	+ 5.2	-	-	
77							
60							
79							
69							
68	21A	1	+ 3.8	- 4.5			
		2	+ 4.1	- 3.6			
		Avg	+ 4.0	- 4.0	+ 0.7	+ 1.0	
74	28A	1	+ 3.5	- 3.4			18.4
		2	+ 3.0	- 3.1			18.1
		3	+ 2.8	- 3.4			18.4
		4	+ 2.6	- 2.7			18.3
		Avg	+ 3.0	- 3.2	- 0.3	+ 1.8	

* Based on most recent ground calibrations. They are + 3.3 for He/N_2 and - 5.0 for Ne/N_2. These corrections are strictly applicable only to analyses for vials 21A and 28A.

\# This run disregarded due to apparent mistake in gas handling procedure.

TABLE 3 (continued)

Westinghouse, Mass Spectrometric Analysis

Bottle No.	Vial No.	He Conc.‡ ($\frac{\text{upper air}}{\text{ground}}$)	% Concentration					
			N_2	O_2	A	CO_2	H_2O(?)*	NO(?)#
32	1C	1.5						
	1D	1.8	63.6	0.04	0.8	0.04	35.0	0.5
45								
35	2D	1.2	50.3	2.2	0.5	0.02	46.5	0.5
37								
63								
61								
42								
65								
77								
60								
79								
69								
68								
74								

‡ These values were obtained from plots of the ion current (m/e peak 4) against pressure of the gas in a gas handling volume (about 50 cc) leading to the analyzer slit as the sample was being depleted by the analysis. The slopes were then divided by the corresponding slope for ground air. The analyses indicated an excess of helium, but the inherent errors precluded their repetition for error analysis because of the small amount of upper air sample available. In addition, it is seen that the helium excesse were not consistent with the A/N_2 ratios obtainable from the analytical data given in columns 4 and 6.

* The unusually large m/e peaks of 18 have been interpreted as being due to water vapor A possible explanation for this is that the water was introduced by the glass sealing-on operation, and this was not pumped sufficiently before the septum was broken for introduction of the sample into the mass spectrometer.

The presence of a fairly small but definite m/e peak of 30 has been attributed as being due to nitric oxide (NO). This peak is evidently not due to a hydrocarbon since there was no contribution to the m/e 29 peak.

TABLE 3 (continued)

Bureau of Standards, Mass Spectrometric Analysis

Bottle No.	Vial (split)	% Concentration N_2	O_2	A	CO_2*	NO*
32						
45						
35						
37						
63						
61						
42	5DIV	87.(5)#	11.4	1.1	Trace	Trace
65	18BIV	95.(6)#	1.4	1.1	1.4	0.5
77						
60	16CIV	82.(6)#	16.4	0.9	-	0.1
79						
69						
68						
74						

* Assumed that all of the m/e 44 peak is CO_2 and that the m/e 30 peak is NO.

The figures in parentheses are uncertain.

Trace is less than .05 mole percent.

TABLE 3 (continued)

University of Virginia (Beams, McQueen) Mass Spectrometric Analysis

Bottle No.	Vial No.	No. of Runs	% Deviation From Ground Values $N^{14}N^{14}/N^{14}N^{15}$
32			
45			
35			
37			
63	19B	4	+ 3.9 ± 0.4
61	15C	6	+ 2.7 ± 0.3
42	5B	?	+ 2.7 ± 0.5
65			
77	25B	?	+ 0.4 ± 0.3
60			
79			
69	20B	4	+ 0.8 ± 0.3
68			
74	28B	?	< + 0.3

6. MEASUREMENTS OF PRESSURE AND TEMPERATURE

Four aerodynamic methods of measuring either ambient pressure, ambient temperature or both have been tried on rockets. The first was a direct measurement of ambient pressure vs altitude by means of pressure gages located at a neutral point on the skin of a V-2. Temperatures were to have been calculated by the hydrostatic equation. This method was flown on V-2 25. The second and third methods made use of the aerodynamic properties of a cone moving at supersonic velocities. In the former, pressure measurements were made at the tip and at three (or four) points on the side of a right circular cone mounted on the front of the rocket. Ambient pressures and temperatures were calculated by the method of Taylor and Maccoll[24] and Stone's[25] extension to the yawed case. This equipment was flown on V-2's 25, 33, and 50. The third method consisted of measuring the angle of the shock wave generated at the tip of a cone of known angle mounted on the front of the rocket. The shock wave was detected by Pirani pressure gages mounted on the ends of probes which were mechanically oscillated through the shock wave parallel to the longitudinal axis of the cone. The angle of the shock cone is a unique function of Mach number. Having calculated Mach number, and using missile velocity data from tracking devices, the local velocities of sound and hence temperatures vs altitude were calculated. This experiment was performed on V-2's 33, 50 and 56. The probe method has been adapted to the Aerobee rocket and will be flown on Aerobee SC-15 in December. The fourth method consisted of photographing by means of a shadowgraph the shock wave formed by a wedge mounted on the front of the rocket. Mach number was to have been calculated from the shock angles. A shadowgraph was flown on V-2 42 but it failed to operate.

6.1 Ambient Pressure at a Neutral Point

Fig. 50 taken from Erdman[26] shows the pressure distribution from wind tunnel measurements on a model of a V-2 as a function of the distance from the tip at various Mach numbers. At the so-called "neutral point" about 6.3 diameters from the tip one may expect to measure ambient pressure. Temperature may then be calculated by the relation:

$$T = -\frac{gp}{R}\frac{dh}{dp} \qquad (3)$$

where

g = acceleration of gravity

p = ambient pressure

h = altitude

R = universal gas constant

Since the ambient pressure vs altitude curve is differentiated to calculate temperatures, the pressures must be measured with a higher order accuracy than the desired accuracy in temperature. This imposes a severe accuracy requirement on the pressure gages.

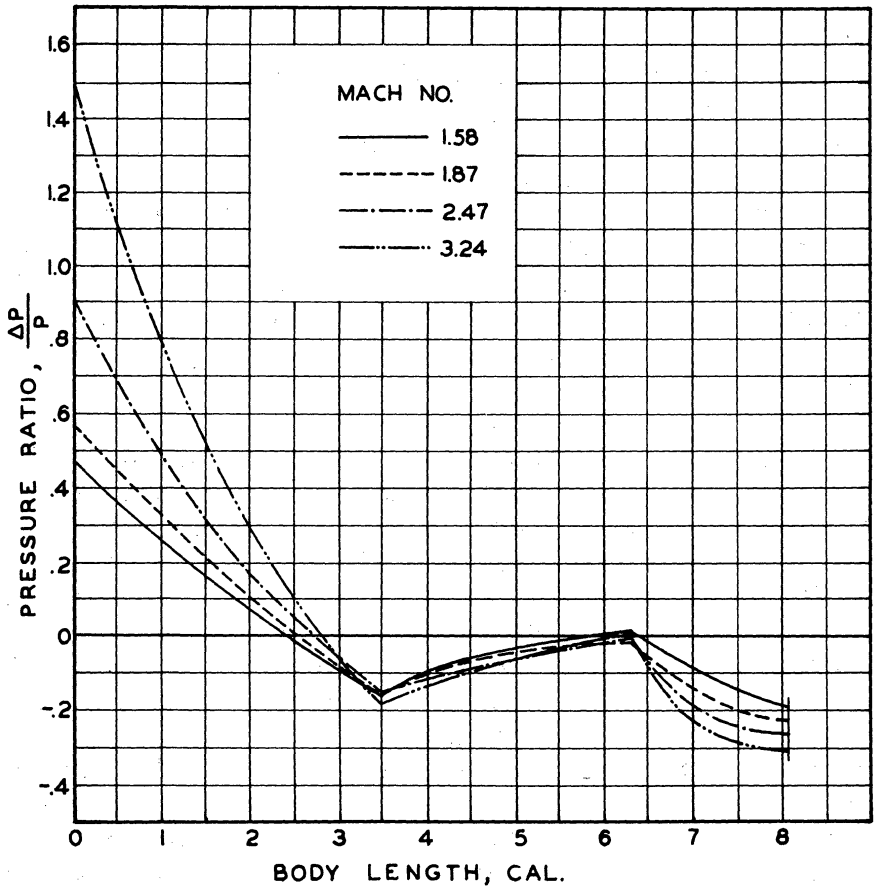

Fig. 50. Pressure Distribution on a V-2

On a V-2 the neutral point is approximately at the most forward part of the fins. V-2 25 was initially equipped with three alphatrons spaced 120° apart at the proper location. However, after the initial misfire of V-2 25 the alphatrons were replaced with the simpler Pirani gages of the first type described in paragraph 6.42. The gages were wrapped with nichrome wire for heating during preflight operations. The temperature was thermostatically controlled. No heat was supplied during flight as it was thought that the thermal capacity of the gage cases would hold the gages at constant temperature throughout the flight.

Two of the three gages operated throughout most of the flight. However, the telemeter record revealed a sporadic shift in the ground or zero volt level of the data. This was thought to be caused by a poor connection between the instrumentation ground and the telemeter ground. The pressures from the two Piranis are shown plotted in Fig. 51 and are compared with a curve derived from Whipple's[2] data for ambient pressure. No calculation of temperature was made because, as noted above, a high order of accuracy in the pressure measurement is required.

Because of the complexity of the rear installation and the inaccuracy of the available gages under the variable temperature conditions prevailing in this section of the V-2, no further attempt of this method was made.

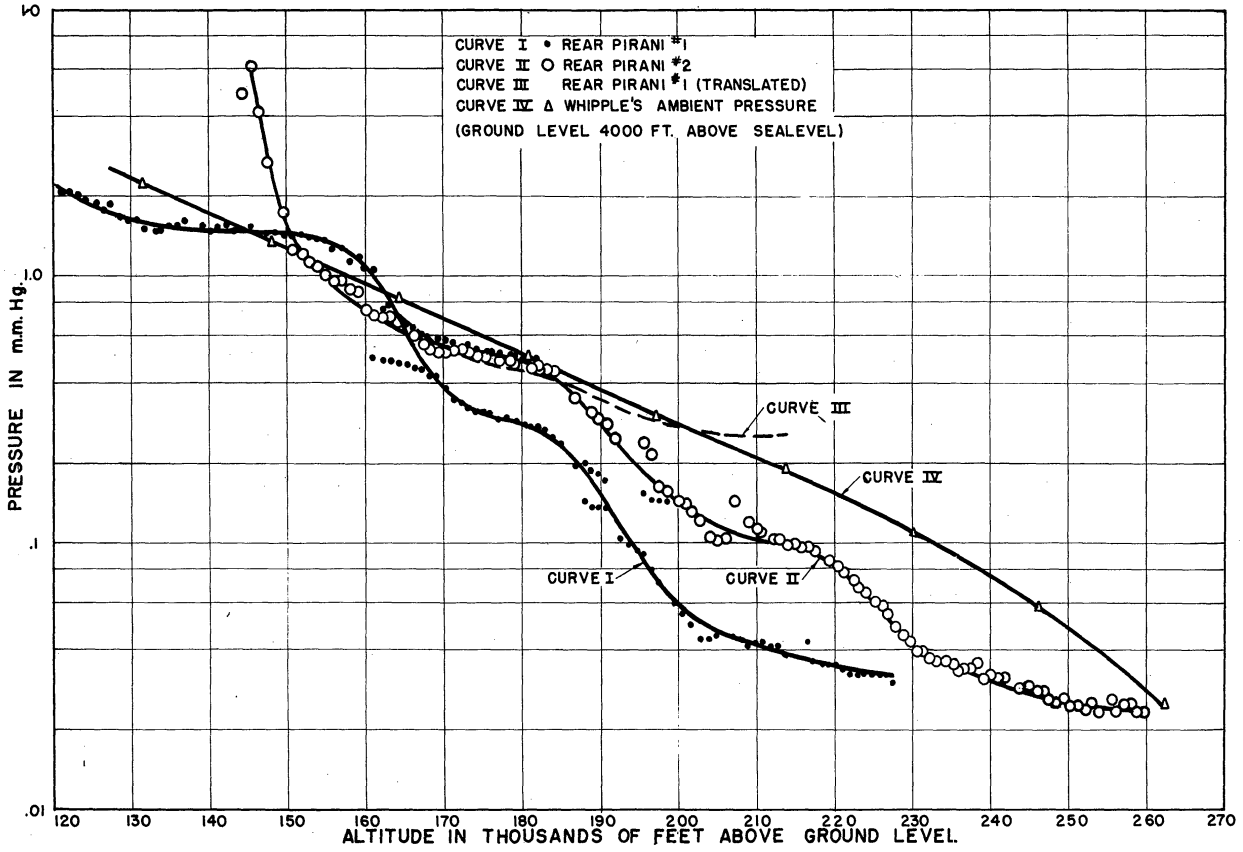

Fig. 51. Rear Pirani Pressures, V-2 25

6.2 Measurement of Ambient Temperature by Measurement of the Aerodynamic Properties of a Supersonic Cone

6.21 Theory

The theoretical method[25] of analyzing the flow about a yawing cone permits a means of determining flight Mach number from impact and surface pressures on a cone, when certain other quantities defining yaw are known. Having found Mach number and having determined missile velocity by some tracking means, the local velocity of sound and ambient temperature may be calculated.

The surface pressure on any point of the yawed cone is:

$$p_s = \bar{p}_s + \epsilon \eta_s \cos \psi \qquad (4)$$

where

$\bar{p}_s$ = surface pressure on unyawed cone

ϵ = net angle of yaw

η_s = perturbation surface pressure per radian of yaw

ψ = central angle between line of maximum pressure, and a line through the tip and the gage opening. The line of maximum pressure and the missile axis lie in the plane of yaw.

From Rayleigh's relation for $\bar{p}_o'/p'$ as a function of M and Kopal's[27,28,29] tabulation of $p_1/\bar{p}_s$ as a function of M, $\bar{p}_o'/\bar{p}_s$ is known as a function of M. In these relations:

$\bar{p}_o'$ = impact pressure behind normal shock wave at tip of unyawed cone

p_1 = ambient pressure

M = Mach number

Correcting for yaw, the impact pressure (p_o') behind the normal shock wave at the tip of the yawed cone is:

$$p_o' = \bar{p}_o' \cos \epsilon \tag{5}$$

From the above relations it is seen that:

$$\frac{\bar{p}_o'}{\bar{p}_s} = \frac{p_o'}{p_s} \left[\frac{1 + \epsilon \left(\eta_s / \bar{p}_s \right) \cos \psi}{\cos \epsilon} \right] \quad * \tag{6}$$

Thus, having measured p_o' and p_s, the Mach number may be determined. The determination is not unique, however, because $(\eta_s/\bar{p}_s)$ is also a function of M so that a trial and error method for M must be used.

From M, the ambient temperature is calculated by:

$$M = \frac{v}{a} = \frac{v}{\sqrt{kRT}} \tag{7}$$

or

$$T = \frac{v^2}{kRM^2} \tag{8}$$

---

* Recent work shows that $\cos \epsilon$ should be replaced with unity for angle of attack less than 20° for a similar configuration. See NACA Technical Note 2261, January, 1951.

where K = ratio of specific heats for air

v = missile velocity

R = gas constant for air

A fundamental difficulty of this method, or any other (such as the probe) method which arrives at temperature by a measurement of Mach number is seen in this relation: since v and M enter as squared terms, they must be measured to a high order of accuracy for reasonable accuracy in T. Although v can be measured with suitable accuracy by doppler, the pressure measurements from which M is calculated were found to require better accuracy than could be obtained from either the alphatron or Pirani gages in their current state of development.

If the surface pressures at two points on the cone are known, an alternate method to the one above may be used. In the relation

$$P_s = \bar{P}_s + \epsilon \eta_s \cos \psi \qquad (9)$$

$\bar{p}_s$, ϵ and η_s are, at any instant, equal for all points on the cone. Taking points 1 and 2 which lie angular distances ψ_1, and ψ_2 around the cone from the maximum pressure line, the expressions for $\eta_s/\bar{p}_s$ are written for each, equated, and simplified:

$$\frac{\eta_s}{\bar{P}_s} = \frac{P_{s_1}/P_{s_2} - 1}{\epsilon\left(\cos\psi_1 - P_{s_1}/P_{s_2}\cos\psi_2\right)}. \qquad (10)$$

Since terms on the right hand side can be measured, $\eta_s/\bar{p}_s$ can be determined, thus eliminating the ambiguity in M. Since $\eta_s/\bar{p}_s$ is a correction factor in the expression for $\bar{p}_o'/\bar{p}_s$, it need be known to only first order accuracy. If $\eta_s/\bar{p}_s$ could be measured with sufficient accuracy, M could be read directly from Kopal's tables. However, this would be difficult because $\eta_s/\bar{p}_s$ is a function of the difference of two nearly equal surface pressures.

One assumption which was made in the reduction of the data from the two trials of this method was that the wind velocity was zero. This is very likely not true and in the complete development of the method a measurement and correction for horizontal winds would have to be made. No method of detecting or correcting for possible vertical winds was known. Errors due to vertical winds apply to all present methods in which sonic or missile velocity is used.

6.22 Experimental Attempt on V-2 25[30]

Calculations[31] were made which showed that the ram and side pressures to be encountered on a cone at the tip of a V-2 would fall within the measurement range of known pressure gages. Therefore, the development of alphatrons and Pirani's as described in Section 6.4 was undertaken. At the

same time the design of a cone and auxiliary circuits for incorporating the method on V-2 25 was started. As noted in the discussion of the gages in Section 6.4, both alphatrons and Pirani gages were flown in the missile.

The 22° nose cone of this rocket had an impact alphatron gage mounted at its tip and three surface alphatron gages spaced 120° apart around the periphery of the cone at a distance of 21.5 inches from the tip. Unfortunately, the impact alphatron gage results were lost due to telemeter difficulties; consequently, no use could be made of the surface pressures since heliographs indicated no pitch or yaw during the portion of the flight in which the side alphatrons recorded pressure. Thus, the second method of Section 6.21 could not be used.

Fig. 52 shows the cone surface pressures indicated by two surface pressure alphatrons. The curves reveal what is believed to be a shift in zero voltage level. Fig. 52 verifies the heliograph result of little pitch and yaw.

Attempts were made to calculate ambient temperature from these surface pressure measurements by use of the hydrostatic equation, but were unsuccessful because of the large cumulative errors in the stepwise calculation.

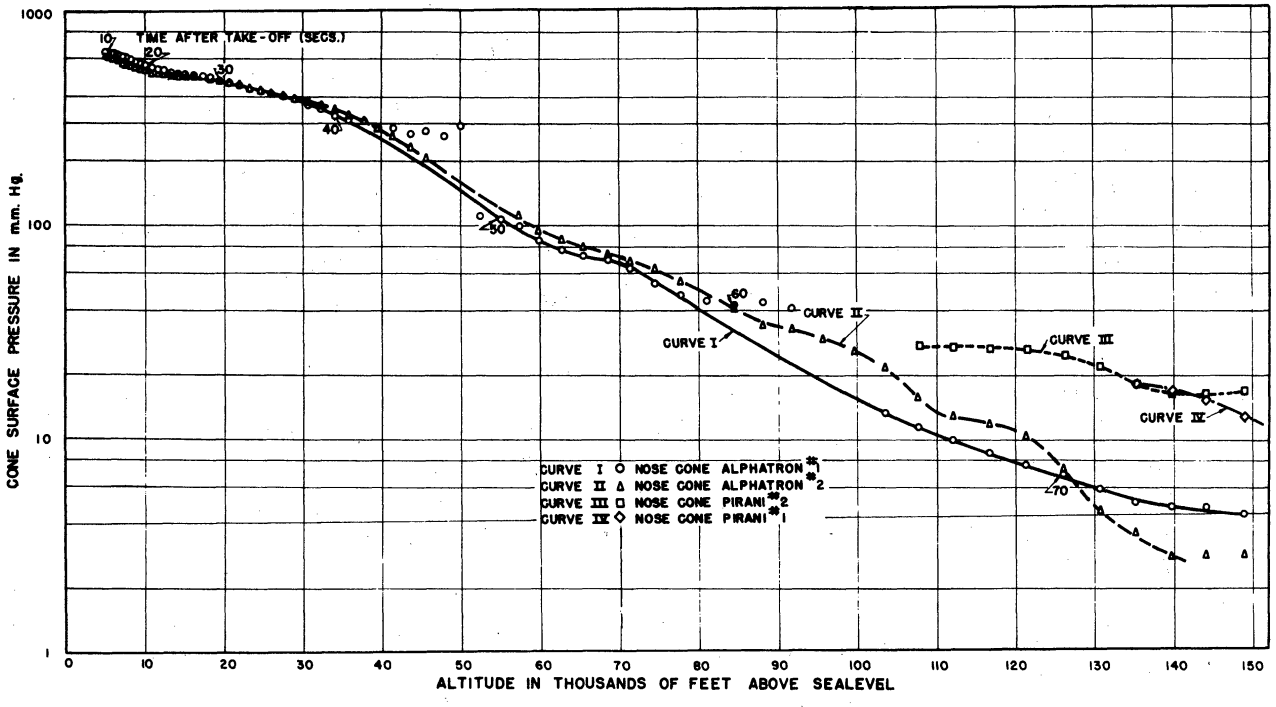

Fig. 52. Cone Pressures, Nose Cone Gages, V-2 25

Four Pirani pressure measuring gages were also installed in the cone for measuring pressures at higher altitudes. The impact Pirani gage used the same duct as the impact alphatron whereas the three surface Piranis were located the same distance back from the tip as the alphatrons but 28° around the periphery. Their pressure sensitivity range overlapped the alphatrons. Pressures were obtained from the impact Pirani gage and two surface Pirani gages but the region during which both were sensitive did not overlap except for a short time. See Fig. 53. The impact alphatron range was to have overlapped the side Pirani range.

By means of the commutator described in Section 6.4, the Pirani voltage output range was broken into three ranges. However, the various ranges for a single gage did not track, probably due to the zero voltage shift. In the case of Pirani No. 1 it was found, that if the end of one range was made to coincide with the beginning of the following range, the intersection of this plot with that of gage No. 2 occurred at a point where the heliographs indicated zero yaw. Further, the expected gage pressure curves were calculated using Whipple's data and found to lie parallel to and above the experimental curves indicating that the experimental pressure readings were off by a constant multiplying factor. The source of this error was not known and since no correction factor could be calculated, none was used.

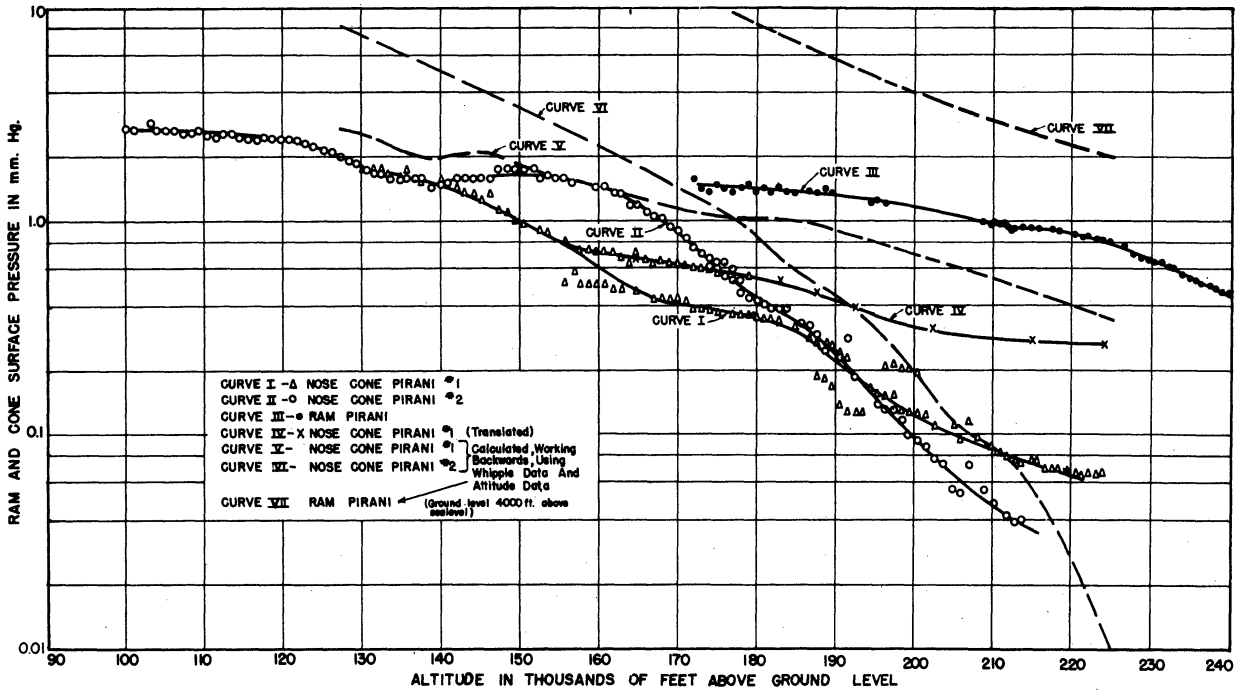

Fig. 53. Cone Pressures, Piranis, V-2 25

Next, an attempt was made to calculate ambient temperatures. Angle of attack and roll data were obtained from heliographs, while altitude and velocity were taken from doppler. All data being given as a function of time, calculations were made at one-second intervals and plotted as a function of altitude in Fig. 54.

Where no impact pressures were recorded in the range where the nose cone surface Piranis operated, ambient temperature was calculated using equation (10). Calculations were made using equation (6) where the impact and surface gage curves did overlap. See Fig. 54.

In these calculations $\eta_s/\bar{p}_s$ was determined using equation (10) and substituted along with p_o' and either p_{s_1} or p_{s_2} into equation (6) to obtain $p_o'/\bar{p}_s$. Two corresponding temperatures were calculated and plotted. The discrepancy in the two temperatures is large and is probably due to the zero voltage error noted above. Another factor, which may have caused considerable error in the impact Pirani reading, is the high temperature which probably existed at the inlet to the duct leading to this gage due to the increase in temperature through the normal shock wave followed by the presence of stagnation temperature in this region.

Figs. 55 and 56 show the alphatron gage assembly and the outside cone of V-2 25. The Piranis are not shown.

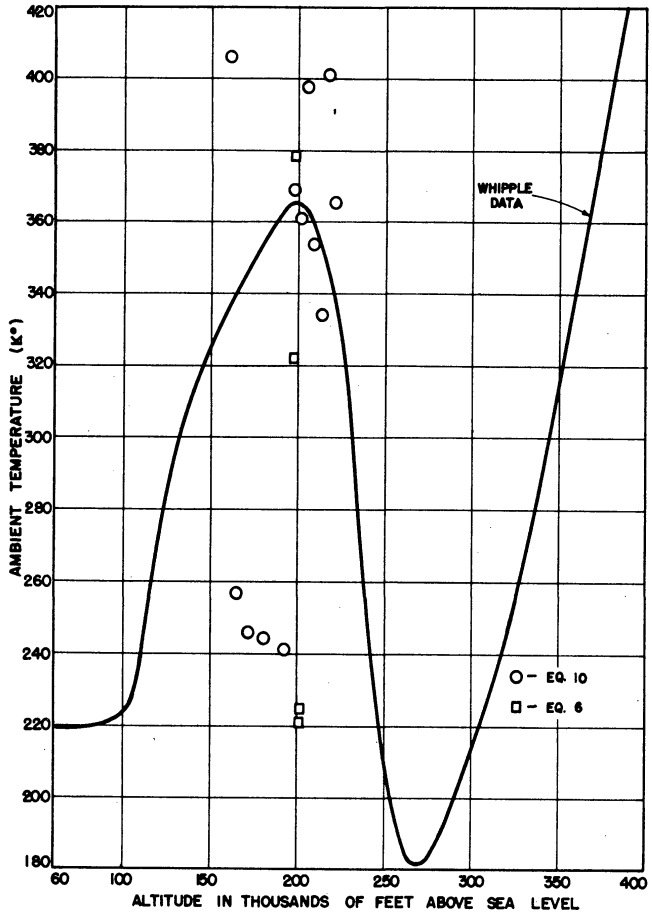

Fig. 54. Ambient Temperature vs Altitude, V-2 25

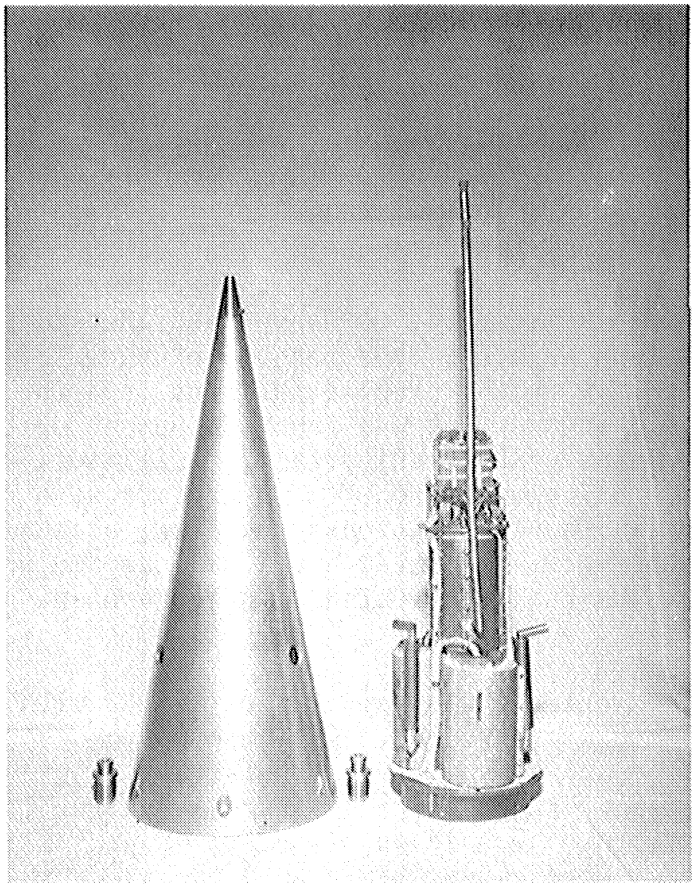

Fig. 55. Alphatrons and Cone, V-2 25

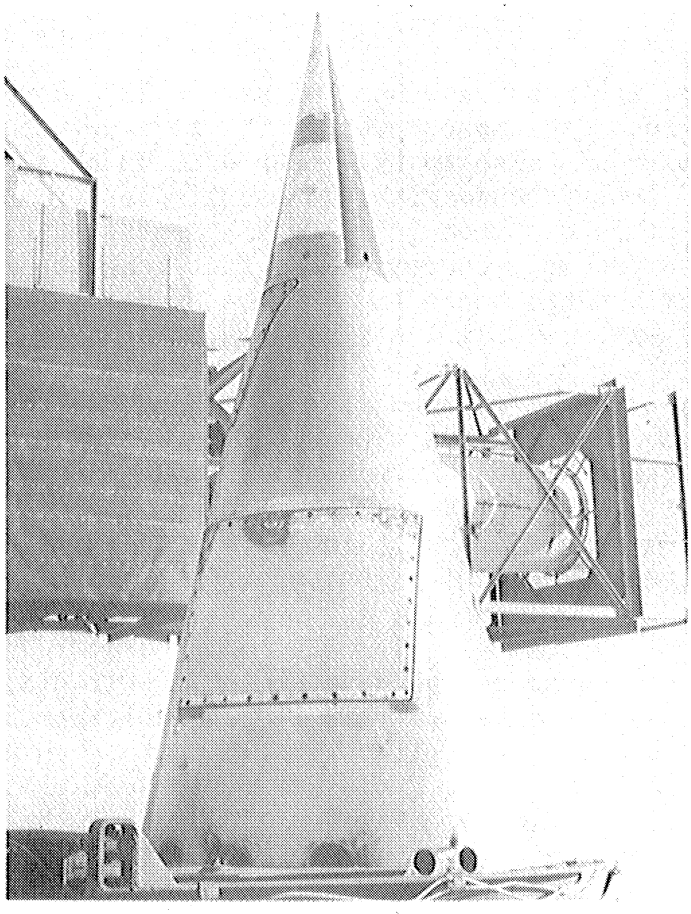

Fig. 56. Nose Cone on Warhead, V-2 25

6.23 Experimental Attempt on V-2's 33 and 50

As a result of the experience gained from V-2 25 some changes were made in the instrumentation for the cone experiment on V-2 33. The cone was accurately machined to 40° included angle. The voltage outputs of the gages were made to time-modulate the telemeter. See Section 6.44. Thermistors were inserted in the Pirani cases to permit telemetering of gage temperatures. One ram and four side gages spaced 90° were used instead of one ram and three side gages. Alphatrons were not used because of their complexity and because the space was given over to the probe experiment described in Section 6.3. Doppler was to have been used but was removed just prior to firing because of interference with the cone-Pirani driving oscillator. Because of nearly complete failure of the telemeter on V-2 33 no data were obtained. The pressure apparatus apparently functioned, however, because a two-second interval of telemetering was received at 50 seconds and showed reasonable signals. Fig. 57 shows the electronics. The gage openings may be seen in Fig. 68.

The cone experiment was repeated on V-2 50 with still further changes. The 40° cone was retained. The circuit changes by which the accuracy was improved and the pressure sensitivity range extended are described in Section 6.44. In addition to thermistors for telemetering Pirani temperatures, the tip of the nose cone was filled with ice water which surrounded the Pirani gage cases. This held the gages at nearly constant temperature thus reducing errors due to temperature correction and also increased the gage sensitivity by increasing the temperature differential between the gage case and the wire.

To insure against telemeter failure, a 12-channel magnetic recorder was carried which recorded the outputs of the most critical channels. See Section 8.2. Doppler was also to have been used on this rocket but was again removed because of interference with the oscillators of the FM magnetic recording system. This occurred in spite of careful shielding and grounding precautions and was probably caused by the fact that the recorder was located between the doppler antenna doors in a region of high field strength. Figs. 58 and 59 show the experimental installations on V-2 50.

The rocket flight was successful in most respects. Good telemetering and magnetic recorder records were obtained. The telemeter record was used for data reduction because it was superior to the magnetic recorder record. However, it is believed that the recorder record was of good enough quality for data reduction had the telemeter failed. Good signals were obtained from all five cone Pirani gages throughout their entire range of sensitivities.

During the course of the development of Piranis, it had been noted that the gages showed hysteresis. That is, the voltage output curve taken on decreasing pressure differed slightly from that taken on increasing pressure. This is shown in Fig. 60. This and other instabilities were thought to have been removed by "flashing" the gages, that is, heating them to higher temperatures than they would expect to encounter in flight. The hysteresis effect, however, appeared to be different for different batches of wire. In the gages for V-2 33, it was reduced to the point where it was masked by the scatter of the calibration points. The gages of V-2 50, however, not only

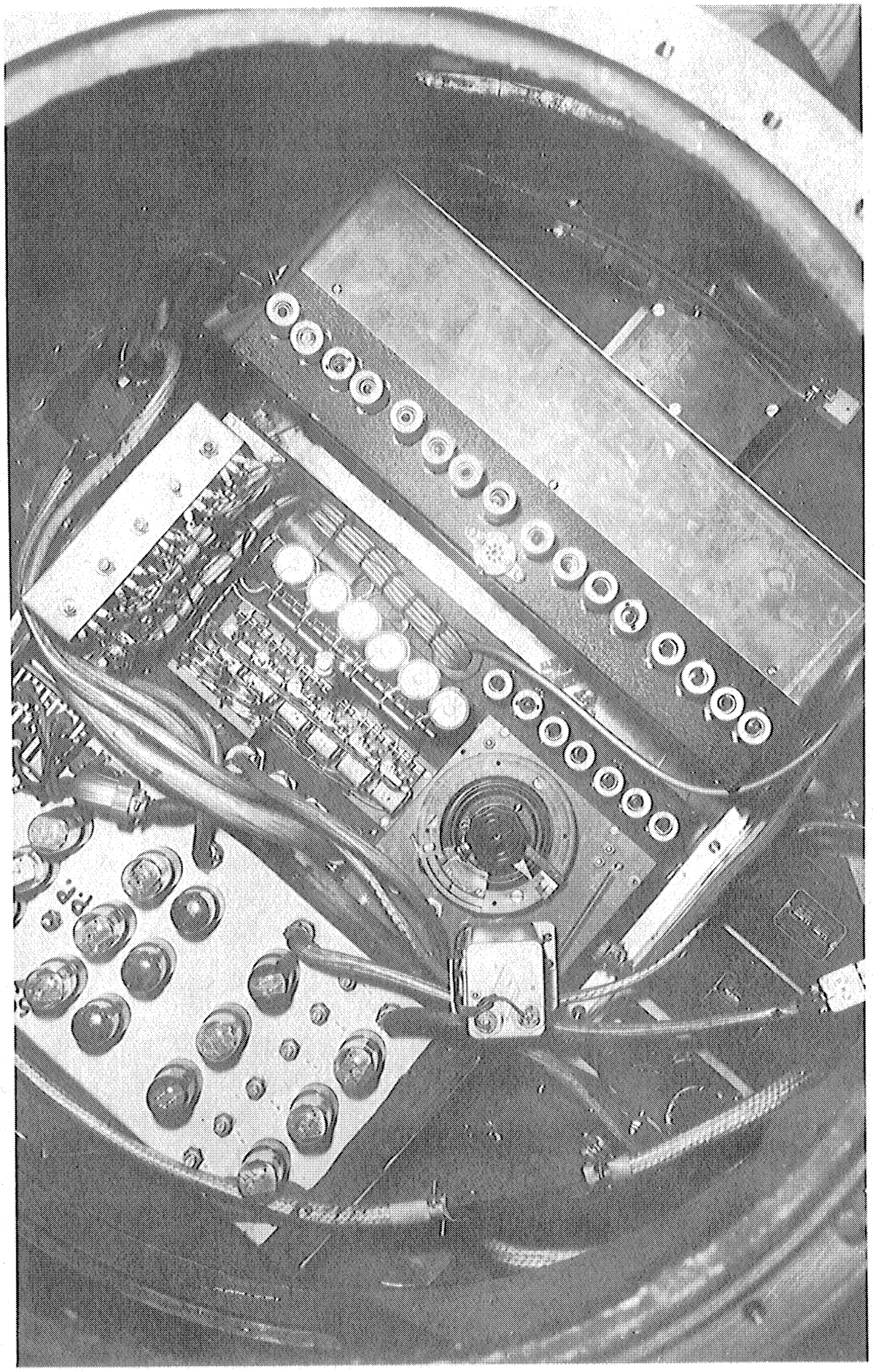

Fig. 57. Electronics, V-2 33

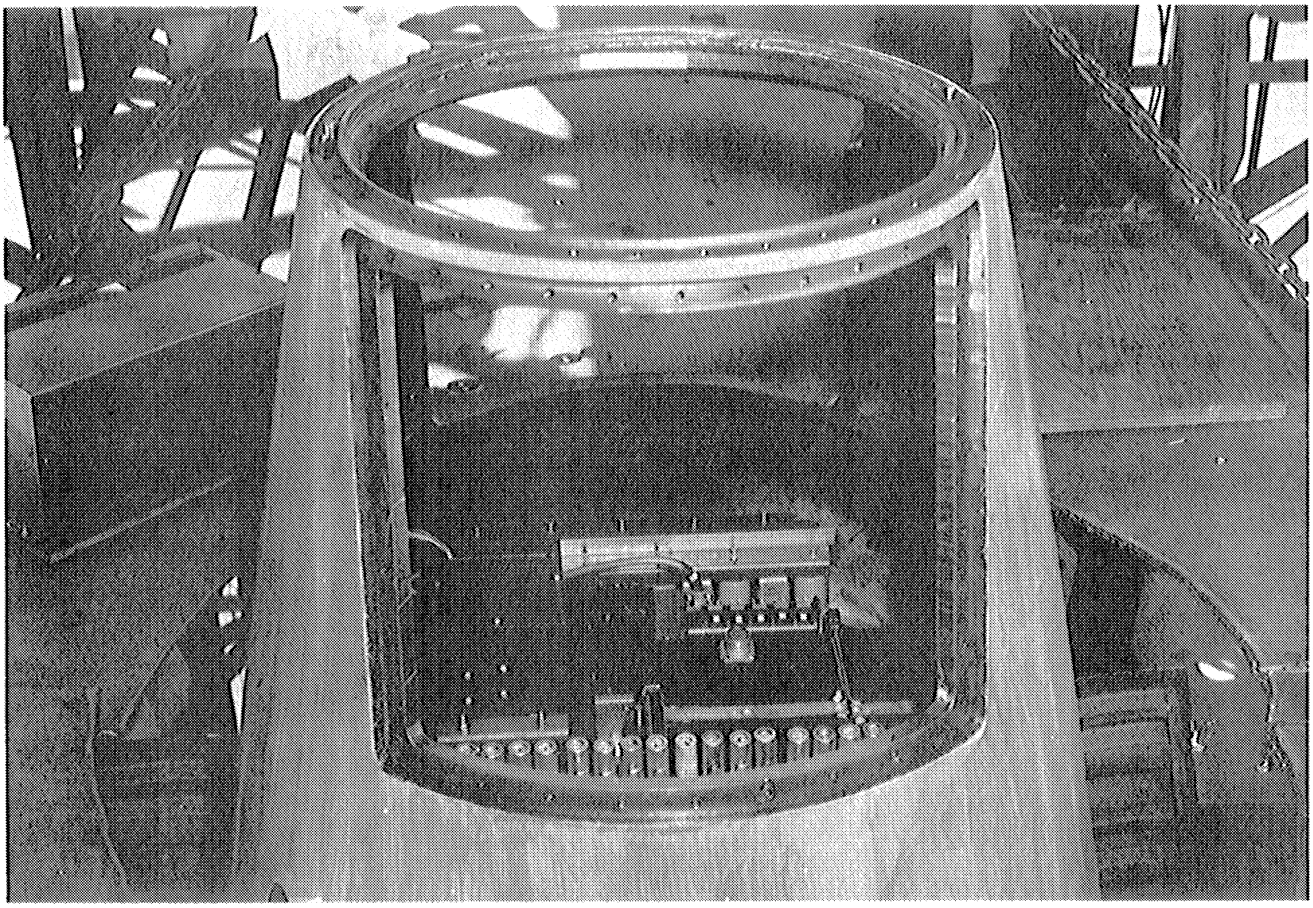

Fig. 58. Electronics, V-2 50

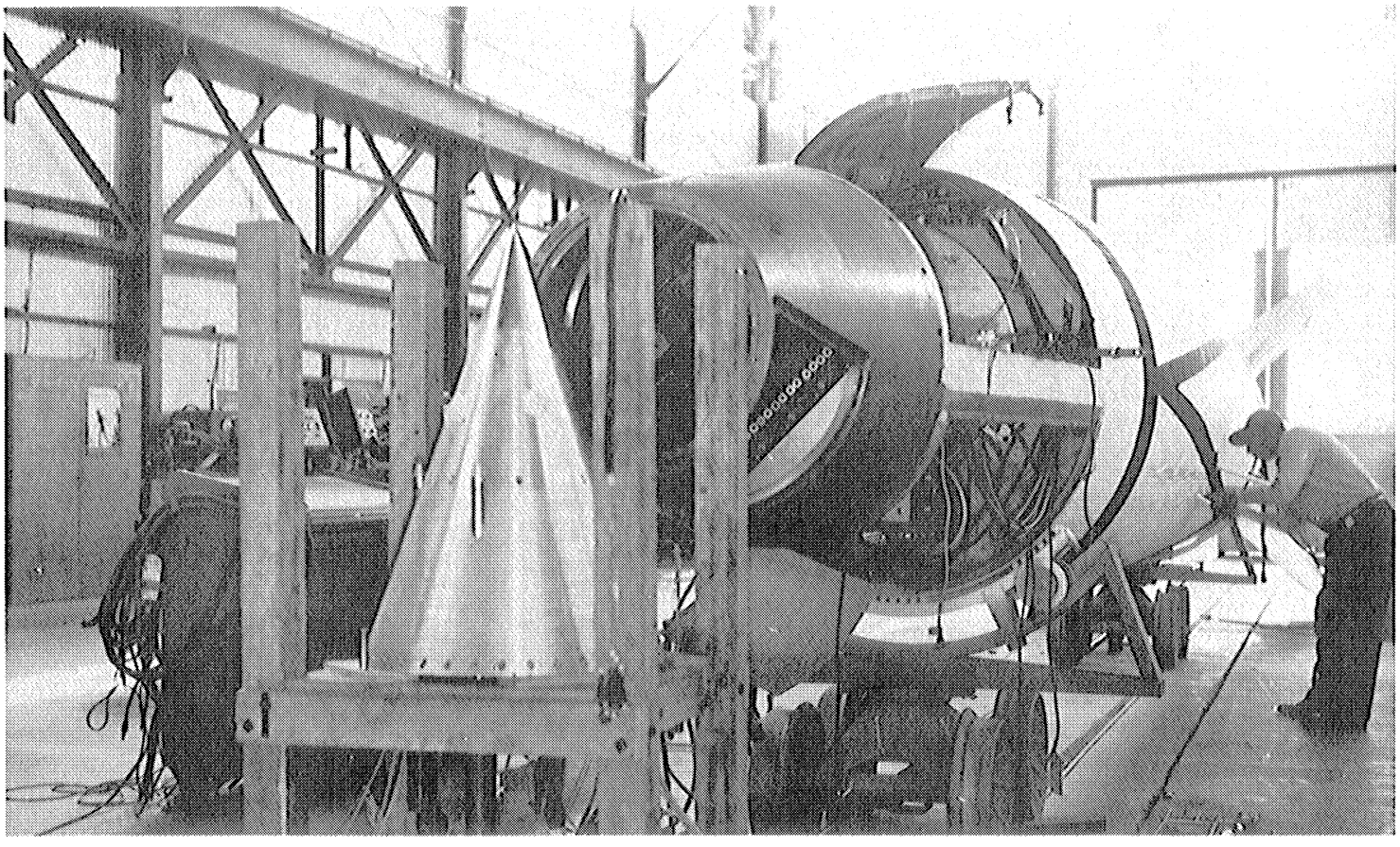

Fig. 59. Nose Cone and Probes, V-2 50

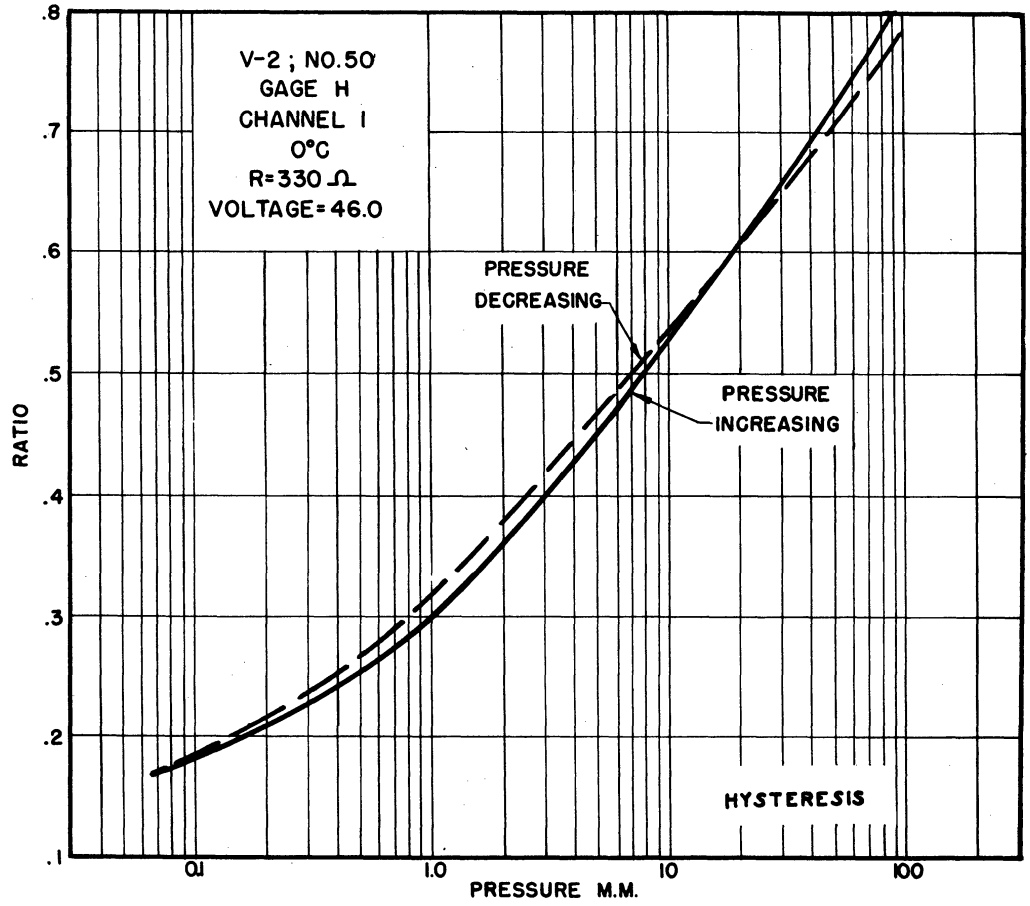

Fig. 60. Pirani Gage Hysteresis, V-2 50

exhibited marked hysteresis but the improved circuit stability and accuracy revealed the effect to be a real instability that could not be eliminated by smoothing the calibration data. The gages were flown, however, on the basis that, since the gages would encounter a continuously decreasing pressure, the corresponding calibration curve would be valid. This is not entirely true, however, because pitch or yaw can reverse the pressure gradient and put the gage on a minor hysteresis loop. The final conclusion was that the errors due to hysteresis alone preclude the calculation of ambient temperature from data obtained with the gages of V-2 50.

One solution to the difficulty might have been to use many gages, each type sensitive over a small range of pressures. This approach was not followed, however, as the experiment was dropped in favor of the probe experiment.

Reduction of the cone Pirani data was carried out. The flight voltage at which the Pirani circuits operated was determined and an interpolation curve drawn on the original calibration curve as in Fig. 61. The telemeter data were then reduced to pressure and corrected for Pirani gage wall temperatures using curves of which Fig. 62 is one and which shows a typical temperature rise for the flight. The corrected pressures were plotted against altitude using Askania trajectory data for altitude. See Fig. 63. From Fig. 63 the zero yaw side pressure can be obtained from the average of the four side pressure if the angle of yaw is not large. However, the side pressure data indicate that the angles of yaw are, for the large

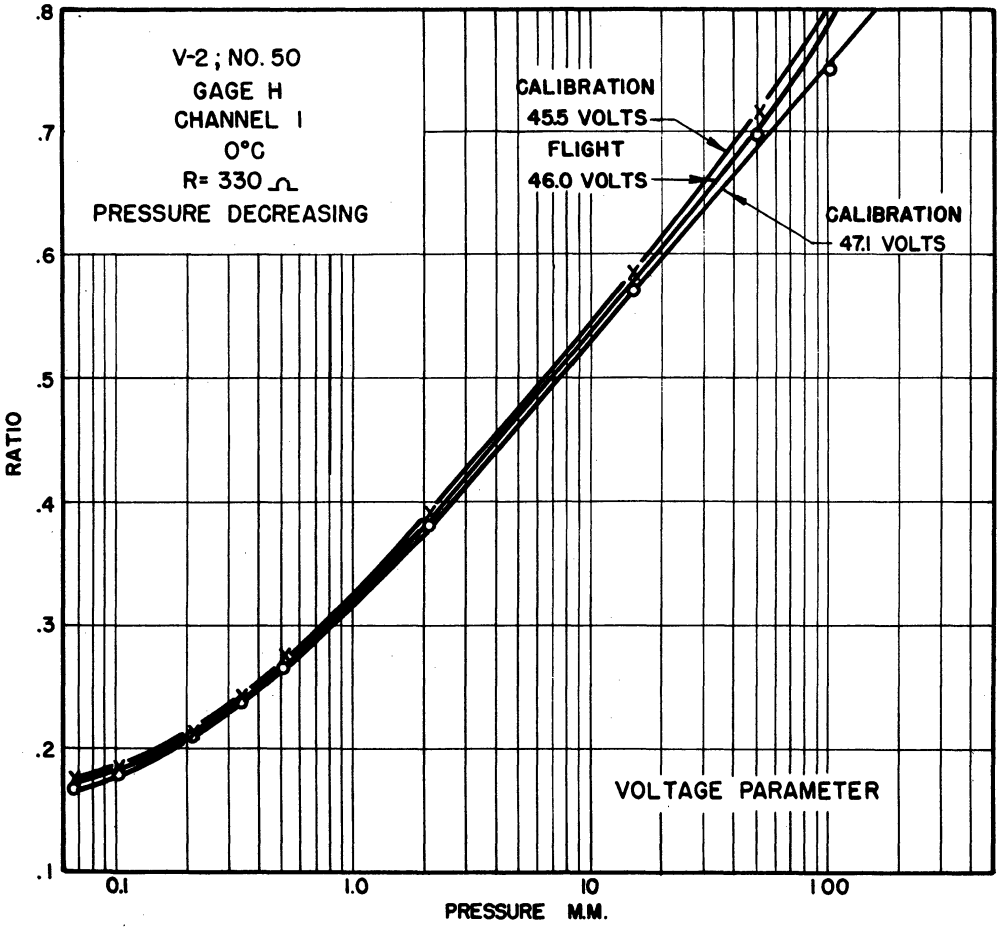

Fig. 61. Pirani Gage Calibration, V-2 50

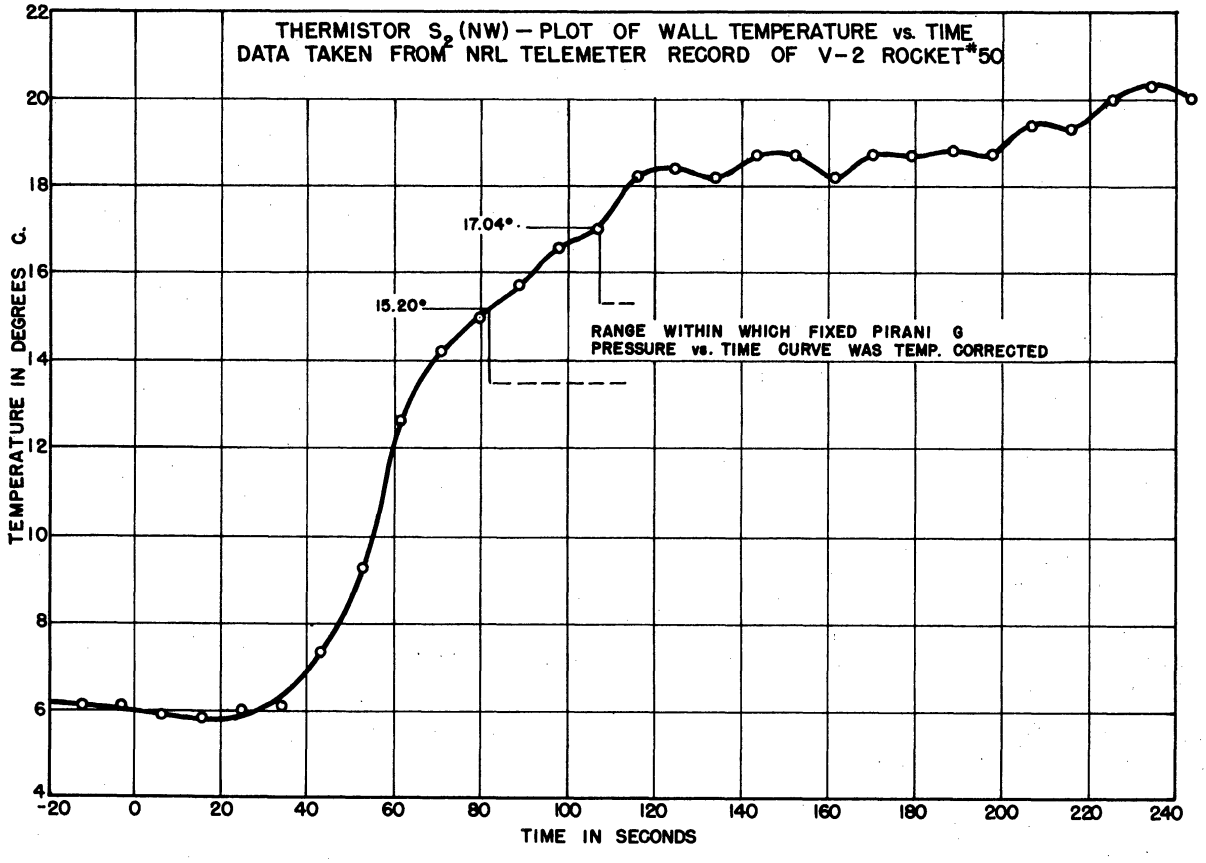

Fig. 62. Pirani Case Temperature, V-2 50

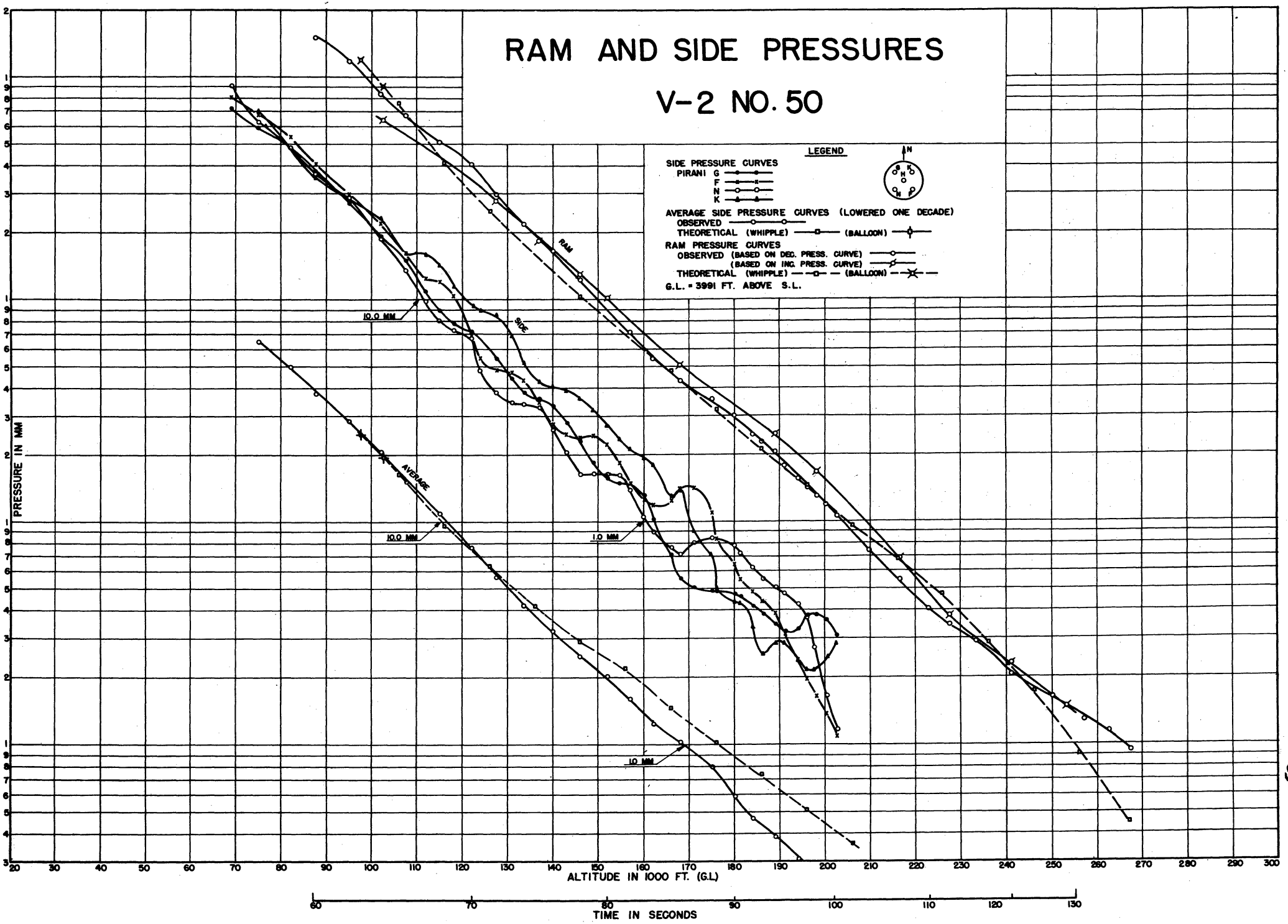

Fig. 63. Pressure vs Altitude, V-2 50

part of the curve, not great enough to modify the ram pressures by more than five percent which is much less than the error due to hysteresis. From the ratio of ram and average side pressures, knowing the rocket velocity, the ambient temperature can be easily obtained from equation (6). The ambient temperature is plotted against altitude in Fig. 64 on which both the NACA curve and the one derived from Whipple[2] are shown for comparison. No agreement is seen. A portion of the telemeter record is shown in Fig. 106.

As a tentative estimate for the accuracy of the observed pressures, the theoretical ram and zero-yaw side pressures based on Whipple's and balloon data are shown in Fig. 63. These were obtained by using the assumed known ambient temperature based on Whipple, together with the rocket velocity. The ram and side pressures were worked out independently so that they could be compared with the corresponding observed pressures. All the observed pressures were evaluated using the decreasing pressure branches of the calibration curves. To indicate how much error in pressure might be attributed to hysteresis, the ram pressure based on the increasing pressure branch of the calibration curve is shown. Although the pressure in the ram gage was always decreasing in flight the magnitude of the hysteresis effect was shown for the ram gage rather than a side gage for simplicity. This treatment merely illustrates that a pressure error due to the hysteresis error alone is large enough to account for the errors in the final calculated ambient temperatures.

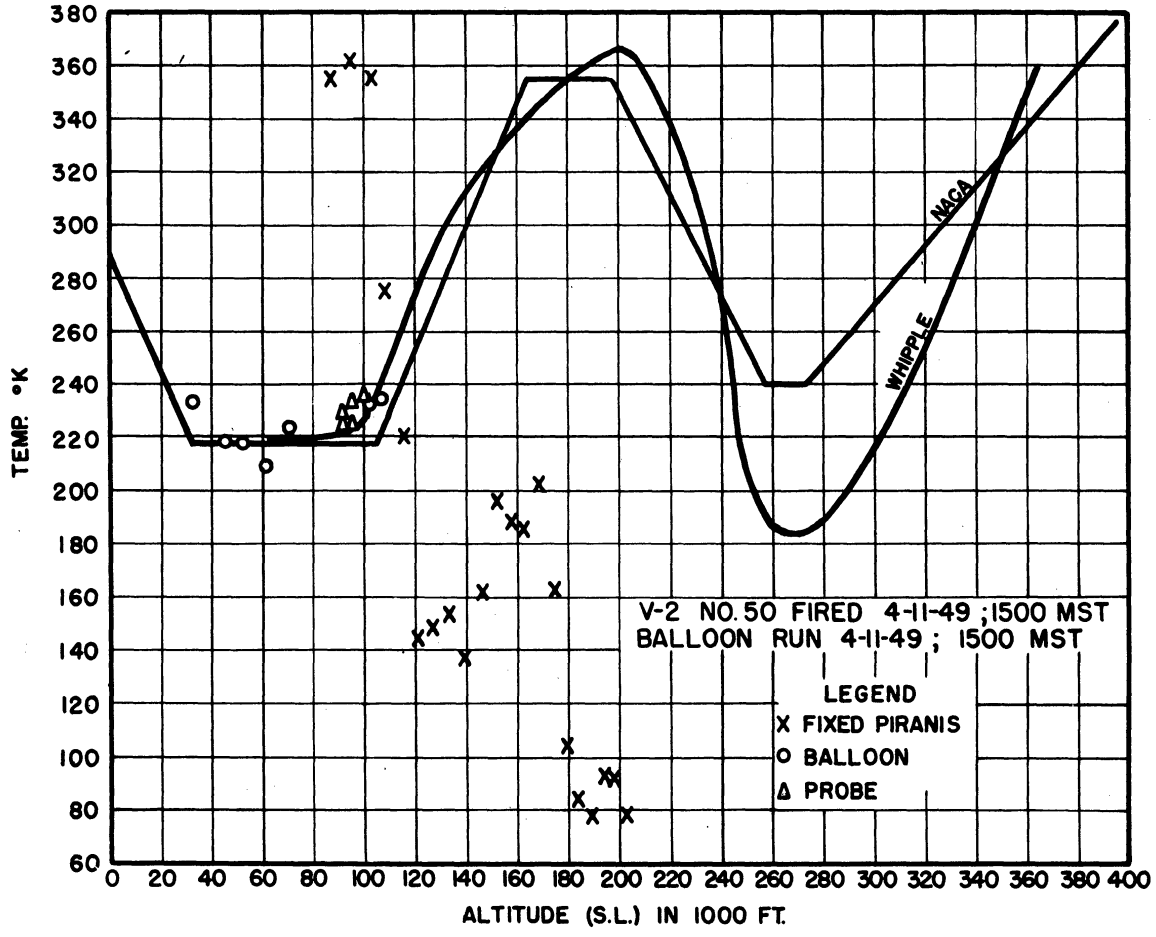

Fig. 64. Ambient Temperature vs Altitude, V-2 50

It is clear from the above results and discussion that the accuracy of the gages and circuits, as developed, was not good enough to make temperature measurements with the cone pressure method. In addition, the method is subject to errors arising from incomplete aerodynamic theoretical analysis of such things as boundary layer thickness. For these reasons, further development of the gages and of the method were dropped in favor of the probe method which is discussed in the next section.

6.3 Measurement of Ambient Temperature by Measurement of the Angle of the Shock Wave Formed by a Supersonic Cone

6.31 Theory

The method consists of measuring the ambient kinetic temperature of air at high altitudes by measuring the angle of the shock wave (the "weak" shock or the "first" solution of the conical flow equations) attached to the nose cone of a missile that moves at supersonic speeds. The shock wave is located by signals obtained from Pirani gage probes which are moved up and down through the shock wave. The method depends only upon the determination of the time of the signal and not its amplitude. This factor was the basis for choosing the probe method as more suitable for intensive development than the cone pressure method. Having located the shock wave position as a function of probe position, the shock angle is calculated from the geometry of the apparatus. Mach number, being a unique function of shock angle, is determined from a tabulation[27,28,29] and temperature derived as in the previous methods.

The theory is again due to Stone[25] who relates the shock wave angle formed by a cone to the free stream Mach number. Certain assumptions must be made in applying the theory to the experiment:

a) Air is a continuous medium.

b) Air is non-viscous.

c) The ratio of the specific heats of air at constant volume and constant pressure is constant.

d) The cone moves at supersonic speeds.

e) Heat transfer between the air stream and the body is negligible.

Not all of these assumptions are valid for all conditions of the experiment. However, they are reasonable enough to permit measurement of ambient temperature by the method with useful accuracy. The effect of viscosity at low density has been the subject of separate investigation described in Section 6.63.

Fig. 65 shows a yawing cone in a rectangular system of coordinates (1,2,3) where r, θ, ϕ denote the usual spherical coordinates.

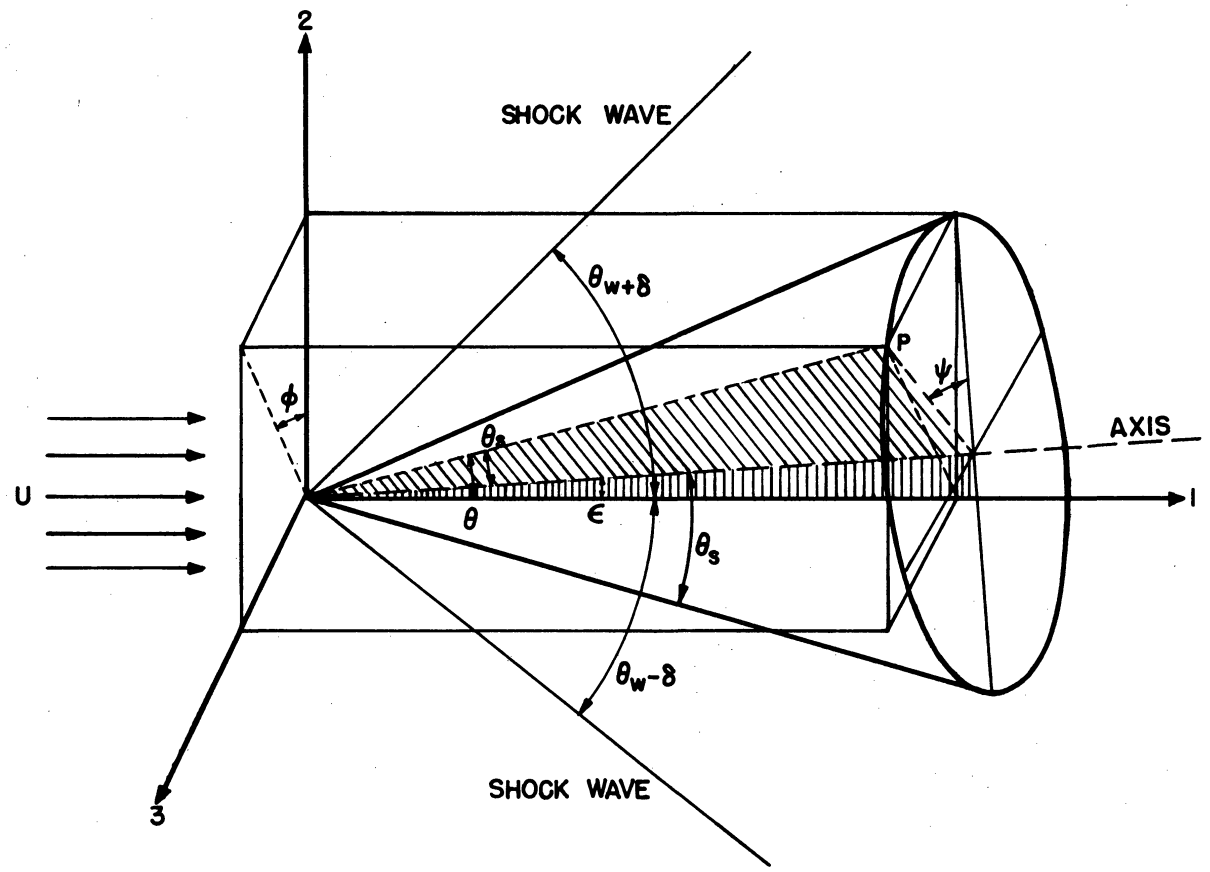

Fig. 65. Yawed Cone

The equations of motion and the continuity equation with the particular boundary conditions of the yawed cone constitute a two-point boundary value problem with a non-linear differential equation. The exact solution of this problem has not yet been developed. The approximate solution has been given by Stone who considers the effects of yaw on the quantities characteristic of the conical flow as perturbations of the corresponding quantities of the non-yaw case. If third and higher order effects of yaw are ignored, the equation of the nose cone and shock wave cone can be reduced to[29]:

$$\theta_s' = \theta_s + \epsilon \cos\phi - \tfrac{1}{2}\epsilon^2 \cot\theta_s \sin^2\phi \qquad (11)$$

and

$$\theta_w' = \theta_w + \epsilon\alpha\cos\phi + \epsilon^2(\beta_0 + \beta_2 \cos 2\phi), \qquad (12)$$

respectively. θ_w, $\alpha = \delta/\epsilon$, β_0, β_2 are shown as functions of the free stream Mach number in Fig. 66. Fig. 67 shows wave angle as a function of Mach number for a conical shock wave. θ_w is the shock wave angle of the non-yaw cone. ϵ is the angle of yaw of the nose cone.

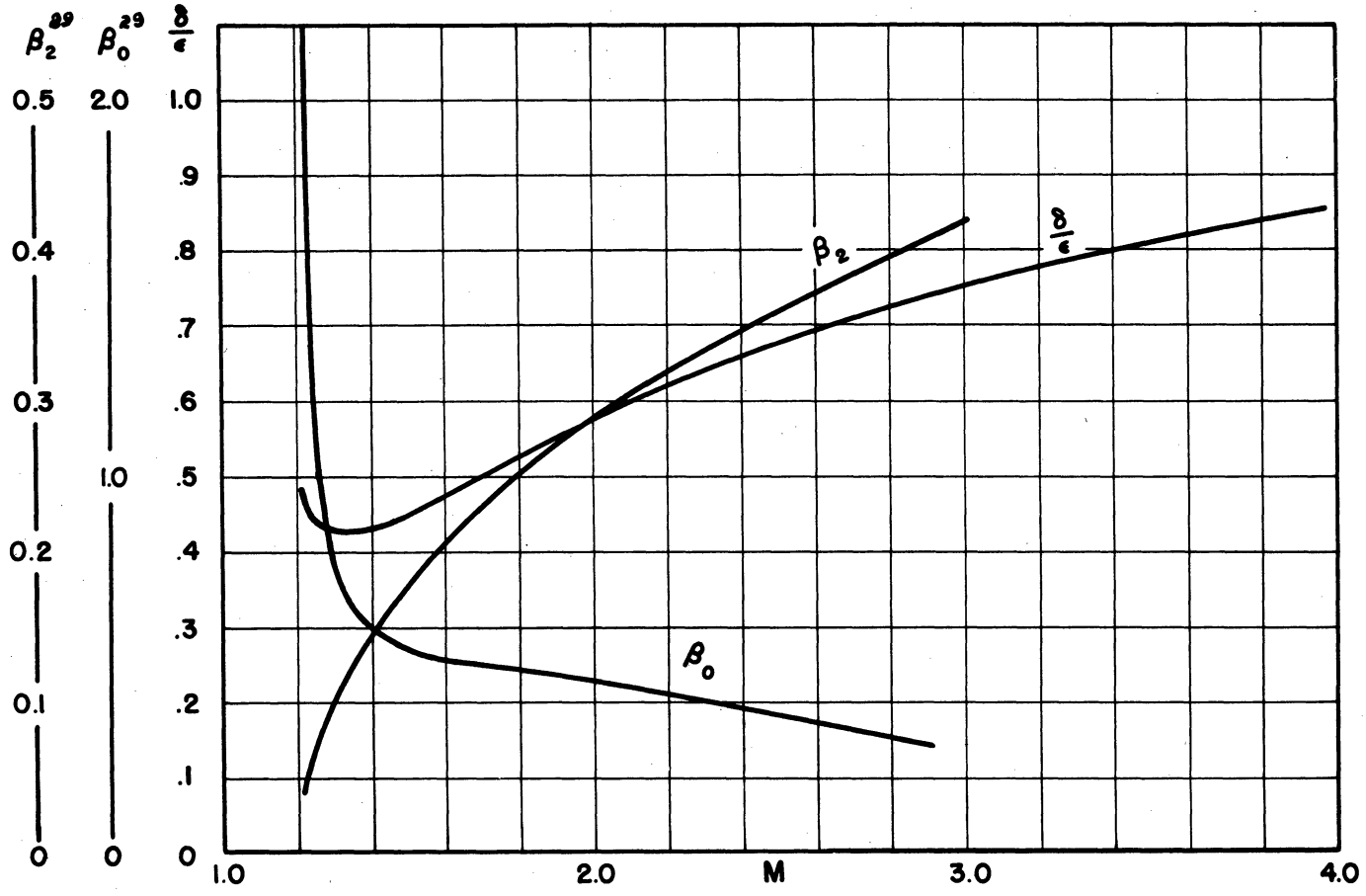

Fig. 66. δ/ϵ, β_0, β_2^{29}

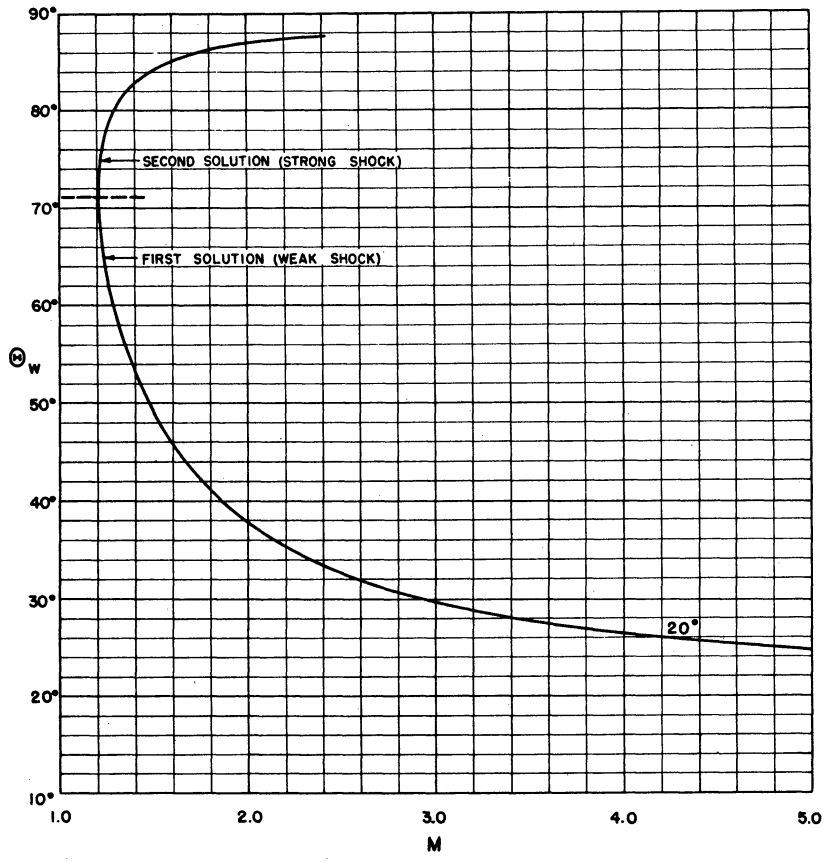

Fig. 67. Wave Angle for a Conical Shock Attached to a 20 Degree Half-angle Cone

It can be seen from equation (12) that if the angle of yaw is so small that the second order effect of yaw is negligible compared to the first order effect, the shock wave attached to a yawing cone in supersonic flight continues to be a circular cone, of the same apex angle as in the non-yaw case, but with a yaw of its own given by:

$$\delta = \alpha \epsilon$$

The plane of yaw of the shock wave will be the same as the plane of yaw of the cone.

However, with yaw so large that the second order effect must be considered, the shock wave cone ceases to be circular. Its normal cross section becomes actually a curve of the sixth degree simulating closely an ellipse of small eccentricity. The magnitude of the second order effect can be obtained from equation (12). The semi-apex angle of the shock cone in the second order case is given by:

$$\theta_w' = \frac{\theta_w'(\phi) + \theta_w'(\phi + \pi)}{2} \tag{13}$$

From (12) we see that this is equal to:

$$\theta_w' = \theta_w + \epsilon^2 (\beta_0 + \beta_2 \cos 2\phi) \tag{14}$$

The amount by which this varies from the first order case is:

$$\Delta \theta_w = \theta_w' - \theta_w = \epsilon^2 (\beta_0 + \beta_2 \cos 2\phi) \tag{15}$$

This quantity is a maximum for $\phi = 0$, and a minimum for $\phi = \pi/2$. The maximum and minimum values of $\Delta \theta_w$ are respectively:

$$\Delta \theta_{w_{max}} = \epsilon^2 (\beta_0 + \beta_2) \tag{16}$$

$$\Delta \theta_{w_{min}} = \epsilon^2 (\beta_0 - \beta_2) \tag{17}$$

6.32 Experimental Attempts on V-2's 33 and 50

The probe shock wave experiment was flown on three V-2's and is being adapted to the Aerobee. The 40° cone and mechanical apparatus for

scanning the probes was similar for all V-2's. Fig. 68 shows this assembly for V-2 33. The probes were moved up and down through an amplitude of 8 inches with a period of 3 seconds. The probes were driven by a large bronze cam which in turn was driven through a gear box by a 1/5 horsepower motor. The probe gages and circuits are described in Sections 6.42 and 6.44, respectively.

V-2 33 was launched successfully but the telemeter failed completely before the probes were started, and no data were obtained from the probe experiment.

V-2 50 was also launched successfully. On this missile two of the probes were of the static or needle type with the orifice about 10 diameters back from the tip at the same level as the orifices of the impact probes. It was thought that there would be less distortion of the main shock wave as a result of interaction with the probe shock wave. See Section 6.62. However, the signals received from the static probes did not have sharply rising wave fronts. This is thought to be because the shock wave and hence the pressure discontinuity, can occur only when the local velocity is supersonic. Due to the existence of a boundary layer in which velocity builds up from zero at the wall to main stream value at the outer edge of the layer, there is no pressure discontinuity in a thin layer of flow in the immediate vicinity of the static type probe. These probes were not used on V-2 56. The impact probes gave sharp signal impulses as they passed through the shock wave. These gages burned out at about 62 seconds after they had given 2 and 3 signals respectively. Burnout in these cases occurred at the instant the probes encountered the shock wave and was possibly due to the time lag of the associated apparatus or shorting of the sagging wire to the support. One of the static probes burned out at 31 seconds, the other gave signals to 80 seconds. However, the signals were not useful, as noted above. Fig. 69 and Fig. 70 show typical signals obtained from this flight. Fig. 71 is the static probe.

The impact probe data from V-2 50 were reduced to temperature vs altitude using Askania data for altitude and velocity. The results are shown in Table 4 with probable error due to error in measuring the position of the shock wave. The error due to viscosity was neglected as small at these altitudes. Corrections for yaw were not made. From Fig. 63 it can be seen that there was little yaw at the time the shock wave was measured. The results are plotted in Fig. 64. They show excellent agreement with the theoretical curves and with temperatures taken by balloon at the same time. On the basis of these results it was decided to attempt the experiment again on V-2 56.

6.33 Experimental Attempt on V-2 56[32]

The most successful trial of the probe method for temperature was accomplished on V-2 56. The probes and circuits for this rocket are described in Sections 6.42 and 6.44, respectively. The mechanical apparatus was very similar to that of V-2's 33 and 50. It is shown in Fig. 72. The rocket peak altitude was 405,700 feet. Excellent data were obtained from all four Pirani gages in the altitude range between 85,000 and 130,000 feet. One of the gages or its circuit failed at this point. Data were obtained

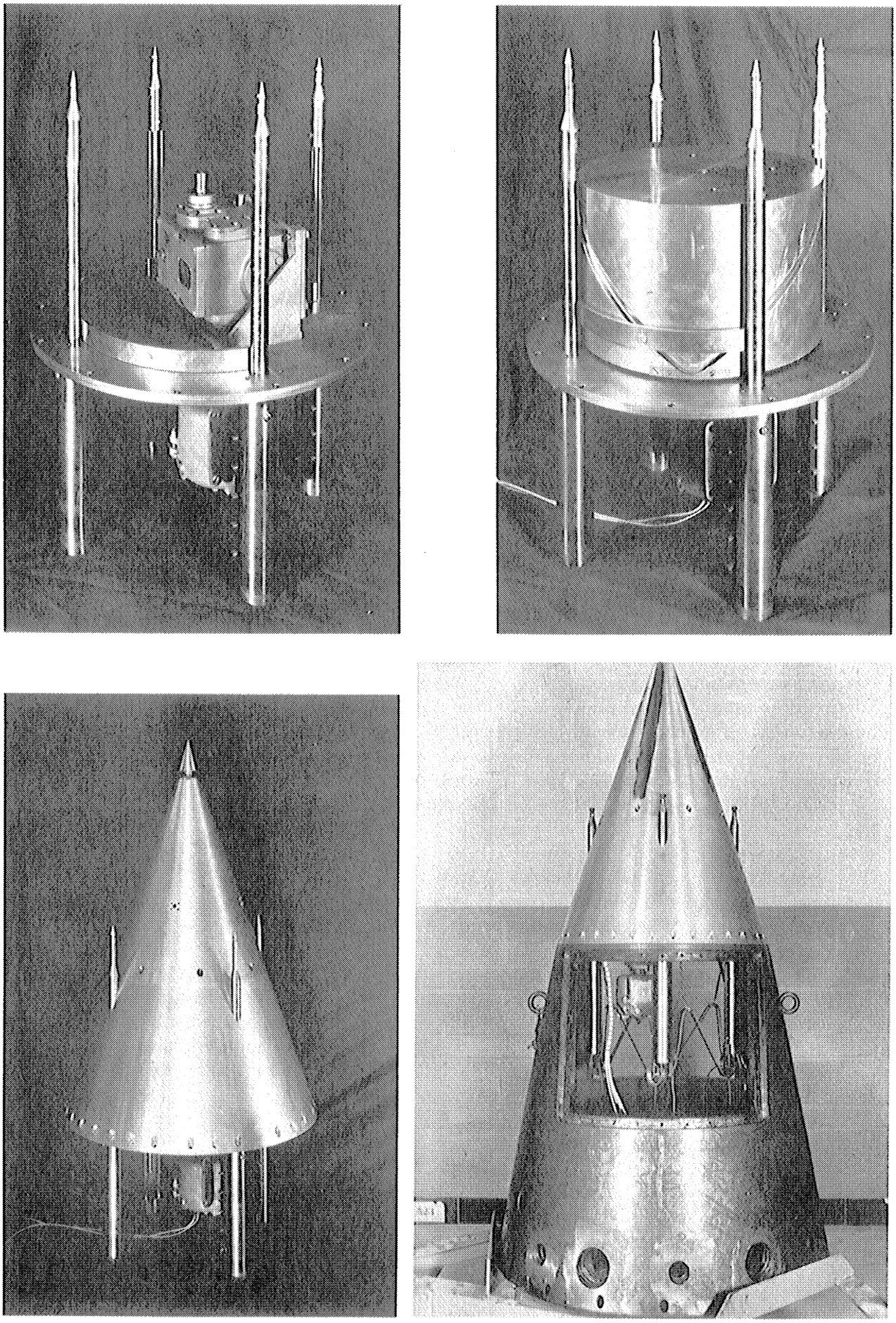

Fig. 68. Probe Apparatus, V-2 33

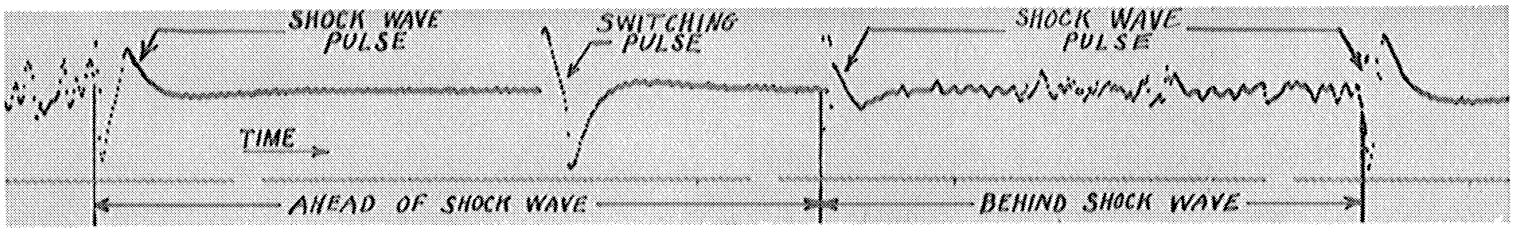

Fig. 69. Probe Signal, V-2 50

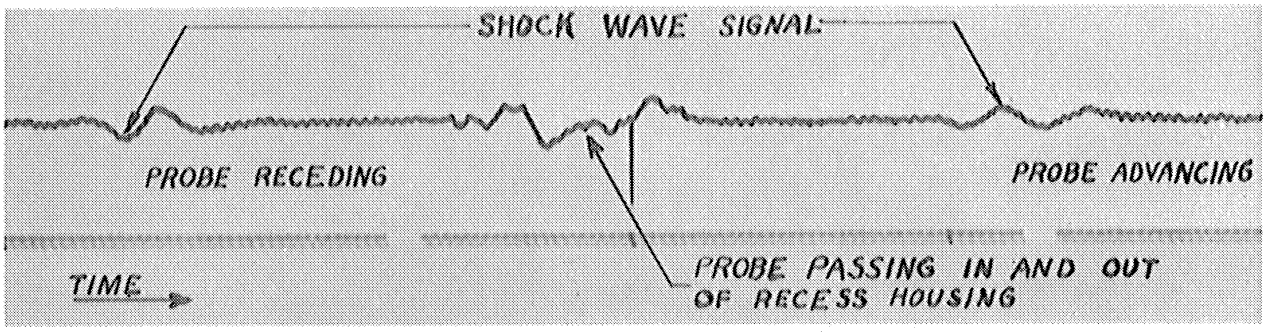

Fig. 70. Static Probe Signal, V-2 50

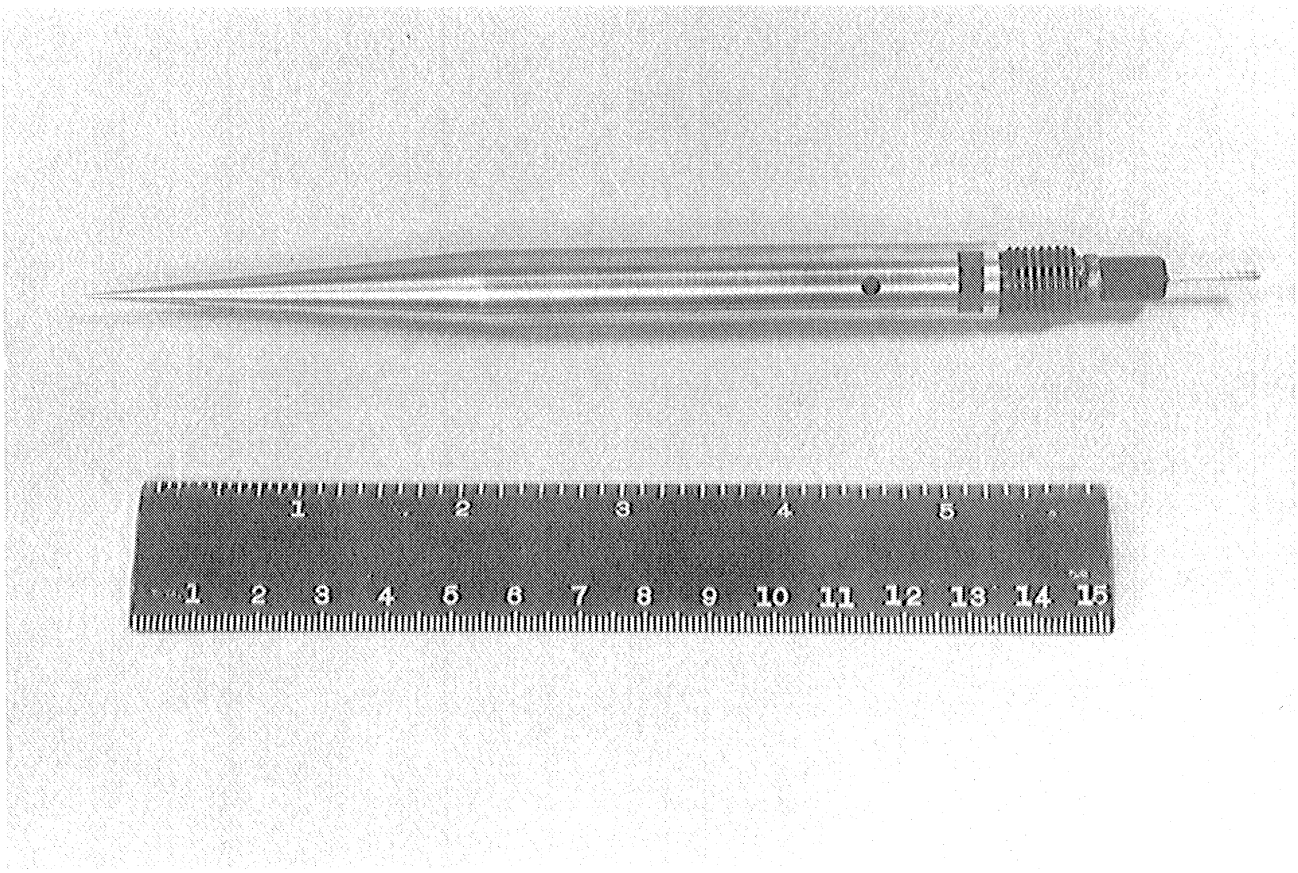

Fig. 71. Static Probe, V-2 50

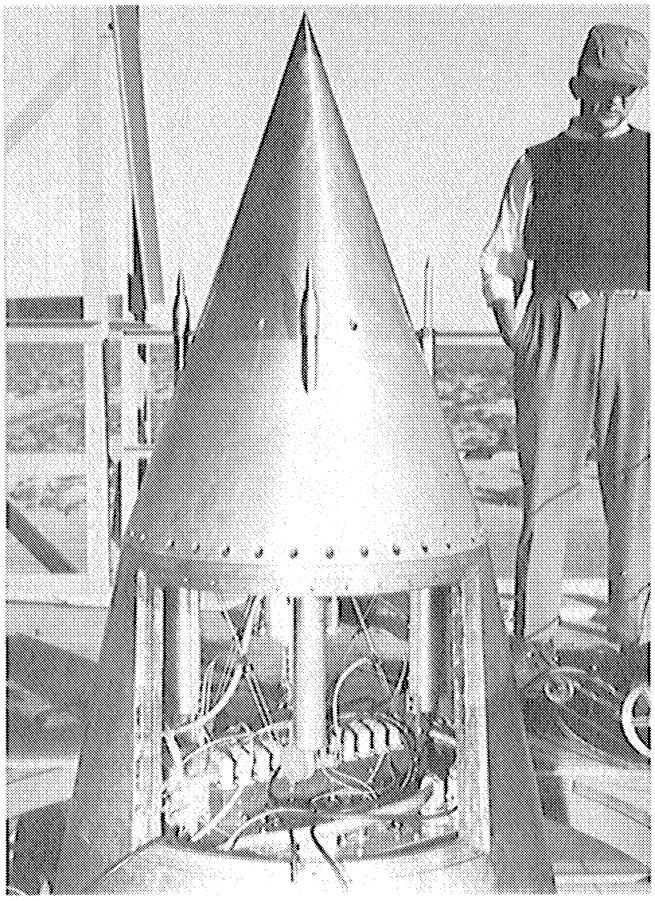

Fig. 72. Probe Apparatus and Electronics, V-2 56

TABLE 4

Results of Probe Experiment, V-2 50

Probe	Time (Sec)	Alt Above S.L. (KM)	Alt Above S.L. (1000 Ft)	Angle (Deg)	Probable Error ± (Deg)	Probable Angles (Deg)	M	V (Ft/Sec)	A (Ft/Sec)	T (°K)	ΔT (°K)
						27.81	3.46		977	221	-5
South	59.802	27.99	91.8	27.93	0.12		3.42	3380	988	226	
						28.05	3.38		1000	231	+5
						28.08	3.39		997	230	-3
North	59.824	27.99	91.8	28.20	0.12		3.37	3380	1003	233	
						28.32	3.35		1010	236	+3
						27.79	3.47		991	227	-6
North	61.240	29.57	96.9	27.91	0.12		3.43	3440	1003	233	
						28.03	3.39		1014	238	+5
						27.69	3.49		986	224	-4
South	61.254	29.57	96.9	27.81	0.12		3.46	3440	994	228	
						27.93	3.43		1003	233	+5
						28.09	3.39		1017	239	-3
North	62.292	30.45	100.0	28.21	0.12		3.37	3450	1023	242	
						28.33	3.35		1030	245	+3

from the other three gages up to 145,00 feet, when a second gage or its circuit failed. Signals were obtained from the remaining two gages up to 230,000 feet at which point they burned out because of overheating at the low pressure. The premature failure of the two gages or their circuits possibly was due to the misfire of a sound grenade from the SCEL temperature experiment also flown on the missile.

Table 5 shows the approximate expected Pirani signals for a 394,000 peak trajectory compared with the nearest actual values obtained on V-2 56.

Prior to the flight a careful calibration of the position of the probes against the probe position commutator signal was made. This was used together with the telemeter record of the probe position signal to plot probe position against time. The time of a given probe position signal was obtained by linear interpolation between the nearest one-second time marks on the telemeter record. The times of the shock wave signals were obtained by the same interpolation method. The probe position corresponding to a shock wave signal was obtained from the graphs of probe position against time. The shock wave angles were then calculated, assuming a right circular shock wave cone and correcting for winds. The winds were estimated on the basis of averaged data from several sources such as grenade and AA bursts, ionospheric and noctilucent clouds and meteor trails[33].

Data reductions differed for the four-probe, three-probe and two-probe sets. In the four-probe case, where the shock cone is over-determined, the angles were calculated by using the data in various combinations. Close agreement was found for the shock angles for all methods. Three-probe data will just determine the shock wave cone without independent yaw data. Two-probe data requires independent yaw data for reduction to shock angle. These were obtained from Askania and a K25 reconaissance camera installed on the missile by APL. No yaw data were available from 183,000 to 230,000 feet so that data from the probes in this range were not reduced. Fig. 73 shows a portion of the telemeter record and Fig. 74 the final temperatures plotted against altitude. The reason for the "up-down" discrepancy in Fig. 74 is not known. An error analysis of the experiment was made. The magnitudes of errors in applying the aerodynamic theory are not known. For example, the effect of viscosity has not been completely investigated. It was shown that experimental errors such as those in calibrating the cone and measuring yaw by ground tracking devices could be fairly large. In further development of the experiment the experimental errors can be expected to be reduced and a theoretical analysis of the affect of viscosity will be attempted.

6.34 Adaptation to Aerobees

Based on the results of V-2 56 it was decided to adapt the probe experiment to Aerobees. Very little information on the attitude of Aerobees above 100,000 feet was available. However, the few observations made indicated a good probability that the Aerobee might have an angle of attack up to 250,000 feet suitable for the probe experiment. It was also thought that, since two or even three Aerobees could be instrumented and flown for the same cost as one V-2, it would prove economical to measure temperature with Aerobees rather than V-2's, even with the calculated risk of failure because of bad angle of attack.

TABLE 5

Pirani Gage Signals V-2 56

Altitude 10^3 Ft	V (Ft/Sec)	P_{01}' mm. Hg.	P_{0W}' mm. Hg.	Pirani Signal peak input volts		Amplified Pirani Signal predicted peak volts		Amplified Pirani Signal obtained on V-2 56 peak volts	
				0.0001"	0.0002"	0.0001"	0.0002"	0.0001"	0.0002"
98.2	4360	186.0	309.0	.015	.013	0.60	0.52	1.00	1.05
131.5	4180	35.6	66.0	.084	.080	1.68	1.60	1.05	0.70
164.2	3839	9.1	14.1	.320	.138	2.88	2.07	0.95	0.82
196.9	3550	2.47	3.63	.190	.172	2.47	2.24	1.75	0.93
229.7	3248	0.447	0.637	.062	.025	1.24	0.70	0.35	0.58

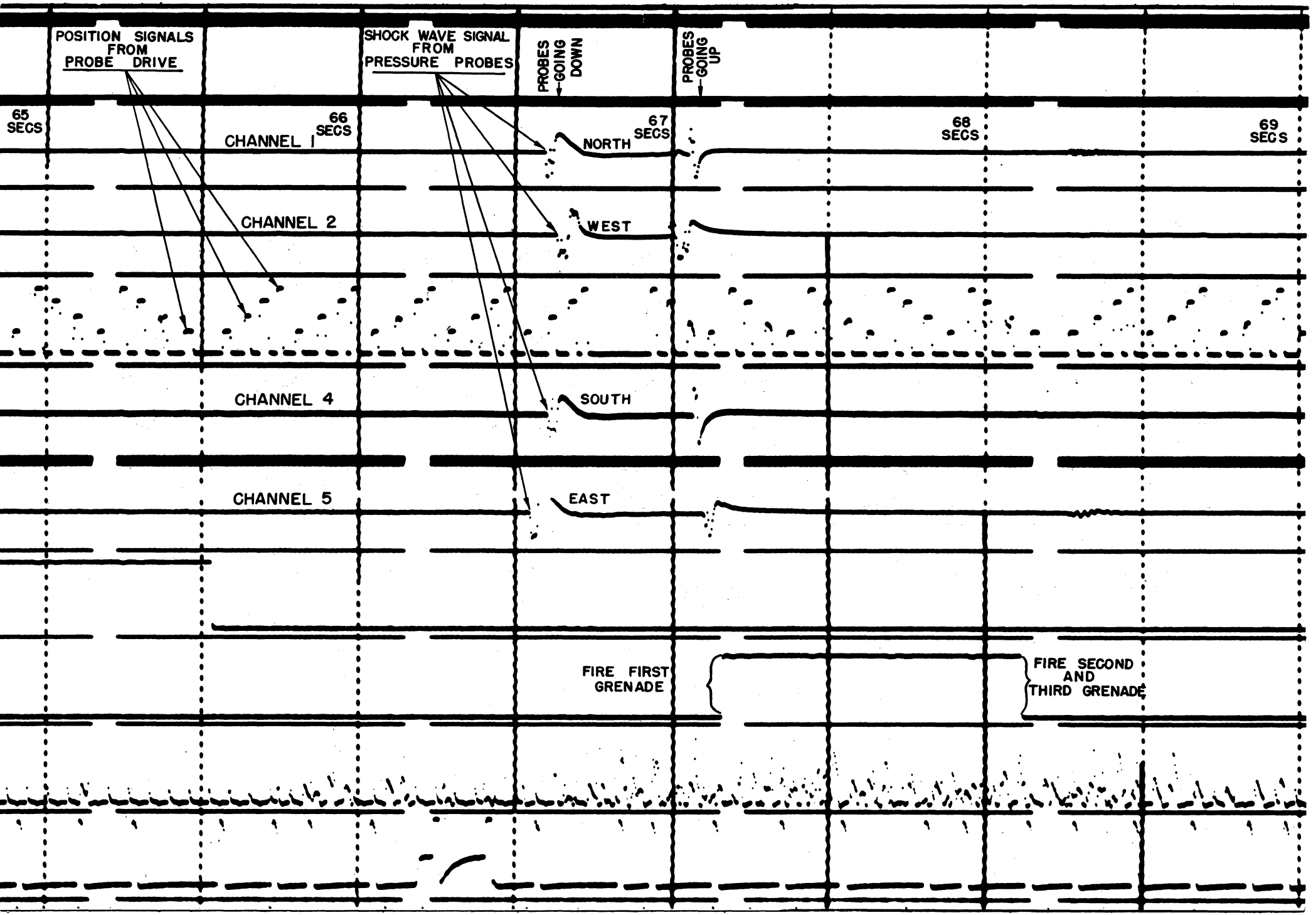

Fig. 73. Portion of Telemeter Record, V-2 56

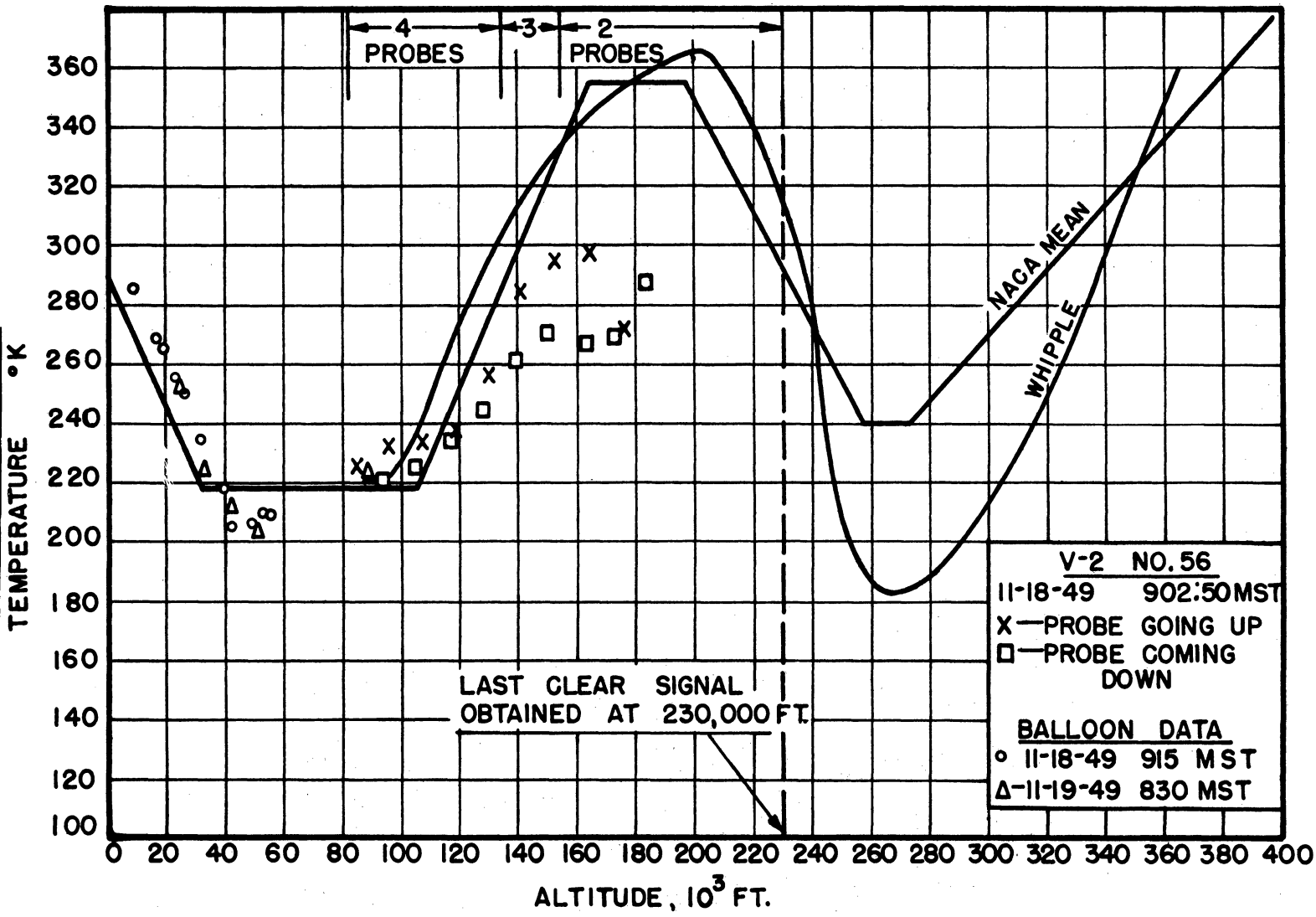

Fig. 74. Ambient Temperature vs Altitude, V-2 56

Consequently, development of the probe Aerobee was undertaken. It was decided to scan the cone rather than the probes and a 2-way reversible motor driven screw shown in Fig. 75 was built to do this. In order to measure shock wave curvature, an array of ten probes, see Fig. 76, was decided upon. Provisions for carrying doppler were made with the cooperation of BRL. A magnetic recorder and associated circuits for recording probe data were developed. These are described in Section 6.45.

6.4 Pressure Gages and Circuits

The first three aerodynamic methods for ambient pressure and temperature described above required small, lightweight, rugged pressure gages operating with good accuracy over a wide range of pressures. (The probe method, being geometric, did not require gage accuracy.) Consequently, a large portion of the effort of the project was directed toward development of suitable pressure gages. Three types were considered: the null-pressure diaphragm gage, the alphatron and the Pirani gage. No development of the first was done but several models of alphatrons and Piranis were developed and used.

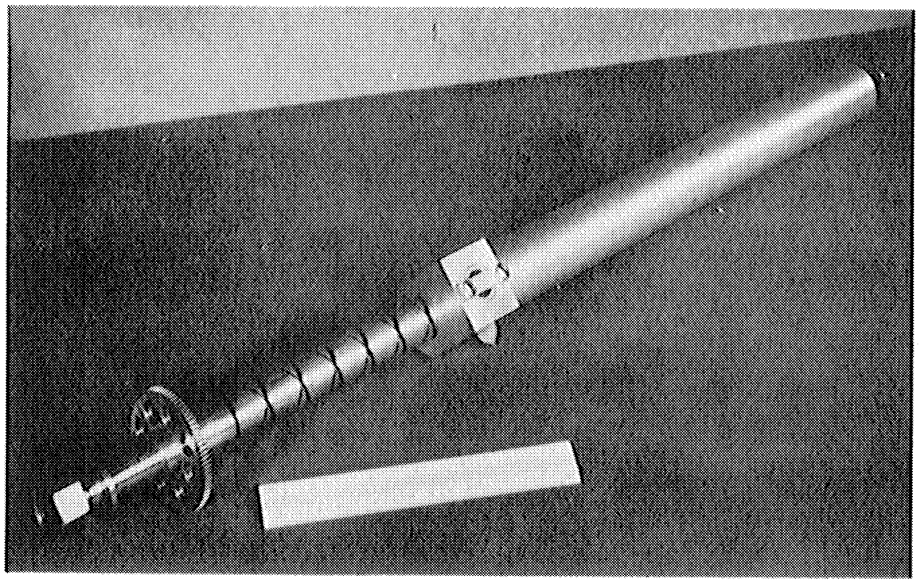

Fig. 75. Reversing Drive Screw, Probe Aerobee

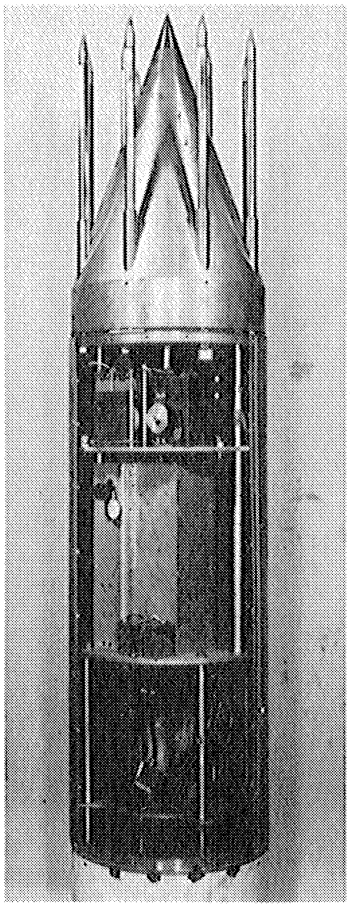

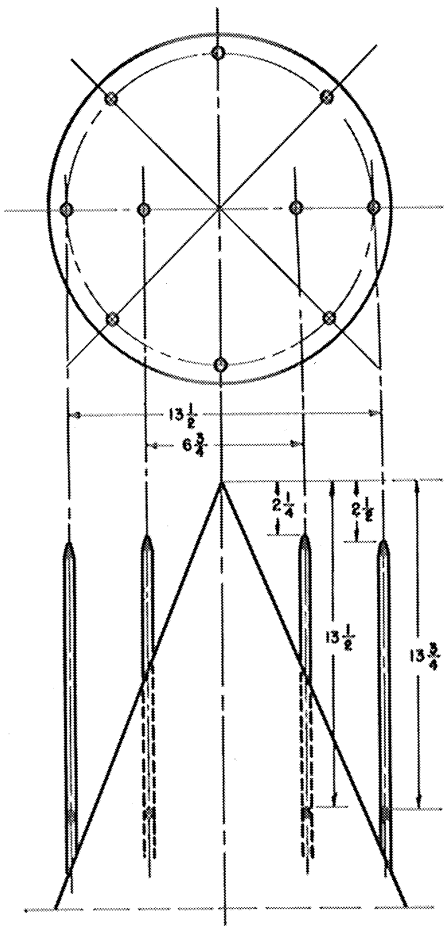

Fig. 76. Probe Array, Probe Aerobee

6.41 Alphatrons

The alphatron is an ionization gage in which ionization occurs as a result of collisions between the gas molecules and alpha particles from a radioactive source, such as polonium. Its advantages are wide pressure range, lightweight and ruggedness. Its disadvantages are that it is an extremely high impedance device, and, being actually a density measuring device, it must be maintained at constant temperature in order to measure pressure. Fig. 77 shows the volt ampere characteristic of the experimental parallel plate alphatron used in preliminary studies. This alphatron is shown in Fig. 78.

Following tests on the parallel plate alphatron, an alphatron for flight use was designed. Fig. 79 shows the ion collector assembly and Fig. 80 the complete alphatron assembly. The alphatron was equipped with a nichrome wire heater which kept the gage temperature at 50°C by thermostat regulation. Fig. 81 is the current-pressure characteristic of the alphatron.

Both AC and DC operation of the alphatrons were considered and tried. The DC circuit was that of Meagher and Bentley[34] shown in Fig. 82. The output voltage of this circuit is nearly proportional to the logarithm of the current. This is accomplished by making use of the velocity distribution of electrons from a thermionic cathode. Such operation of a tube causes it to have very high grid resistance at low currents which may lead to leakage current difficulties in a humid atmosphere. However, this was

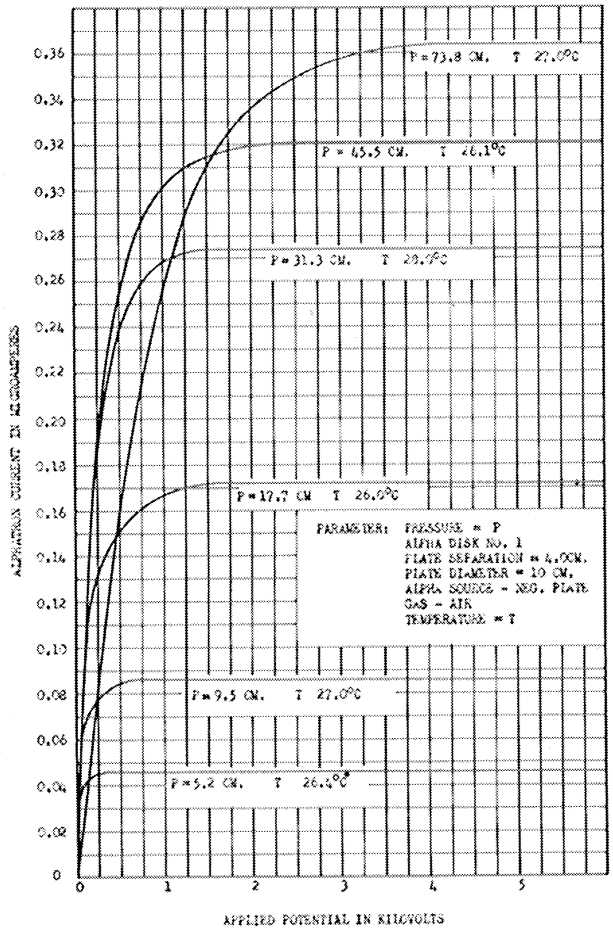

Fig. 77. Parallel Plate Alphatron Characteristics

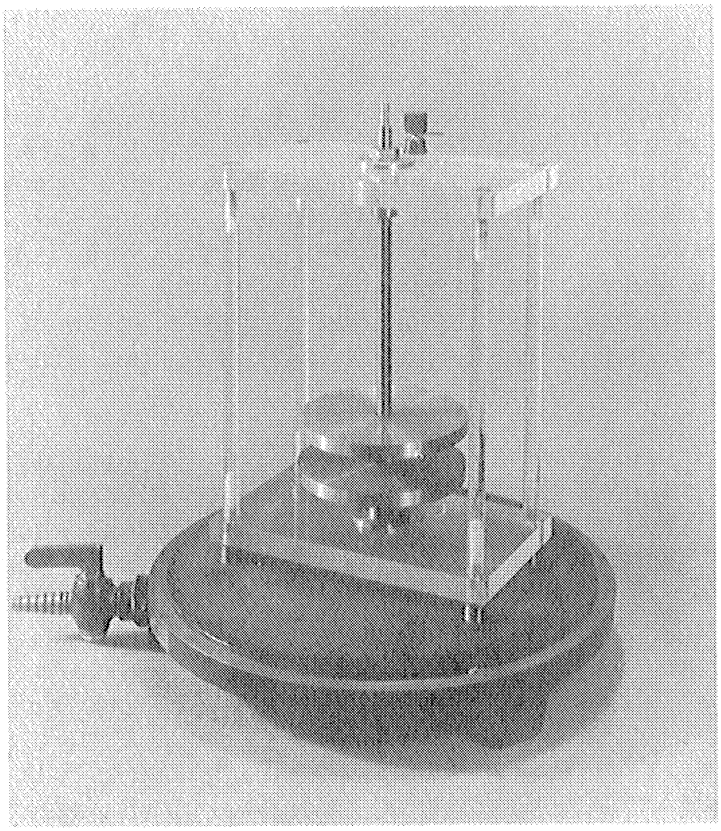

Fig. 78. Parallel Plate Alphatron

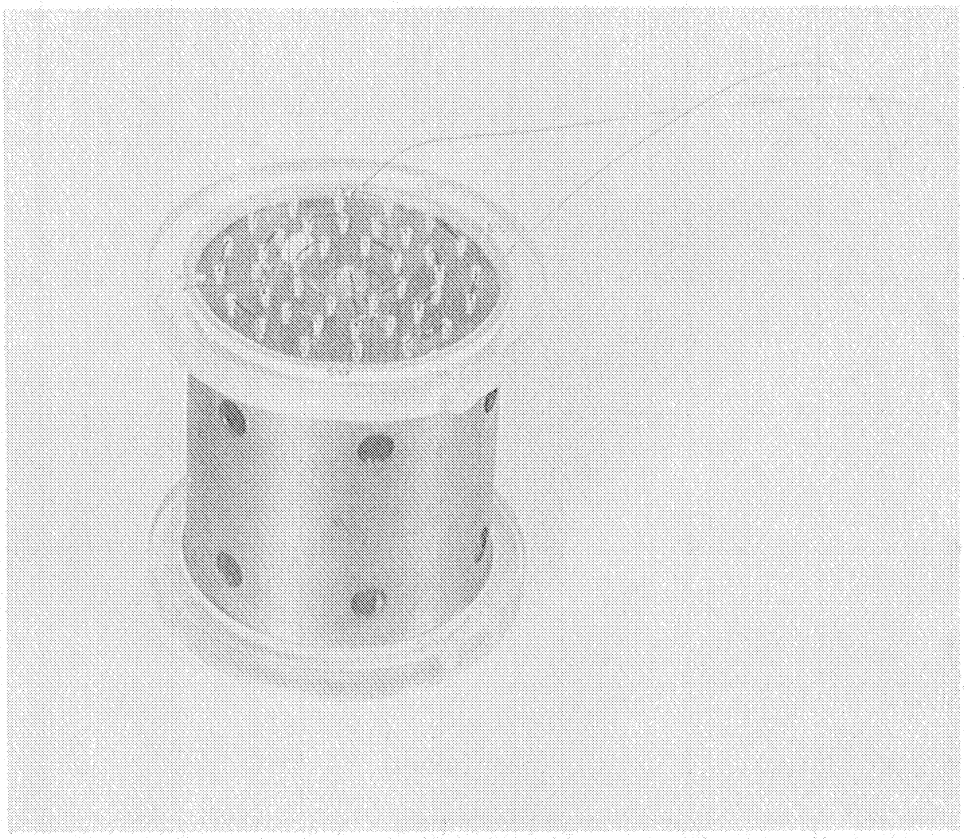

Fig. 79. Alphatron Ion Collector

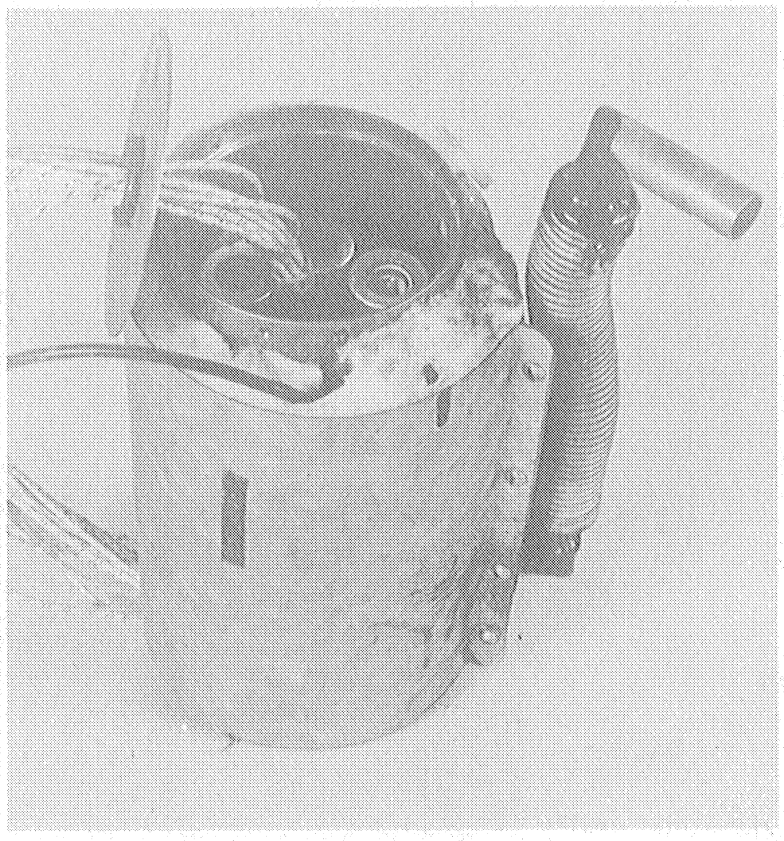

Fig. 80. Flight Alphatron with Oven

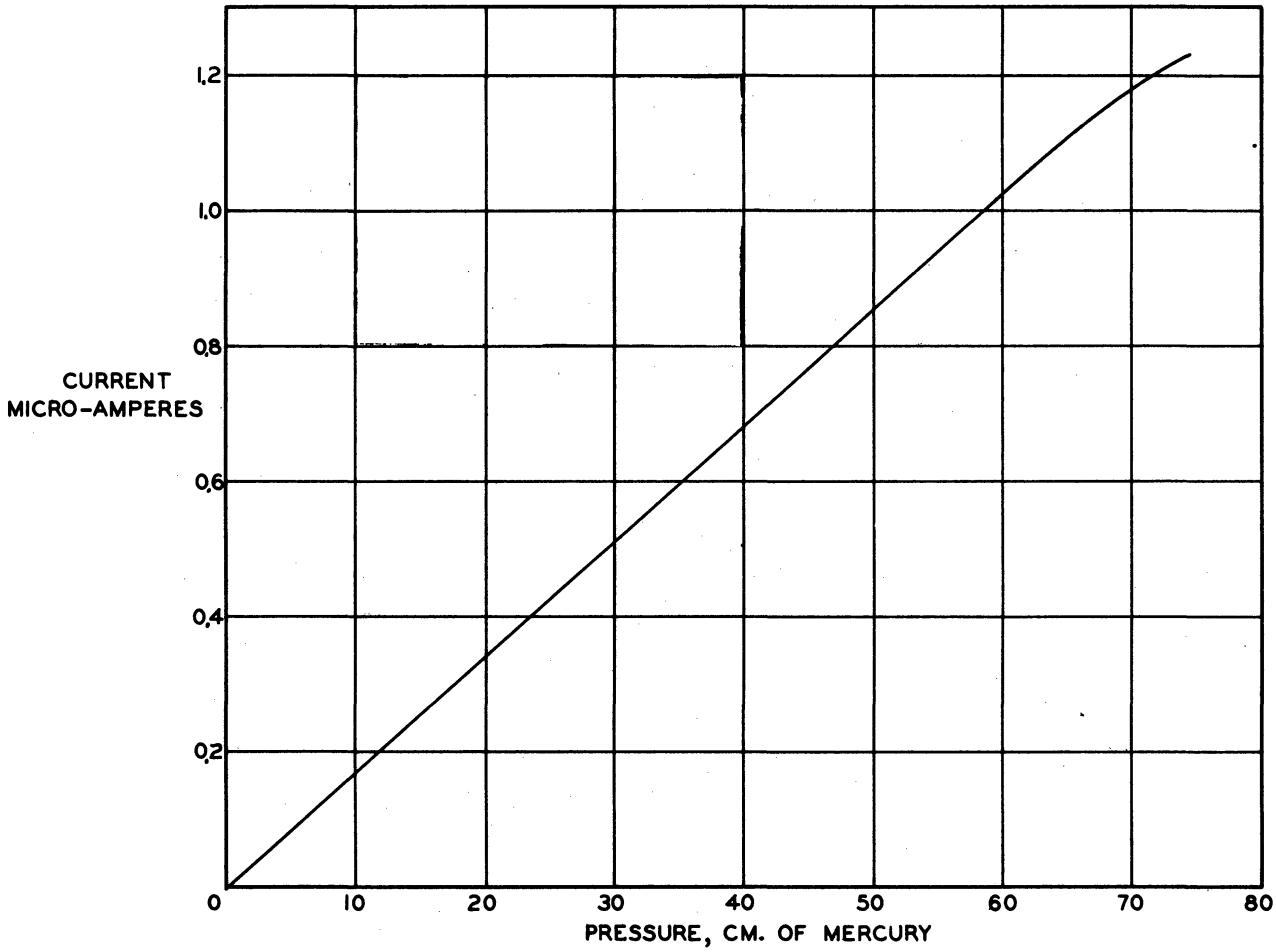

Fig. 81. Alphatron Current vs Pressure Characteristic

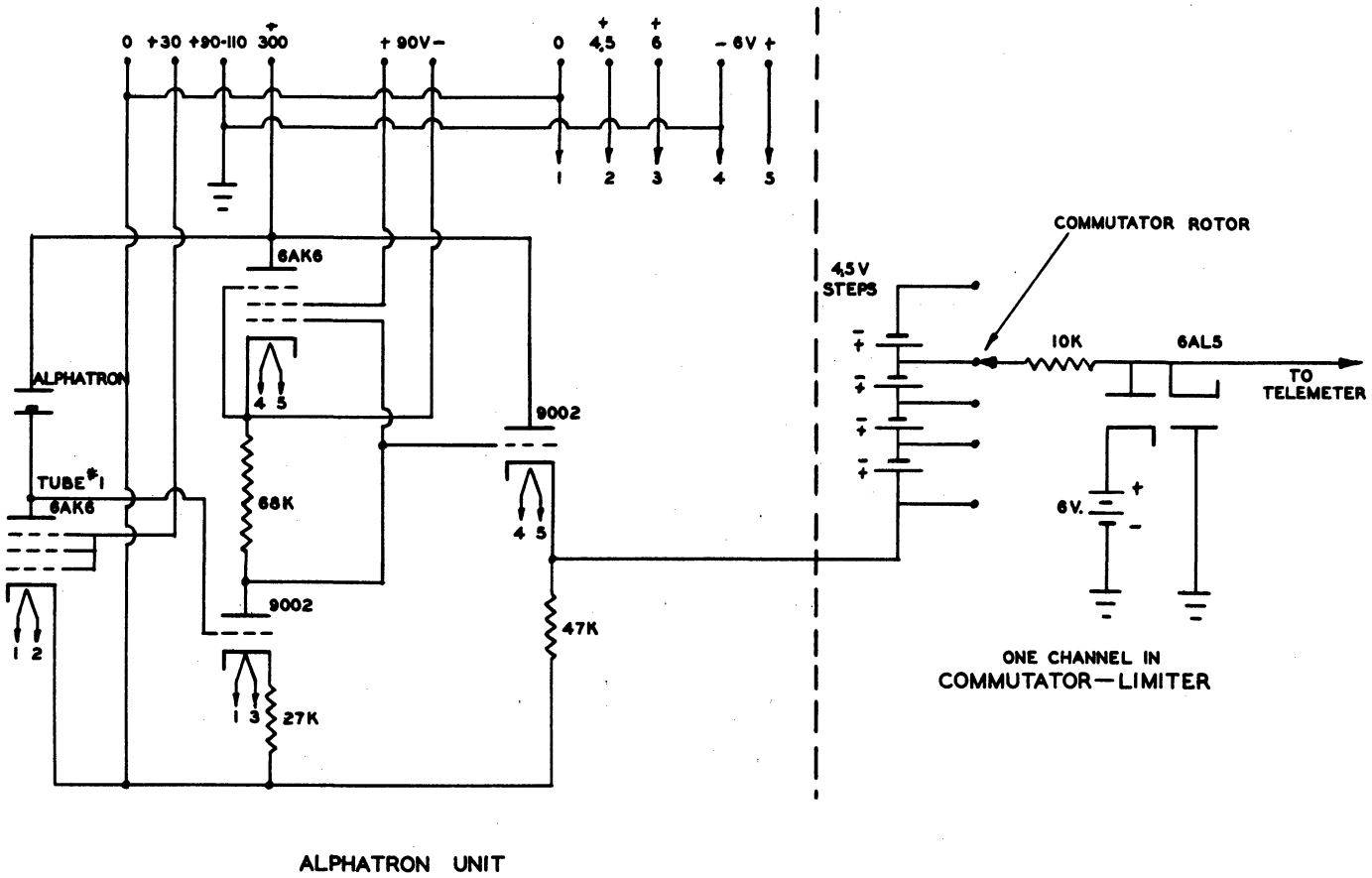

Fig. 82. Meagher-Bentley Circuit

not thought to be objectionable inasmuch as the same problem had to be solved for the alphatron itself: the electronic circuit was included within the regulated oven. The pressure-voltage characteristic of the alphatron and DC circuit is shown in Fig. 83. Experience in the field with the logarithmic circuit showed it to be very unstable. The logarithmic tube was replaced with a 20-megohm fixed resistor. This improved the stability but aggravated the flatness of the pressure-voltage characteristic at 5 mm as seen in Fig. 84. The voltage range of this characteristic was broken up into four 0 to +5-volt steps with bucking batteries switched by means of the motor driven commutator shown in Fig. 85.

As a consequence of the several postponements of V-2 25, it was necessary to supplement the alphatron gages in the low-pressure range with Pirani gages because of the loss in alphatron sensitivity due to the 140-day half-life of the polonium sources. Another consequence of the delay was that further development of the alphatrons and circuits was possible. Investigation showed that the flat part of the characteristic of Fig. 84 was caused by an avalanching phenomenon. This was eliminated by using a lower ion collection voltage in this range. The gages and circuits were rearranged for ease of assembly. The new circuit with ion collector voltage switching is shown in Fig. 86 and the output voltage vs pressure characteristics in Fig. 87. This was the alphatron and circuit (with commutator) flown on V-2 25.

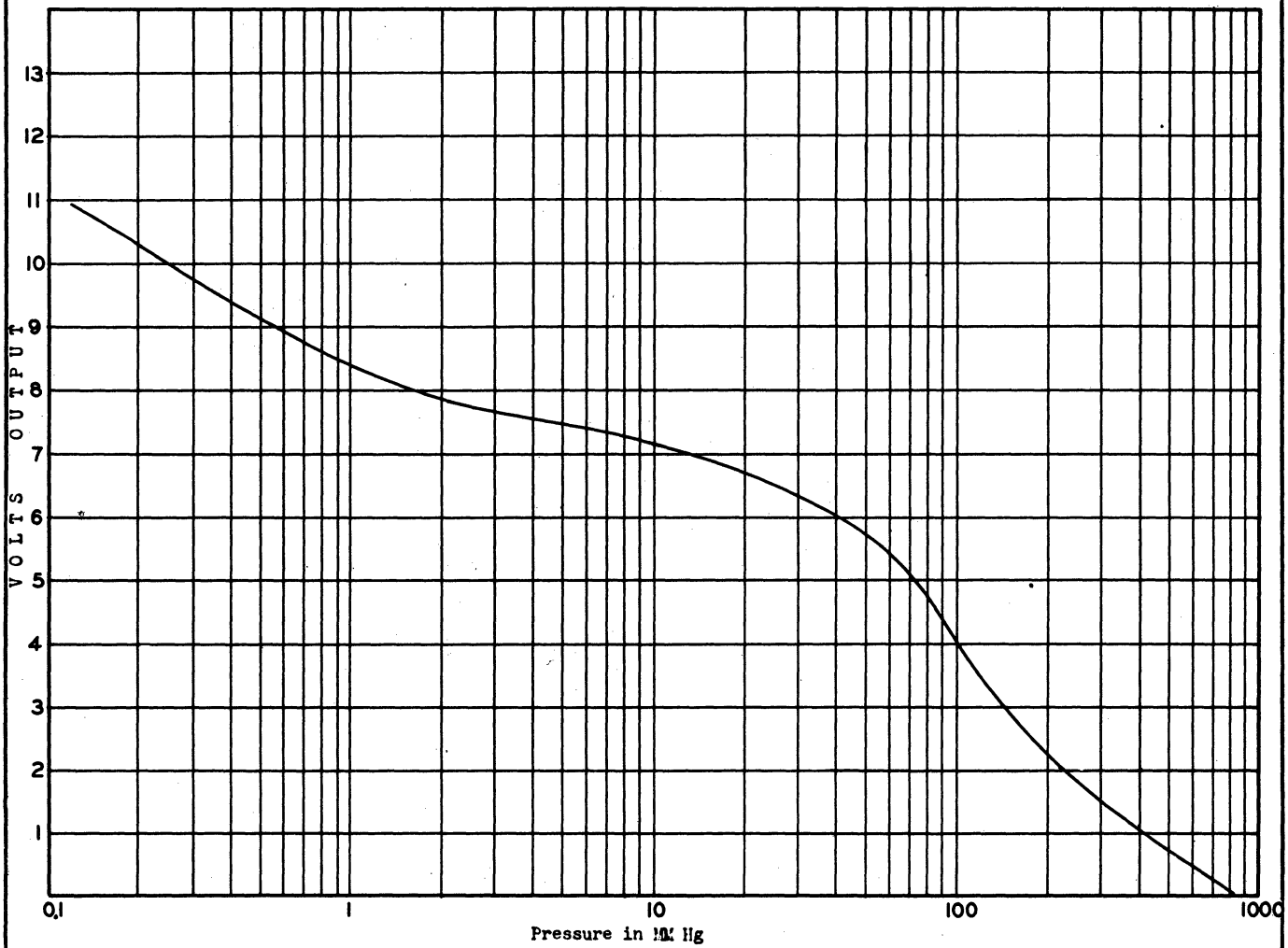

Fig. 83. DC Alphatron Output vs Pressure Characteristic, Meagher-Bentley Circuit

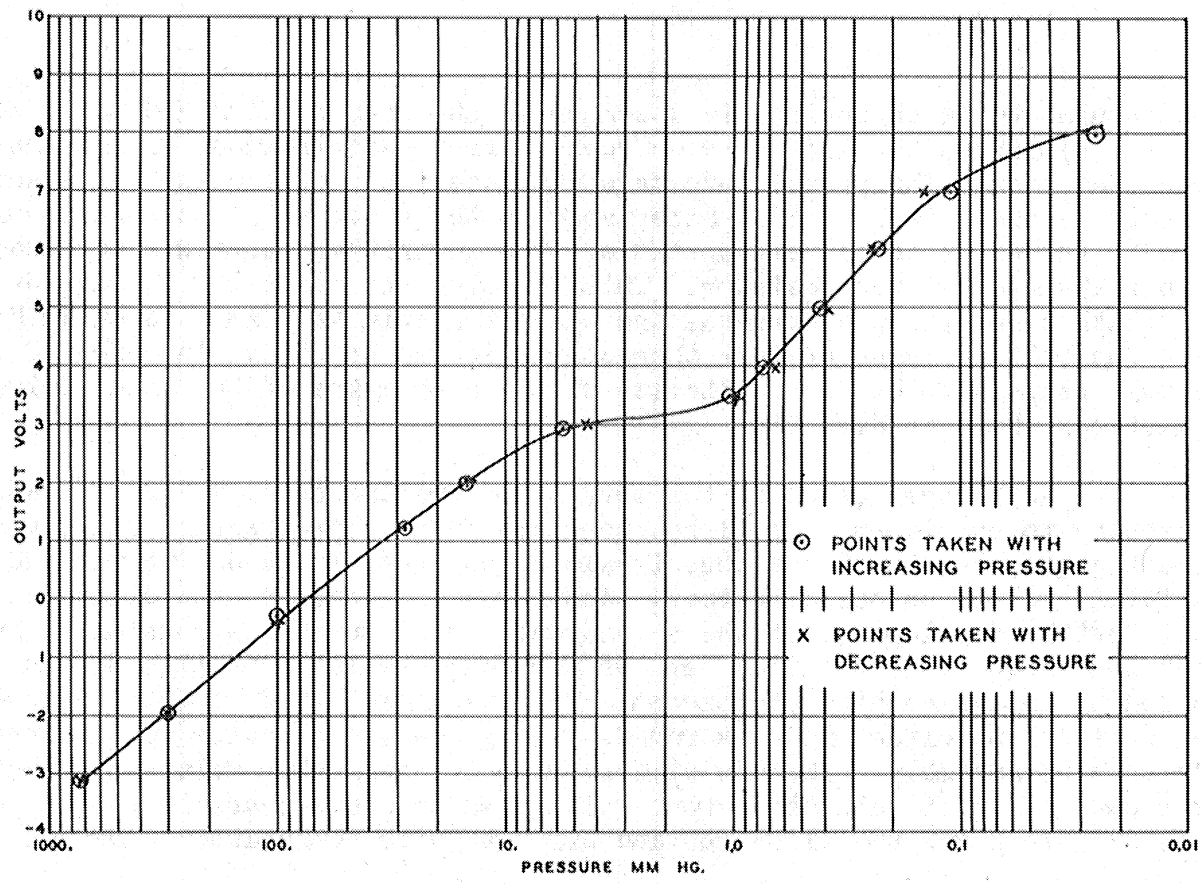

Fig. 84. DC Alphatron Output vs Pressure Characteristic, Modified Circuit

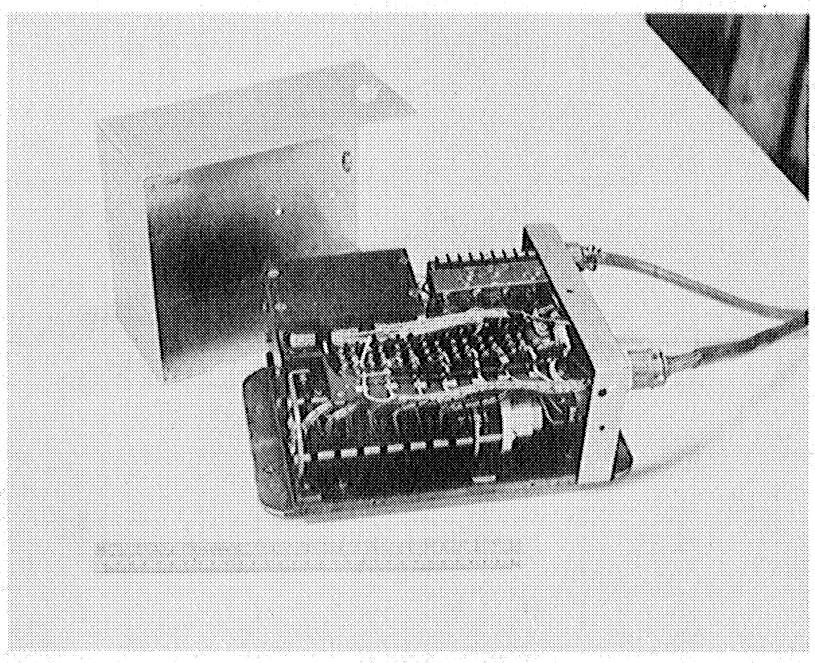

Fig. 85. Commutator

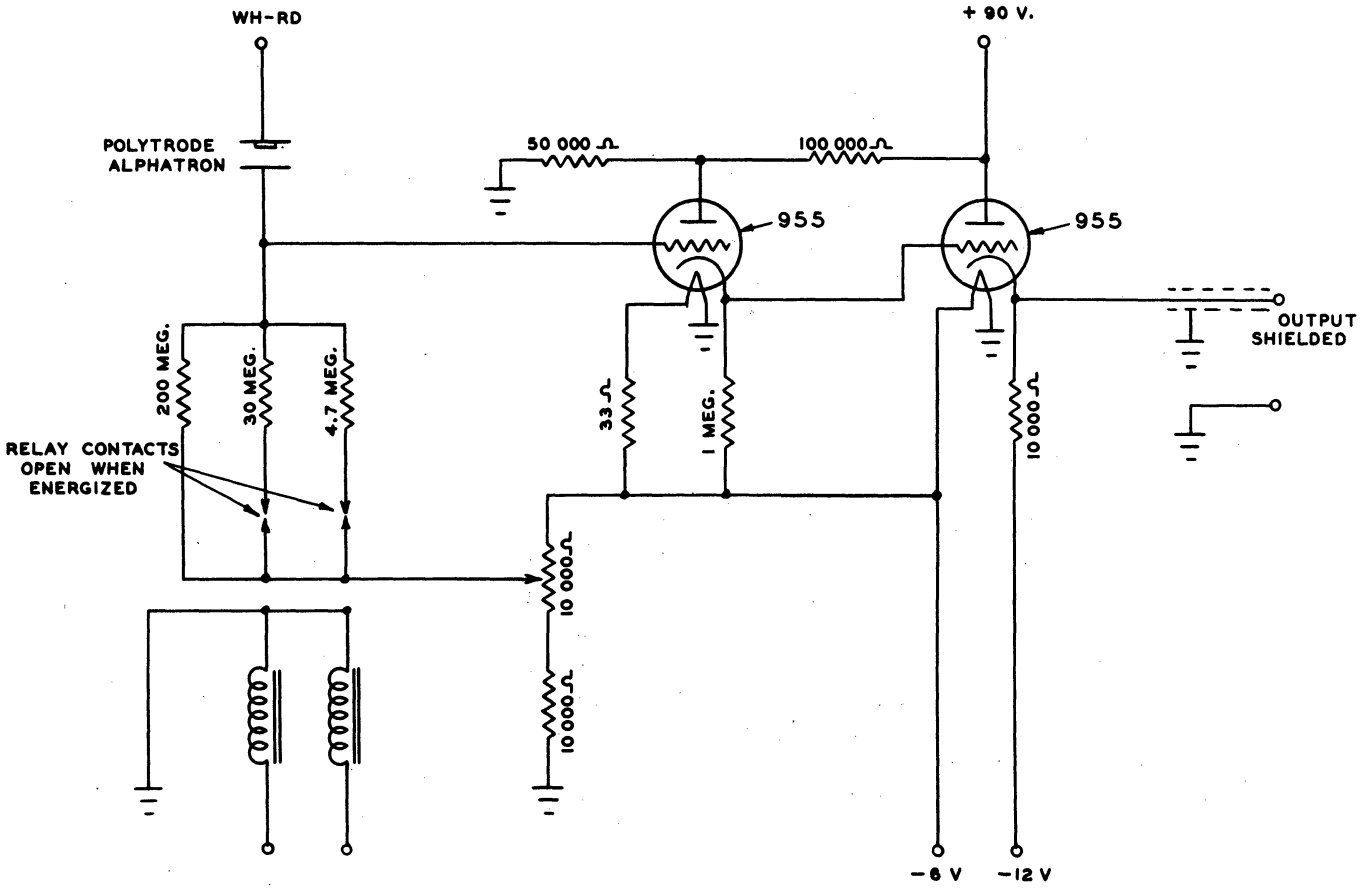

Fig. 86. Alphatron Circuit, V-2 25

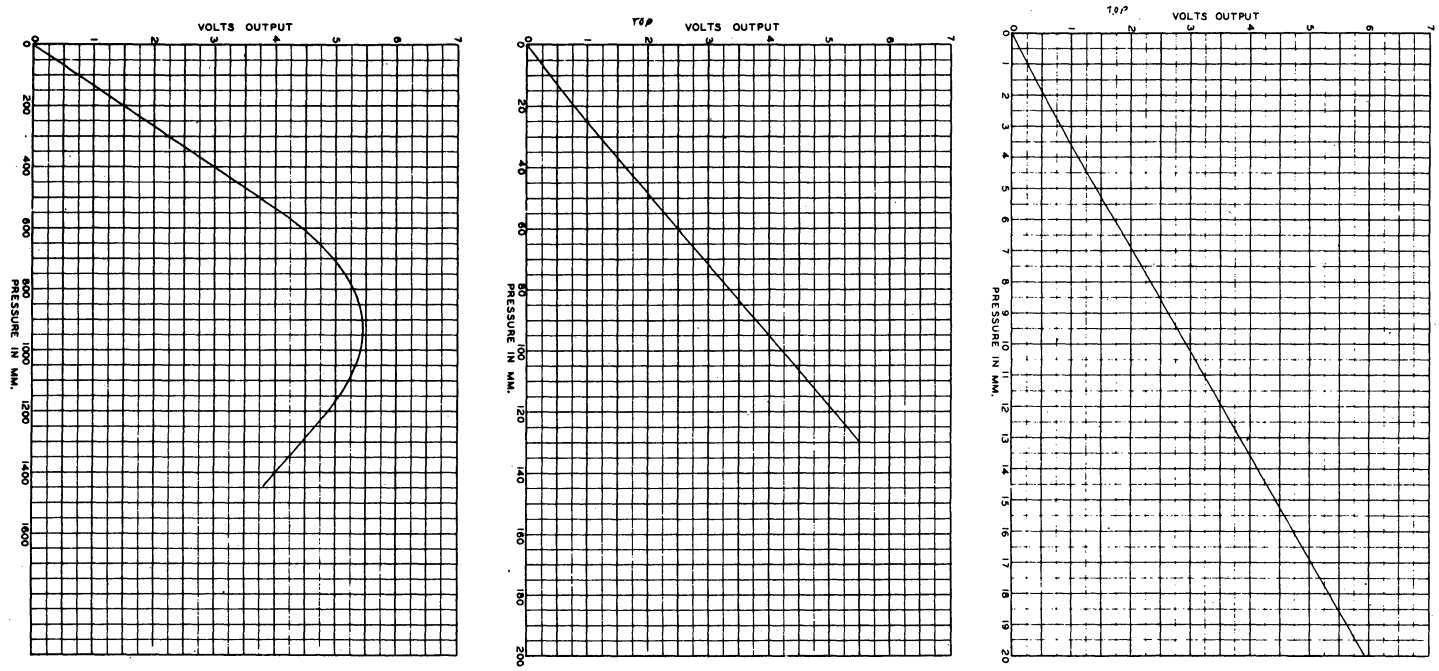

Fig. 87. Multiple Range Alphatron Characteristics, V-2 25

An investigation of AC operation of the parallel plate alphatron of Fig. 78 was made but not designed for flight because of the relative complexity compared to the DC circuit. The advantages of AC operation are that stable high gain AC amplifiers are simple to construct and that DC leakage currents can be blocked by condensers. The circuit for AC operation is shown in Fig. 88 and its characteristics in Fig. 89. An alternating ion collector voltage of 60 cps was used. It was required that the capacity of the collecting electrodes be balanced out. In Fig. 88 tube No. 1 is balanced against tube No. 2 in order to balance out the reactance current due to the capacity of the ion collector.

6.42 Pirani Gages

The Pirani gages developed were used for three purposes: to supplement the alphatrons used on V-2 25 at low pressures, to measure cone pressures on V-2's 25, 33 and 50 and for the probe experiment of V-2's 33, 50 and 56. Figs. 90 and 91 shows the construction of the gage used in the cone pressure measurements. Platinum and tungsten wires of various diameters were investigated. Tungsten was rejected as being unstable as illustrated in Fig. 92. Platinum (etched Wollaston) wire appeared to be quite stable and gages were made using wire 0.0002 inch in diameter and 2 inches long. These were used in the ambient and cone pressure measurements and were operated at constant voltage, although the associated circuits differed.

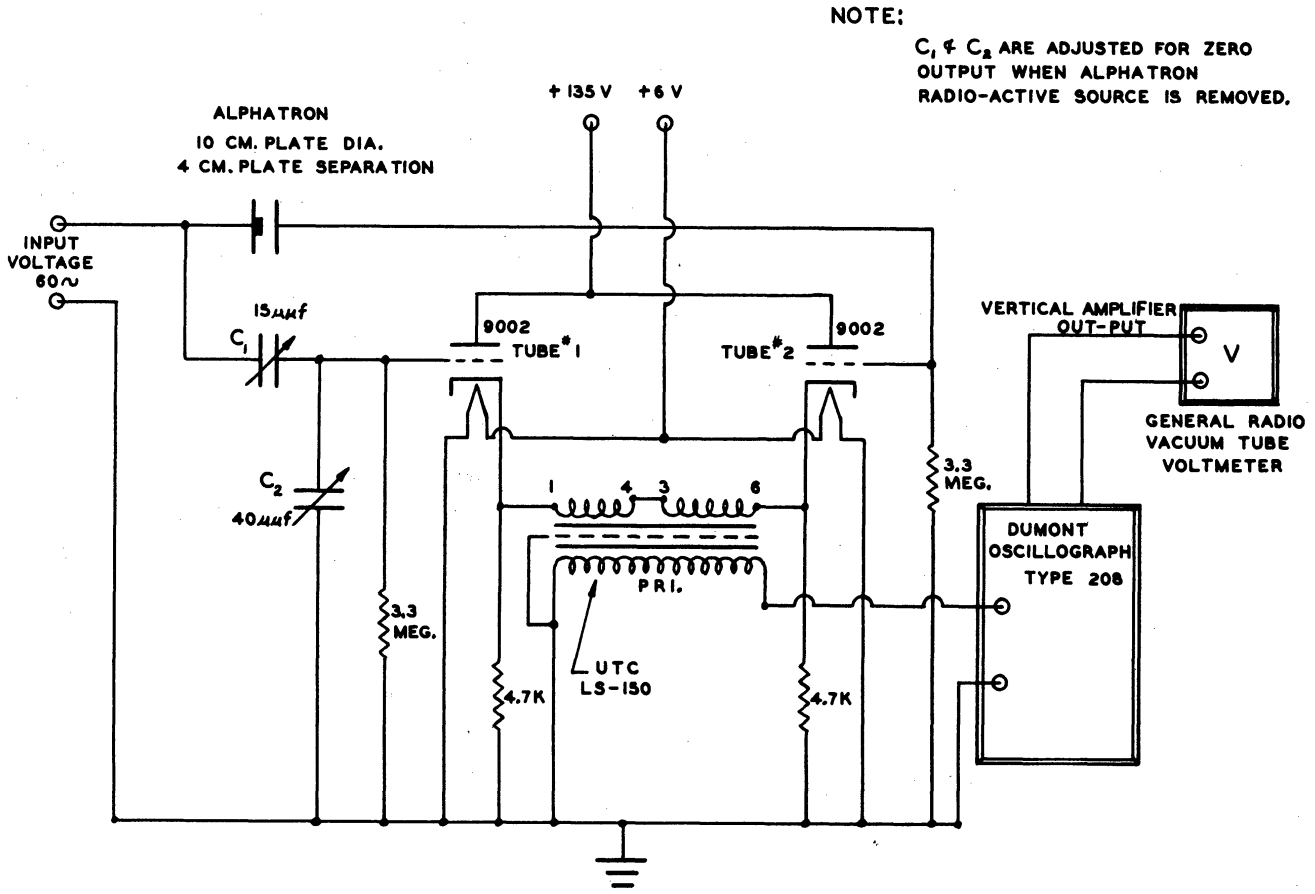

Fig. 88. AC Alphatron Circuit

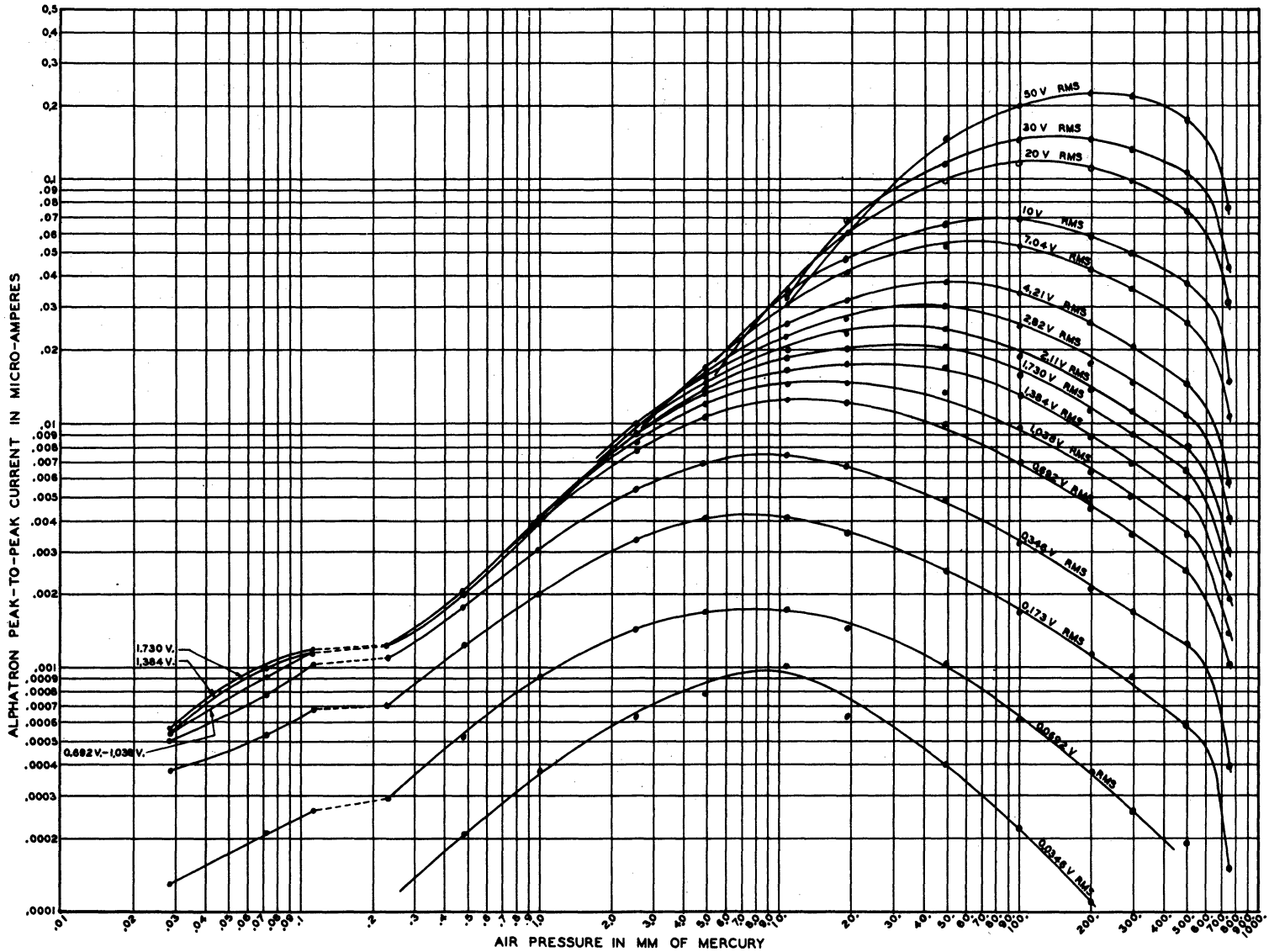

Fig. 89. AC Alphatron Characteristics

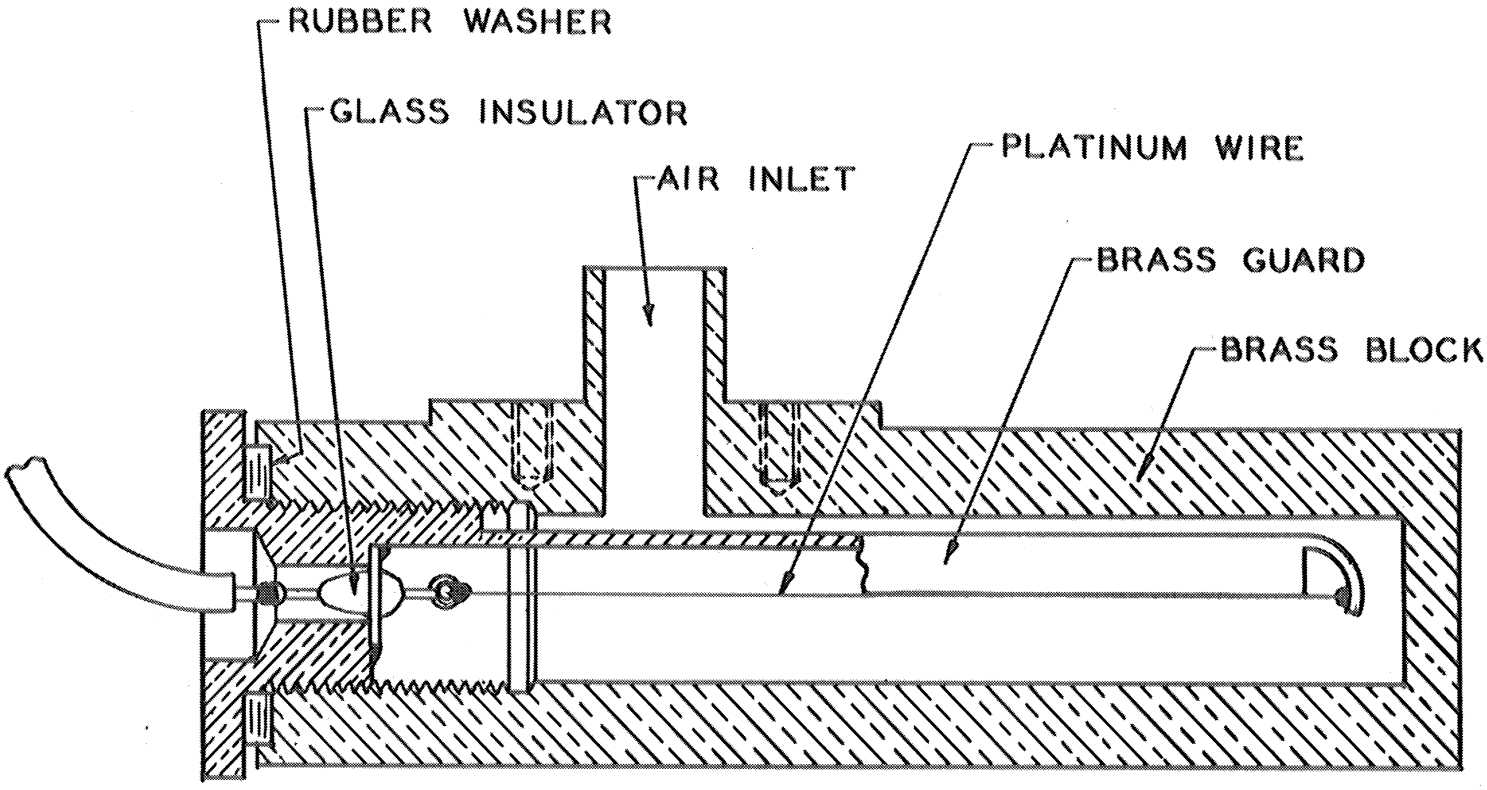

Fig. 90. Cone-Pressure Pirani

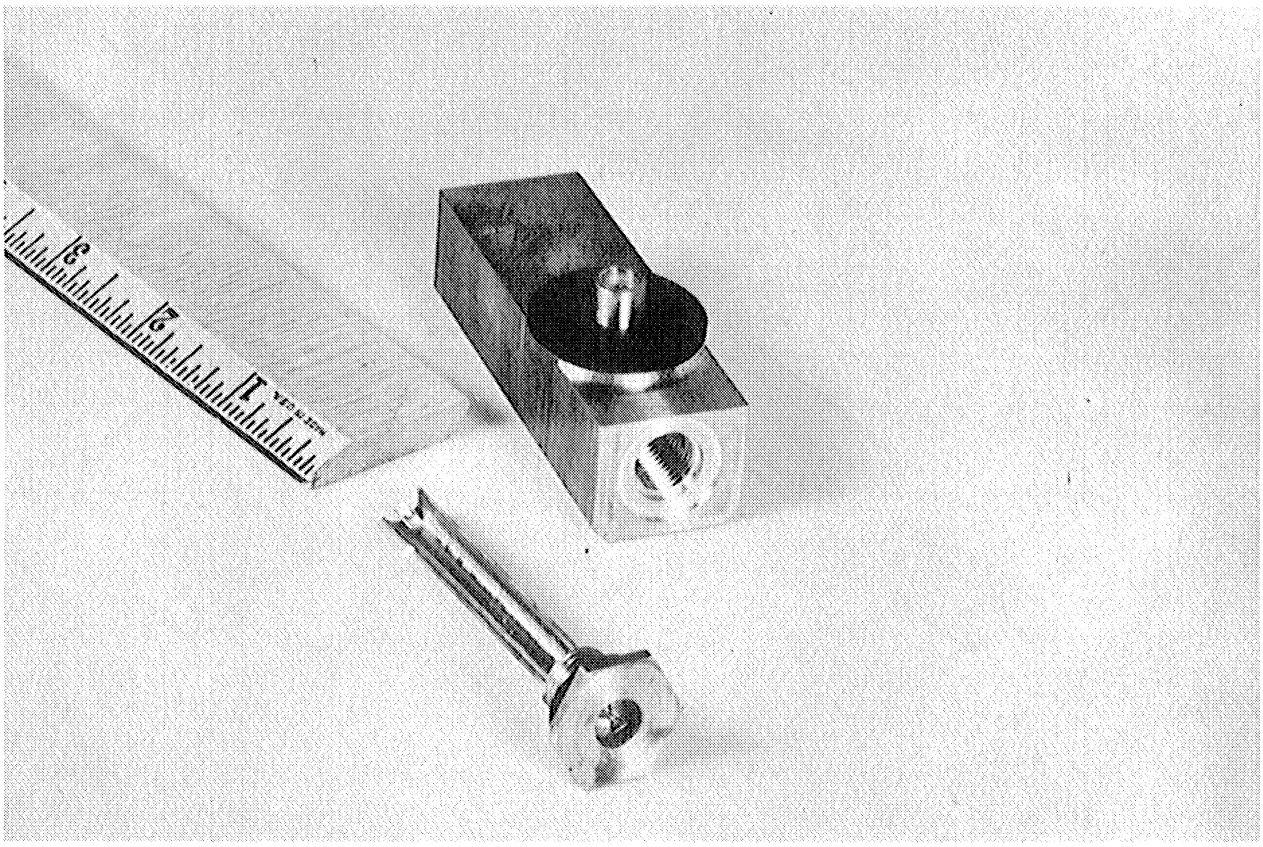

Fig. 91. Cone-Pressure Pirani

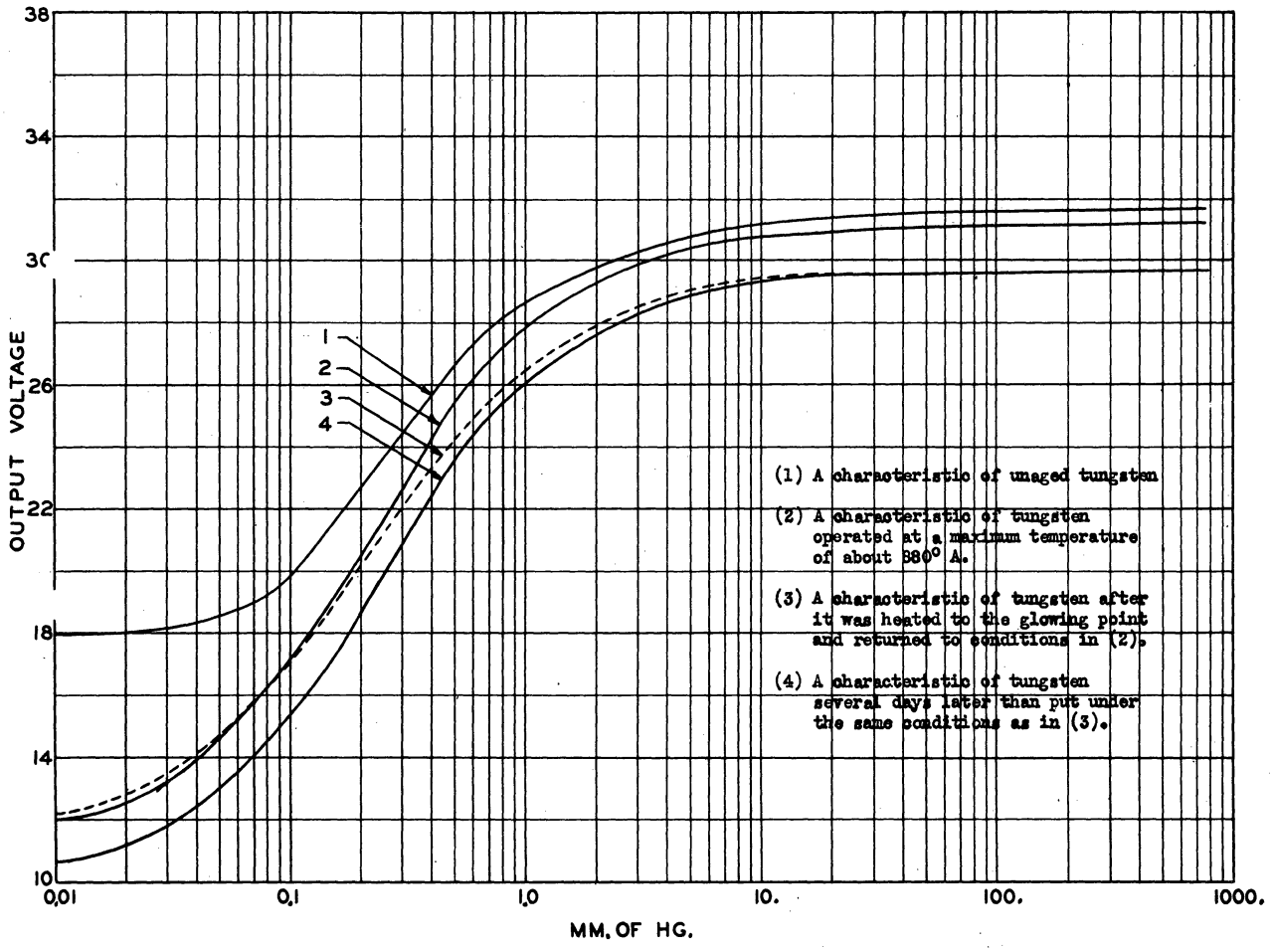

Fig. 92. Tungsten Pirani Characteristics

Tests performed on this type of gage with the circuit of V-2 25 are typical and are shown in Figs. 93 and 94. The curves of Fig. 92 were also obtained with this circuit. The characteristic of these gages which prevented the successful operation of the cone ram and side pressure experiment for temperature is their hysteresis which was brought to light in the work on V-2 50. See Section 6.23.

The development of the probe experiment required the development of a Pirani gage with the following characteristics: ruggedness, small orifice, small size, short time constant and sensitivity over a wide range of pressures. Experience with the gages of Fig. 90 led to the selection of platinum as the most suitable wire. Etched Wollaston wire, in which the platinum was 0.0001 inch in diameter, 1/2 inch long was used. This diameter wire has been used in the majority of probes flown, but on V-2 56, two 0.0002 inch diameter wires were tried for increased ruggedness. However, these survived no better than the 0.0001 inch diameter wires and have been discarded because of their longer time constant. The first probe gage design is shown in Fig. 95. In this gage the wire was soft-soldered. As a result of an experiment flown on V-2 42, see Section 6.61, in which the probe temperature due to aerodynamic heating was measured with thermistors, it was decided that soft solder might melt in flight. Lead and lead-indium solders were used on V-2's 33 and 50, respectively, but the soldering technique proved difficult. The gage wires for V-2 56 were welded and this construction has proved highly satisfactory. Other changes made to increase ruggedness after the experience gained in V-2 50 were: shortening the wire to

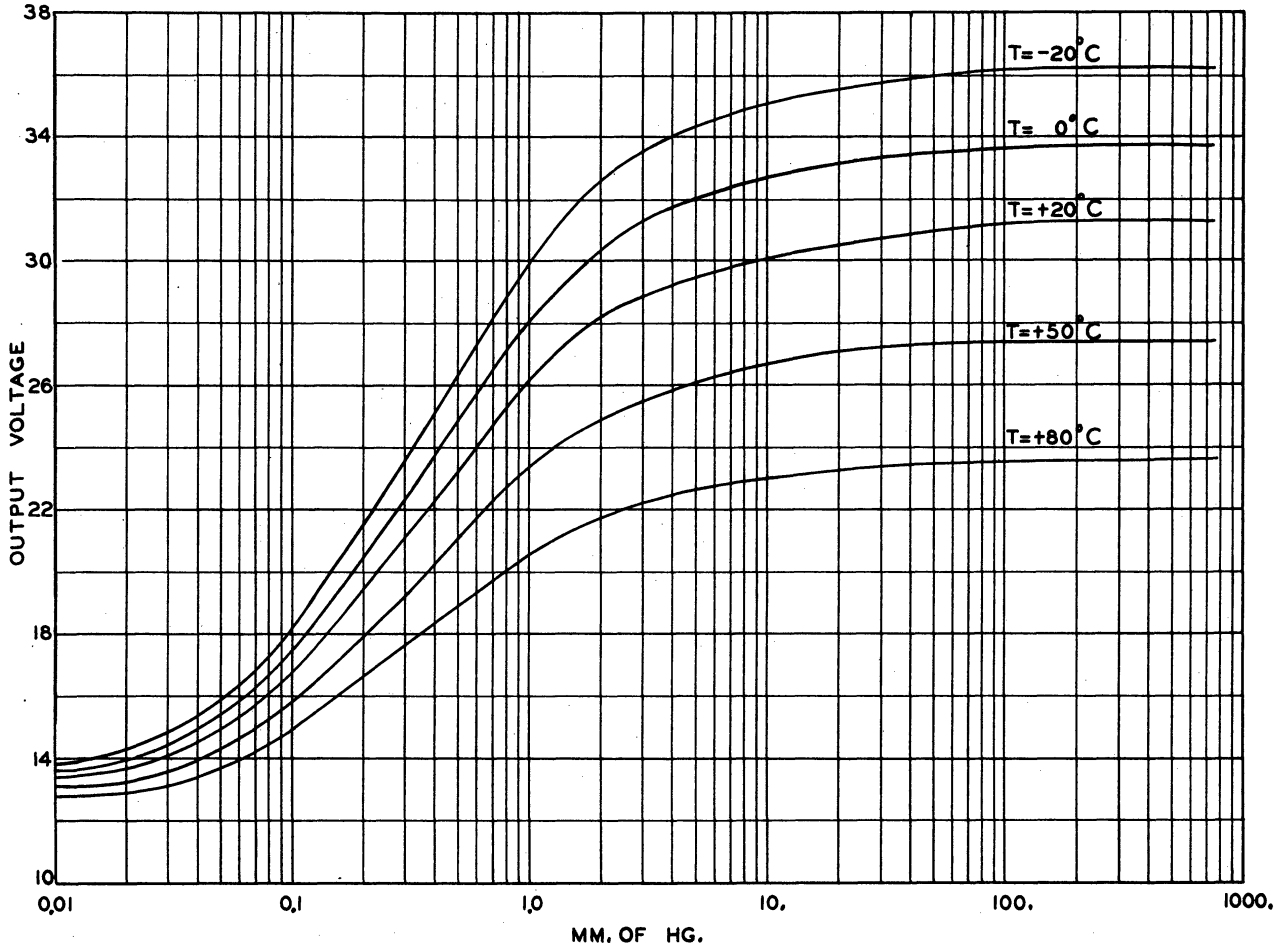

Fig. 93. Cone-Pressure Pirani Characteristics

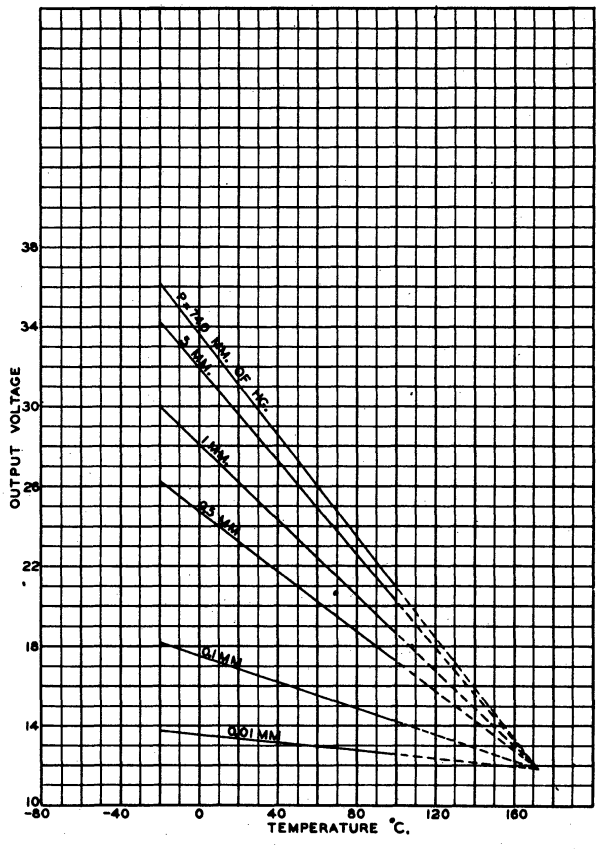

Fig. 94. Cone-Pressure Pirani Characteristics

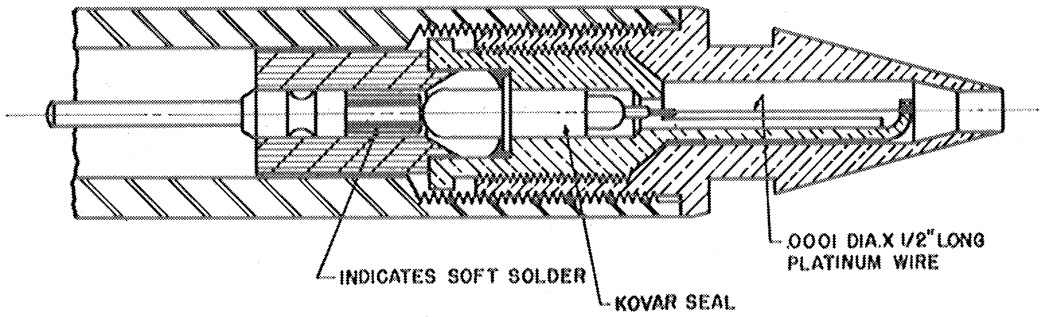

Fig. 95. Early Probe Pirani

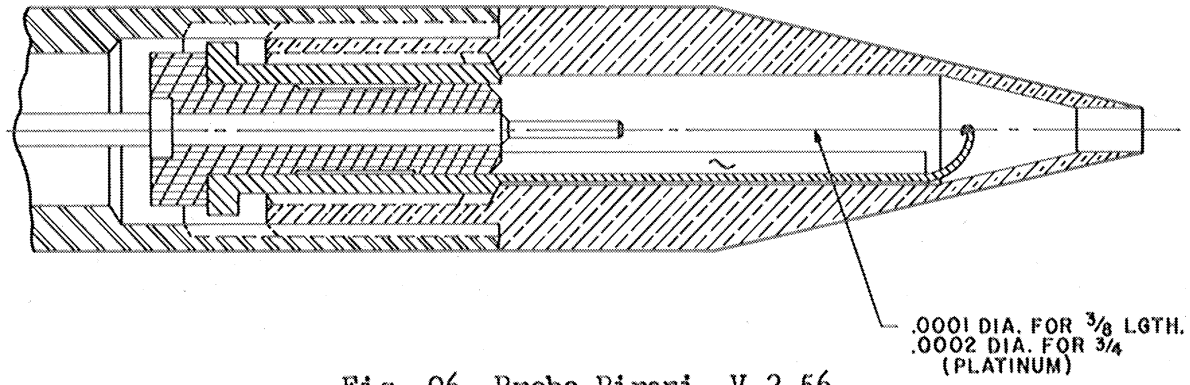

Fig. 96. Probe Pirani, V-2 56

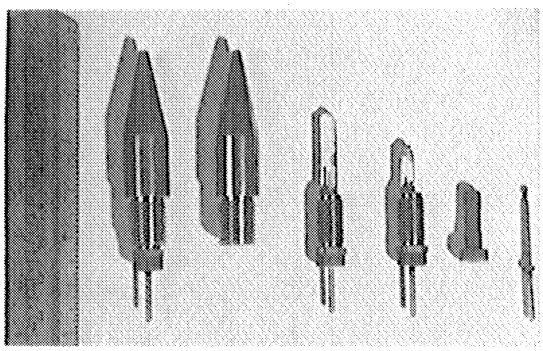

Fig. 97. Probe Pirani, V-2 56

3/8 inch, enlarging the cavity diameter to prevent touching when the hot wire sags, coating the wire support with Sauereisen cement to prevent grounding and too-rapid cooling in the event that the sagging hot wire touches the support. The current gage is shown in Figs. 96 and 97. To simplify welding on the Aerobee probes, the wire holder will be changed to stainless steel and its shape altered.

6.43 Pirani Gage Time Constants

The accuracy with which the pressure change of the shock wave in the probe method can be determined depends upon the time constant of the Pirani gages. The time constant, which is the time required to complete 63 percent of the voltage change caused by a rapid change in pressure, of the probe Pirani gages is determined by two factors; the time required for the pressure change at the tip of the probe to propagate into the cavity, and the time required by the hot wire to change its resistance after the air pressure inside of the cavity has changed. The time constants of gages similar to those used on V-2 56 were investigated in two ways. In the first

method a solenoid-operated bellows was used to produce a pressure change at the opening of the probe. The resulting change of voltage across the Pirani was recorded with a Hathaway oscillograph through a cathode follower. See Fig. 98. Because the mechanical system itself required 17 to 33 milliseconds to operate, the time constants determined with this method are higher than the true values. A lower limit for the gage time constant was arrived at with a second method. This consisted of applying a square wave of voltage to the Pirani wire and observing the change in Pirani current on a cathode ray oscilloscope. The time constants determined with this method are smaller than the true values because that portion of the time constant due to propagation of the pressure change into the cavity has been neglected.

The average values of these measurements are plotted in Fig. 99. The measurements were made for Pirani wires 0.5 inch in length. The investigation also showed that, for a given diameter of wire, increasing the length decreased the time constant, whereas decreasing the length increased the time constant. The 0.0002 inch diameter wires used on V-2 56 were 0.75 inch long and the 0.0001 inch diameter wires 0.375 inch long. In the temperature calculations from the probe data, it was assumed that the accuracy of a signal determination corresponded to the time ($T_{0.1}$) required for the Pirani gage signal to complete one-tenth of its total change. The probable range of values for $T_{0.1}$ are also plotted in Fig. 99.

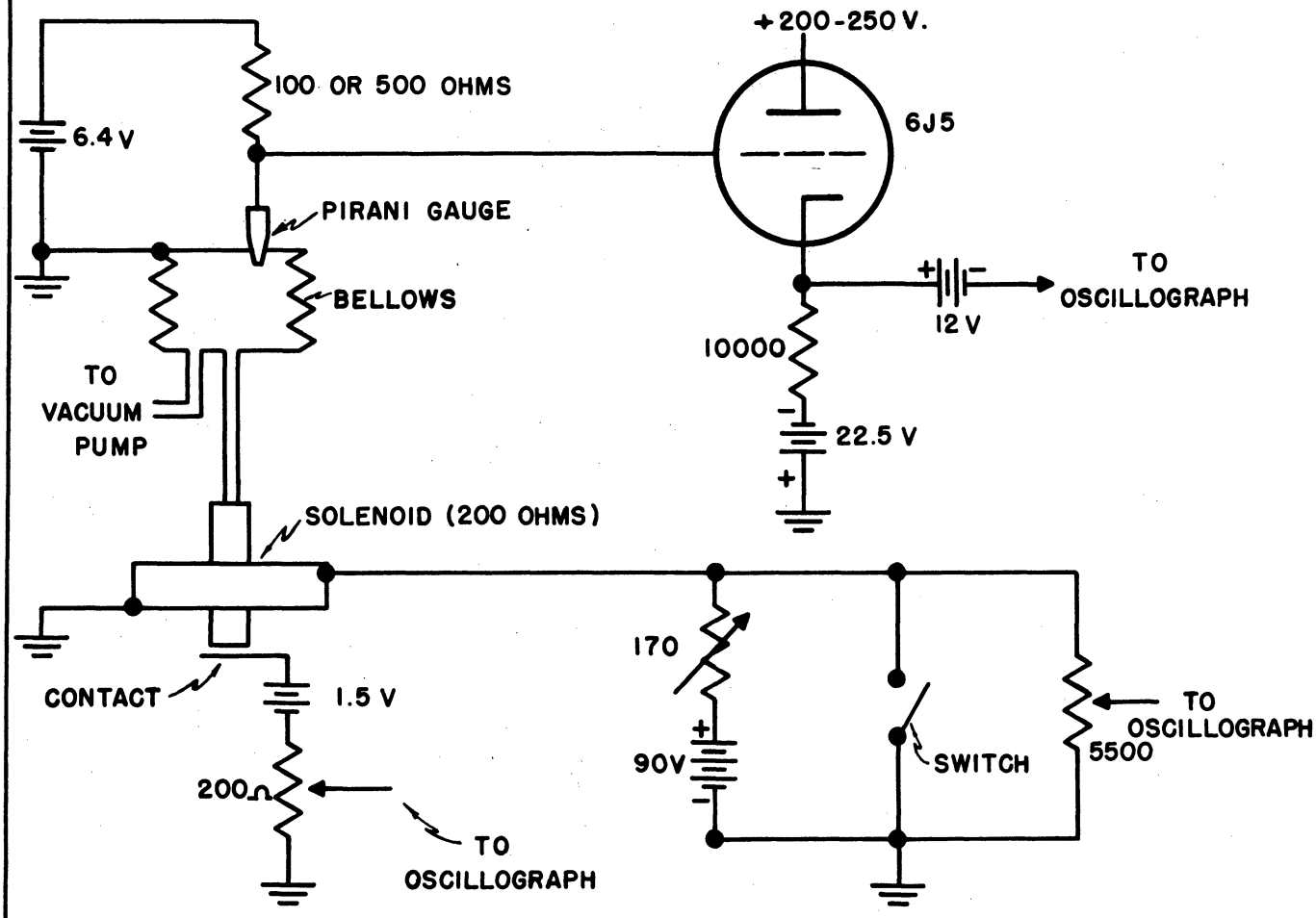

Fig. 98. Pirani Time-Constant Set-up

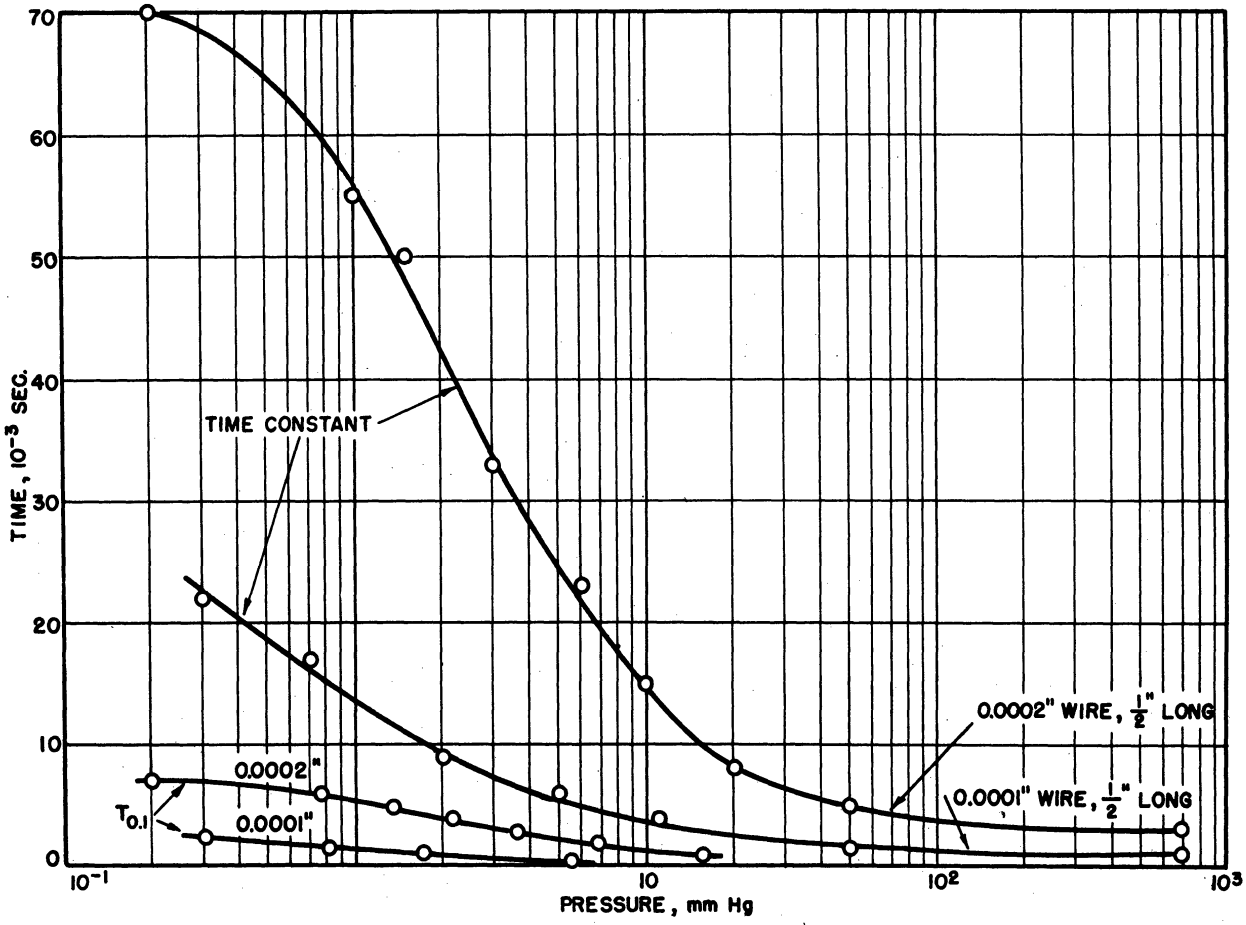

Fig. 99. Pirani Time-Constants

6.44 Pirani Gage Circuits

The circuits in which the Pirani gages were used are described separately because in most cases the characteristics desired were independent of the gages used. That is, a circuit with certain desirable characteristics could be easily adapted for use with any Pirani gage. The gages may be operated at constant current, constant voltage, constant resistance or in such a way that all three vary. Each mode of operation has advantages and disadvantages. Constant current operation requires only a simple series circuit consisting of a source voltage, a high series resistance to control the current and the Pirani. The output voltage is taken across the Pirani. The arrangement gives high sensitivity at low pressures and low sensitivity at high pressures. The gages burn out at higher pressures than in other arrangements. In constant voltage operation a series circuit is also used but the fixed resistance is small compared to the Pirani and the output voltage is taken across the resistance. Constant voltage operation gives moderate sensitivity over a fairly wide range of pressures and the gages do not burn out at as high pressures as in the constant current circuit. By making the series resistance about equal to the Pirani resistance in the measurement range the sensitivity can be improved in a certain pressure region of interest over that obtained with constant voltage. In addition, the pressure at which the gage burns out is lower than for the constant current method. The signal voltage may be taken from across either the Pirani or the series resistance. Constant resistance operation gives good sensitivity over a wider range of pressures than constant voltage operation

and, in addition, the gages will not burn out at any pressure. However, the circuits required for this kind of operation are elaborate.

Constant voltage operation was employed for all of the Piranis flown on V-2 25 and for the cone pressure Piranis of V-2 33. On V-2 25 the circuit used was a conventional low gain negative feedback AC amplifier. See Fig. 100. The output is rectified and fed to the telemeter through a cathode follower and the commutator of Fig. 85. The gages are driven by a regulated RC power oscillator. The 8-channel amplifier and oscillator chassis is shown in Fig. 101.

The cone pressure gages of V-2 33 were also AC-operated at constant voltage, but, in order to eliminate amplitude errors from the range switching commutator and the telemeter, the output voltage was used to time-modulate the telemeter. The circuit is shown in Fig. 102. Time modulation is accomplished by generating a saw tooth envelope in an AC scanning voltage of the same frequency as the driving voltage. The envelope is generated by a rotating potentiometer driven by a governor controlled motor. The scanning voltage is added to the gage output voltage 180° out of phase so that when the two voltages are equal the input to the amplifier is zero, resulting in a dip in the telemetering record. The scanning potentiometer also provides a pip marking the beginning of the scanning (as well as two calibrating voltages) so that Pirani output and hence pressure are a function of the time interval between starting pulse and dip. This circuit performed satisfactorily in the laboratory and for the one or two seconds of telemeter operations on V-2 33. The apparatus is seen in Fig. 103 and a typical record in Fig. 104.

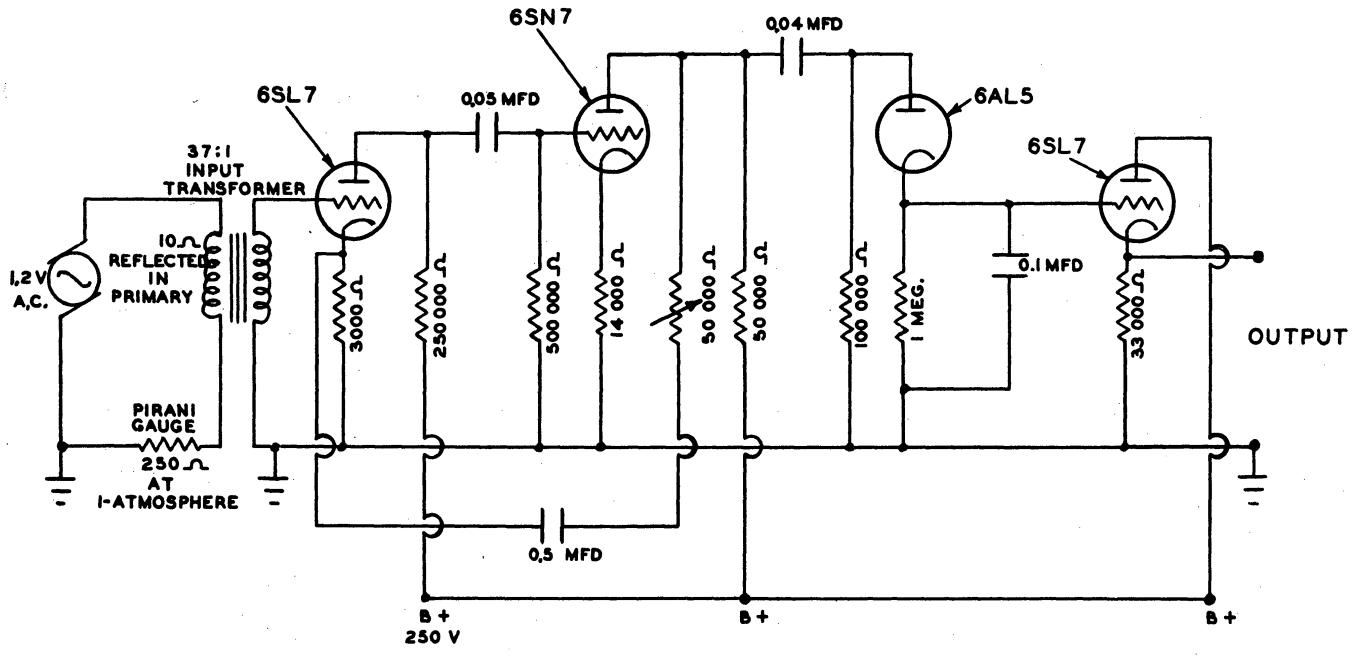

Fig. 100. Cone-Pressure Pirani Circuit, V-2 25

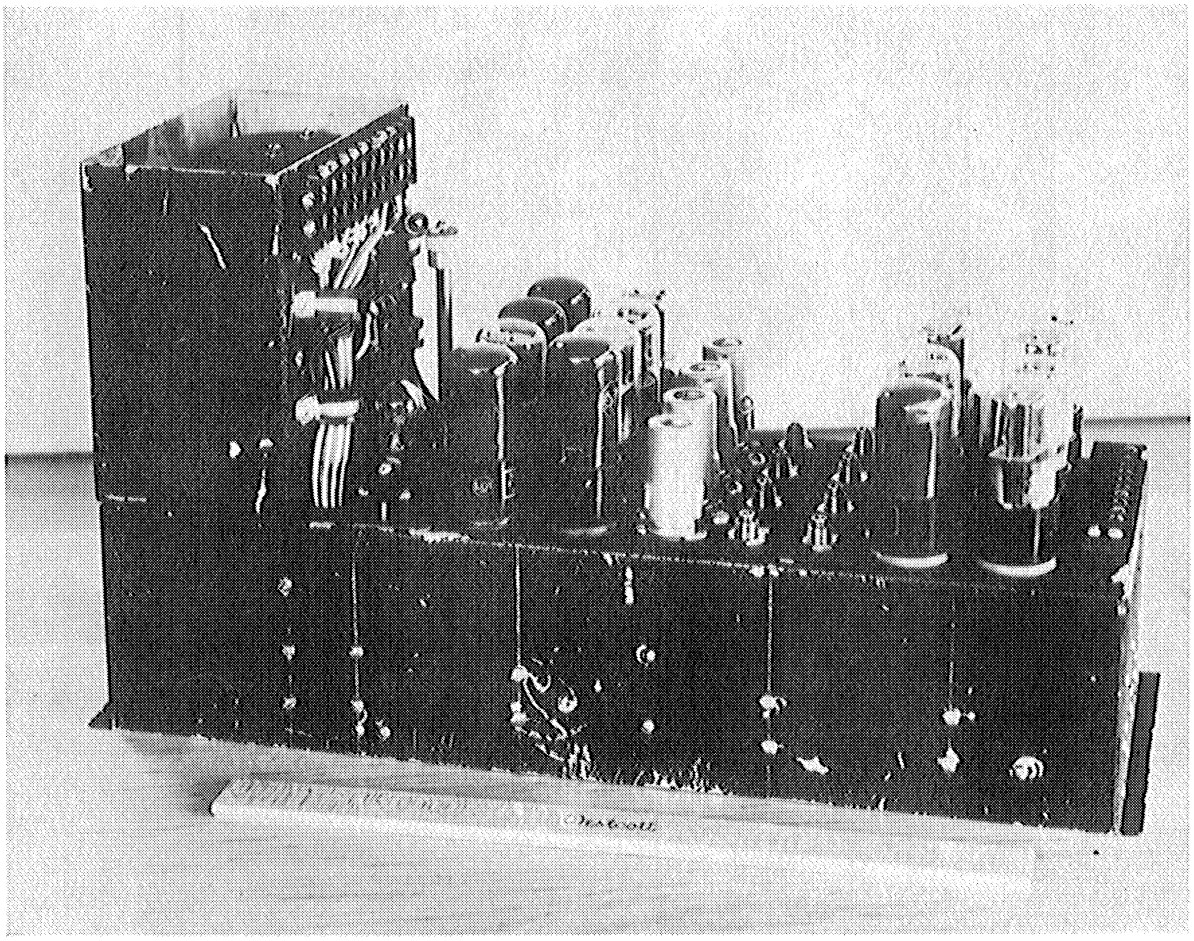

Fig. 101. Cone-Pressure Pirani Electronics, V-2 25

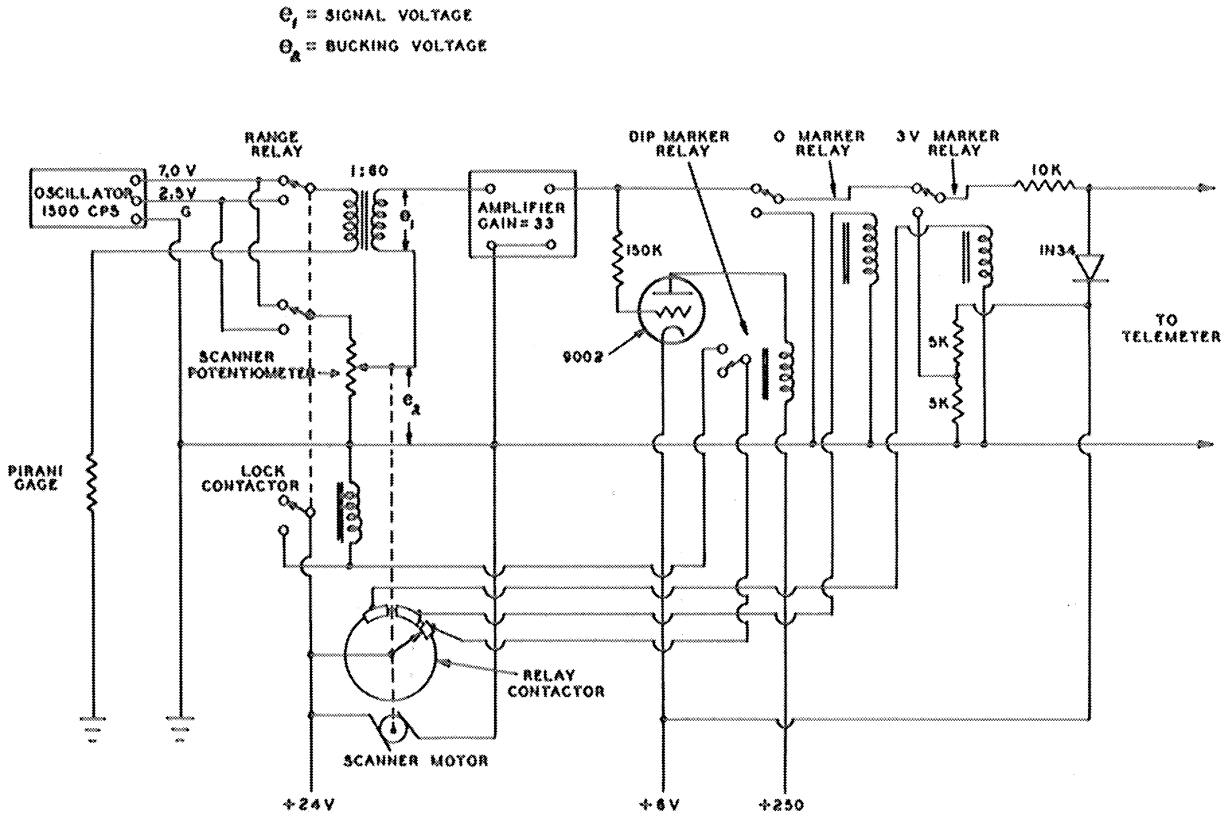

Fig. 102. Cone-Pressure Pirani Circuit, V-2 33

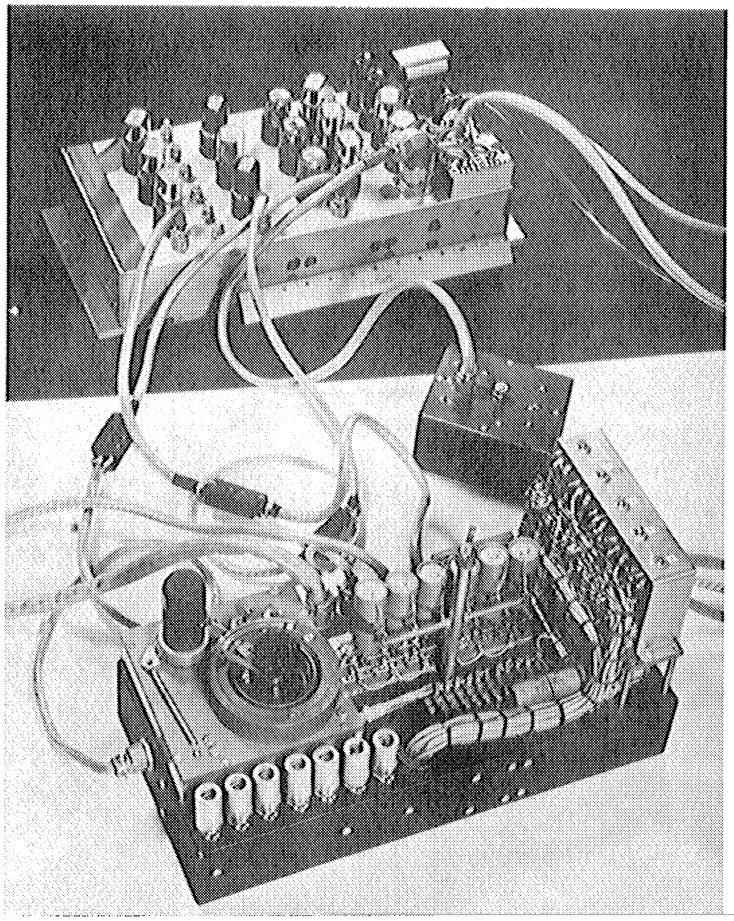

Fig. 103. Cone-Pressure Pirani Electronics, V-2 33

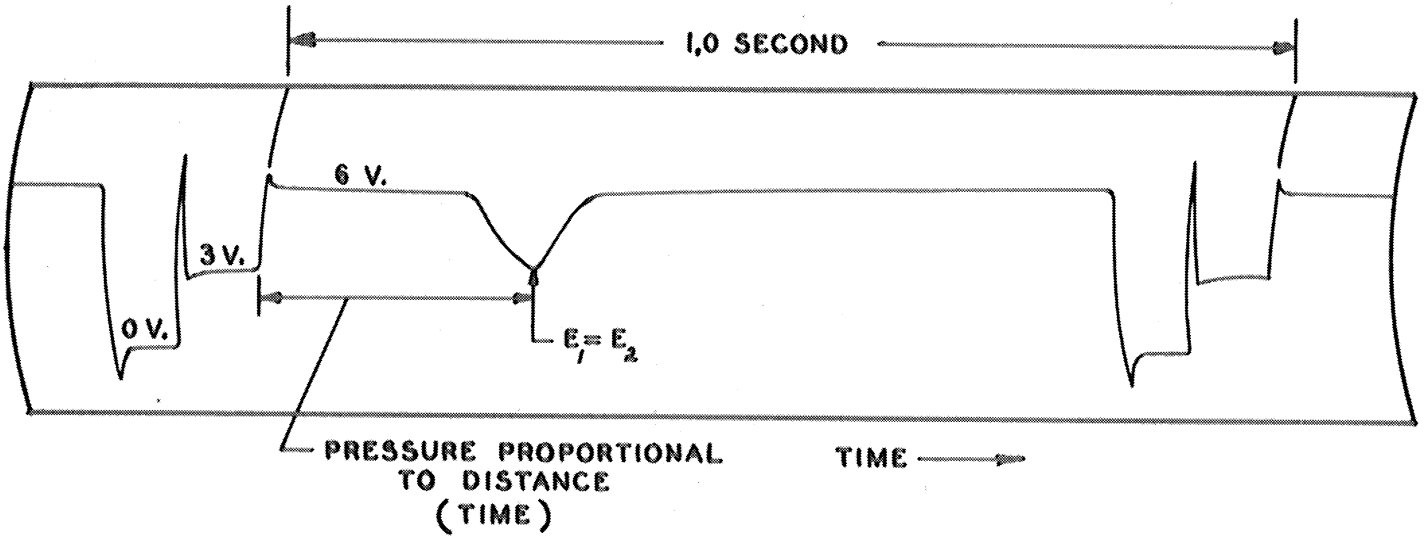

Fig. 104. Typical Record, V-2 33

The time-modulation circuit for cone pressure Piranis was further developed for V-2 50. On this missile the circuit contained the Pirani gage as one arm of a DC Wheatstone bridge. See Fig. 105a. The driving voltage to the bridge is scanned by a rotating non-linear potentiometer driven by a governor controlled motor. During each cycle the voltage increases, thus increasing the current to the Pirani and increasing its resistance. When the Pirani reaches a resistance that balances the bridge (600 ohms), it is dropped out by a relay and then reconnected to the bridge at the beginning of the next cycle. The bridge output voltage is converted to AC by a chopper and amplified for bridge balance detection. This time-modulation circuit, which extended the wide pressure range of constant resistance operation by use of the non-linear potentiometer, was linear and accurate over three decades of pressure although the overall accuracy of the system was poor because of the hysteresis in the Pirani characteristic. The apparatus is shown in Fig. 105b. The apparatus operated as designed on V-2 50 and gave the data discussed in the pressure measurements of V-2 50 in paragraph 6.23. A typical set of signals is seen at the bottom of Fig. 106.

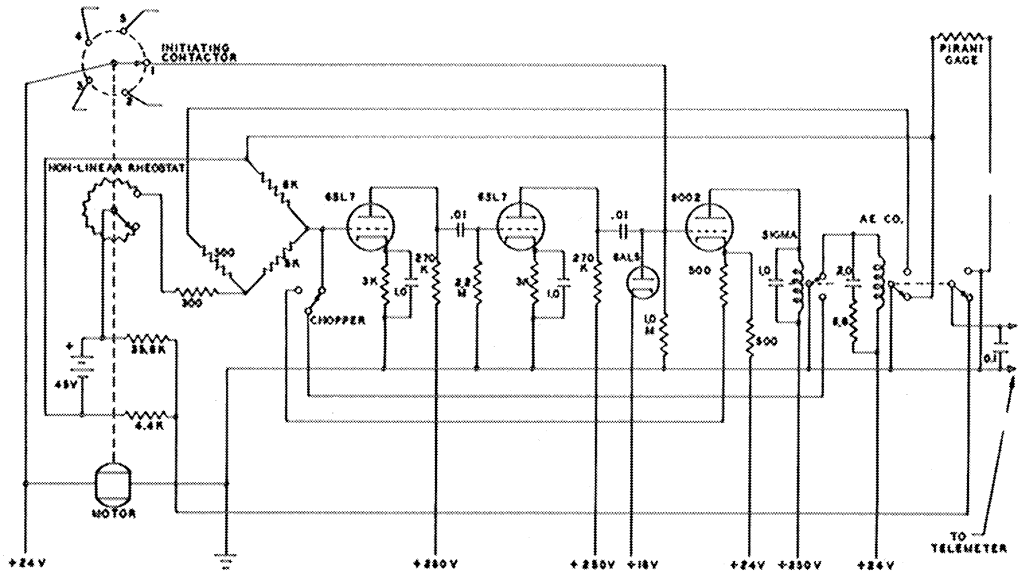

Fig. 105a. Cone-Pressure Pirani Circuit, V-2 50

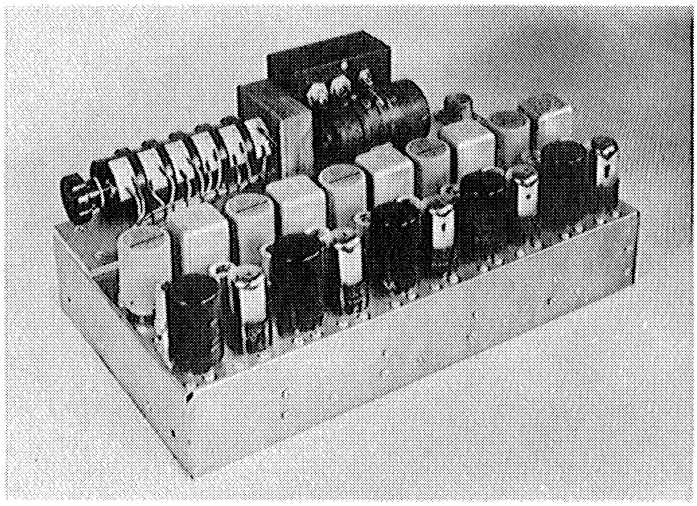

Fig. 105b Cone-Pressure Pirani Electronics, V-2 50

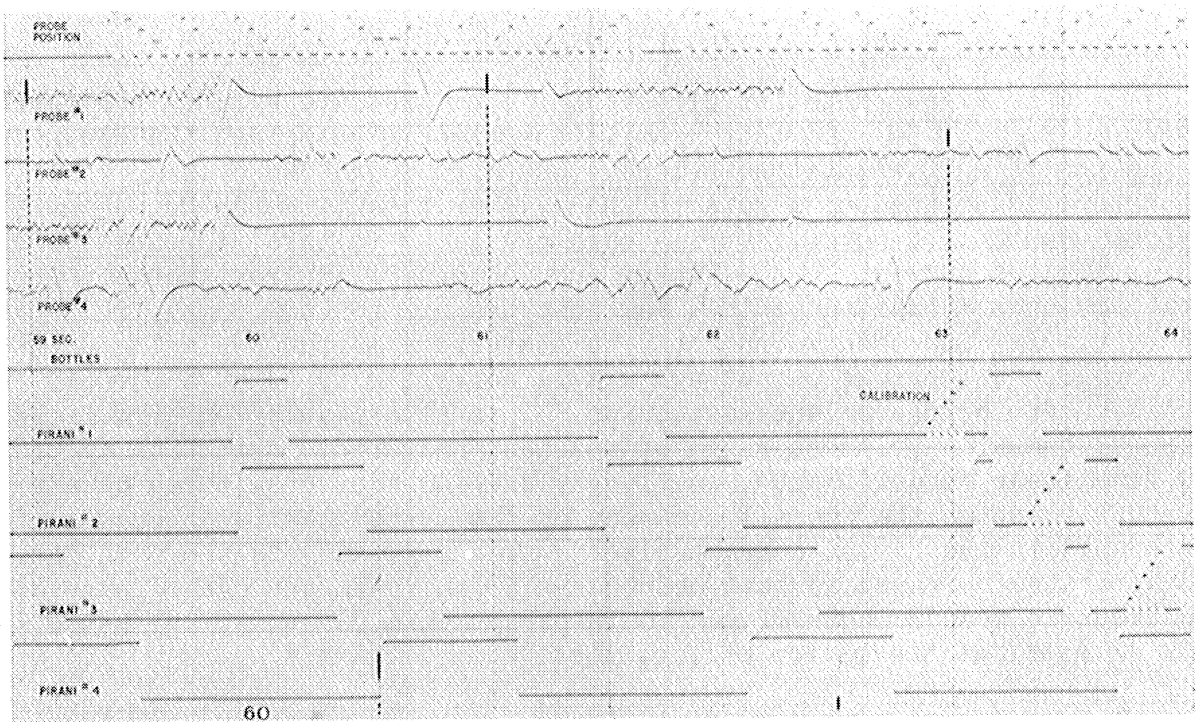

Fig. 106. Portion of Telemeter Record, V-2 50 Showing Cone-Pressure Pirani Signals

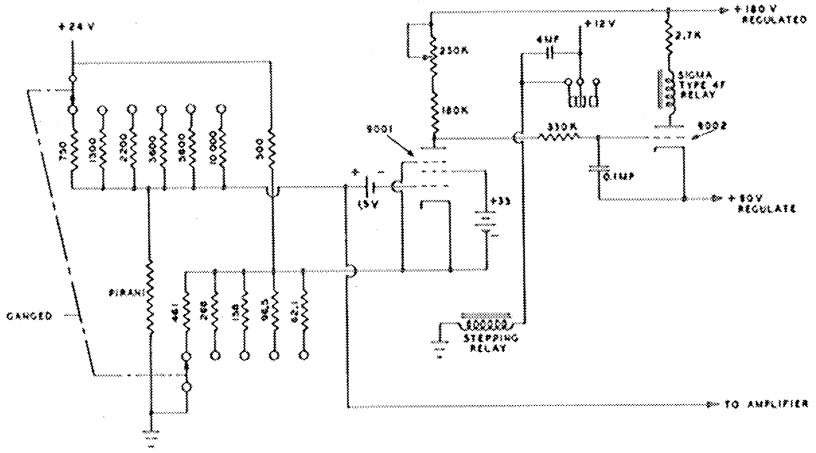

Fig. 107a. Probe Pirani Circuit, V-2 33

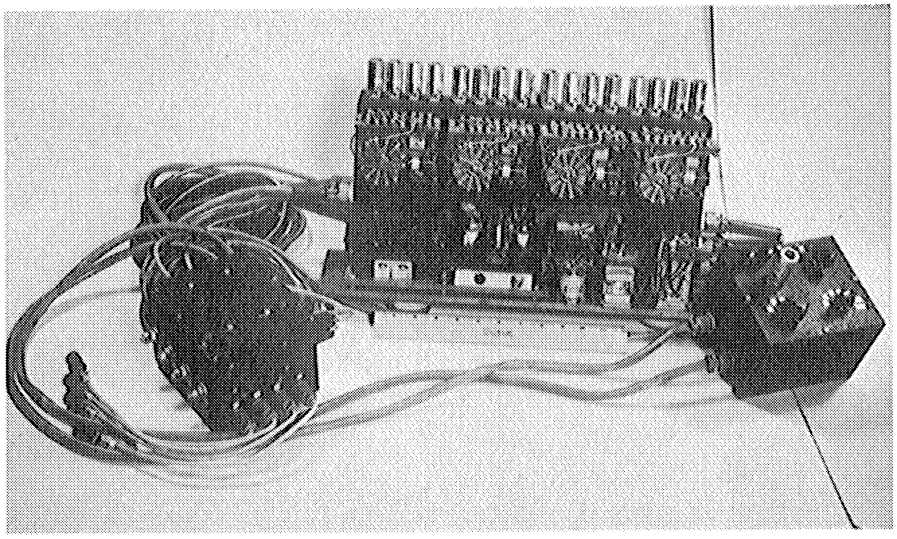

Fig. 107b. Probe Pirani Electronics, V-2 33

Several circuits were developed for the operation of the Piranis of the probe experiment. The circuit of Fig. 107 was used for V-2 33 and with minor changes on V-2 50. In this arrangement the Pirani is one leg of a DC Wheatstone bridge. The bridge arm resistances are chosen so that at high pressures the Pirani operate in the variable voltage, variable current condition. As the pressure decreases, the Pirani resistance increases. When the Pirani reaches 700 ohms the electronic circuit detects balance and switches a higher resistance into the bridge arm through which the Pirani is driven. At low pressures the Pirani operates at constant current. The transient output of the Pirani gage which is generated as the probe intersects the shock wave is fed into the amplifier of Fig. 108. The amplifier gain characteristic, shown in Fig. 109, is made non-linear with Thyrite in order to limit the input to the telemeter on large signals. The frequency characteristic is shown in Fig. 110. The high frequency cut-off is introduced to discriminate against noise and signals at the resonance frequency of the Pirani chamber. This apparatus was flown on V-2 33 and with only minor modifications on V-2 50.

It was determined from the data on V-2 50 that the signal to noise ratio to be encountered under flight conditions would be good. Therefore, it was decided to simplify the Pirani driving circuit for V-2 56 using a variable current, variable voltage arrangement. The series resistance was chosen to give best sensitivity in the region of 200,000 feet and the gain of the amplifiers was increased to give ample signal above and below this altitude. Figs. 111, 112, 113, and 114 show the gage driving circuit, the gage characteristics of the apparatus, the amplifier and the frequency characteristic used on V-2 56.

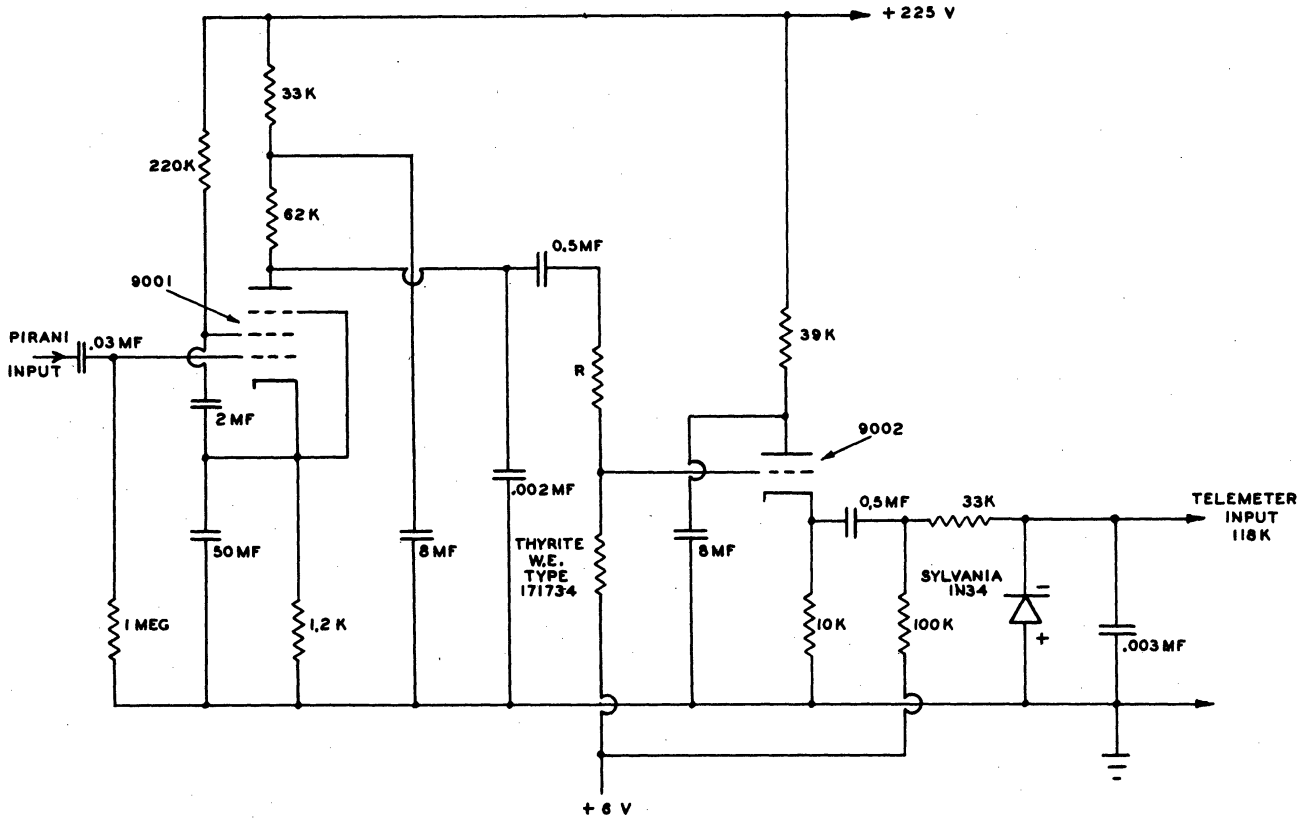

Fig. 108. Probe Amplifier Circuit, V-2 33

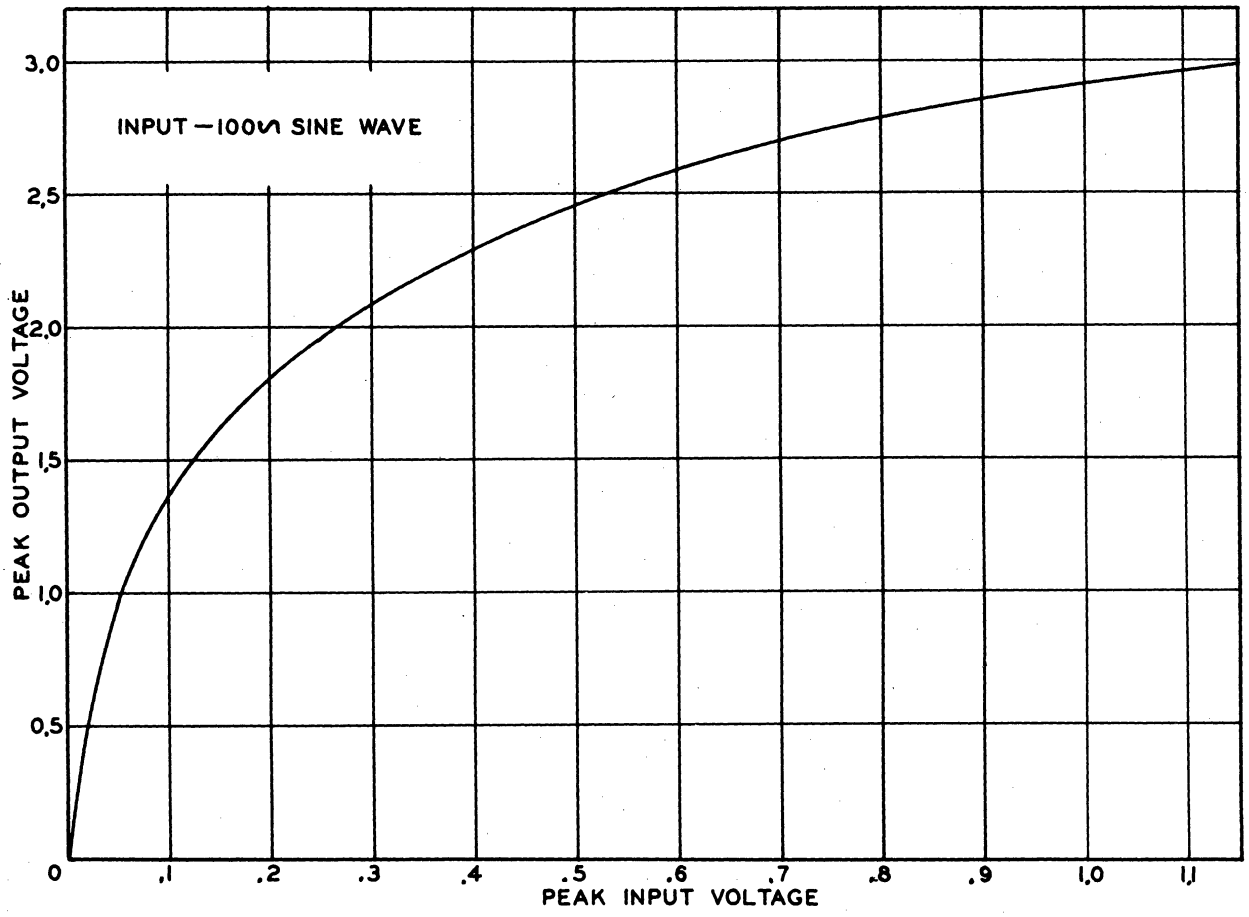

Fig. 109. Probe Amplifier Input-Output Characteristic, V-2 33

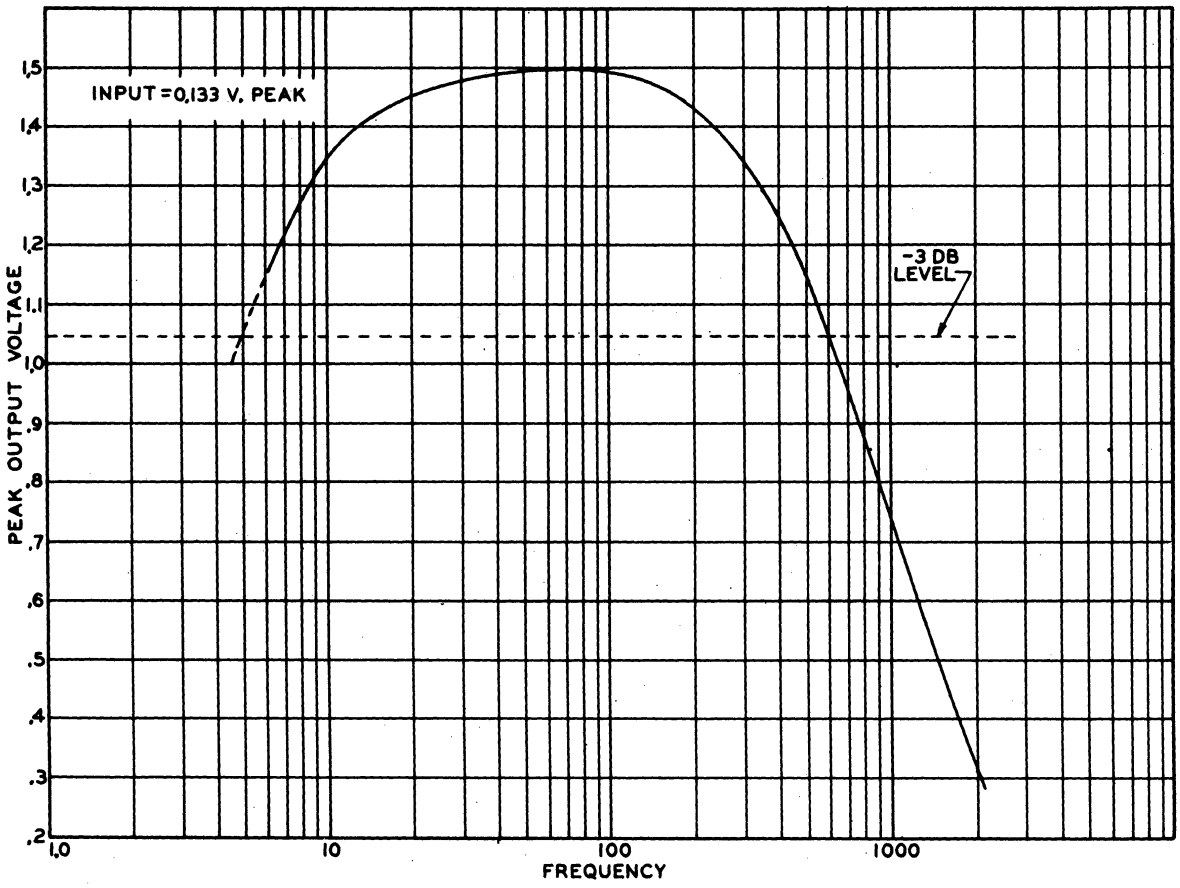

Fig. 110. Probe Amplifier Frequency Characteristic, V-2 33

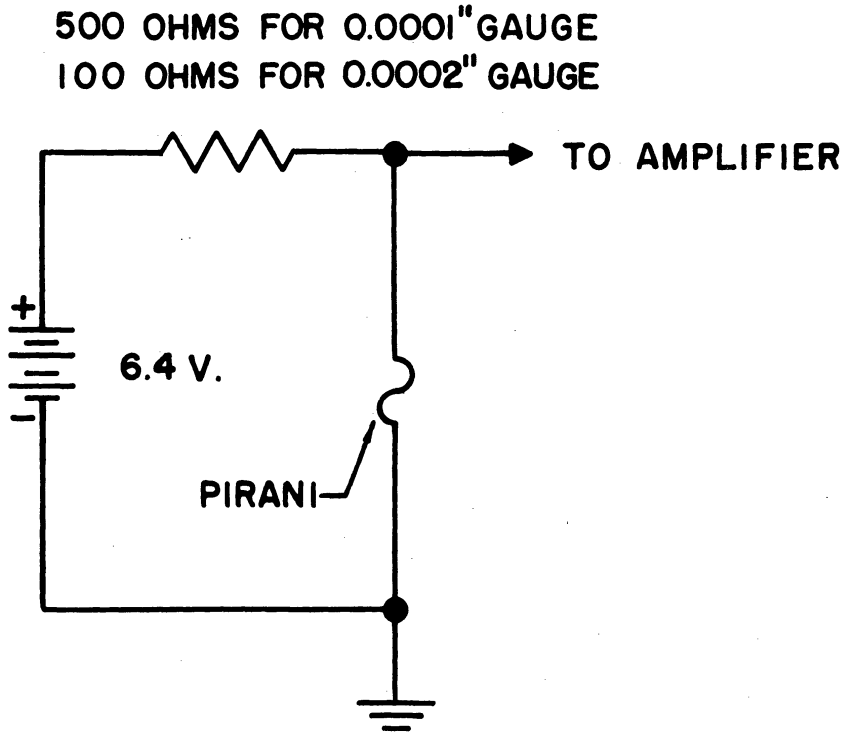

Fig. 111. Probe Pirani Circuit, V-2 56

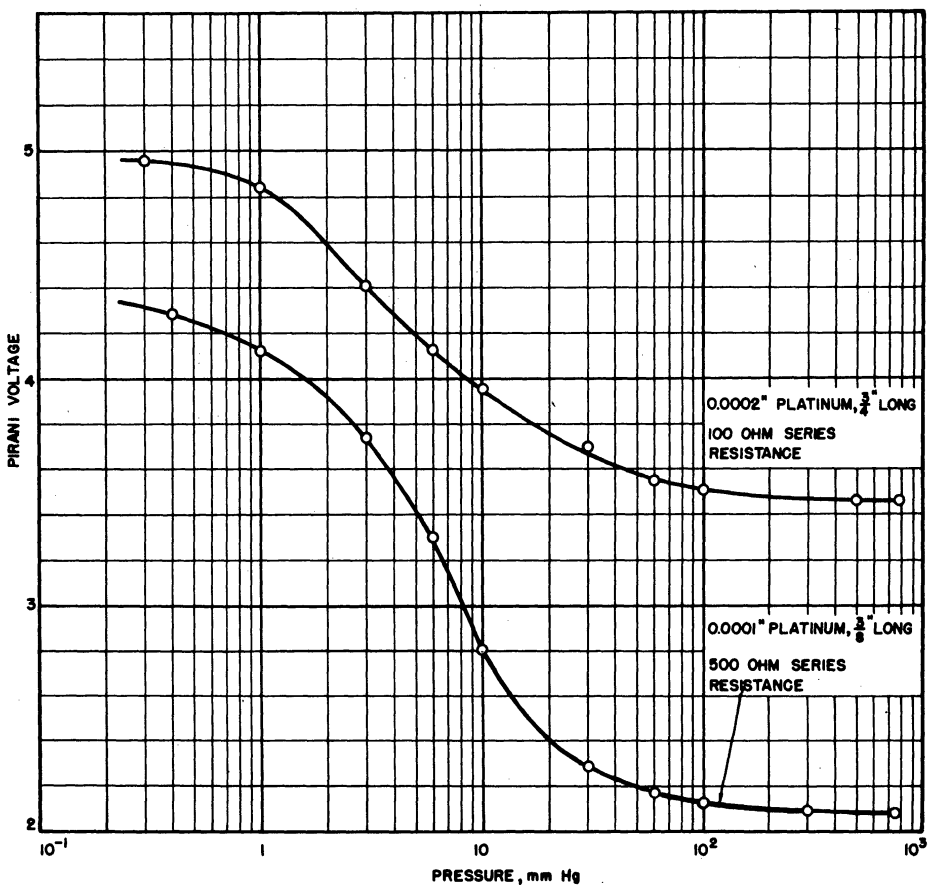

Fig. 112. Probe Pirani Characteristics, V-2 56

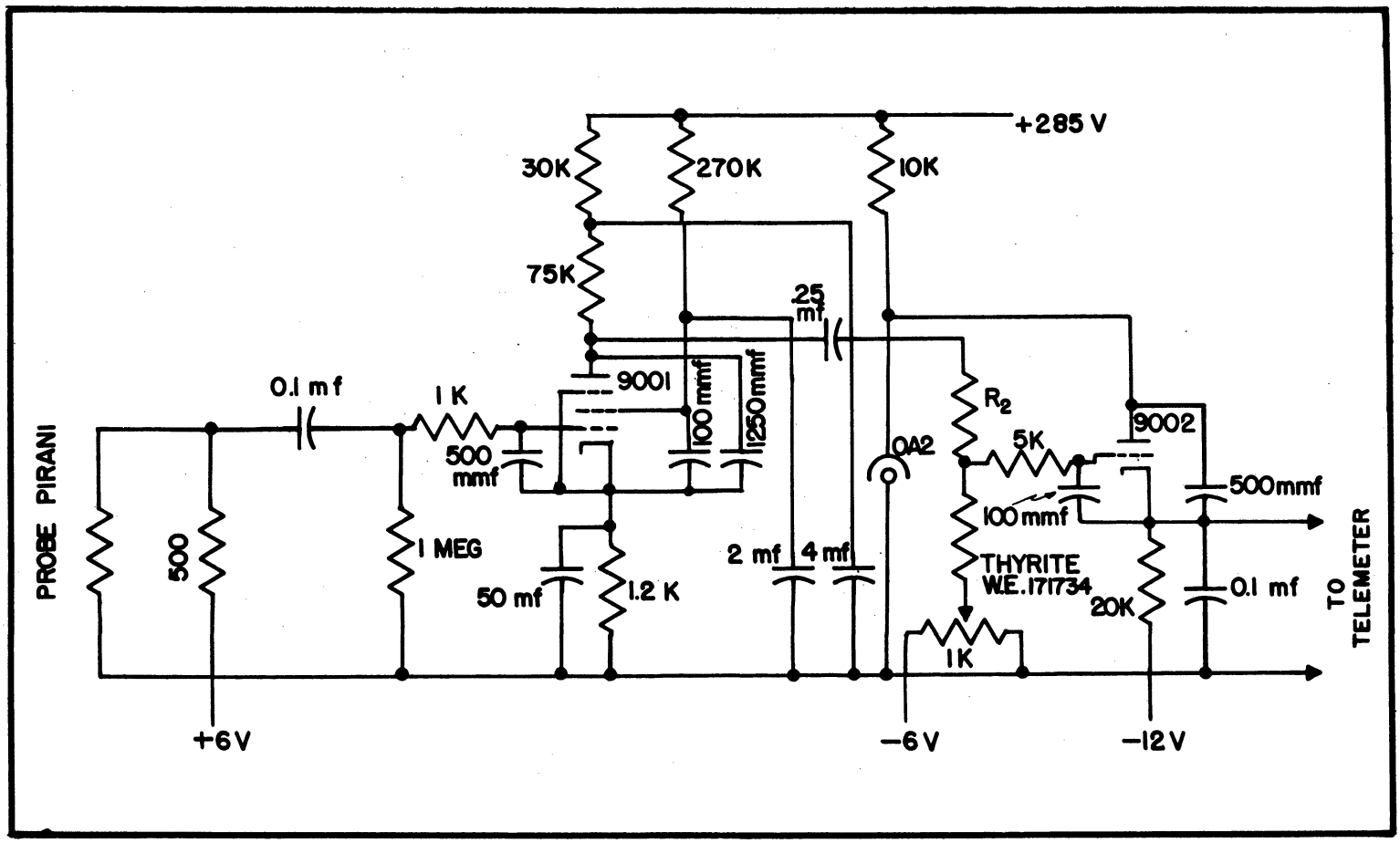

Fig. 113. Probe Pirani Amplifier, V-2 56

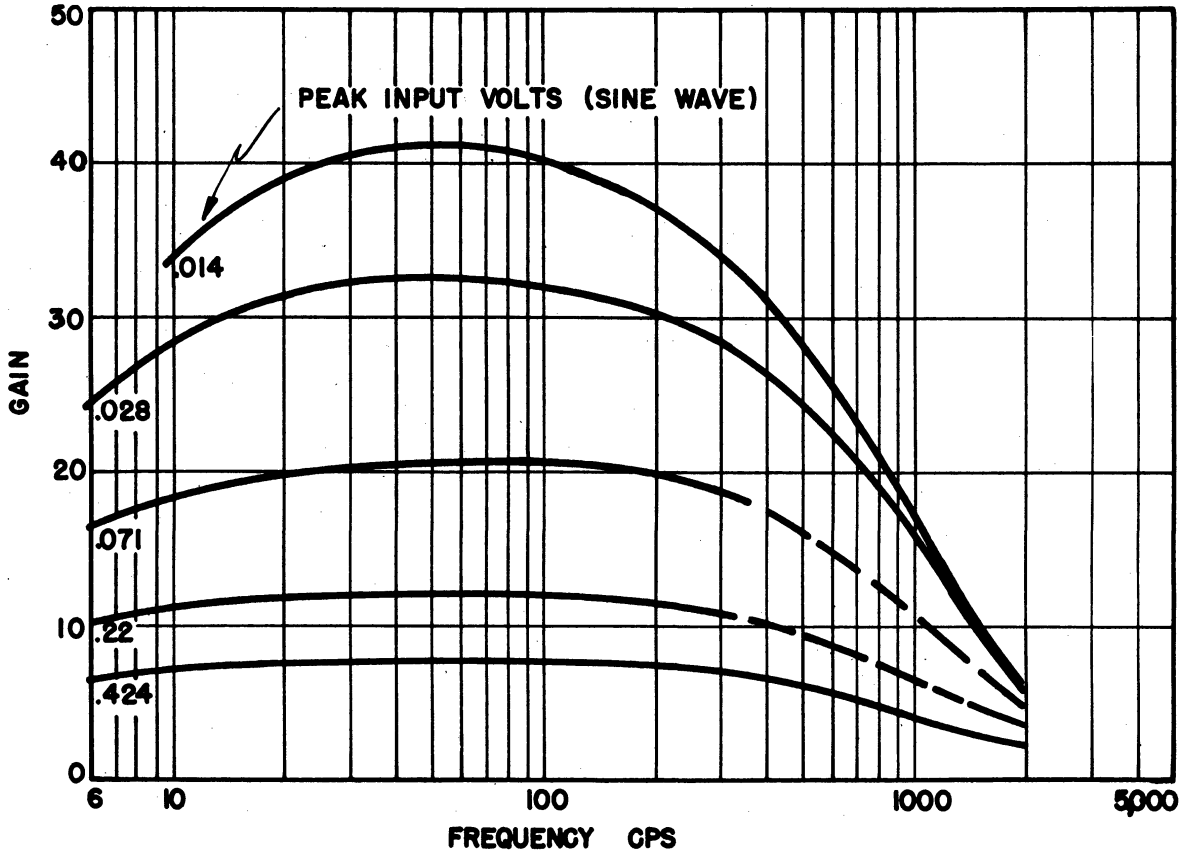

Fig. 114. Probe Pirani Amplifier Characteristics, V-2 56

6.45 Circuits for Probe Aerobee - Magnetic Recorder

The circuit containing the Piranis on the probe Aerobee is essentially the same as that used on V-2 56. However, the adaptation of the experiment to the Aerobee required a data system capable of handling 11 channels continuously. It was thought that a 13 channel magnetic recorder could be developed which would be lighter and simpler to use than two units of the FM-FM Bumblebee telemeter currently used on Aerobees. Since amplitude accuracy is not required it was decided to use an AM system. Good time accuracy could be obtained by recording a time signal from the timer and also transmitting the time signal to the ground over the single channel of doppler telemeter. Thus ground time and rocket time could be correlated.

The development of the recorder started with an investigation of the Cook 13 in-a-row heads salvaged from V-2 56. However, because of better availability and higher playback signal outputs attention was turned to Brush Development Co. heads similar to those used in the Cook recorder of V-2 50. See Section 8.2. An experimental tape transport mechanism, Fig. 115, was built for tests on the heads and for playback of flight records. Amplifiers were built for playback and tests on the system were run. The final tape transfer characteristics are shown in Fig. 116, and the frequency response in Fig. 117. It was noted that the overload characteristic for a 17 volt bias gave the same type of non-linearity sought in the probe amplifiers on V-2s to keep a wide range of signals within the modulation range of signals within the modulation range of the telemeter unit. Hence, it was unnecessary to introduce non-linearity in the probe amplifier described below.

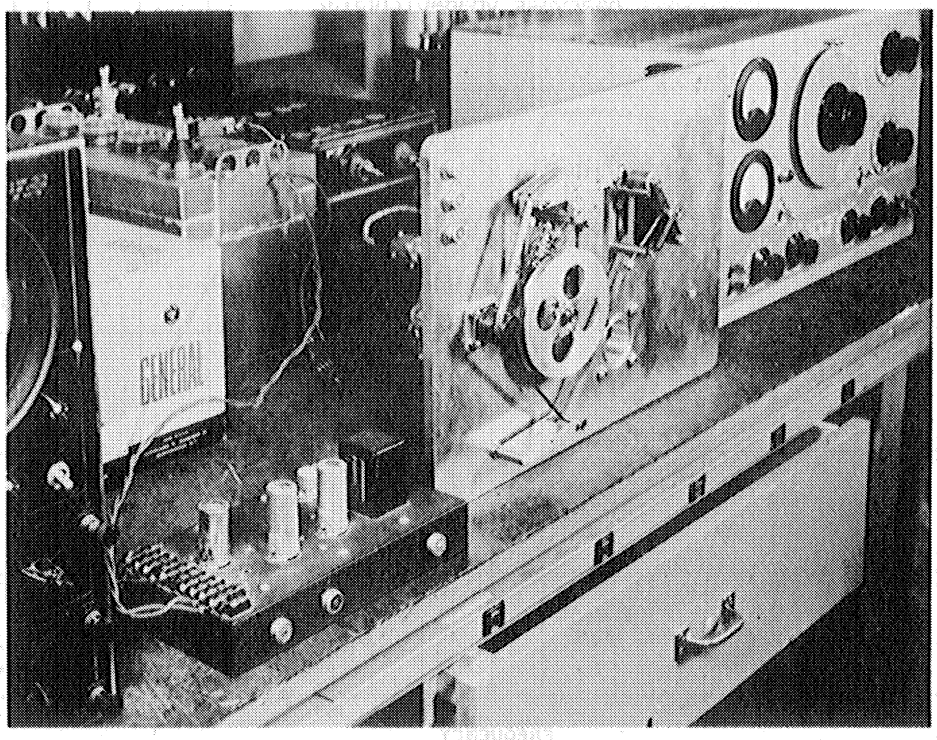

Fig. 115. Experimental Tape Puller

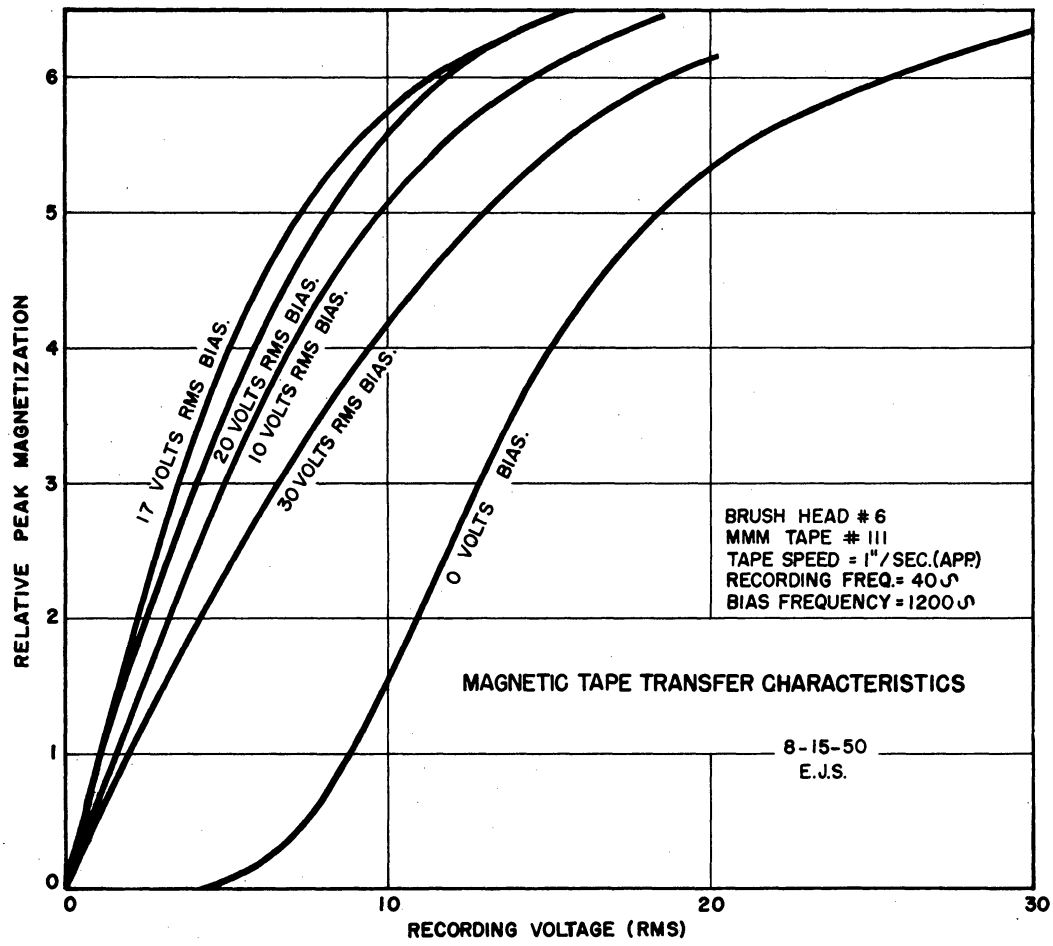

Fig. 116. Transfer Characteristics, Recorder and Playback

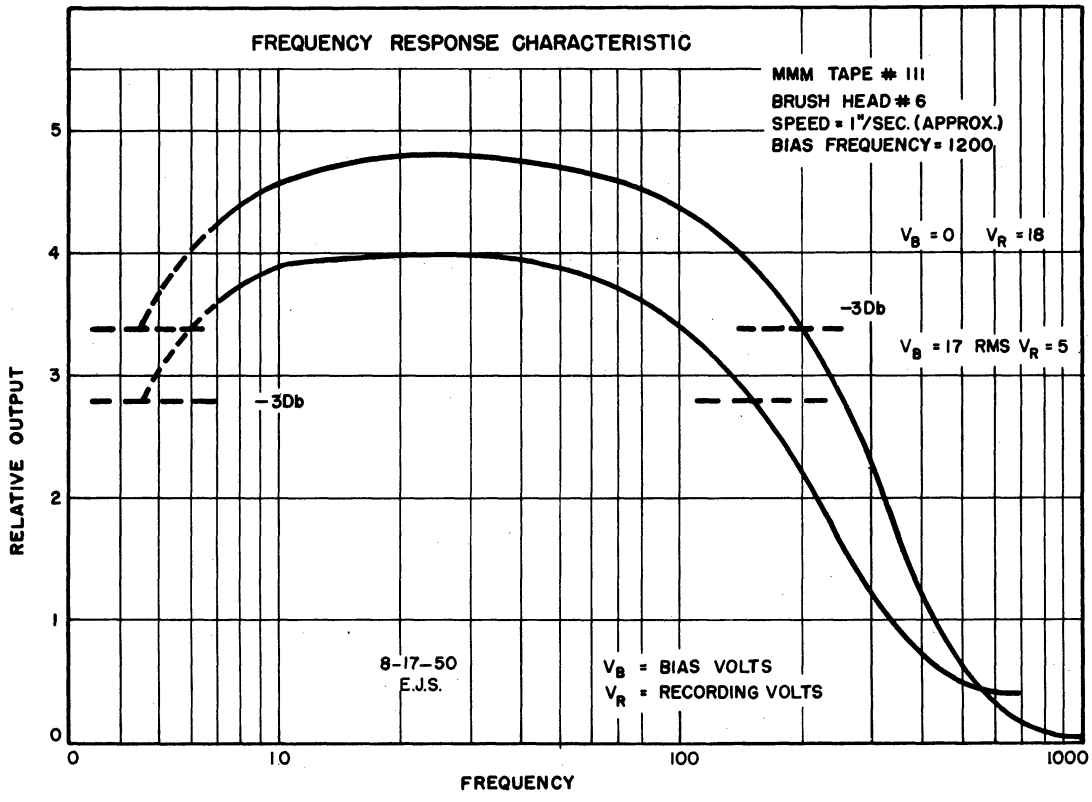

Fig. 117. Frequency Response, Recorder and Playback

It is seen in Fig. 117 that bias causes little change in the frequency response characteristic. The high frequency -3 db point occurs at the point at which it was desired. The low frequency -3 db point occurs at about 5 cps.

Following the successful test of the breadboard system, development of the flight electronics and tape puller was carried out. The Brush heads were arranged in a 13 channel configuration similar to that on the first Cook recorder. See Fig. 118. Tests of the system revealed two difficulties:

a) Crosstalk of the order of 50% between adjacent channels was encountered. This was a playback phenomenon caused by fringing flux on the tape. It was remedied by additional shielding of the heads from each other by means of a sheet of .013" thick transformer steel on top of the heads next to the tape. The shield, shown in Fig. 118, reduced crosstalk to 5% at 10 cps and less at higher frequencies.

b) Simulated probe signals showed an "anticipation" on playback evidently caused by fringing flux preceding the actual signal on the tape. The problem was solved by reducing the tape speed to one inch per second which, in effect, shortened the anticipation to a negligible value. The slower tape speed also reduced crosstalk to 1% or less at any frequency. Fig. 119 shows a simulated probe signal with and without anticipation.

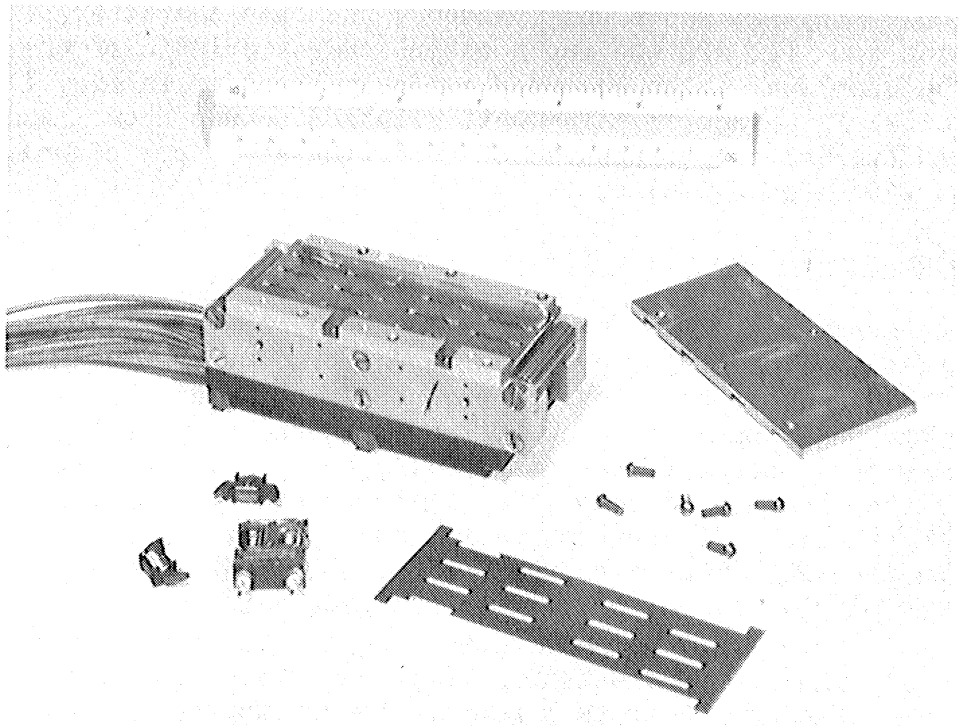

Fig. 118. Magnetic Head Assembly and Crosstalk Shield

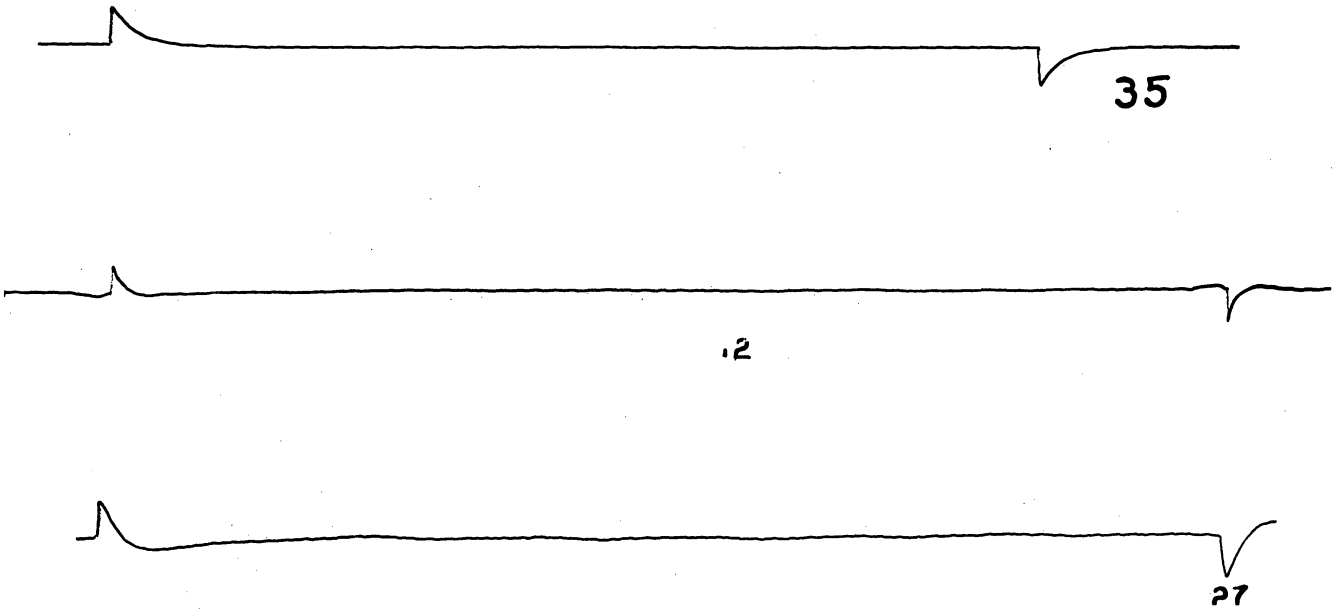

Fig. 119. Top: Signal Impressed on Recorder
Center: Playback Signal Showing Anticipation
Bottom: Playback Signal Showing No Anticipation

The flight electronics and their circuits are shown in Figs. 120, 121, 122, 123 and 124. The chassis are extremely light and have plug-in installation. Fig. 125 shows the frequency response characteristic of the entire system and Fig. 126 the input-output characteristic of the entire system. The complete flight recorder assembly is shown in Fig. 127. Much of the material is magnesium. The unit weighs 3 pounds when loaded with 1" wide tape sufficient for 30 minutes of recording at 1" per second. The motor draws 250 ma at 24 volts.

6.46 Constant Resistance Circuits for Probe Piranis

As mentioned above, constant resistance operation of Piranis has the advantages of sensitivity over a wide range of pressures and prevention of gage burnout at low pressures. Consequently, considerable effort was devoted to the development of a constant resistance circuit for flight. The circuits developed operated reasonably well, but in each case were not used in flight either because of complexity, microphonics, or excess power requirement. The development of constant resistance type circuits was dropped when it was found on V-2 50 that a good signal to noise ratio existed in the probe outputs. The simpler series circuit with higher gain amplifiers was adopted for V-2 56 and the Aerobee. One circuit used a saturable reactor to control the current flowing into a Wheatstone bridge. A later version, seen in Fig. 128 used a magnetic amplifier in place of the reactor for greater sensitivity. In operation a 400 cycle A.C. voltage controlled by the magnetic amplifier is rectified and applied to the Wheatstone bridge which contains the Pirani gage.

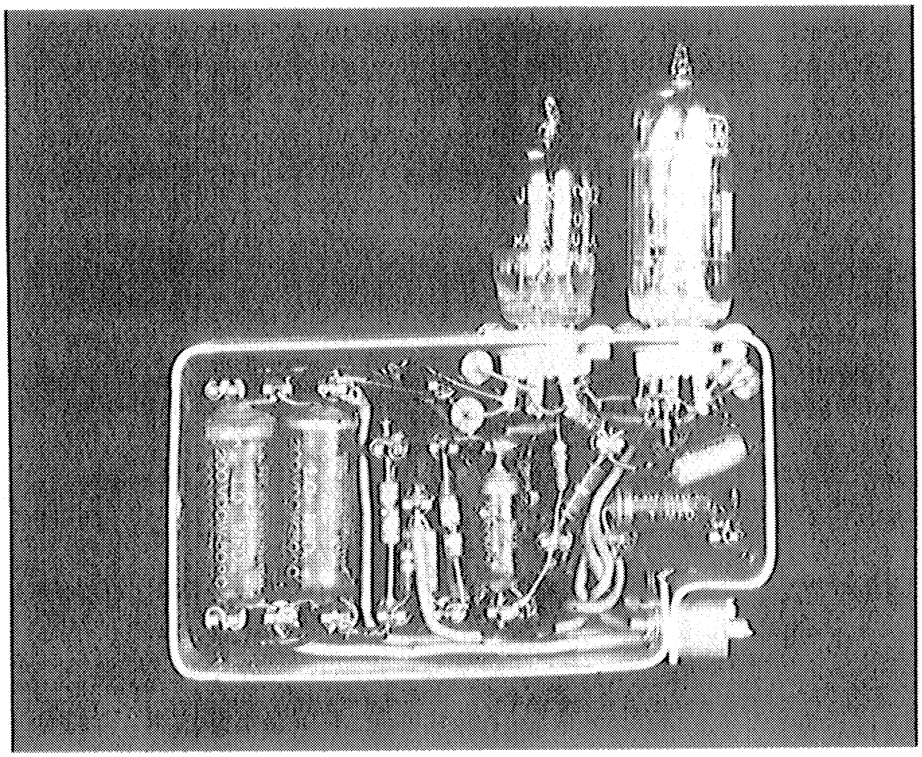

Fig. 120. Probe Amplifier, Aerobee

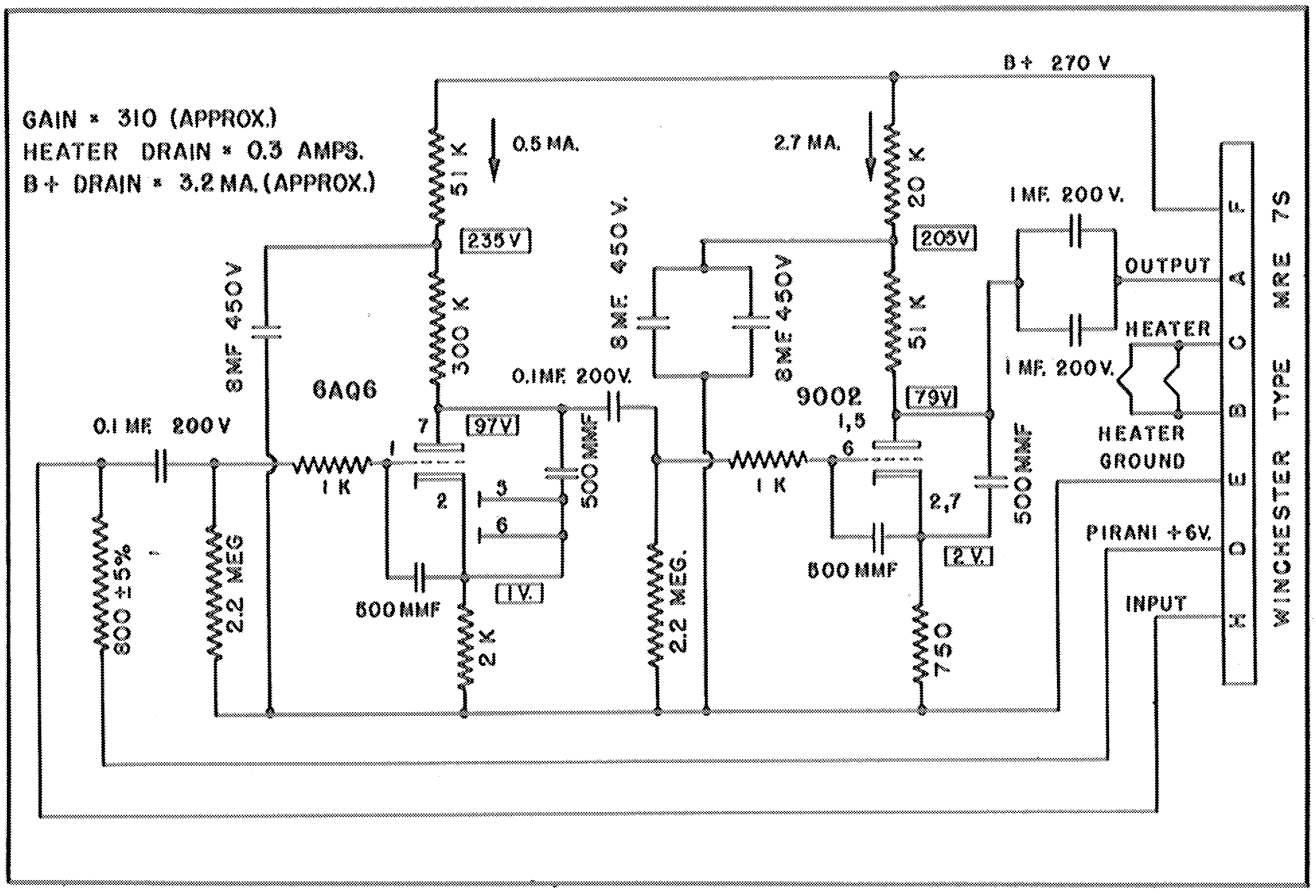

Fig. 121. Probe Amplifier Circuit, Aerobee

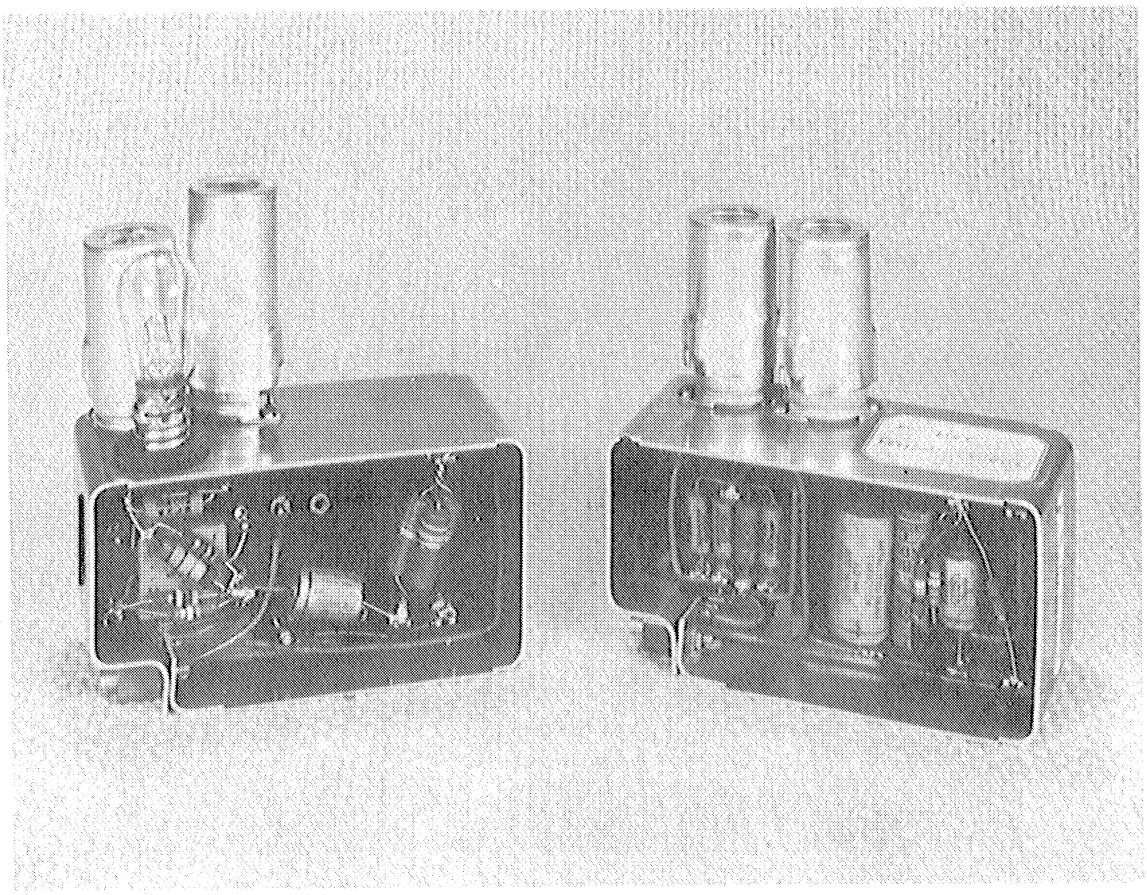

Fig. 122. Left: Bias Oscillator, Probe Aerobee
Right: Marker Oscillator, Probe Aerobee

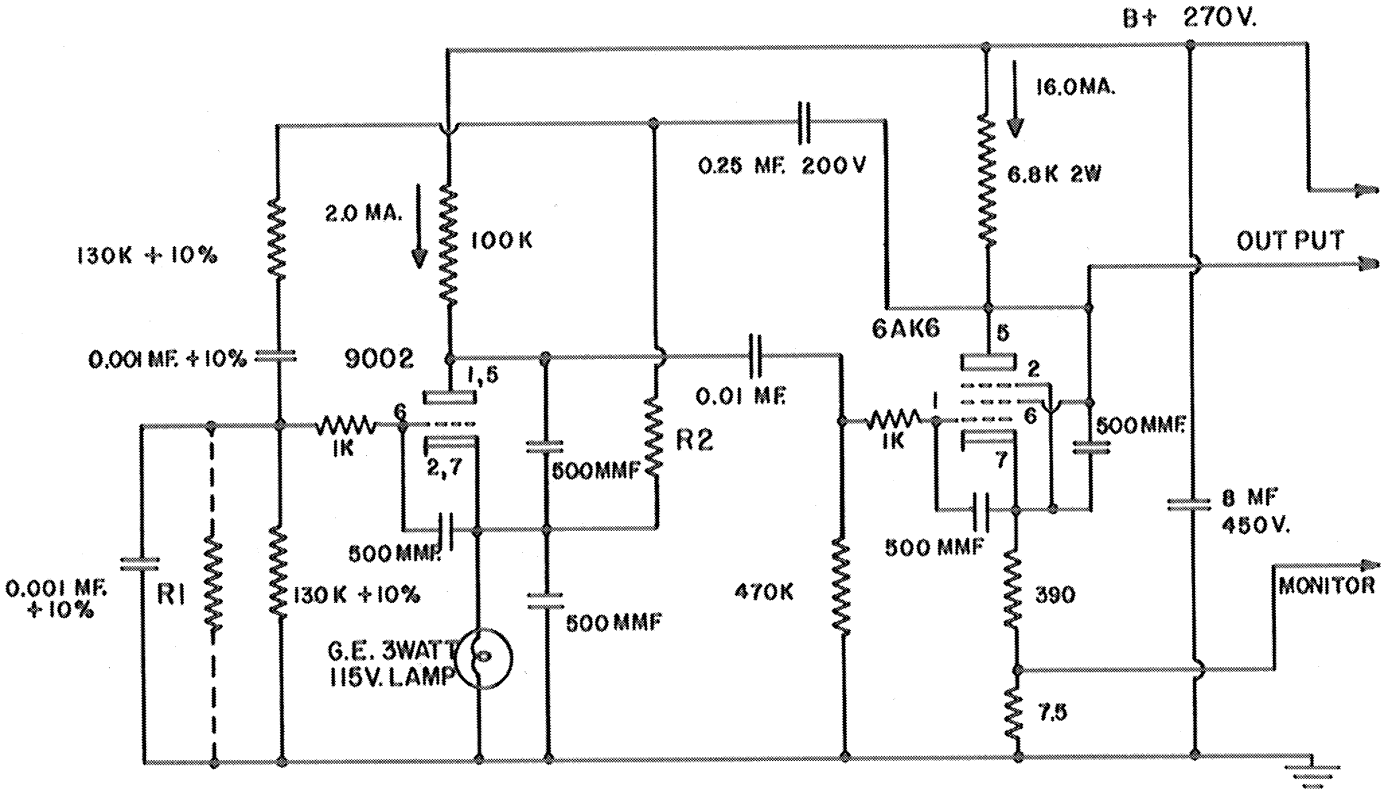

R_1 ADJUSTED FOR 1200Ω OPERATION UNDER LOAD
R_2 ADJUSTED FOR 16V. RMS OUTPUT UNDER LOAD (APP.3K)

Fig. 123. Bias Oscillator Circuit, Probe Aerobee

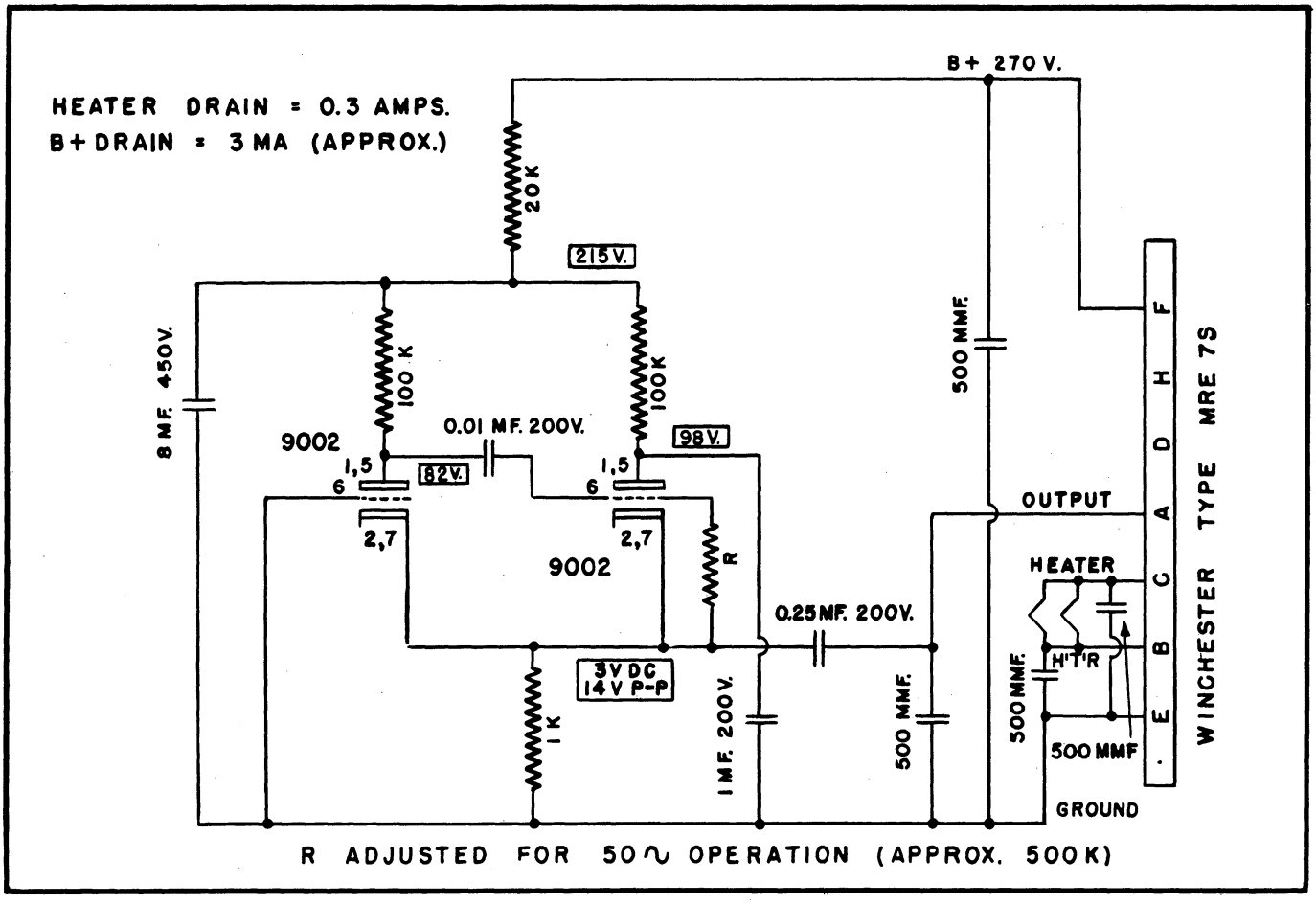

Fig. 124. Marker Oscillator Circuit, Probe Aerobee

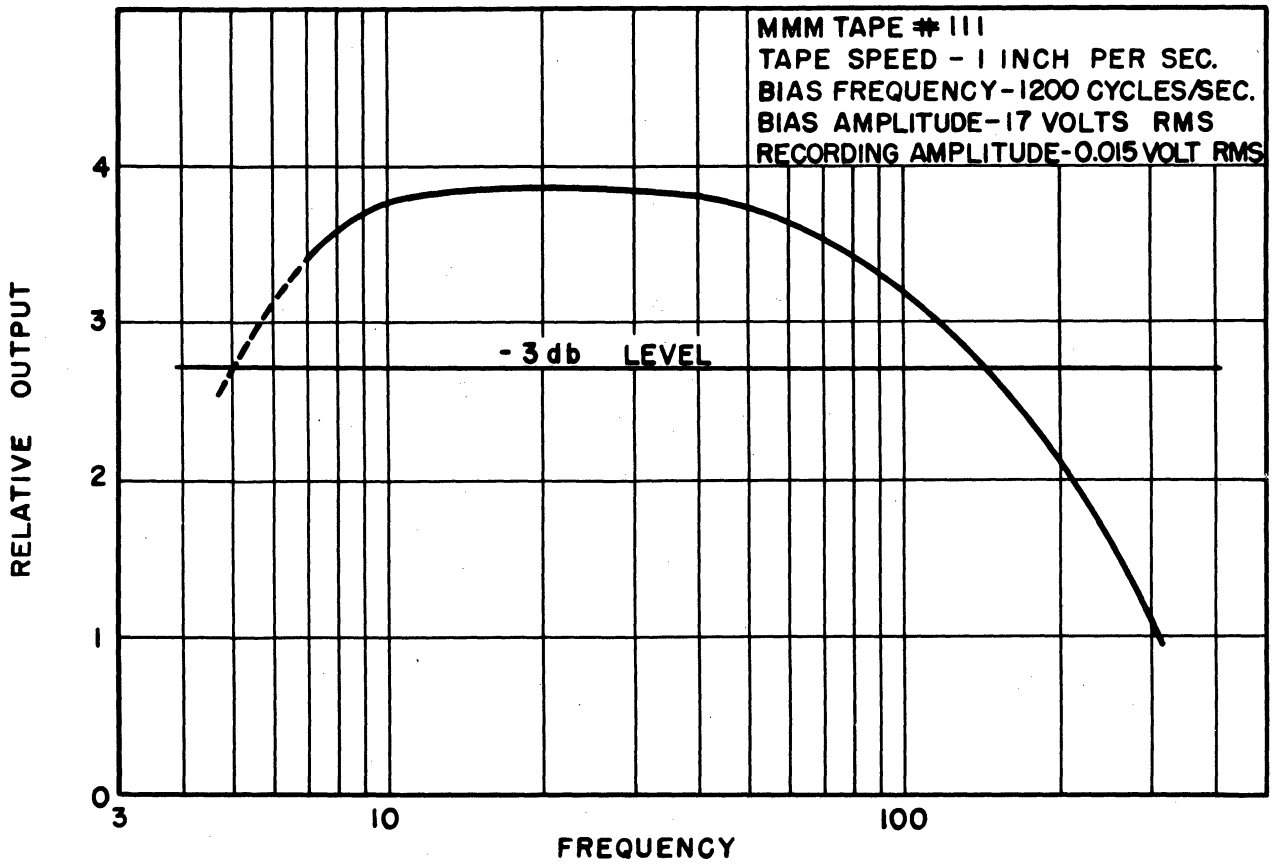

Fig. 125. Frequency Characteristic, Entire System

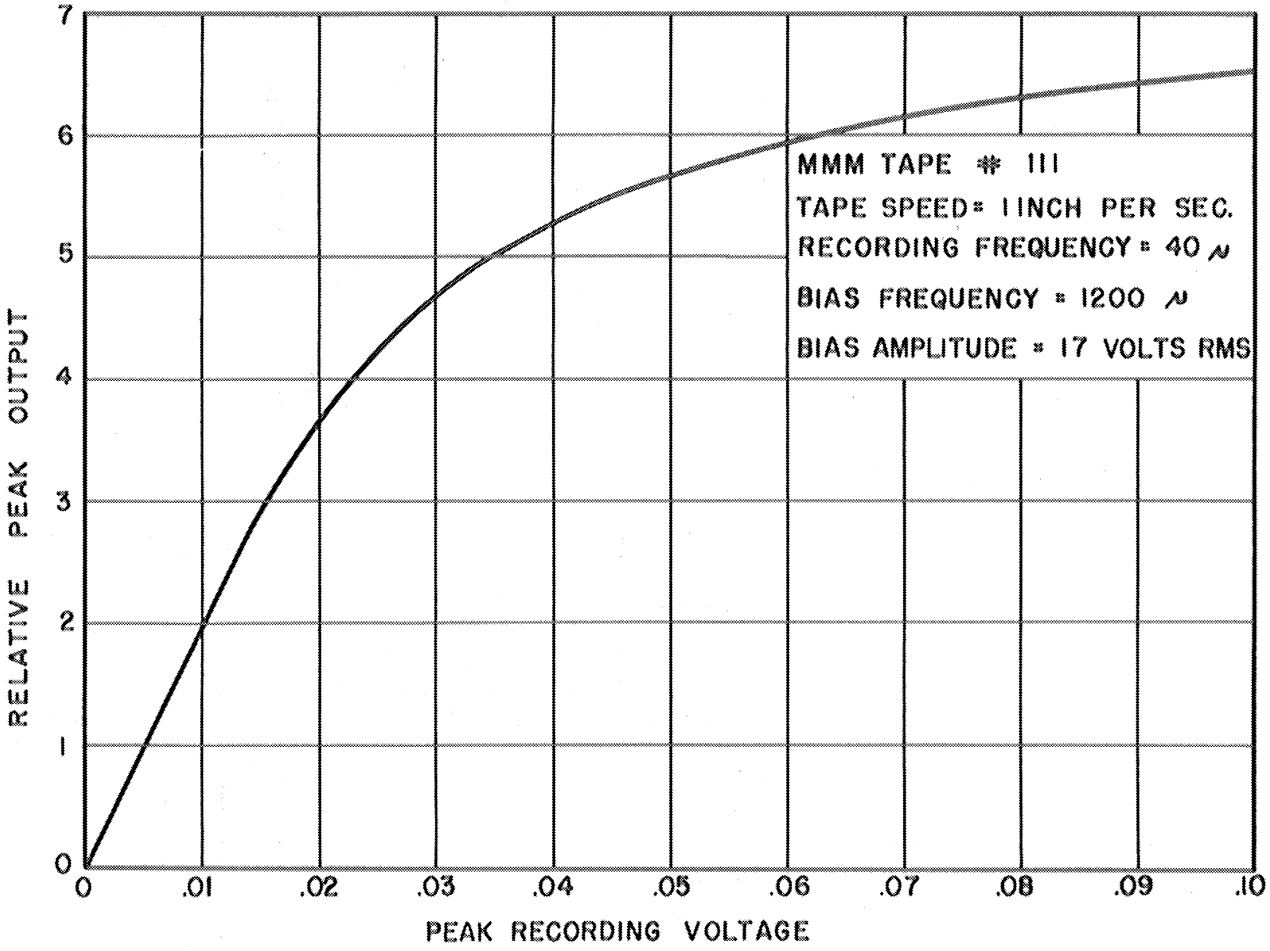

Fig. 126. Transfer Characteristic, Entire System

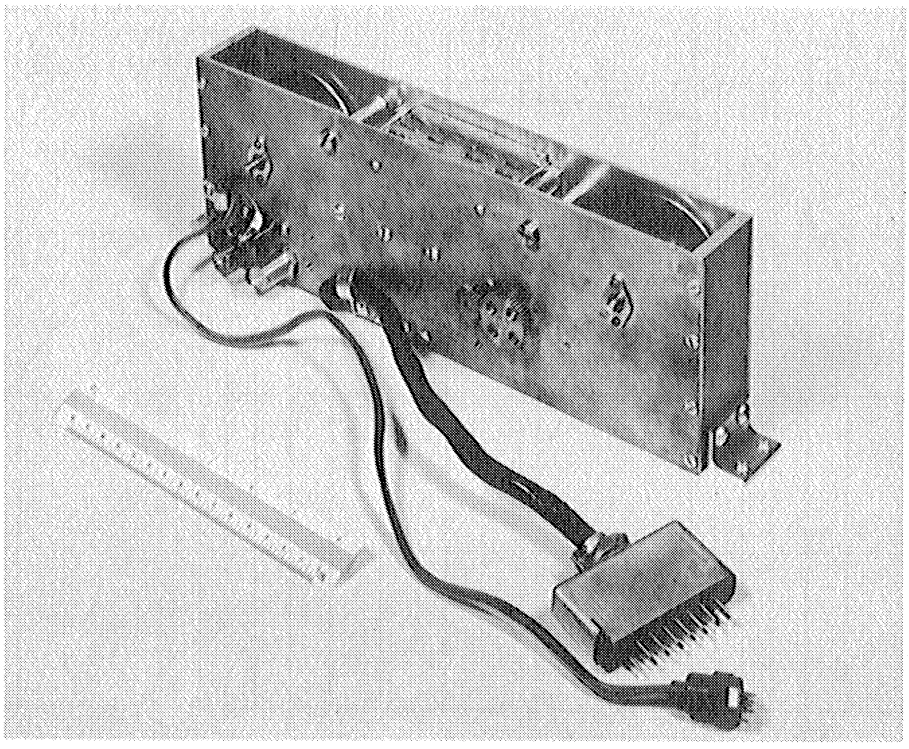

Fig. 127. Magnetic Recorder Assembly, Probe Aerobee

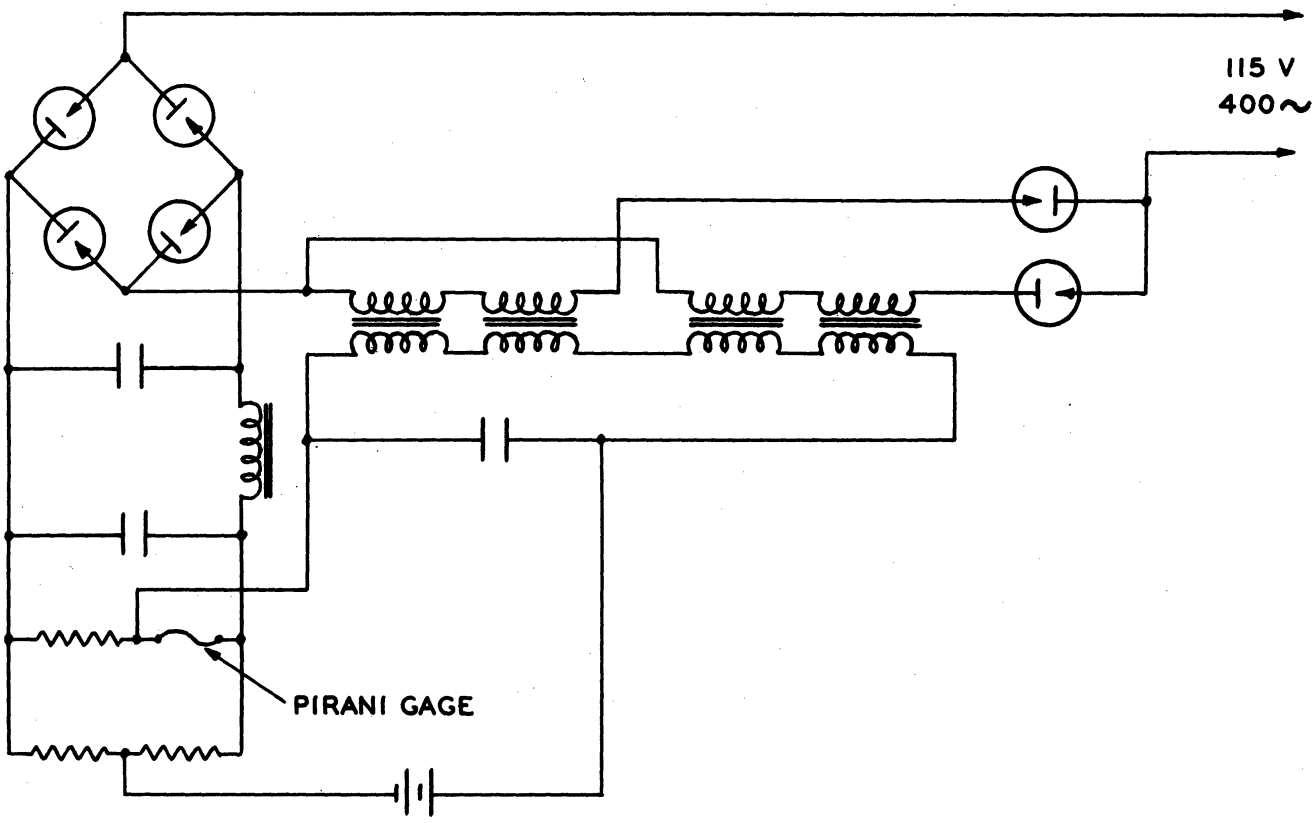

Fig. 128. Magnetic Amplifier
Constant-Resistance Circuit for Piranis

The output of the bridge is fed directly into the magnetic amplifier. Fig. 129 shows a typical Pirani resistance vs pressure characteristic obtained with this circuit.

Another circuit, shown in Fig. 130, consists of an oscillating amplifier with both positive and negative feedback loops. Positive feedback is from the output to the input. Negative feedback is from the Pirani to the input. In addition a negative feedback loop was incorporated containing a bridged-T filter to degeneratively feed back all output frequencies except those in a narrow band around 10 kilocycles. In operation, as the Pirani resistance increases, the ratio of negative to positive feedback increases and the amplitude of the oscillations decreases. Since the gain of the amplifier is relatively large at 10 KC, the amplitude of oscillations tends to adjust itself to maintain the feedback ratio constant. Laboratory tests showed that this circuit held a probe Pirani wire at constant resistance within 0.2% from atmospheric pressure to 20 microns. The chief undesirable feature, however, was the large power requirement of the 6L6 cathode coupled output stage. Further experimentation led to a transformer coupled output stage with usable power requirement but this circuit was too microphonic for rocket use. The latter circuit is seen in Fig. 131.

A third circuit, due to Von Ubisch[35], is shown in Fig. 132. It consists of a tuned audio amplifier phase inverter and push-pull output stage. The output is transformer coupled to the bridge circuit which contains the Pirani gage. The bridge unbalance provides positive feedback to maintain oscillations at the one kilocycle frequency of the tuned circuit. An increase

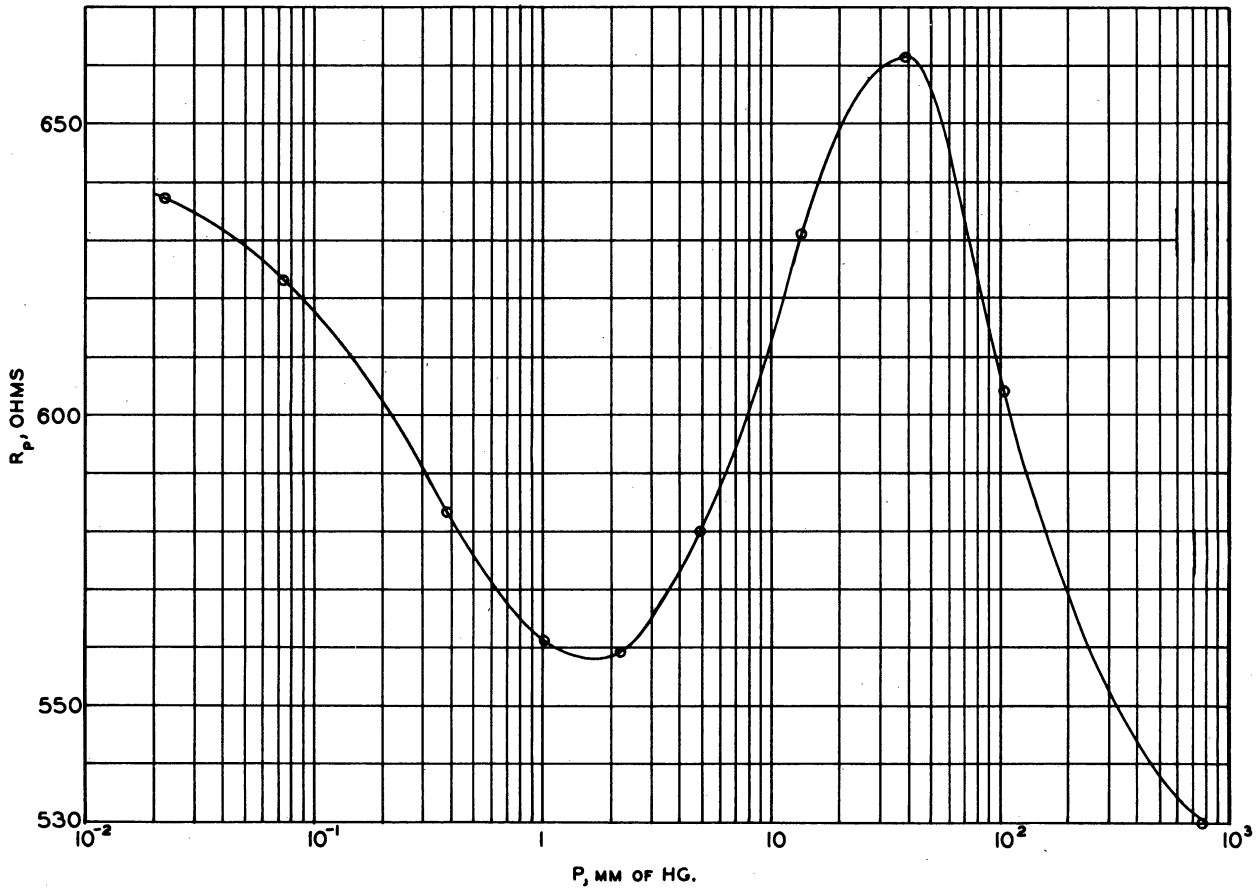

Fig. 129. Resistance vs Pressure Characteristic, Magnetic Amplifier Constant R Circuit

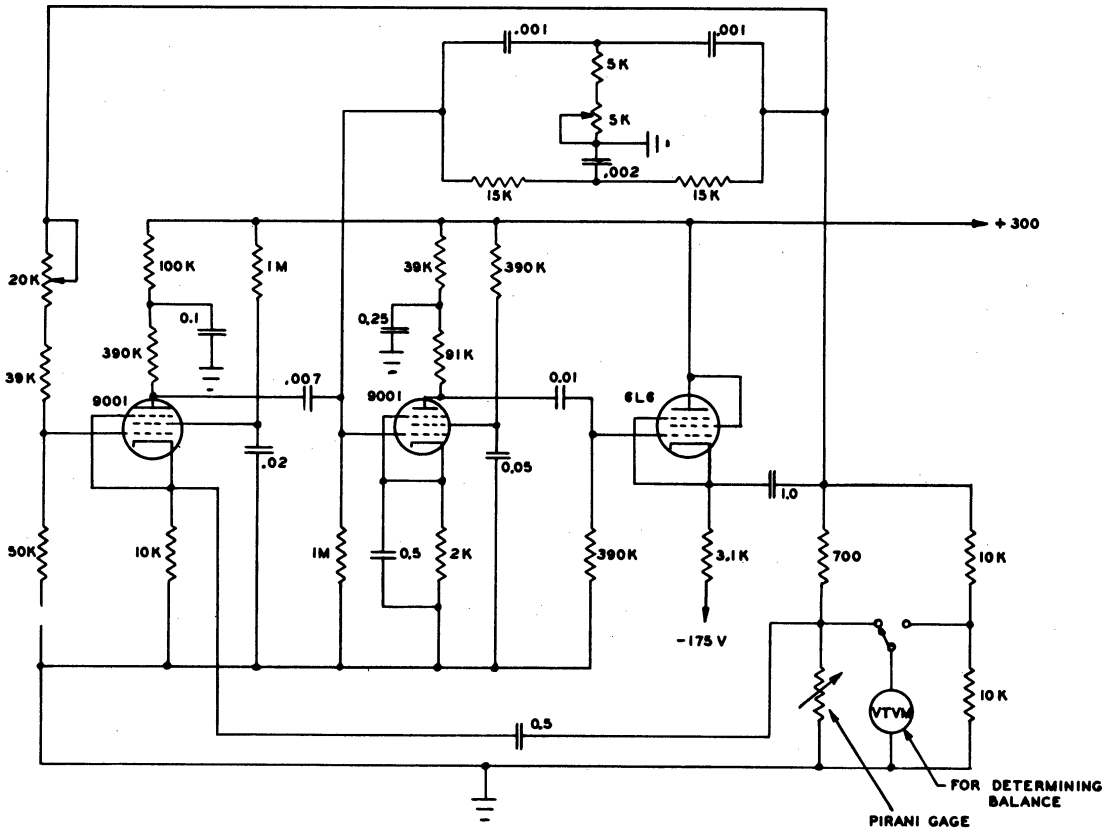

Fig. 130. Constant R Oscillator, 6L6 Output

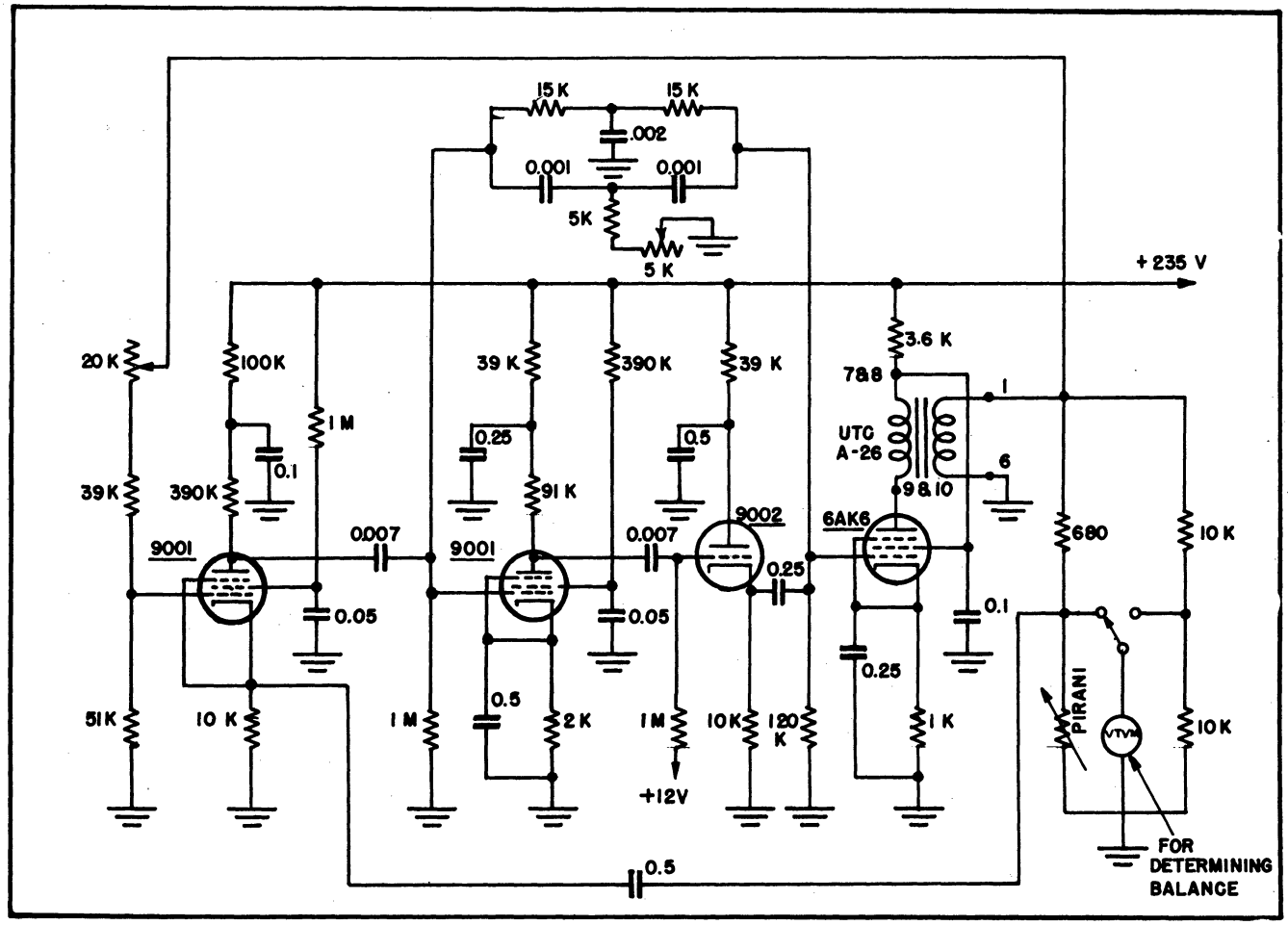

Fig. 131. Constant R Oscillator, Transformer Output

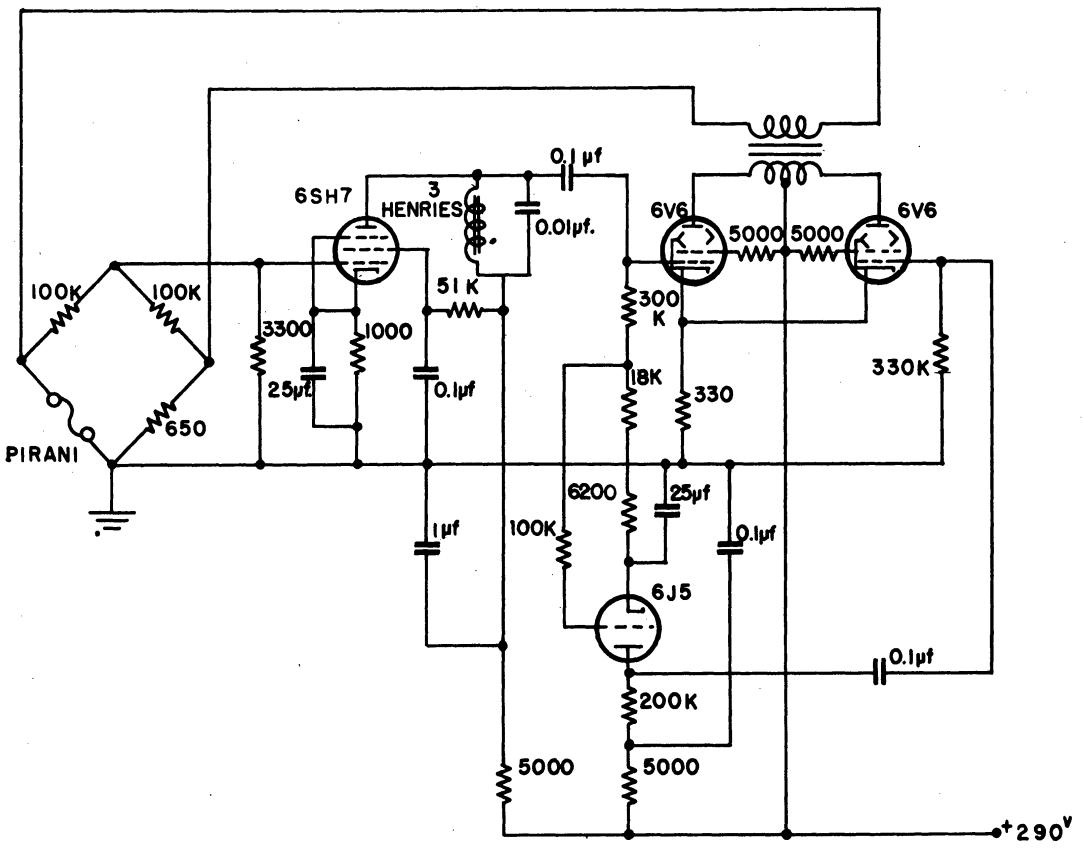

Fig. 132. Von Ubisch Constant R Circuit

in Pirani gage resistance decreases the bridge output voltage and, through the amplifier, the voltage across the bridge. Thus the circuit tends to maintain the Pirani gage at constant resistance. Fig. 133 shows the resistance-pressure characteristic obtained with this circuit and a platinum Pirani 0.0001 inch in diameter and 0.5 inches long. At low voltage levels the experimental model was microphonic. Further, attempts at increasing the operating frequency to decrease the overall response time were not successful. The circuit was unstable above 2500 cps.

6.5 Shadowgraph[36]

Flow visualization provides a very direct approach to the measurement of shock wave angle from which Mach number and temperature may be obtained. Shadowgraph and schlieren techniques, widely used in wind tunnels, were both considered for application to rockets. Schlieren, which is sensitive to density gradient, will perform at lower densities than the shadowgraph but is more complex, and it was thought that a rather long development period would be necessary. The shadowgraph, sensitive to the second derivative of the density, is much simpler and was chosen for the first experimental attempt on V-2 42, assigned to the Signal Corps. The major experiment, a sulphuric acid smoke generator, was instrumented by Edgewood Arsenal.

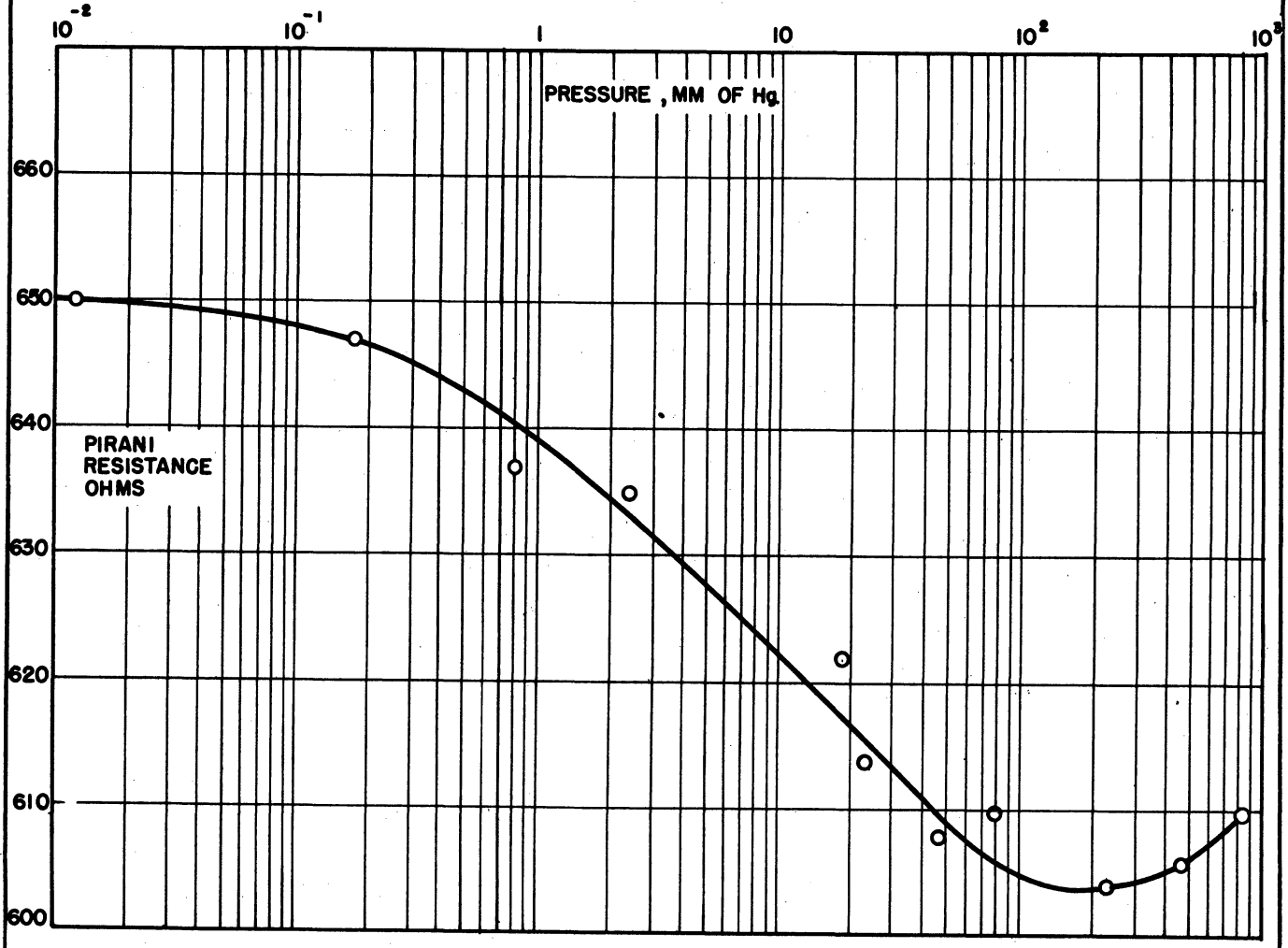

Fig. 133. Resistance vs Pressure Characteristic, Von Ubisch Circuit

Figs. 134, 135 and 136 illustrate the shadowgraph that was flown on V-2 42. The Western Union H-2 concentrated arc serves as essentially a point source (0.003" diameter). The lens forms a parallel beam of light which, by means of prisms, throws a shadow of the wedge and shock wave onto the photographic film. Two discs driven at different speeds by a governor controlled motor form the shutter mechanism to take two frames per second. The exposure is about 0.002 seconds. The film is wound into a heavy steel casette to facilitate recovery. The wedge has a twenty degree half-angle. Fig. 137 shows a shadowgram taken with the flight shadowgraph using an open jet with a Mach 1.4 nozzle. Since the wedge was wider than the jet, the flow traversed by the light was not uniform. This, together with the high sensitivity, accounts for the width of the shock wave shadow.

Prior to the firing of V-2 42 tests were run on a model of the shadowgraph in the University of Michigan wind tunnel to check on undesirable interference of the shock waves from the tubes carrying the prisms with the main shock wave from the wedge. Schlieren pictures taken at Mach 2 and 4 and several angles of attack revealed that no undesirable interference occurred. Fig. 138 shows the model in the tunnel at Mach 2 and an angle of attack of 7°.

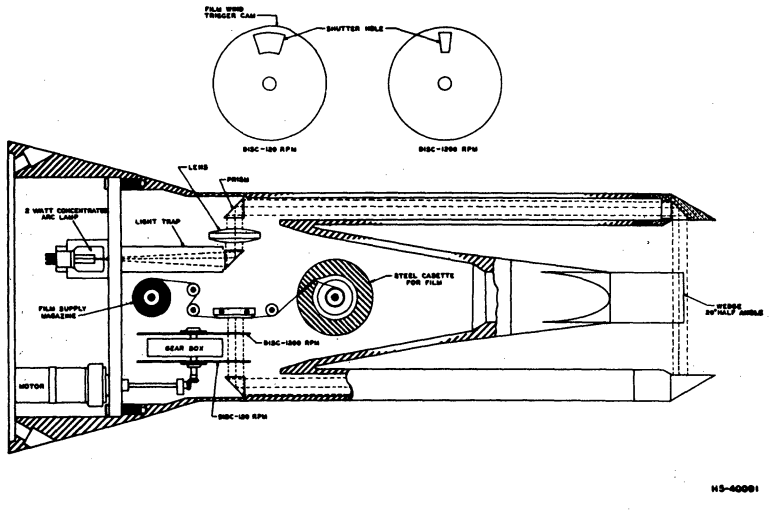

Fig. 134. Shadowgraph Schematic, V-2 42

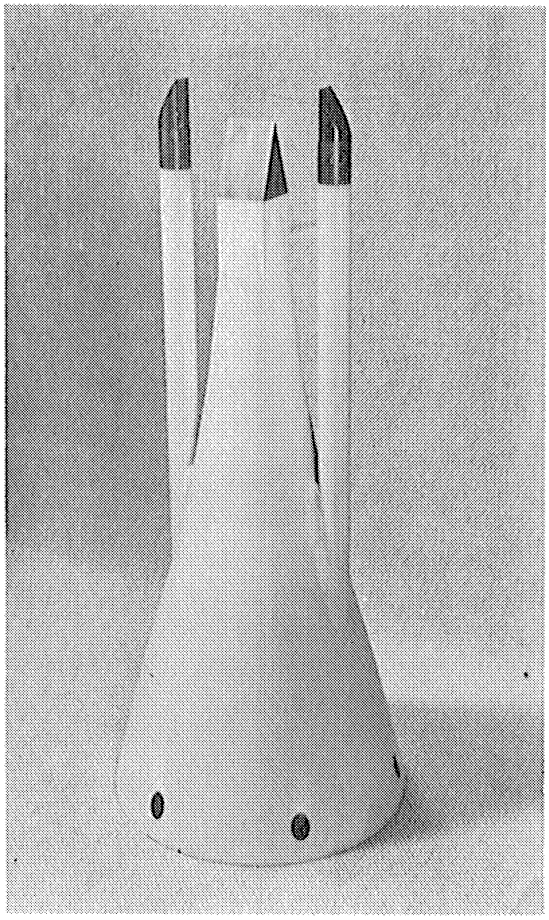

Fig. 135. Shadowgraph, V-2 42

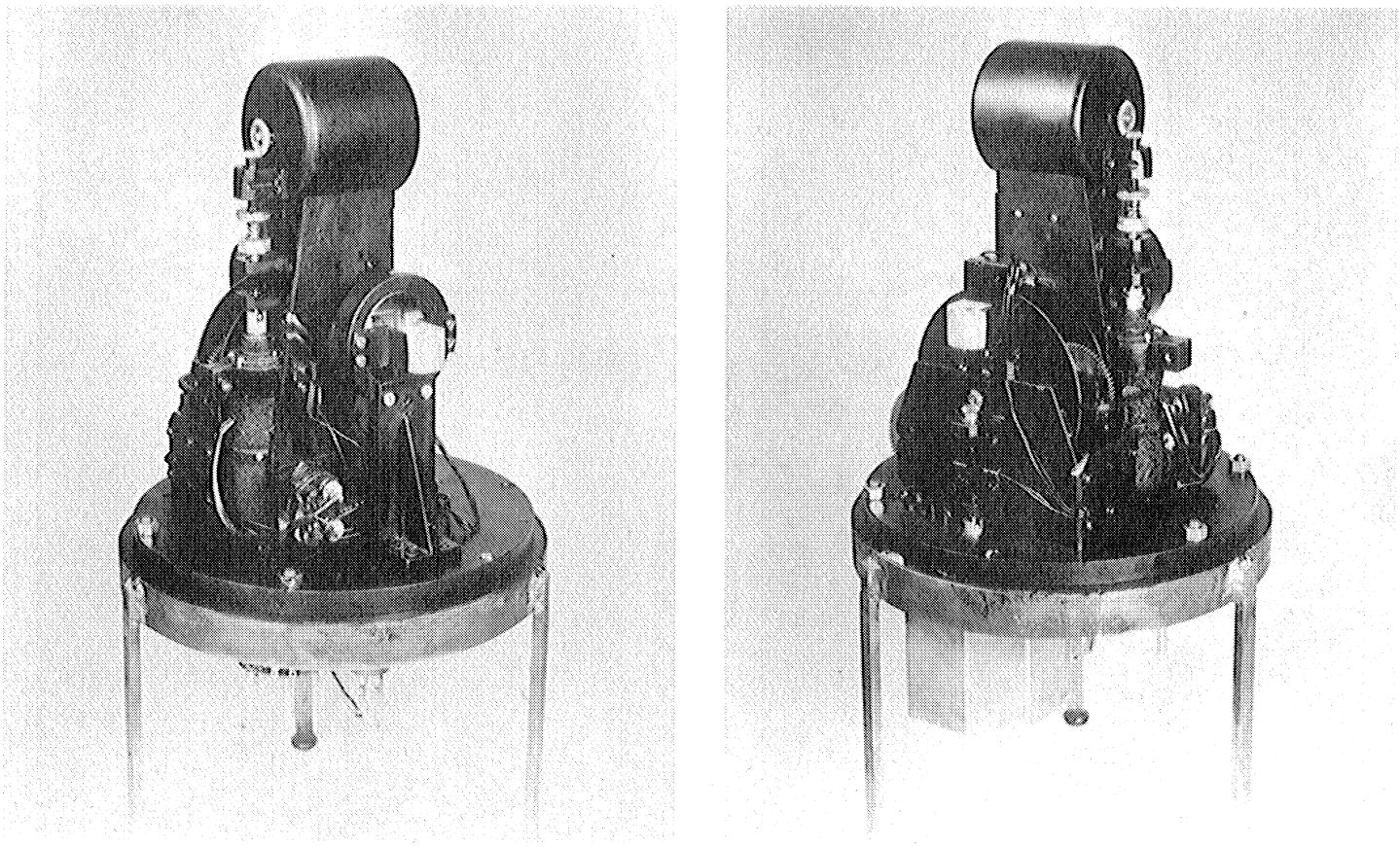

Fig. 136. Shadowgraph, V-2 42

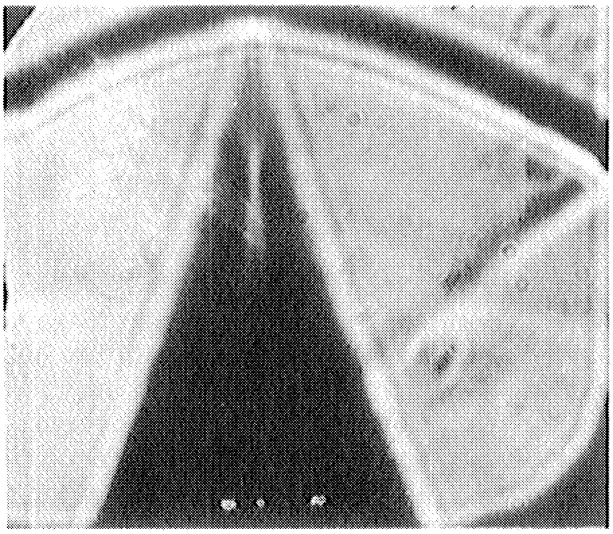

Fig. 137. Jet Shadowgram Taken with Shadowgraph of V-2 42

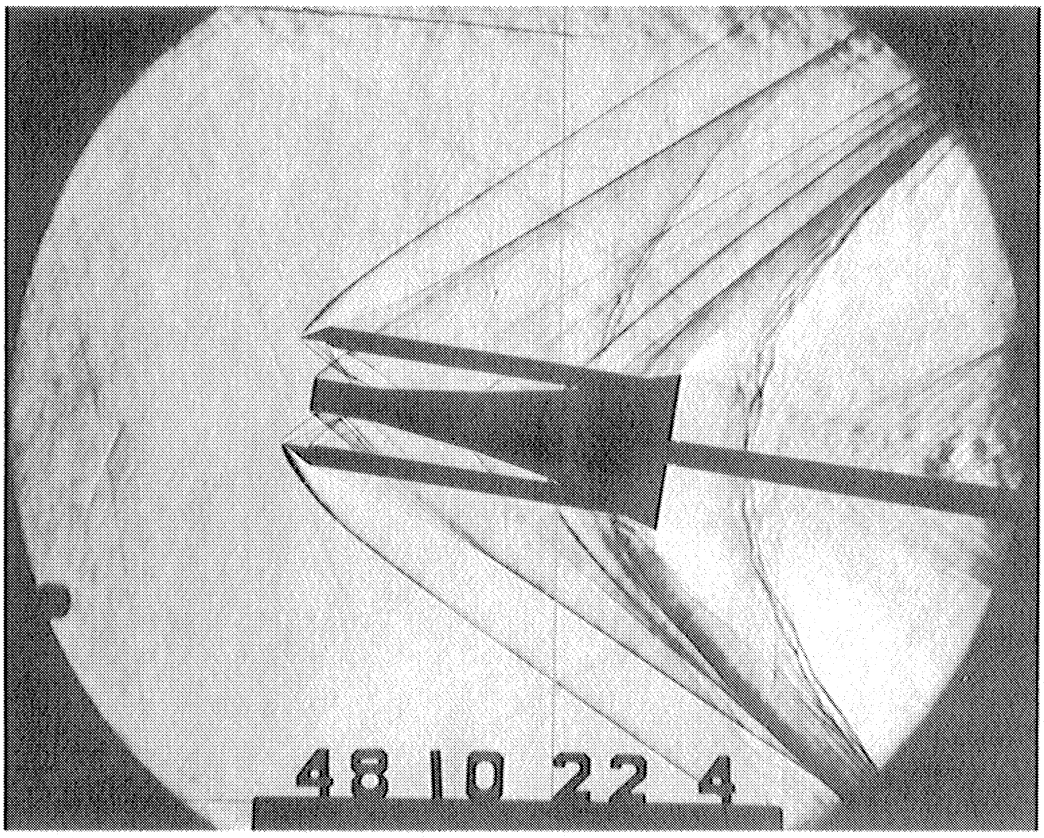

Fig. 138. Wind Tunnel Test, Shadowgraph Model

V-2 42 was fired successfully on December 9, 1948. However, the film mechanism failed to start at take off for an undetermined reason and no pictures were taken. Development of a new model incorporating features to improve reliability was started. This apparatus was to have been flown on V-2 56 but was shelved when tests of shadowgraph and schlieren at the Langley Field low density wind tunnel revealed that the altitude limits of both techniques would be considerably lower than that of the probe apparatus. The Langley experiments are described in Section 7.

6.6 Subsidiary Experiments Related to the Measurement of Pressure and Temperature

6.61 Probe Temperatures and Signals in Flight

In order to test heating effects and noise effects for the probes of the type used for the shock wave angle experiment, probes of the type to be used on V-2 50 were installed on the warhead doors of V-2 42. Two probes were installed inside guards, where in the major shock wave angle experiment, they remained during powered flight. One of these contained a thermistor to measure temperature during flight. This is the right hand probe in Fig. 139. The other probe contained a regular Pirani gage and is the right hand probe in Fig. 140. Two other probes were installed without the guard. One of these contained a thermistor for temperature measurement and is the left hand probe in Fig. 139. The other contained a regular Pirani gage and is the left hand probe in Fig. 140. The probes containing the Piranis were swept by a wedge rotated by a motor as shown in Fig. 140. The purpose of the wedge was

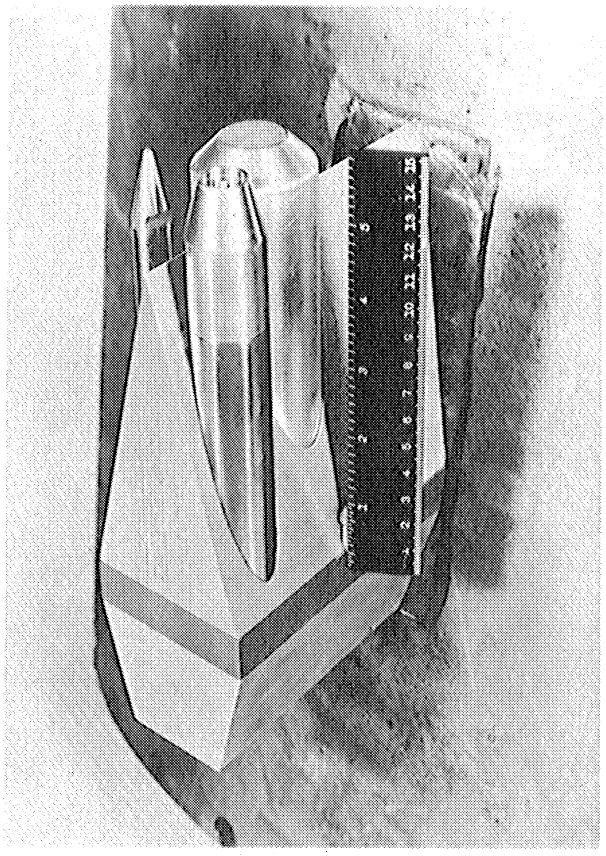

Fig. 139. Test Probes, V-2 42

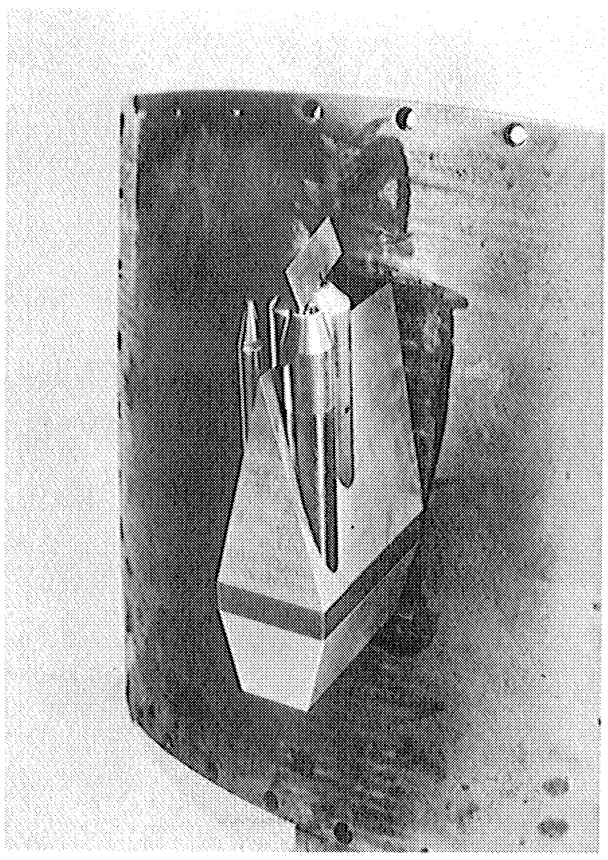

Fig. 140. Test Probes, V-2 42

to set up a shock wave to test the sensitivity of the gages and to check on the relative effect of the shock wave and noise from turbulence, vibrations, etc. In each case, the thermistor was in series with a battery and linear resistance. The voltage across the thermistor was telemetered. The Piranis were in series with a transformer and battery, the secondary of the transformer feeding an A.C. amplifier capable of passing the expected transient signal.

The rocket firing was successful (Section 6.5) and useful data were obtained from the experiment. The probes which were scanned by the wedges both gave records. The interpretation was difficult because of the configuration of the scanning motor and the probe shield. The unshielded probe burned out at 10.5 km and the shielded probe at 90 km. Fig. 141 is a reproduction of parts of the telemeter record showing the pips obtained. The wedge width is indicated. The gage is excited by the shock wave off the tip of the wedge and by the stream off the trailing edges of the wedge. An examination of the record of the shielded probe at 33 km indicated a Mach number ahead of the wedge of about 3 which seems reasonable. It was noted that noise did not blot out the signal from the wedge.

Fig. 142 shows the results from the thermistor probes. The temperature in the unshielded probe reached 196°C which is under the melting point of 40-60 tin-lead solder so that a soldered gage might not melt loose. However, this temperature would reduce the gage sensitivity. The shielded probe showed no increase in temperature which is unlikely and it is thought that the thermistor failed.

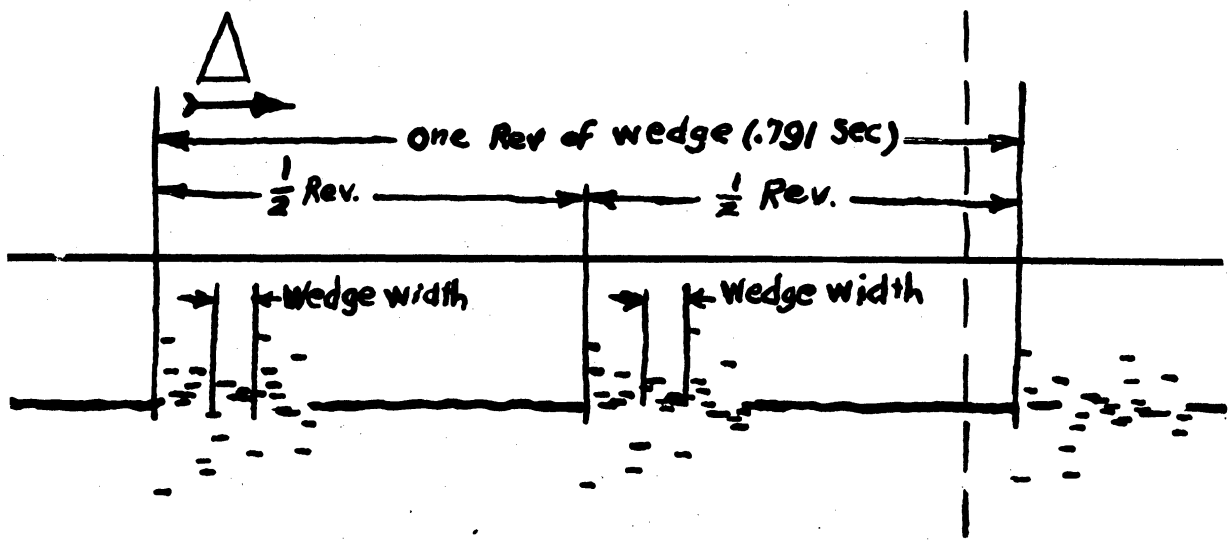

Fig. 141. Test Probe Signal, V-2 42

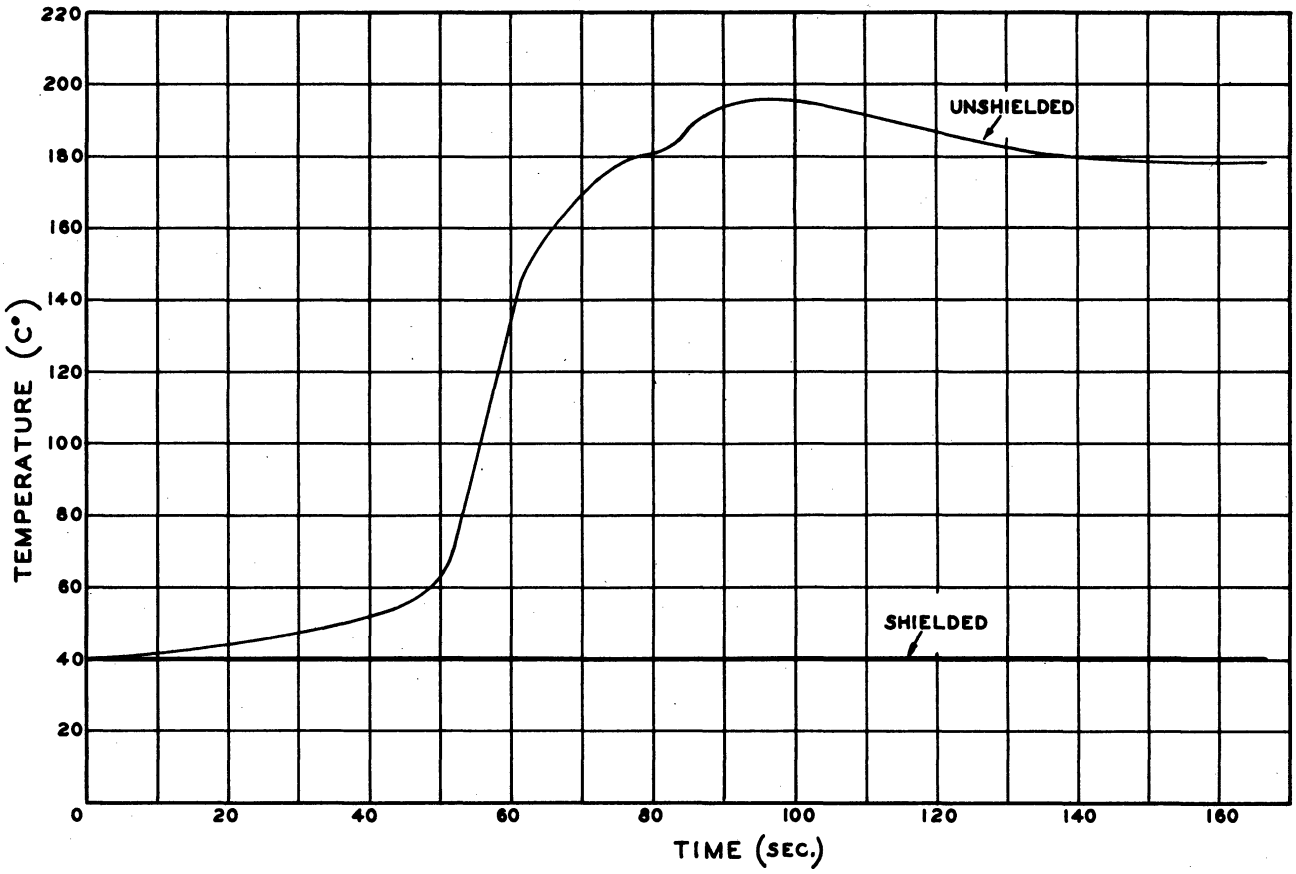

Fig. 142. Thermistor Test Probe Results, V-2 42

The following conclusions were drawn from the results of this experiment:

a) Unshielded gages using common solder might survive the early part of a V-2 flight. It would be safer to use shields and a high melting point solder or welds.

b) A good signal to noise ratio could be expected from the gages in the probe experiment. This was later verified in the flights of V-2's 50 and 56.

6.62 Model Test of Probes

A model test of the probe experiment was undertaken for two reasons:

a) By schlieren photographs to discover if the shock wave to be detected is distorted by the probe.

b) By recording probe Pirani signals to correlate with the schlieren photographs the time of the signals and position of the probe with respect to the shock wave.

The tests were performed in the University of Michigan supersonic wind tunnel at Willow Run. A one-eighth scale model of a V-2 nose cone with a reciprocating probe and facilities for a one-tenth scale probe or full scale probe was built. A one-tenth scale static probe was also provided. The model is shown in Fig. 143. The probe circuit was similar to that used on V-2 33. See Section 6.44.

Three tests at angles of attack of 0°, +12° and -12° were run. The test Mach number was 1.93; the test section pressure about 100 mm Hg. Schlieren photos were taken with a Fastax camera at 700 frames per second.

Fig. 144 shows typical signals obtained from the gages and recorded on a Brush recorder. Fig. 145 show the schlieren pictures.

Examination of the pressure records and photographs shows that a signal was given by the Pirani gage when the point on the gage inlet orifice closest to the shock wave actually came in contact with the wave. Therefore, when the probe was moving forward the signal was received when the point on the Pirani gage opening most distant from the axis of the cone came in contact with the shock wave and on the return excursion when the point closest to the cone axis came in contact with the wave. This conclusion is subject to possible error due to the distortion of the shock wave by the probe. The error could change in sign and magnitude when the probe direction is reversed. However, it was found that the shock wave angle, with the probe at its signal-issuing position, checked with the theoretical results (with no probe present) within the experimental accuracy which was of the order of ± 0.5°. Because the static probe appeared to give smaller distortion to the shock wave, two static probes were flown on V-2 50. However, as noted in Section 6.3 the pressure signals were not as sharp as from the impact probes and they were not used again.

The position correlation information gained from this experiment was used in the reduction of the shock wave data from V-2's 50 and 56.

6.63 Shock Wave Curvature Investigation

To our knowledge, the Taylor-Maccoll theory has not been extended to the case of low density flow taking into account viscosity and the effect of a thick boundary layer. It is expected that as the density decreases the displacement effect of the thickening boundary layer will distort the shock wave. This has been shown in our theoretical analysis for a small wedge[36] and confirmed by Kane in wind tunnel tests at the University of California. Although small models give rise to curvature in wind tunnel tests it was thought that since the rocket cone is larger with respect to the mean free path that the curvature might be less.

A series of tests in the supersonic wind tunnel at the University of California was performed in which the shock waves from cones of constant angle but different size (hence different Reynold's number) were photographed. It was hoped to discover the variable controlling curvature, e.g. M/R or M/R^2 or some other and to plot curvature against this variable for the tunnel conditions. The curve would then be extrapolated to the rocket conditions. It was hoped either to show that curvature in the rocket case was negligible or to establish a correction for curvature.

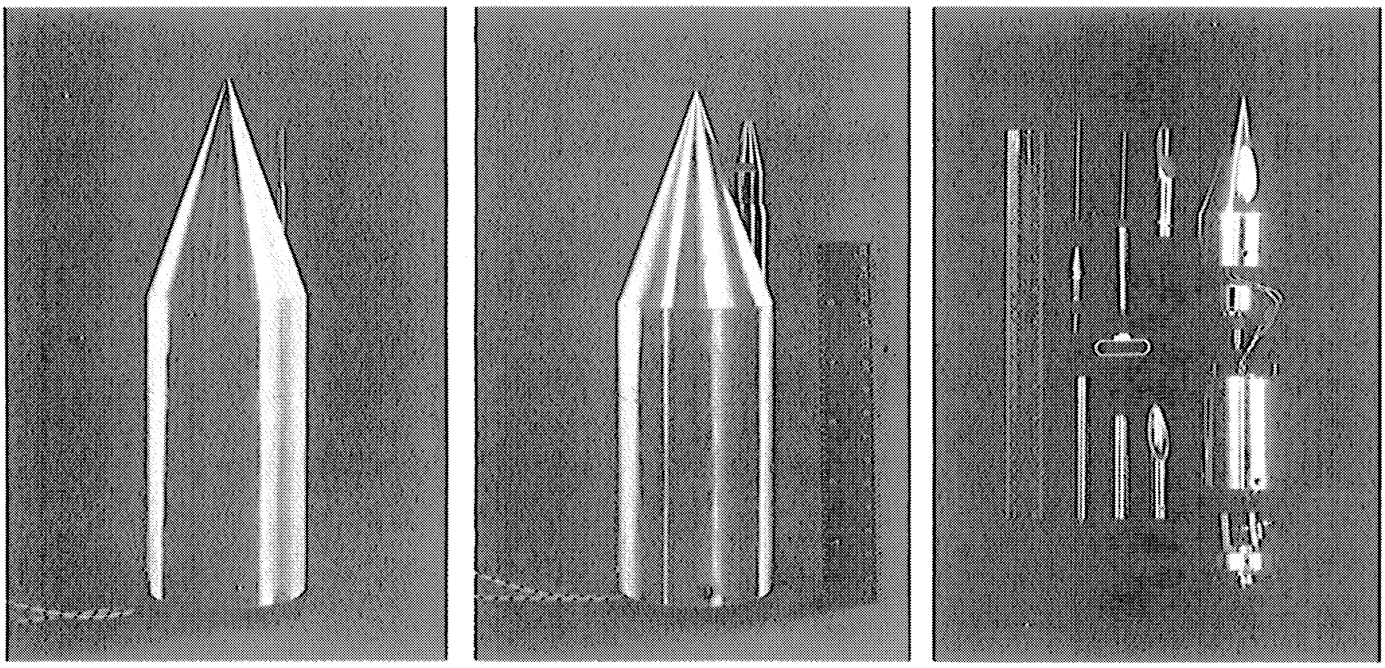

Fig. 143. Probe Experiment Wind Tunnel Model

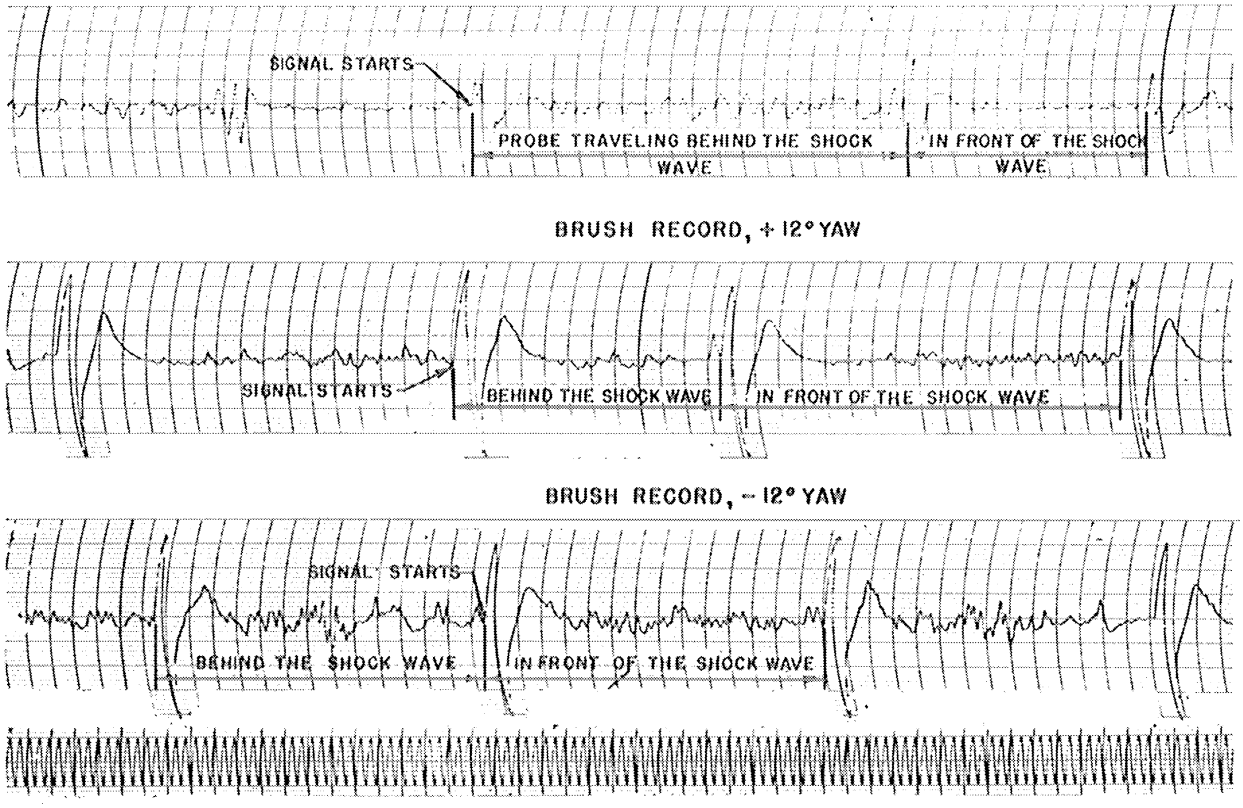

Fig. 144. Probe Signals, Tunnel Model Test

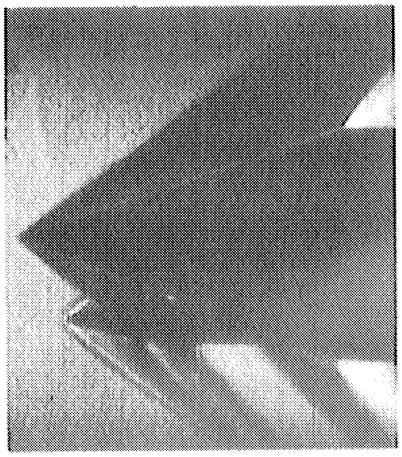

PIRANI PROBE, 0°

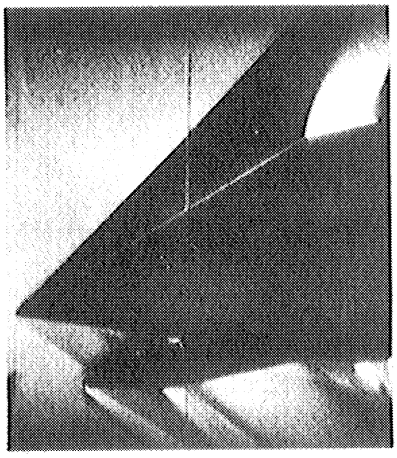

PIRANI PROBE, +12°

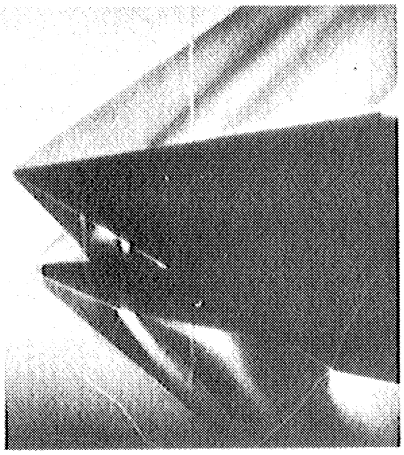

PIRANI PROBE, -12°

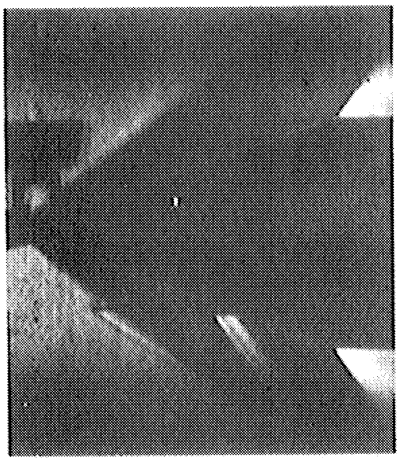

SCALE IMPACT PROBE, 0°

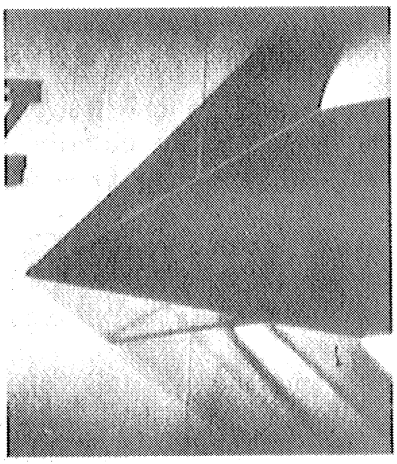

SCALE IMPACT PROBE, +12°

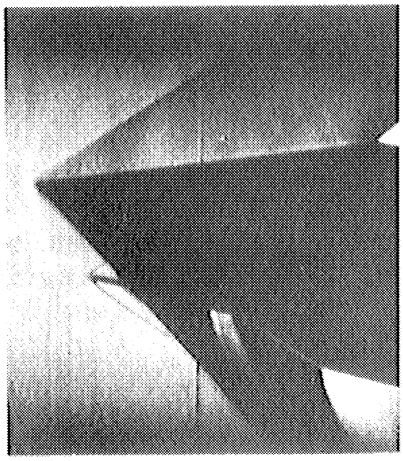

SCALE IMPACT PROBE, -12°

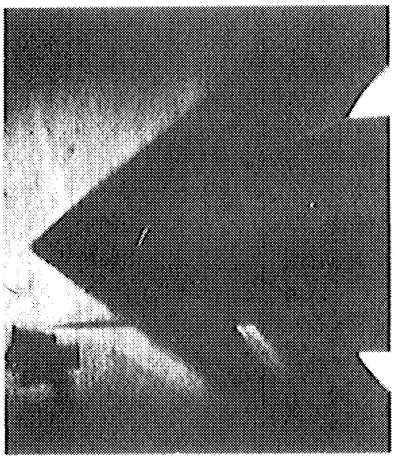

SCALE STATIC PROBE, 0°

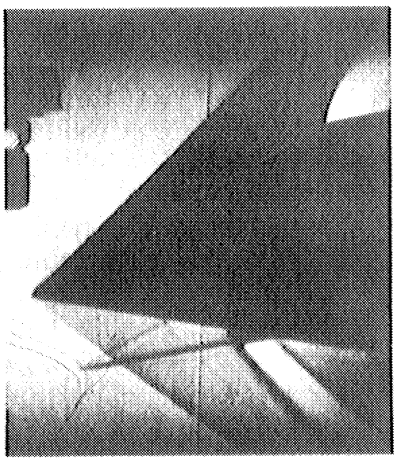

SCALE STATIC PROBE, +12°

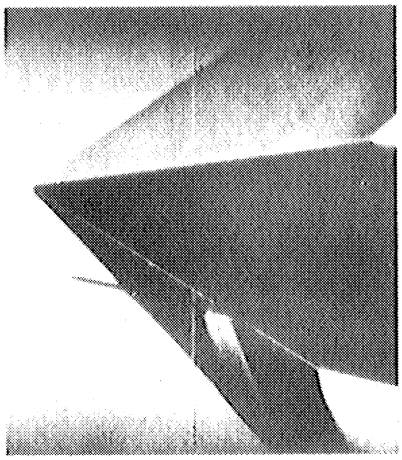

SCALE STATIC PROBE, -12°

Fig. 145. Schlieren Pictures, Tunnel Model Test

The following memorandum dated July 28, 1950 from the University of California describes the tests:

"SUBJECT: SHOCK CONTOUR TEST PROGRAM

1.0 OBJECT OF TEST

At the request of Dr. V. C. Liu of the Engineering Research Institute of the University of Michigan, an experimental study of shock wave contours about conical probes was carried out at the Low Pressures Research Laboratory at the University of California in Berkeley. The object of this program was to obtain photographs of the shocks about four different axially symmetric models under several flow conditions using the nitrogen glow technique (Ref.1). Pressure determinations at selected points in the test section were also made for each flow condition.

2.0 DESCRIPTION OF EQUIPMENT

The tests were performed in the No.3 Wind Tunnel (Ref.2) using the No.2 and No.3 nozzles. The No.2 nozzle covers a Mach range from 2.1 to 2.8, while the No.3 nozzle extends this range from 2.8 to 3.5.

All photographs were made using 3 1/4 in. x 4 1/4 in. Defender 428 cut film. A view camera was used to hold the film and was equipped with a 6 in. focal length, f-4.5 maximum aperture lens.

The pressure traverses were made with a source-shaped impact tube (No.14) 0.300 in. dia. and with a hole dia. of 0.060 in. The conical probe (No.15) was used to determine the static pressure. This probe consists of a 5° half-angle cone joined to a 0.300 in. dia. cylinder, with pressure orifices located on the cone surface.

The four models used in this program were all 20° half-angle cones mounted on cylindrical supports. The physical dimensions were as follows:

(1) Cone base dia. 0.700 in., cylindrical support dia. 0.700 in.
(2) Cone base dia. 0.350 in., cylindrical support dia. 0.350 in.
(3) Cone base dia. 0.100 in., cylindrical support dia. 0.100 in.
(4) Cone base dia. 0.700 in., cylindrical support dia. 0.060 in.

A remotely controlled traversing mechanism within the test section of the No.3 Wind Tunnel provided means for mounting and moving models or probes in the test section. Selsyn motors and generators gave position coordinates on standard 5-place counters located outside of the vacuum chamber. The two probes - No.14 and No.15 - were mounted on this mechanism together with a vertical support rod which held the four models. Either of the two probes or any of the four models could be moved into the test section as required without alteration of the air stream.

3.0 PROCEDURE

Two test runs were made - Run 116 using the No.2 nozzle and Run 117 using the No.3 nozzle. During Run 116 photographs of the four models

were obtained with N_2 flow rates of 21, 10.3 and 4.1 lbs/hr (Table 1)[37]. The exposure times, aperture settings, etc. are listed in Table 3[37]. Pressure measurements were made at 15 points for each flow condition, but with the discharge off. The location of these points is shown on Figs. 1, 2 and 3.[37] These plots also indicate the Mach number at each point as calculated from the probe pressure measurements using the non-viscous theory (Ref.3). Additional pressure measurements were made with the nitrogen glow energized, to determine the possible effect on the flow conditions.

During Run 117, photographs of the four models were obtained at two flow conditions. A third flow condition was attempted, but the nitrogen glow technique would not operate satisfactorily at the highest stagnation pressures encountered with the No.3 nozzle. The same experimental procedure was used in Run 117 as is outlined above for Run 116, and the data are summarized in Tables 2 and 3.[37]

4.0 RESULTS

A total of 20 photographs, one each of four models at five flow conditions, were obtained during Runs 116 and 117. Each photograph is identified by a number which is listed in Table 3[37]. The negatives are enclosed with this memorandum.

The pressure measurements made at 15 points in the test area for each flow condition are listed in Tables 1 and 2. These data have been reduced to give the Mach numbers, Reynolds numbers and static pressures in the test area. The Mach number distribution has been plotted for each flow condition, on Figs. 1, 2 and 3 (for Run 116) and Figs. 4 and 5[37] (for Run 117).

No attempt has been made to analyze the data, in accordance with the request of the University of Michigan. Attention is drawn to the rows marked with an asterisk in Tables 1 and 2, which indicate pressure measurements obtained with the glow energized. The computed Mach numbers and static pressures differ slightly under these conditions as compared with the measurements made with a "cold" stream. The effect is believed to be due primarily to an observed increase in stagnation pressure and temperature caused by the heating effect of the discharge in the stagnation chamber.

5.0 REFERENCES

1) R.A. Evans and G.J. Maslach - "Status Report on Wind Tunnel Flow Visualization by Glow Method", Univ. of Calif. Eng. Projects Report HE-150-68, May 1950.

2) S.A. Schaaf, D.O. Horning, E.D. Kane - "Design and Initial Operation of a Low Density Supersonic Wind Tunnel", Univ. of Calif. Eng. Projects Report HE-150-62, August 1949.

3) E.D. Kane - "Drag Forces on Spheres in Low Density Supersonic Gas Flow", Univ. of Calif. Eng. Projects Report HE-150-65, February 1950." (End of quote)

Tables and figures are shown in the original report.[37]

Several methods of examining the photographs were tried: slide projector, optical projecting comparator, densitometer, (recording and non-recording). The comparator provided too much magnification and the densitometer spots were too large for acceptable resolution. Therefore the negatives were projected by slide projector and the screen images traced on paper. The following significant conclusions may be drawn from an analysis of the tracings:

a) The angle between the axis of the cone and the tangent to the shock wave contour at the station corresponding to the base plane of the cone approaches the Taylor-Maccoll shock wave angle asymptotically. See Fig. 146. This asymptotic value is actually reached with the 0.700 in. dia. cone.

b) The influence of disturbances traveling upstream in the boundary layer appears to be negligible.

Experimental errors in the method are estimated to not cause an error of larger than ± 10% in the Mach numbers and to not affect the above conclusions. The sources of error are:

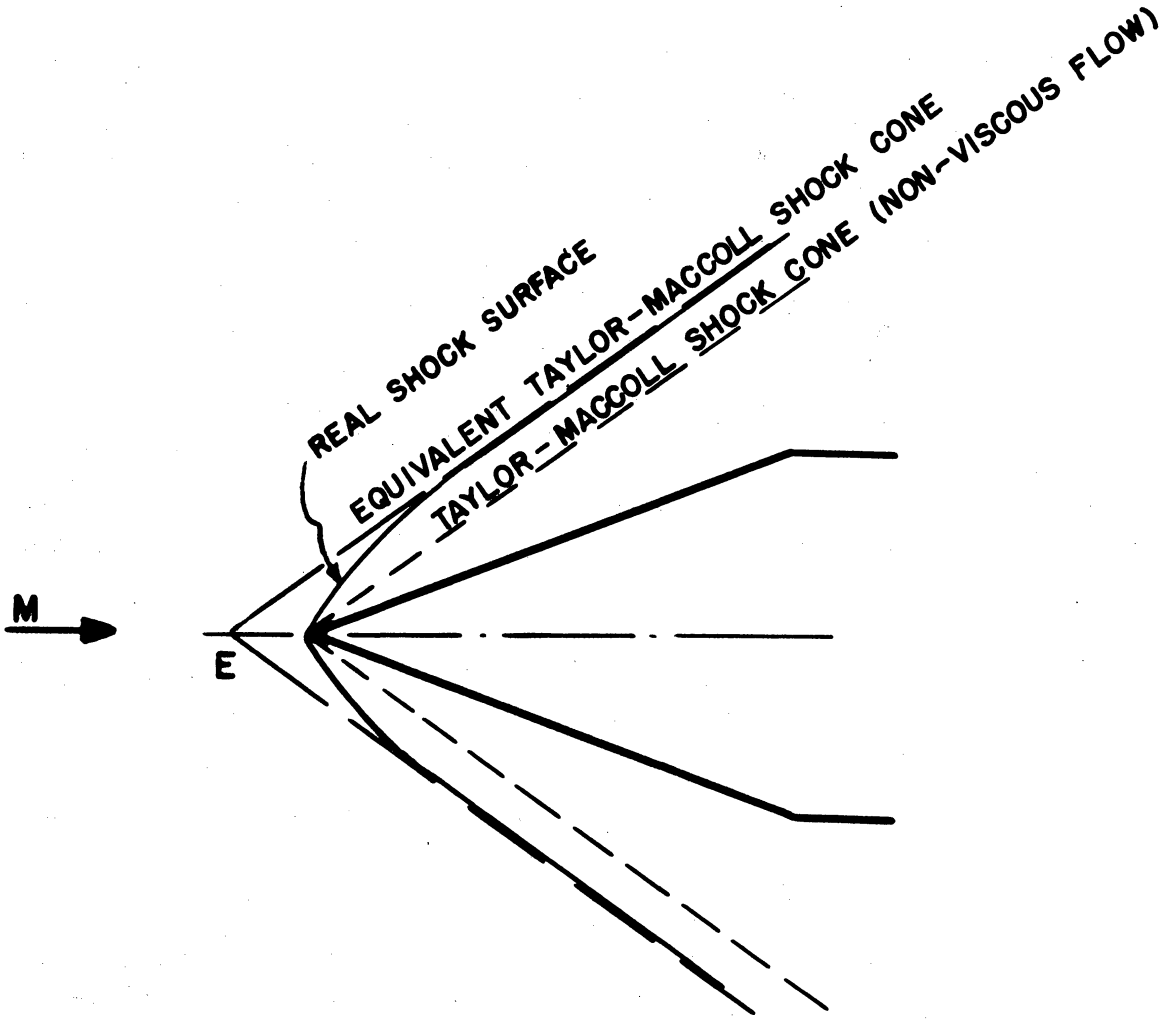

Fig. 146. Asymptotic Shock Cone

a) Non-uniformity of Mach number distribution in the wind tunnel section.

b) Error in Mach number calibration for the tunnel.

c) Variation in flow conditions from run to run.

d) Uncertainty about the nitrogen after-glow technique of flow visualization at low densities.

e) Error in making and measuring the tracings.

Fig. 147 shows a typical photograph (at M = 3.1, test section static pressure about 50 mm) taken by the nitrogen after-glow technique (enlarged).

On the basis of the above conclusions it is suggested that in the evaluation of the free stream Mach number of the supersonic flow around a cone in a slightly viscous fluid through measurements of shock wave surface as in the probe experiment, an equivalent Taylor-Maccoll shock cone vertex be determined by using the two inner probes and the two corresponding outer ones, as in Fig. 146. In other words, the conical surface tangent to the real shock surface at large distances from the tip is considered as the equivalent Taylor-Maccoll shock cone in non-viscous flow.

The above suggestion, based on a limited number of wind tunnel runs, is considered to be tentative only, due to the possible errors in the wind tunnel technique as mentioned and the limited size of models used.

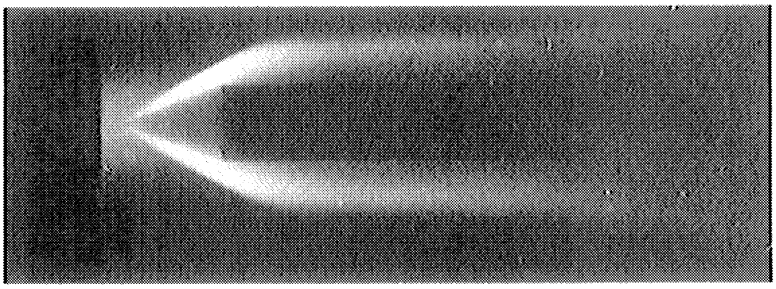

Fig. 147. Shock Wave Curvature

6.64 Evaluation of Shadowgraph and Schlieren Techniques for Measuring Temperatures in the Upper Atmosphere

Following the unsuccessful trial of the shadowgraph on V-2 42 it was learned that low pressure supersonic wind tunnel facilities were available at the NACA Laboratories at Langley Field, Va. It was decided to investigate the limits of the optical techniques in the tunnel before proceeding with further development for rocket use.

Optical parts for assembling two different shadowgraphs and two different schlierens on an optical bench were taken to Langley Field. The wedge was 1 1/2 inches wide by 1/2 inch high with a 40° included angle. Fig. 148 shows the optical components and Figs. 149 and 150 schematics of a schlieren and shadowgraph, respectively. Fig. 151 illustrates the wedge and tunnel test section. Runs were taken for various values of pressure in the settling chamber, all at approximately Mach 2.5. In order to estimate the maximum altitude at which shock wave photographs could be made with either device, the photograph for which the shock wave could just be seen in a given set was selected and the corresponding altitude calculated according to the relation:

$$\frac{\rho_o}{\rho} = \left(1 + \frac{\gamma - 1}{2} M^2\right)^{\frac{1}{\gamma - 1}} \qquad (18)$$

where ρ_o = the density of nitrogen in the settling chamber.

ρ = the density in the test section at Mach M.

M = Mach number.

$\frac{\rho}{\rho_o}$ was calculated from pressure measurements with T assumed = 300°K. Then was calculated and the corresponding altitude taken from Whipple.

Table 6 shows the results and Figs. 152 and 153 typical schlieren and shadowgraph runs respectively. Certain rocket conditions would tend to extend the altitude at which shock wave photographs might be expected to be obtained. It is estimated that only 1" of the wedge width was effective in the tunnel because of boundary layer on the tunnel walls. The rocket wedge was 2" wide and would be effective all the way across. From this consideration it was estimated that shadowgrams could be made to 40 km. In the case of the schlieren, in addition to the wider wedge, other factors could be used to extend the altitude limit. For instance, the use of first surface concave mirrors instead of lenses would remove the chromatic aberration present in the test apparatus. This would permit reducing the width of light over the knife edge from 0.005" to an estimated 0.002". The focal length of the mirrors could be increased to 36" over the 27" of the lenses in the test. The sensitivity of a schlieren system is directly proportional to the focal length of the lenses or mirrors and inversely proportional to the width of light over the knife edge. From these considerations and the full use of a

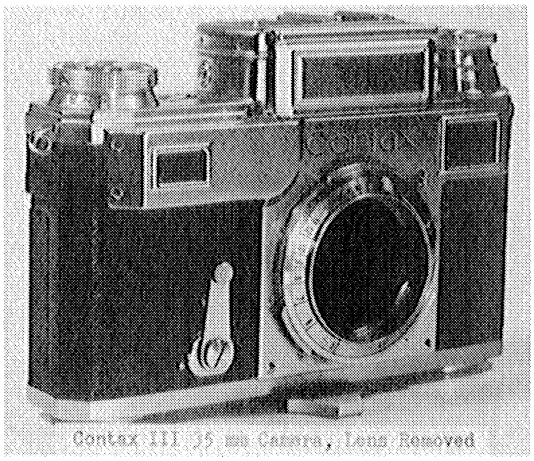

Contax III 35 mm Camera, Lens Removed

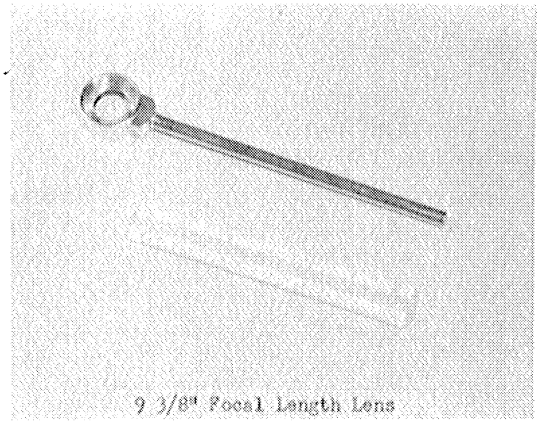

9 3/8" Focal Length Lens

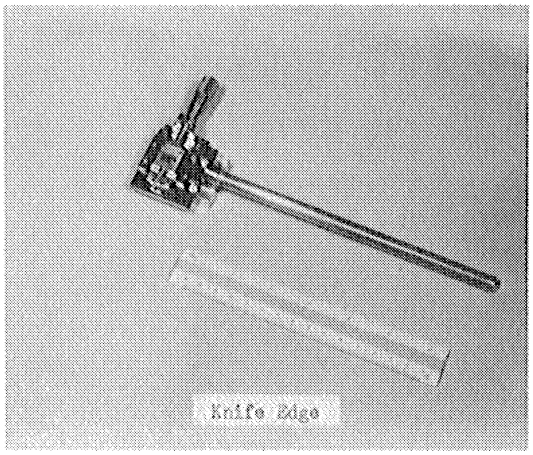

Knife Edge

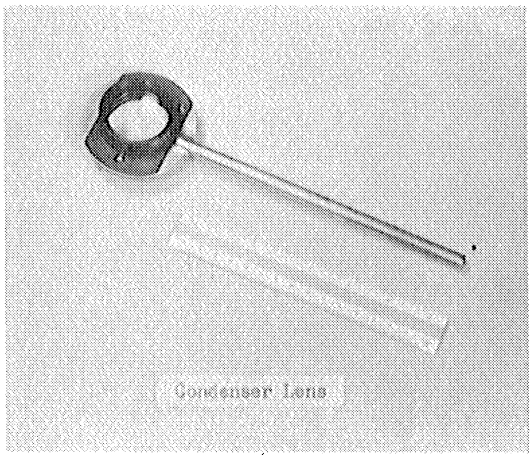

Condenser Lens

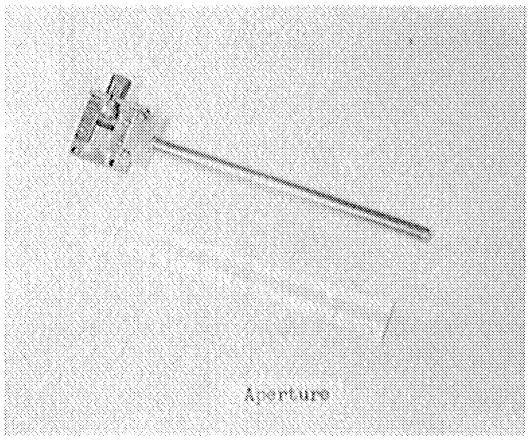

Aperture

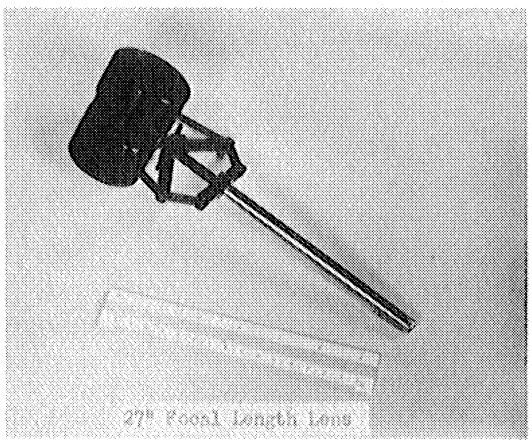

27" Focal Length Lens

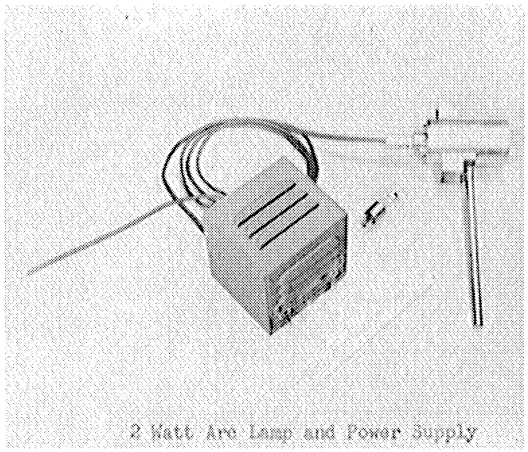

2 Watt Arc Lamp and Power Supply

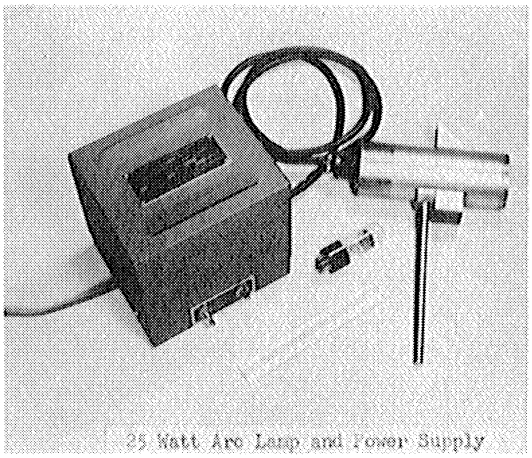

25 Watt Arc Lamp and Power Supply

Fig. 148. Optical Components, Langley Field Tests

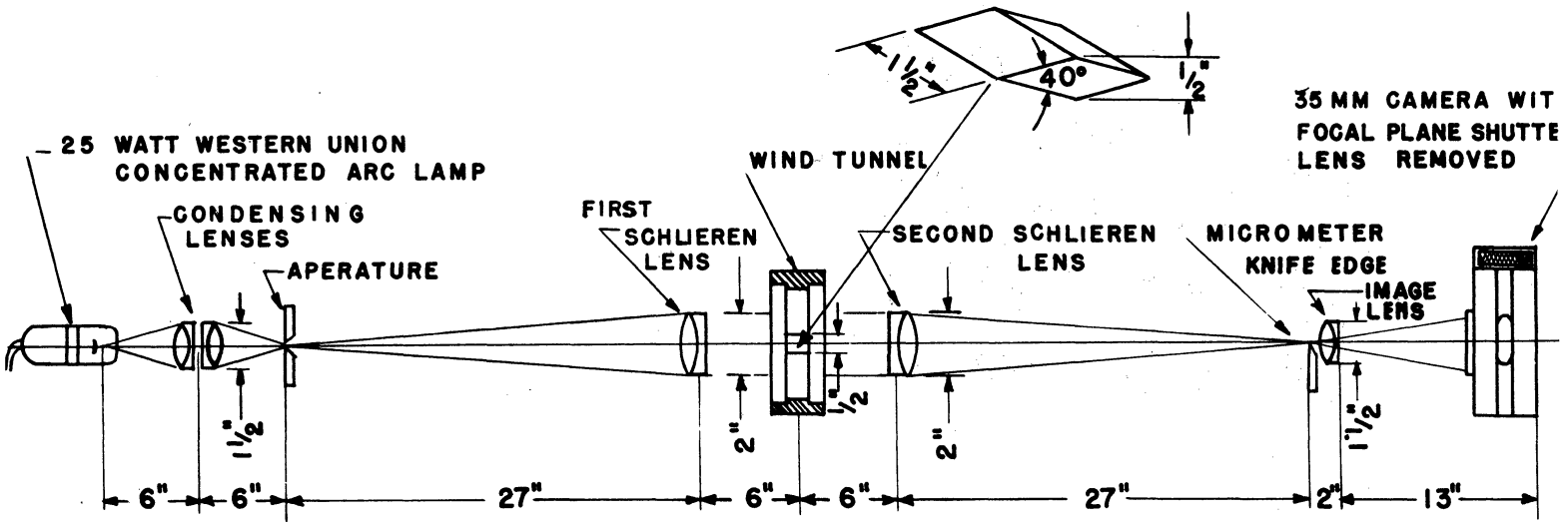

Fig. 149. Schlieren Schematic, Langley Field Tests

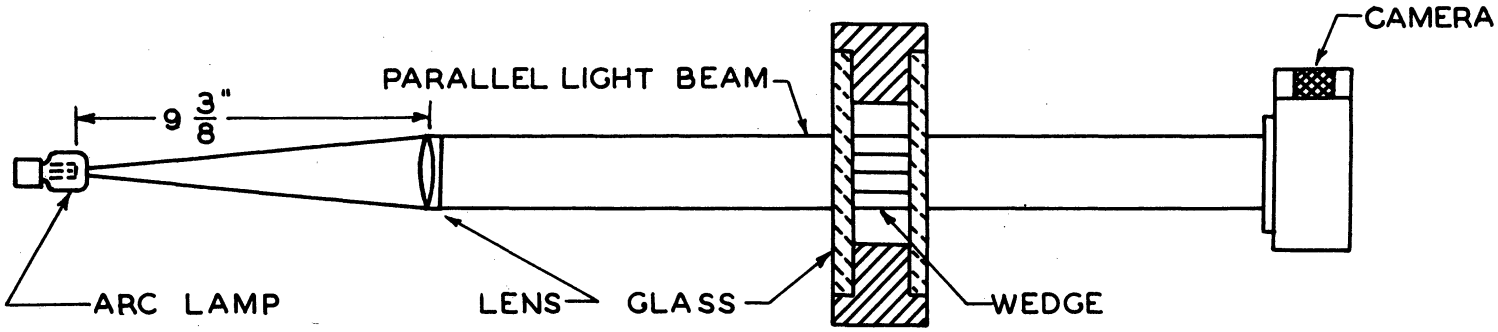

Fig. 150. Shadowgraph Schematic, Langley Field Tests

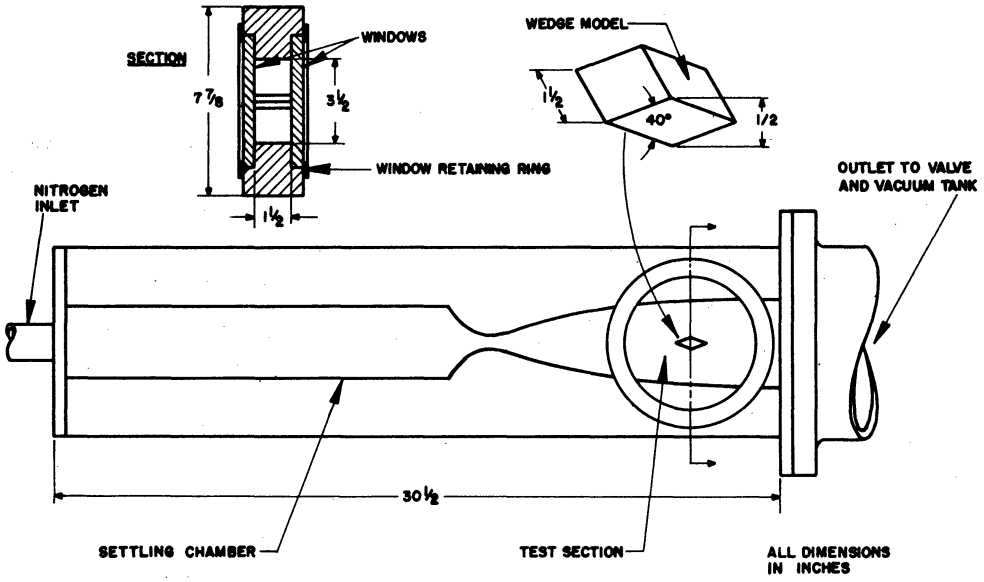

Fig. 151. Wedge and Tunnel Test Section

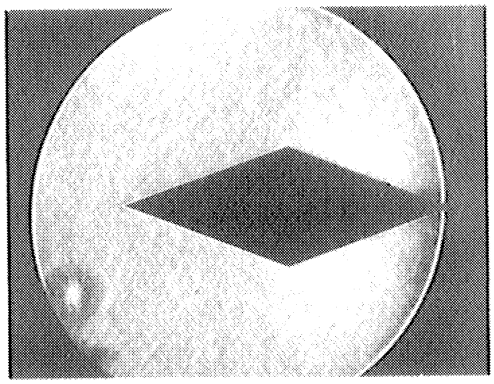

P_o = 10 mm., P_1 = .50 mm.

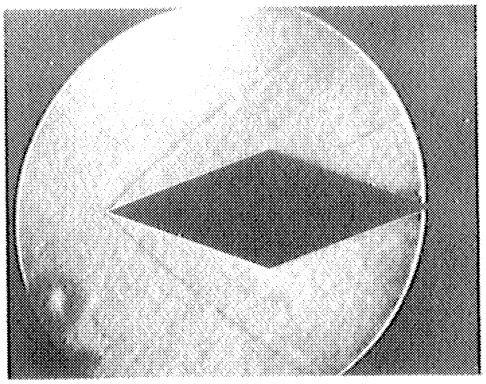

P_o = 40 mm., P_1 = 1.26 mm.

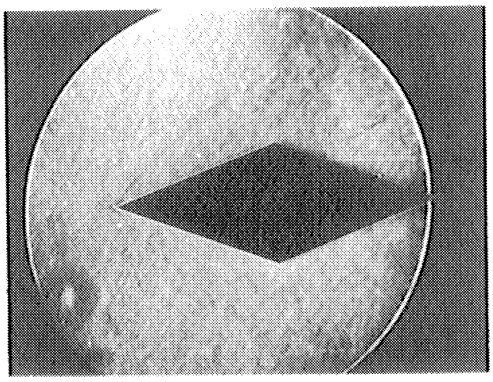

P_o = 15 mm., P_1 = .63 mm.

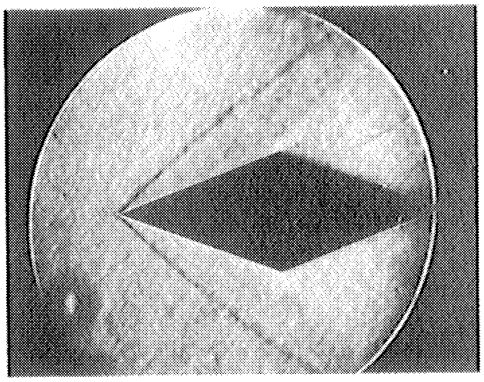

P_o = 60 mm., P_1 = 1.68 mm.

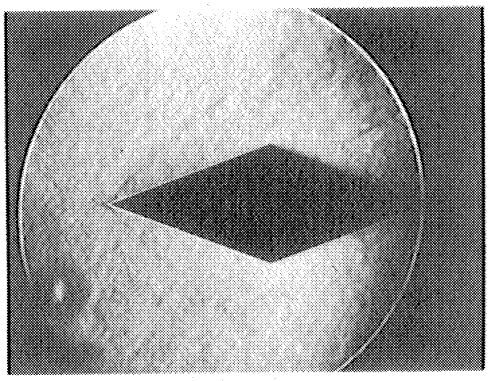

P_o = 20 mm., P_1 = .76 mm.

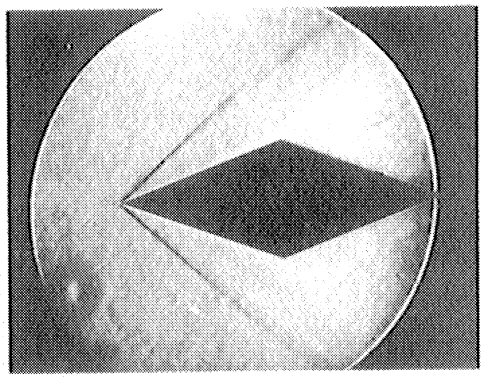

P_o = 100 mm., P_1 = 2.50 mm.

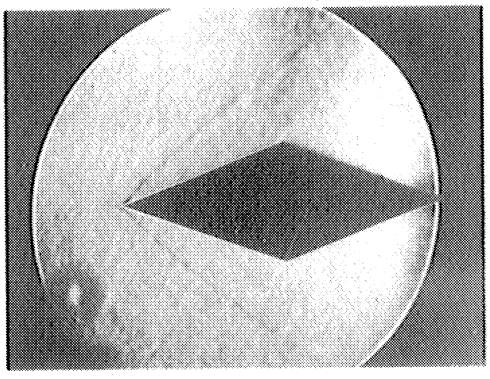

P_o = 30 mm., P_1 = 1.02 mm.

SCHLIEREN SERIES SCH-51

P_o = SETTLING CHAMBER PRESSURE

P_1 = TEST SECTION PRESSURE

ALL PRESSURES IN mm. Hg.

Fig. 152. Schlieren Photographs, Langley Field Tests

TABLE 6

Summary of Shadowgraph and Schlieren Results

Series	Run No.	Settling Chamber Pressure (mm.)	Mach No.	Corresponding Altitude
SG-21	2			
SG-41	2			
SG-11	1	30 mm.	2.65	37.2 km.
SG-22	2			
SG-42	5			
SCH-31	1	20 mm.	2.45	38.5 km.
SCH-51	2	15 mm.	2.47	41 km.
SCH-10	5			

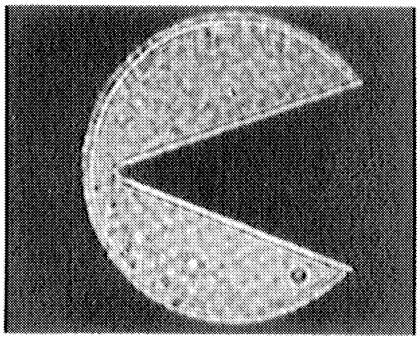

P_o = 20 mm., P_t = .76 mm.

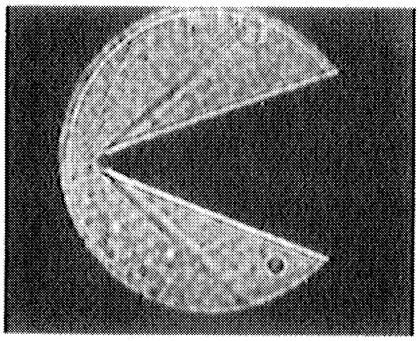

P_o = 60 mm., P_t = 1.68 mm.

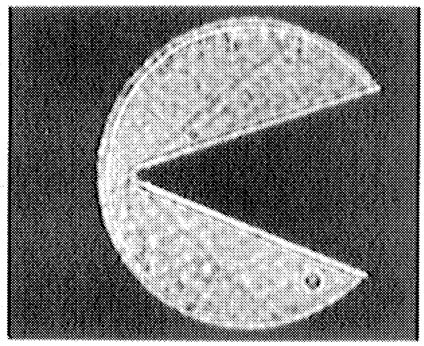

P_o = 30 mm., P_t = 1.02 mm.

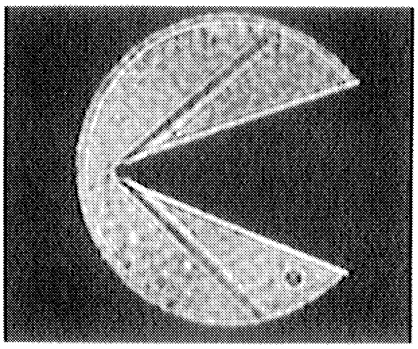

P_o = 100 mm., P_t = 2.50 mm.

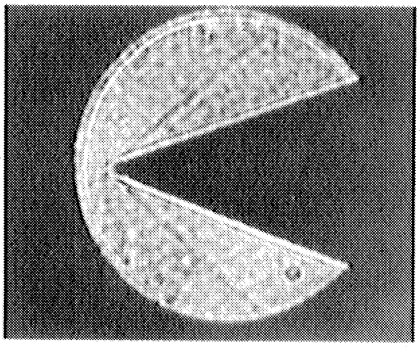

P_o = 40 mm., P_t = 1.26 mm.

SHADOWGRAPH SERIES SG-21
P_o = SETTLING CHAMBER PRESSURE
P_t = TEST SECTION PRESSURE
ALL PRESSURES IN mm. Hg.

Fig. 153. Shadowgrams, Langley Field Tests

2" wedge it was conservatively estimated that a rocket schlieren could be built with ten times the sensitivity of the one used in the tests. A schlieren system is sensitive to the density gradient of air across a shock wave. For low pressures, the shock wave thickness is approximately proportional to the mean free path[38]. Therefore, the ability of a schlieren system to detect a shock wave is proportional to ρ/mfp. At 41 km the limit of the lens schlieren system, ρ/mfp = 9×10^{-4}. The mirror schlieren should then detect a shock wave when ρ/mfp = 9×10^{-5}. This corresponds to an altitude, based on Whipple[2], of 51 km. The units of ρ/mfp are grams/cm^2.

An investigation of the precision of the measurements led to the result that the included angle between the two sides of the shock wave could be measured, by making four independent measurements, with a probable error of $\pm 0.2^{\circ}$. Neglecting boundary layer effects, this corresponds to a probable error in temperature of $\pm$ 2.5°C at Mach 3 and $\pm$ 4.2°C at Mach 4.

It was concluded, then, that the shadowgraph could measure temperature with acceptable accuracy to about 40 km and the schlieren to about 50 km. Since the probe experiment showed promise of measuring shock wave angles with comparable accuracy up to 70 km and since the probe experiment is subject to no greater error due to boundary layer, it was concluded that the shadowgraph and schlieren techniques for rockets should be shelved in favor of the probe technique.

7. WINDS

The investigation of winds in the University of Michigan project has been confined to cooperation with Edgewood Arsenal and Evans Signal Laboratory in providing auxiliary circuits for the rocket tests of the sulphuric acid and talc smoke trail generators and the smoke puff grenades.

A brief investigation[32] of the possibility of measuring winds with the probe experiment was made. It was shown that horizontal winds could be calculated from probe data if the attitude of the nose cone of the missile with respect to earth were known with good precision.

8. AUXILIARY ROCKET COMPONENTS

During the course of the research some apparatus of general interest in missile work has been developed or purchased and used. Two, into which went a great deal of development effort, were timers and two magnetic recorders (the Michigan recorder is described in Section 6.45).

8.1 Timers

The nature of the Michigan rocket experiments has been such that the operation of instruments and rocket apparatus (such as parachute) could be programmed by a timer. Various timers have been tried and one evolved which has the following characteristics:

a) Single main cam: once the cam has been notched it needs no further adjustment and the time intervals

cannot change. The cam is simple and a new one can be notched in the field in a few minutes.

b) Governor controlled motor: the total timer cycle of 200 seconds will repeat within ± 0.5 second on operating voltages between 15 and 30 volts.

c) Automatic recycling: the timer, having been started goes through one cycle and stops on the zero position ready to be started.

d) Manual cycling: the timer relay can be cycled by push button as quickly as is desired without operating the motor.

e) Multiple circuits: four separate circuits can be stepped through ten positions each. The relay contacts can handle 20 amperes.

f) Moderate current drain: the motor draws 250 ma at 24 volts during operation. The relay draws 2 amps at 24 volts for a fraction of a second on each of 12 steps.

g) Blockhouse monitoring: the fact that the timer is in zero position may be monitored in the blockhouse.

h) Light weight: the timer and relay weigh 2.3 lbs total.

The timer is shown in Fig. 154 and a typical circuit in Fig. 155.

8.2 Cook Magnetic Recorder

As a result of the telemeter failure on V-2 33 it was decided to parallel the telemeter of V-2 50 with a recorder. A 12 channel FM recorder using one inch tape was purchased from Cook Research Laboratories, Chicago. It had the following characteristics:

a) Input: 0 to +1.5 volts DC at 50,000 ohms resistive.

b) Output: 0 - 40 mm deflection on Brush recorder.

c) Frequency response: same as Brush recorder.

d) Timing: an intervalometer provided time marks 1/100 second long spaced 1.0 ± 0.01 seconds apart.

e) FM system: the DC inputs modulated 12 FM signal converters between 2500 and 4500 cps. A fixed frequency oscillator provided a recorded signal on a 13th channel which was subsequently used to regulate the speed of the playback motor and to provide an amplitude compensating signal.

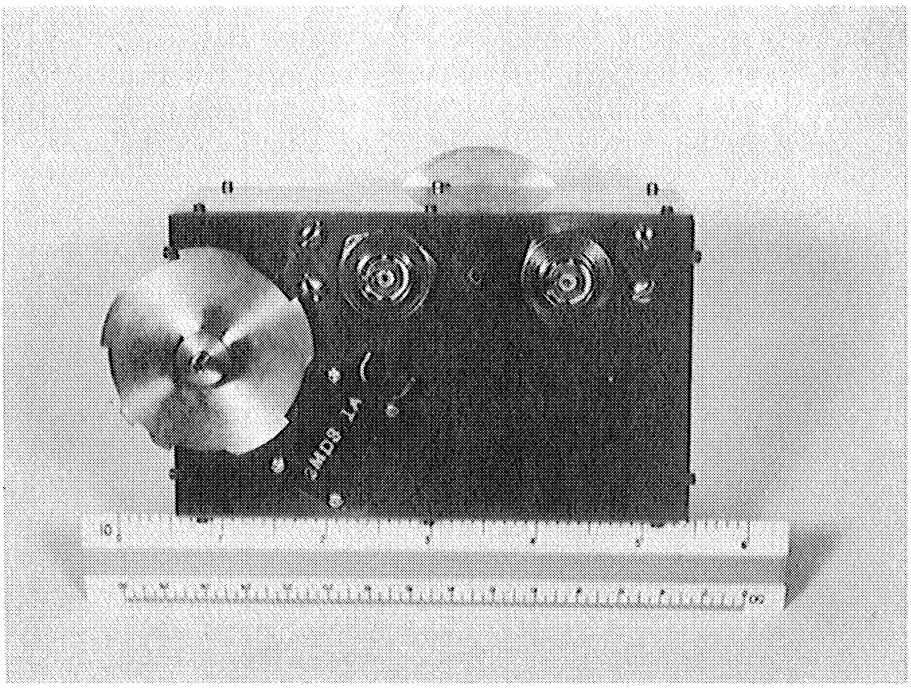

Fig. 154. Timer

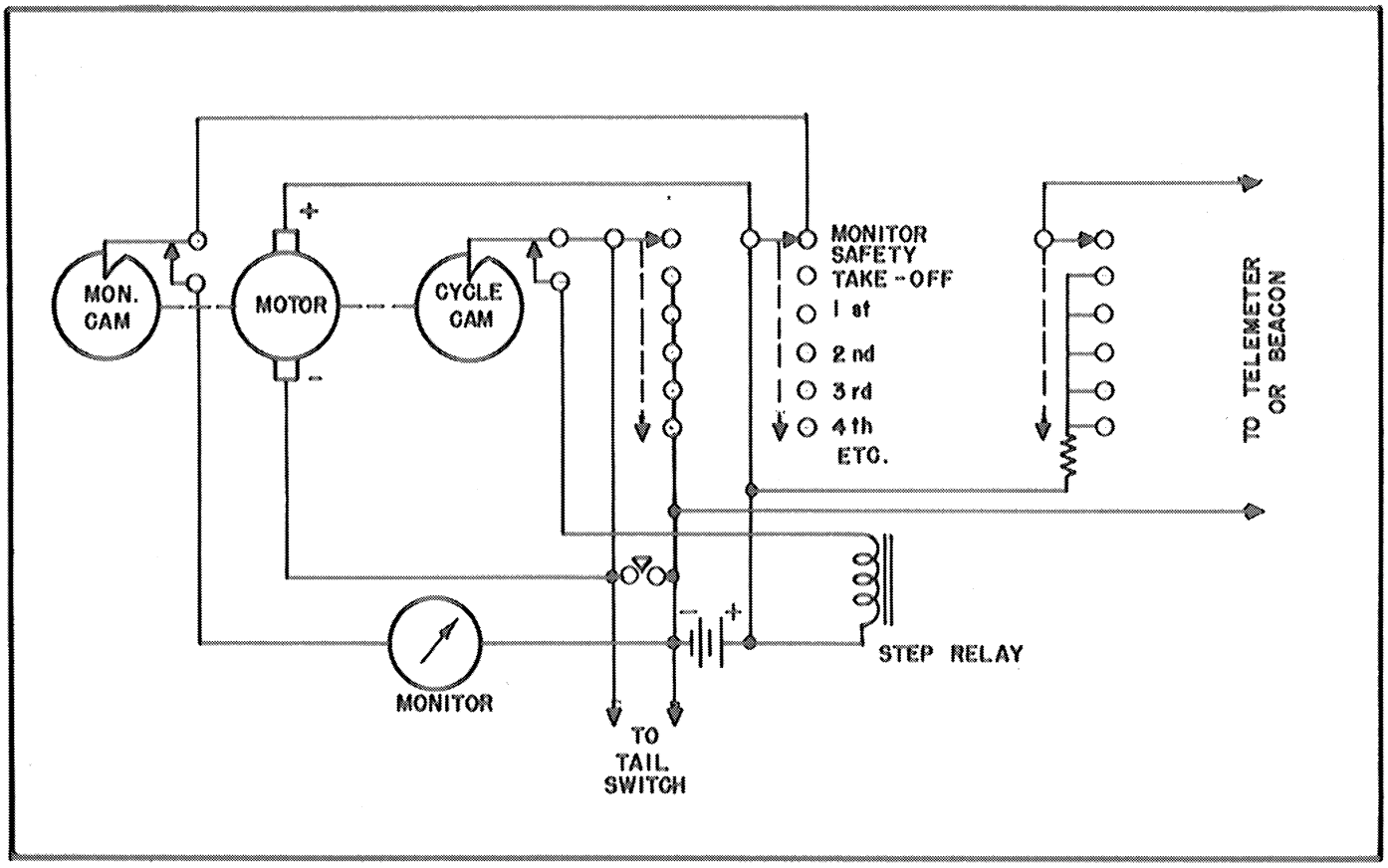

Fig. 155. Typical Timer Circuit

f) Recording time: seven minutes of recording time was provided.

g) Weight, size: the signal converter unit was 22" x 9" x 9" and weighed 45 lbs. The recorder unit was 11 x 4 1/2 x 3 3/4 and weighed about 10 lbs.

h) Performance: the performance characteristics were such that in flight operation an amplitude accuracy of ± 5% or better and a time accuracy of ± 0.5% were obtained.

On V-2 50 the reference oscillator was blocked by the doppler transponder signal. However, since the oscillator (converter) unit was mounted between the doppler doors, this is not surprising. The doppler was removed. The recorder performed successfully in flight up to the point where the first Pirani failed. It is thought that the failure of the recorder and Pirani may have been caused by the misfire of a sound grenade. A few minor changes were made in the system used on V-2 56. The recorder was pressurized, the tape supply was monitored, the converter chassis was mounted in the warhead and the 13 heads were arranged in a line instead of being staggered. The system performed satisfactorily throughout the flight.

In each case, since a good telemeter record was obtained, the telemeter record was used for data reduction. The telemeter records had less noise and better recording contrast. Further, the amplitude axis is straight rather than curved. Nevertheless, the recorder record was suitable for data reduction, if no telemeter record had been available. Fig. 156 and 157 show the two units flown on V-2 56.

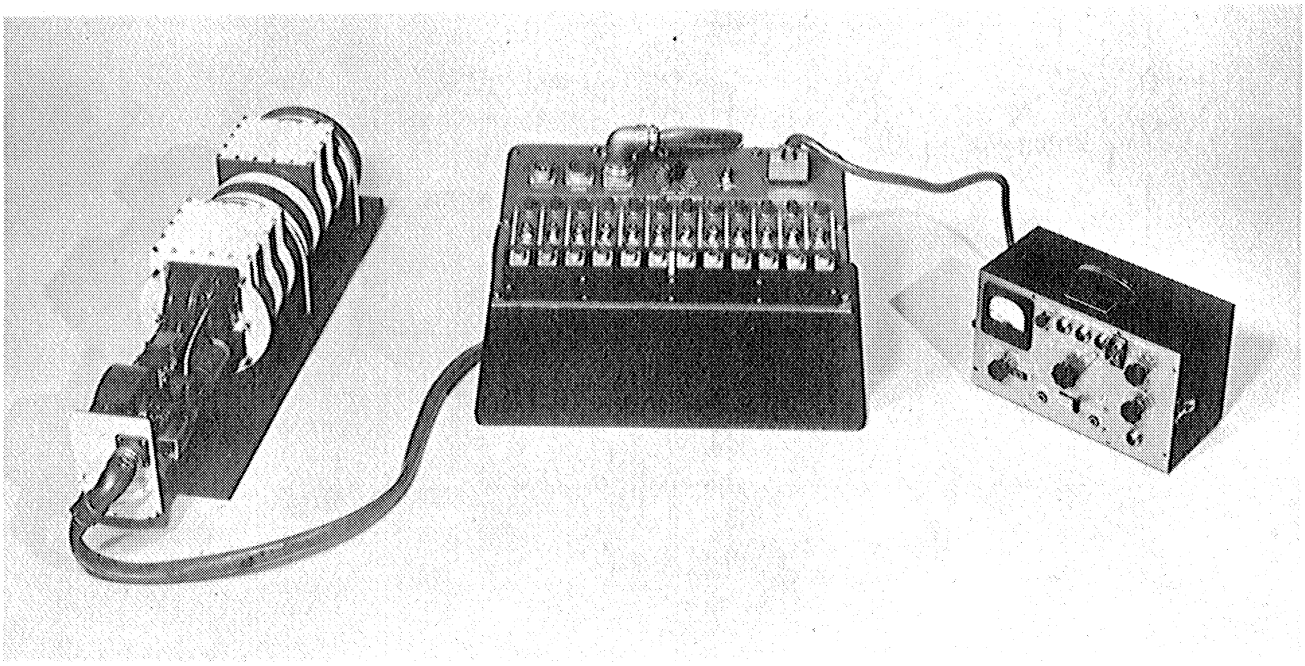

Fig. 156. Cook Magnetic Recorder, V-2 56

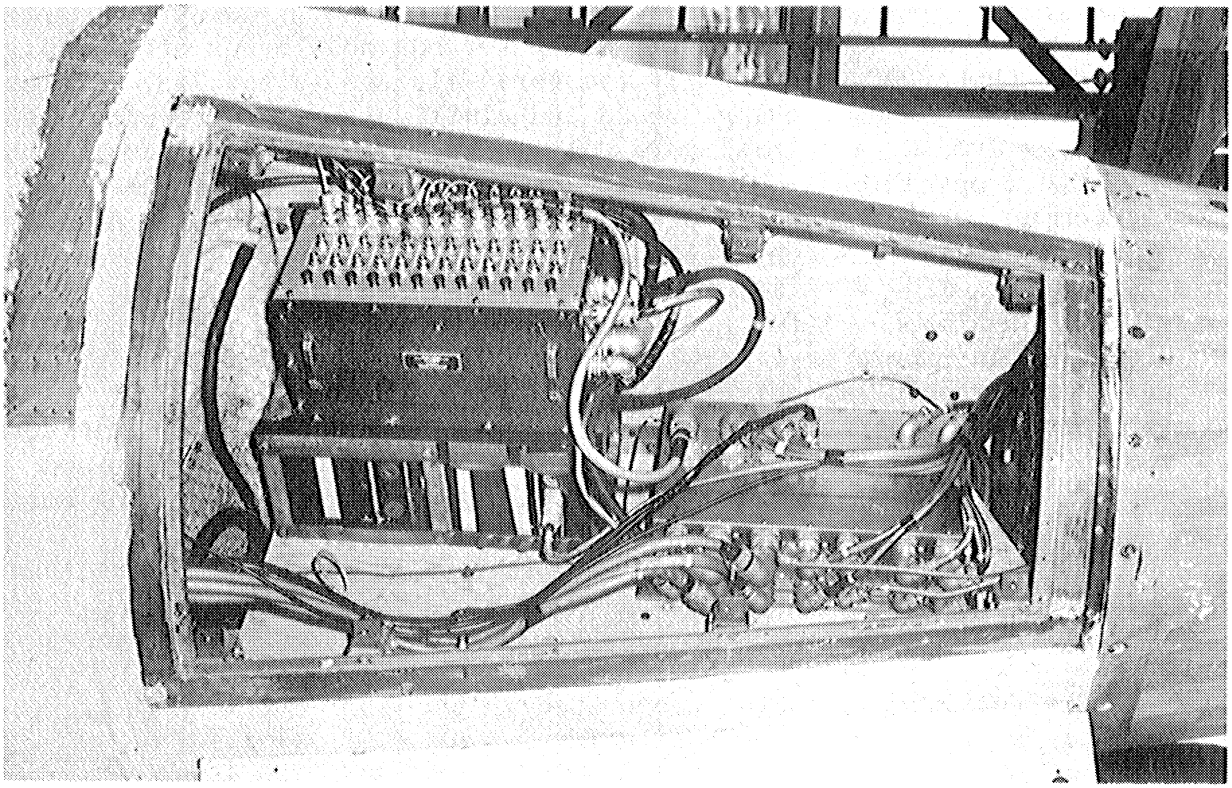

Fig. 157. Cook Magnetic Recorder, V-2 56

9. RECOMMENDATIONS

9.1 Composition

In view of the expectation from theoretical considerations that measurable diffusive separation may exist at 100 kilometers it is recommended that sampling at this altitude or above be attempted. It is also important to seek an explanation for the increase in the ratio $N^{14}N^{14}/N^{14}N^{15}$ indicated by McQueen since this increase cannot be reconciled with the constancy of the $He/A+N_2$ and $Ne/A+N_2$ ratios and it appears unlikely that the latter ratios are in error.

9.2 Pressure, Density, Temperature

The probe experiment should be given a complete test on Aerobees and developed further if initial trials show promise. The need for a simple, reliable method for measurement of pressure, density, and/or temperature is still very great and efforts should be continued to develop one.

10. ACKNOWLEDGMENT

The entire research program was supported financially by the Meteorological Branch, Evans Signal Laboratory. We are indebted to ESL also for great aid in evaluating the research, providing equipment and giving

assistance in the firings at White Sands Proving Ground. The development by ESL of the parachute technique for lowering Aerobee nose cones effectively increased the number of successfully recovered air sample bottles. Military personnel at White Sands Proving Ground and civilians associated with agencies at the Proving Ground gave invaluable help to the Michigan staff during the course of field operations. Particular mention must be made of the General Electric Company group in charge of launching V-2s, the 1st Guided Missiles Battalion in charge of launching Aerobees, Ballistics Research Laboratories for providing tracking facilities and data, Signal Corps Engineering Laboratories Field Station No. 1 for providing radar tracking and sound ranging, Army Ordnance for providing V-2s, the Naval Unit at White Sands for providing laboratory and Aerobee launching facilities, and White Sands Proving Ground for quarters, food, recreation, search and recovery facilities and many other services. Thanks are also due to Picatinny Arsenal for their design and construction of the pyrotechnic hammer-anvil sealers for the sampling bottles.

We are particularly grateful to Dr. F. A. Paneth and his colleagues at Durham University for analyzing the upper air samples and providing information useful in constructing the Michigan charcoal adsorption analyzer.

The following agencies cooperated in the sampling program by providing space on V-2s for sample bottles:

Applied Physics Laboratory
Cambridge Field Station
General Electric Company

The overall instrumentation of V-2 25 was a combined effort among Naval Research Laboratory, Edgewood Arsenal and the University of Michigan. We are indebted to the Naval Research Laboratory for providing the warheads and telemetering services for all Michigan V-2 firings in addition to making available laboratory facilities in Washington for instrumentation checks on V-2 25. Edgewood Arsenal also provided space on V-2 42 for the Michigan shadowgraph.

The privilege of consultation with the following people was greatly appreciated:

Drs. J. A. Hipple (now at the National Bureau of Standards) and R. E. Fox of the Electro-Physics Dept., Westinghouse Research Laboratories, East Pittsburgh, Pa.

Drs. Fred L. Mohler and Vernon H. Dibeler, Mass Spectrometry Section, Division of Atomic and Molecular Physics, National Bureau of Standards, Washington, D.C.

Professors John T. Tate and Alfred O. Nier, Dept. of Physics, University of Minnesota, Minneapolis, Minn.

Professor William Lipscomb, Dept. of Chemistry, University of Minnesota, Minneapolis, Minn.

Professor J. W. Beams and Dr. John McQueen, School of Physics, University of Virginia, Charlottesville, Va.

Professor Sydney Chapman, Oxford University, England. Currently at California Institute of Technology, Pasadena, Calif.

Dr. Eric T. Clarke, Tracerlab, Inc., Boston, Mass.

Professor Charles H. Townes, Dept. of Physics, Columbia University, New York City, N. Y.

Dr. A. O. Beckman, Pasadena, Calif.

Dr. C. H. Hahner, Glass Section, National Bureau of Standards, Washington, D. C.

Dr. R. H. Dalton, Chemical Laboratory, Corning Glass Works, Corning, N. Y.

Professors Leo Goldberg and Orren Mohler, McMath-Hulbert Solar Observatory, Pontiac, Mich.

Professor G. B. B. M. Sutherland, Dept. of Physics, University of Michigan, Ann Arbor, Mich.

Mr. James L. Waters, Framingham, Mass.

Thanks are also due to the mass spectrometry sections of the following corporations for their advice as to possible procurement of ultimate exploitation of mass spectrometry for our needs:

Ethyl Corporation, Baton Rouge, Louisiana
General Electric Company, Schenectady, N.Y.
Consolidated Engineering Corp., Pasadena, Calif.

Photographs

V-2 on ground, V-2 take-off, Aerobee on ground (Frontispieces), Figs. 7, 19, 20, 21, 22, 24, 28, 32, 34, 55, 56, 57, 88, 59, 72, 157, U. S. Signal Corps; Aerobee take-off (Frontispiece), Wenk; Figs. 137, 152, 153, Turner; Fig. 147, Univ. of Calif.

11. REFERENCES

1. Chackett, K. F., Paneth, F. A., and Wilson, E. J., Chemical Analysis of Stratosphere Samples from 50 and 70 Km Height, J. Atm. and Terr. Phy., 1 (1950), 49. A preliminary note was published in Nature, 164 (1949), 128.

2. Whipple, F. L., Meteors and the Earth's Upper Atmosphere, Rev. Mod. Phy., 15 (1943), 246.

3. A list of the earlier papers on the "Helium Researches" can be obtained by reference to Proc. Roy. Soc., A165 (1938), 238.

4. Glückauf, E., A Micro-analysis of the Helium and Neon Contents of Air, Proc. Roy. Soc. A185 (1946), 98.

5. Glückauf, E. and Paneth, F. A., The Helium Content of Atmospheric Air, Proc. Roy. Soc., A185 (1946), 89.

6. Paneth, F. A., Composition of the Upper Atmosphere---Direct Chemical Investigation, Quart. J. Roy. Met. Soc., 65 (1939), 304.

7. Maris, H. B., The Upper Atmosphere, Terr. Mag. Atm. Elec., 33 (1928), 233; 34 (1929), 45.

8. Epstein, P. S., Über Gasentmischung in der Atmosphäre, Gerl. Beit. z. Geophy., 35 (1932), 153.

9. Mitra, S. K. and Rakshit, H., Distribution of the Constituent Gases and their Pressure in the Upper Atmosphere, Ind. J. Phy., 12 (1938), 47.

10. Langer, A., A Gas Blending System, Rev. Sci. Inst., 18 (1947), 101.

11. Stueckelberg, E. C. G., and Smythe, H. D., The Ionization of Nitrous Oxide and Nitrogen Dioxide by Electron Impact, 36 (1930), 478.

12. Goldberg, L., Recent Advances in Infra-Red Solar Spectroscopy, Rep. Prog. in Phy., XIII (1950), 24. (This review article gives references to all of the earlier papers. Later work discussed at the 1950 Columbus, Ohio, Symposium on Molecular Spectroscopy has yet to be reported in the literature.)

13. Chapman, S. and Price, W. C., The Upper Atmosphere, Rep. Prog. in Phy., III (1936), 42.

14. Bamford, C. H., Photochemical Processes in an Oxygen-Nitrogen Atmosphere, Rep. Prog. in Phy., IX (1942-43), 75.

15. Nicolet, M., Contribution a l'etude de la strucute de l'Ionosphere, Mem. Inst. Royal Met. Belge., XIX, 1945; L'Adsorption de la radiation solaire dans la haute Atmosphere, 6th Report. Int. Comm. on Solar-Terrestrial Relations, Orleans, (France), 1948, 125.

11. REFERENCES (continued)

16. Williams, Van Zandt, Infra-Red Instrumentation and Techniques, Rev. Sci. Inst., 19 (1948), 135.

17. Snell, F. P., and Snell, C. T., Colorimetric Methods of Analysis, Vol. I, Van Nostrand, 1936.

18. Gordy, W., Microwave Spectroscopy, Rev. Mod. Phy., 20 (1948), 668.

19. Patty, F. A., and Petty, G. M., Nitrite Field Method for the Determination of Oxides of Nitrogen (Except N_2O and N_2O_5), J. Ind. Hyg. and Tox., 25 (1943), 361.

20. Regener, E., Messungen des Sauerstoffgehaltes der Stratosphärenluft, Luftfahrtforschung, 13 (1936), 361.

21. Shepherd, M., The Composition of the Atmosphere at approximately 21.5 Kilometers, Nat. Geog. Soc. Tech. Papers, Stratosphere Series 2 (1936), 117.

22. Pauling, L., Wood, R. E., and Sturdivant, J. H., An Instrument for determining the Partial Pressure of Oxygen in a Gas, J. Amer. Chem. Soc. 68 (1946), 795.

23. McQueen, J. H., Isotopic Separation due to Settling in the Atmosphere, Phy. Rev., 80 (1950), 100.

24. Taylor, G. I., and Maccoll, J. W., The Air Pressure on a Cone Moving at High Speeds, Proc. Roy. Soc., A139 (1933), 278; J. W. Maccoll, Proc. Roy. Soc., A159 (1937), 459.

25. Stone, A. H., On Supersonic Flow Past a Slightly Yawing Cone, J. Math. Phys., 27 (1948), No. 1.

26. Erdmann, Archiv., 66/100 (Peenemünde).

27. Tables of Supersonic Flow Around Cones, Center of Analysis Technical Report No. 1, M.I.T., Cambridge, Mass., 1947.

28. Tables of Supersonic Flow Around Yawing Cones, Center of Analysis Technical Report No. 3, M.I.T., Cambridge, Mass., 1947.

29. Tables of Supersonic Flow Around Cones of Large Yaw, Center of Analysis Technical Report No. 5, M.I.T., Cambridge, Mass., 1949.

30. Leite, R. J. and Liu, V. C., Analysis of Pressure Measurements Recorded During the Flight on V-2 No. 25, Engr. Res. Inst., Univ. of Mich., April 1949.

31. Mills, R. G., Calculations of Pressures on Cones Moving at Supersonic Velocities in the Upper Atmosphere, Engr. Res. Inst., Univ. of Mich., October 1946.

32. Bartman, F. L., Liu, V. C., Schaefer, E. J., An Aerodynamic Method of Measuring the Ambient Temperature of Air at High Altitudes, Engr. Res. Inst., Univ. of Mich., July 1950.

33. Roberts, H. E., The Earth's Atmosphere, Aero. Eng. Rev., 8 (1949), 18.

34. Meagher, R. E. and Bentley, E. P., Vacuum Tube Circuit to Measure Logarithm of Direct Current, Rev. Sci. Inst., 10 (1939), 336.

35. von Ubisch, H., A New Hot-Wire Vacuum Gauge, Nature, 161 (1948), 927.

36. Liu, V. C. and Turner, E. B., An Evaluation of Shadowgraph and Schlieren Optical Methods for Determining Temperatures in the Upper Atmosphere, Engr. Res. Inst., Univ. of Mich., July 1949.

37. Shock Contour Test Program, Inst. of Eng. Res., Univ. of Calif., Series No. UCB 336, July 1950.

38. Rutkowski, J., The Schlieren Method in Flow Observation of Rarefied Gases, UMM 22, Aero. Res. Center, Univ. of Mich.